NOVEL BMP ANTAGONISTS AND NEURAL INDUCTION IN THE MOUSE

by

Lisa Sue De Boer Emmett

A dissertation submitted in partial fulfillment
of the requirements for the degree of
Doctor of Philosophy
(Cell and Developmental Biology)
in The University of Michigan
2009

Doctoral Committee:

      Professor Kathy Sue O'Shea, Chair
      Associate Professor Catherine Ellen Krull
      Assistant Professor Scott E. Barolo
      Assistant Professor Deneen Wellik

Dedication

To my parents, Robert & Sheryl De Boer, my loving husband, John, and my precious son, Aidan.

Acknowledgements

advice in making several transgenic animals, and to Stephanie Schmoll and Dr. Marta Dzaman from the Organogenesis Morphology Core for their assistance in cryosectioning and equipment usage.

My acknowledgements would be incomplete without recognizing the people that influenced my early scientific career. I am indebted to my former employers at GlaxoSmithKline, Dr. Karen Augustine-Rauch and Dr. Rogely Boyce, whom gave an inexperienced undergraduate her first opportunity to work in a laboratory.

Finally, I would like to thank my family, particularly my parents, Robert and Sherry De Boer, and friends for their understanding and support throughout this process. Without their love and friendship, my achievements would not have been possible. I would like to express my heartiest thanks to Susan Johnson and Matt Velkey for taking the time to edit and format this thesis. Sincere thanks go out to my husband John for not only his patience, but his undying love and encouragement over these years. Lastly, I would like to thank my son Aidan. Not only were you a good baby but the joy that you bring to my life has made this entire process worthwhile.

Table of Contents

List of Figures

Figure

List of Figures (continued)

Figure

List of Tables

viii

List of Appendices

Appendix

ABSTRACT

NOVEL BMP ANTAGONISTS AND NEURAL INDUCTION IN THE MOUSE

by

Lisa Sue De Boer Emmett

Chair: Kathy Sue O'Shea

  At induction, the embryonic ectoderm is transformed via a series of
morphogenetic changes and alterations in gene expression to form the neural
ectoderm. A transient structure, the node, expresses factors including noggin,
chordin, and follistatin that antagonize signaling by bone morphogenetic proteins
(BMPs), causing the midline embryonic ectoderm to express neural genes. The
cells at the border between the epidermal and neural ectoderm give rise to the
future neural crest cells and are located at the site of neural tube closure; thus,
tight regulation of signaling molecules in this area is crucial. What additional
genes are involved in inducing and patterning the neural ectoderm remains to be
determined.

  To test the hypothesis that antagonism of BMP signaling sets the boundary
between the neural and epidermal ectoderm as well as to identify novel effectors
of this process, a series of independent experiments was carried out.
Misexpression of the BMP antagonist noggin or knock-down of BMP4 expression

using shRNAs both expanded the neural ectoderm at the expense of the epidermal ectoderm. In a differential display-RT-PCR screen for genes downstream of noggin, we identified the bi-functional protein Geminin. In the early post-implantation embryo, Geminin is required for epithelial to mesenchymal transition at gastrulation as well as neural crest differentiation and migration. Geminin knock-down inhibited the migration of endoderm and mesoderm from the primitive streak and decreased the size of the neural crest cell population while overexpression expanded the neural ectoderm and neural crest. We also identified uncharacterized genes potentially involved in neural induction using laser capture microdissection of neural ectoderm, embryonic ectoderm, primitive streak, node, and anterior visceral endoderm, followed by RNA extraction and microarray analysis. Overall, this work indicates that inhibition of BMP signaling plays a critical role in setting the neural ectoderm/ epidermal ectoderm boundary in the mouse embryo and sets the stage to examine the role of additional genes in this process. These results have implications in understanding normal development, the genesis of birth defects, and may suggest novel strategies for the neural differentiation of stem cells.

Chapter 1

Introduction

1. Patterning the Early Post-Implantation Stage Embryo

In the mouse embryo, the epiblast is patterned by multiple signaling pathways that first establish the embryonic axes and then specify the three germ layers. These signals include members of the TGFβ/Nodal, Wnt, and FGF families (reviewed by Beddington and Robertson, 1999; Tam and Loebel, 2007). In the early post-implantation embryo prior to gastrulation, the proximal-distal (P-D) axis is established by the cross-talk between three cell populations: the epiblast, the primitive visceral endoderm (VE), and the extra-embryonic ectoderm (ExE). Nodal expression in the epiblast with BMP expression in the ExE creates a gradient of high Nodal in the distal region of the embryo and high Bmp in the proximal. At E5.5, Smad2 expression in the VE is activated by Nodal in the overlying distal epiblast cells giving rise to the anterior visceral endoderm (AVE) (reviews Beddington and Robertson, 1999; Lu et al., 2001). The anterior-posterior (A-P) axis of the embryo emerges gradually as the AVE begins to secrete Nodal and Bmp inhibitors such as mDkk1, Cer1, and Lefty1 (Belo et al., 1997; Mukhopadhyay et al., 2001). With coordinated cell movements, the expression domain of Nodal is pushed from the AVE and towards the posterior region of the embryo causing a rotation of the P-D axis of the embryo (Pfister et al., 2007) (Figure 1-1).

As the A-P axis emerges, expression domains are segregated: Wnts, Fgfs, Nodal, and Bmps are restricted to the posterior region of the embryo while their antagonists and pro-neural genes such as *Otx2* are induced in the anterior by the

AVE (Ang et al., 1996). At E6.5, a subset of proximal epiblast cells in the posterior region of the embryo expressing Fgfs, Wnts, and their target genes are induced to form mesoderm and initiate the formation of the primitive streak (Thomas and Beddington, 1996; Ding et al., 1998; Rhinn et al., 1998; Kimura et al., 2000).   Epiblast cells egressing through the streak give rise to definitive (embryonic) endoderm (DE) and mesoderm collectively referred to as mesendoderm. At the anterior most end of the primitive streak (APS), a transient structure known as the node, forms (Beddington and Robertson 1999; Tam and Loebel et al., 2007; Sulik et al., 1994). Mesendodermal cells emerging from the streak and APS displace the VE as they migrate anteriorly giving rise to the anterior definitive endoderm (ADE) and form two major signaling centers: the prechordal plate which lies underneath the most rostral end of the neural tube, and notochord (Sulik et al., 1994). Both of these structures are necessary for not only conveying A-P identity along the neural tube but dorsal-ventral (D-V) patterning as well (Tam and Loebel, 2007).

The node is a key structure involved in neural induction. It begins secreting the BMP antagonists, Noggin, Chordin, and Follistatin which induce expression of pan-neural genes *Sox 1*, *2*, *3*, and *Zic 1* inhibiting BMP binding to its receptor and later induce the neural ectoderm form the floor plate of the neural tube (Levine and Brivanlou, 2007). The neural plate, comprised of neuroectoderm, will eventually give rise to all the nervous tissue of the embryo. Cells adjacent to the neural plate express Bmps and induce the epiblast to form the surface/epidermal ectoderm (Lawson et al., 1999b).

Patterning the early embryo requires the coordinated expression of signaling molecules that specify cell fate and regulate cell movement. Since the process of gastrulation not only converts the epiblast into the three germ layers but creates the signaling centers that will accomplish this, tight regulation is necessary. Genes including Wnt, TGFβ (*Bmp* and *Nodal*), and FGF family members are all expressed at various times and locations during embryogenesis

and play numerous roles in the sequential migration and differentiation of cells from the epiblast. Teasing out their roles and interactions is complicated not only by the cross-talk but by redundancy as well.

2. Signals that Pattern the Embryo

Anterior Visceral Endoderm (AVE)

In the early post-implantation embryo, Nodal is initially expressed throughout the epiblast and the VE (Varlet 1997). Nodal expression in the distal epiblast activates Smad2 in the VE promoting the formation of the AVE (Brennan et al., 2001). These cells are then displaced toward the prospective anterior side of the embryo as gastrulation proceeds (Thomas and Beddington, 1996; Thomas et al., 1998). The AVE begins to secrete molecules such as mDkk1, Cer1, and Lefty1 which antagonize Wnt, BMP, and Nodal signals giving rise to anterior cell fates (de Souza et al., 2000) by inhibiting expression of primitive streak specifying genes in the anterior epiblast (Perea-Gomez et al., 1999; Rhinn et al., 1998; Perez-Gomez et al., 2001b; Kimura et al., 2000). For example, expression of the Wnt antagonist mDkk1 in the anterior mesendoderm specifies anterior neuroectoderm (Mukhopadhyay et al., 2001). Lefty1 inhibits Nodal (Meno et al., 1999) and Cerberus-like 1 inhibits both Nodal and BMP (Belo et al., 1997; Piccolo et al., 1996).   Cer1 and Lefty1 are also expressed later in the ADE after Goosecoid (Gsc), a downstream target of Nodal required for the formation of definitive endoderm, expression in the APS has been activated. Single mutations have little effect but double *Cer1* [-/-]; *Lefty1* [-/-] mutants have an expanded APS (Perea-Gomez et al., 2002) (Figure 1-1).

This illustrates the multiple, redundant roles these regulators play during gastrulation. Loss of the AVE following genetic manipulation not only results in a lack of anterior markers in the epiblast but A-P identity is lost as embryos take on a proximal identity (Waldrip et al., 1998; Perea-Gomez et al., 2002). Nodal/Smad2 signaling is required for the formation of the primitive streak and

AVE, which in turn specify axial mesoderm and anterior mesendoderm required to maintain forebrain specification (Vincent et al., 2003).

Like many other of the TGFβ family members, Nodal signals through a heteromeric complex of type I and type II receptor kinases, of which there are seven and five respectively, that activate the Smad2/Smad3 complex via phosphorylation of the type II receptor. This complex in turn associates with Smad4 which translocates to the nucleus and regulates transcription of target genes (review Whitman et al., 1998; review Wotton and Massague, 2001). Members of the BMP family and Activin bind the same receptors as Nodal, including ALK3 for BMP (Mishina et al., 1995) and ALK4 for Activin (Gu et al., 1998). Mutations in either of these receptors leads to developmental arrest prior to gastrulation. Nodal also positively regulates expression of Bmp4 in the ExE (Brennan et al., 2001; Liu et al., 1999). In addition to Smad2 signaling required for AVE formation, Nodal is also regulated by a co-receptor, Cripto (Ding et al., 1998). Cripto is expressed in a P-D gradient and is induced by Wnt/ β-catenin signaling (Morkel et al., 2003). Nodal also induces Cripto directly in the epiblast and indirectly via inducing Bmp4 in the ExE (Beck et al., 2002).   Regulation of Nodal also plays a role in the temporal expression of genes in the APS. Gsc is activated at the early streak phase whereas Chordin and Noggin, two BMP antagonists, and Brachyury (T), a mesoderm marker, are expressed later in the APS (Bachiller et al., 2000; Perea-Gomez et al., 2002). At the node, Nodal is expressed at the edges of the notochordal plate with a higher concentration on the left-side in later embryos (Norris et al., 2002).   Embryos are highly sensitive to hypomorphic levels of Nodal signaling (Lowe et al., 2001) and pathway mutants such as Fast1 (Hoodless et al., 2001; Yamamoto et al., 2001) have highly variable phenotypes. *Nodal* [-/-] embryos fail to form a primitive streak and die prior to gastrulation (Zhou et al., 1993; Conlon et al., 1994).   They also fail to express posterior markers such as T, Fgf8, Wnt3, and Eomes indicating a requirement for Nodal in mesodermal specification and primitive streak formation (Brennan et al., 2001). Nodal also promotes acquisition of posterior fates in the

4

epiblast via a Smad2-independent pathway by patterning the VE which conveys anterior identity to overlaying epiblast cells (Brennan et al., 2001). It is also required for left-right patterning of the early embryo (Collignon et al., 1996). Taken together, Nodal can be considered a master regulator of embryonic patterning due to the number of roles it plays in early embryo patterning.

Node

The homolog of the node was first discovered in *Xenopus* when tissue from the dorsal blastopore lip was transplanted to the ventral region of the embryo forming a secondary axis. This signaling center became known as Spemann's organizer (Spemann and Mangold, 1924). Since then, organizers in other vertebrate embryos have been identified and include the shield of teleosts (Luther et al., 1935), Henson's node in the chick, and the node in mammals (Waddington et al., 1932; Waddington et al., 1936). The murine node is a bi-layered structure composed of ciliated VE cells at the ventral surface and a dorsal layer of epiblast cells (Sulik et al., 1994) (Figure 1-2). The node is often incorrectly referred to as the anterior primitive streak or APS as it is the most anterior aspect of the primitive streak located at the distal tip of the embryo (Beddington and Robertson, 1999; Tam and Loebel, 2007). Several signaling pathways are involved in correctly inducing, patterning, and maintaining the node including Bmp, Nodal and Wnts. The node has complex signaling activities which include neural induction and patterning (review Harland, 2000). Although the organizer has been studied in numerous species for over seventy years, only a few signaling molecules have been well characterized in the mouse embryo *i.e. Noggin* (Valenzuela et al., 1995), *Chordin* (Pappano et al., 1998), *Follistatin* (Albano et al., 1994), and retinoic acid (Ribes et al., 2009) and several more have been identified in extensive cDNA library screens *i.e.* m8708a22, p7822b53, t8130b59 (Sousa-Nunes et al., 2003). Although factors secreted by the node were originally thought to be the sole source of inducing factors, recent evidence suggests a role for additional players in neural induction. In mice without a functional node whether following genetic ablation *i.e.* the *Foxa2*^{-/-}

(Klingensmith et al., 1999), *Fgf8*^{-/-} (Ding et al., 1998), or *Cripto*^{-/-} (Sun et al., 1999) null mutants that fail to form a node or by surgical removal of the node (Davidson et al., 1999), neural induction does occur albeit in a limited manner. Fgf and retinoic acid (RA) are also factors that play an important role in the node. RA-synthesizing enzyme (Raldh2) is active in the primitive streak, node, and notochord whereas RA-responsive elements (RARE) are expressed in the epiblast (Ribes et al., 2009). Loss of Raldh2 increases the size of the primitive streak and mesoderm at the expense of the neural ectoderm (Molotkova et al., 2005; Vermot et al., 2005). Fgfs can act as neuralizers as they attenuate Bmp signaling (Storey et al., 1998) and in chick, induce Churchill expression (Sheng et al., 2003). Fgfs, in particular, Fgf8, also inhibits neural differentiation by inhibiting RA secreted from mesendoderm cells. RA signaling is required for neuronal differentiation and ventral neural patterning (Diez del Corral et al., 2003; Diez del Corral et al., 2004). Together with Follistatin, another BMP antagonist, RA is expressed in response to Shh signals that regulate neural patterning (Liem et al., 2000). These signaling molecules are released from cells in and around the node and interact with each other to attenuate and/or induce the expression of each other. There is a tremendous amount of redundancy as single mutations of genes such as *Noggin* or *Chordin* are unable to fully disrupt patterning but double *Noggin*^{-/-};*Chordin*^{-/-} mutants fail to form a head (Bachiller et al., 2000; Anderson et al., 2002). Wnt8 and Wnt11 are also expressed in the node where they may regulate Nodal signaling (Bouillet et al., 1996; Kispert et al., 1996). Thus, the multiple roles these signaling families in the developing embryo are still being uncovered.

The first cells emerging from the primitive streak form the APS and become the organizer region. The derivatives of the APS include: the ADE, prechordal plate, and the notochord. These tissues are all essential for patterning of the neuroectoderm. The APS is induced and patterned by two fork-head transcription factors: Foxa2 and FoxH1 which are important regulators of Nodal signaling. Foxa2 is expressed in the VE and in anterior streak cells where it is required for

node formation (Ang and Rossant, 1994; Dufort et al., 1998). FoxH1 is expressed in the epiblast and VE, where it regulates Nodal pathway targets, and promotes expression of Foxa2 in the streak (Weisberg et al., 1998; Hoodless et al., 2001; Yamamoto et al., 2001). Loss of either results in embryos lacking an APS (Ang and Rossant, 1994; Dufort et al., 1998; Weisberg et al., 1998; Hoodless et al., 2001; Yamamoto et al., 2001; Perea-Gomez et al., 2002). Null mutations in *Arkadia*, a modulator of Nodal signaling, also leads to a loss of the APS. Consequently, without Foxa2 induction, the node and axial mesendoderm fail to form, indicating a high level of Nodal is necessary for APS formation (Episkopou et al., 2001).

Brachyury (T) is also necessary for the formation of mesoderm and is expressed in the entire primitive streak including the APS (Herrmann et al., 1990; Lowe et al., 2001). Loss of *T* in the embryo results in embryos that exhibit defects in notochord differentiation and mesoderm formation, lack a trunk and tail, and die around embryonic day 10 (Chesley et al., 1935; Bennett et al., 1975; Herrmann et al., 1991). Brachyury is induced by not only Fgf8 but by Wnt3a in the primitive streak, linking two major signaling pathways to APS formation (Arnold et al., 2000; Yamaguchi et al., 1999; Herrmann et al., 1995).

The Primitive Streak

At E6.5, a transient structure, the primitive streak, forms at the posterior pole of the mouse embryo with the anterior primitive streak (APS) positioned at its distal tip. The primitive streak is the site of cell movements in the epiblast and the source of the three germ layers, giving rise to mesoderm and definitive endoderm (Beddington and Robertson, 1999; Tam and Loebel, 2007). As cells egress through the streak, they contribute to various tissues in the embryo based on the level at which they exit. Cells at proximal levels contribute to the extra-embryonic mesoderm and those from the middle streak region form the lateral plate and paraxial mesoderm (Lawson et al., 1999b). Finally, APS cells become the organizer region. Although some of the signaling factors and pathways involved

have been identified, there is still a significant lack of understanding regarding the formation, regulation, and maintenance of the primitive streak (Figure 1-1; Figure 1-3).

Nodal, a TGFβ superfamily member, plays a major role in the formation and positioning of the primitive streak and the node as mice that lack *Nodal* fail to gastrulate and form mesoderm (Zhou et al., 1993; Conlon et al., 1994). Mice double homozygous null for *Cer1*; *Lefty1* (Nodal antagonists) have an expanded APS and some develop multiple ectopic primitive streaks. Paraxial mesoderm also fails to form (opposite of *Nodal*$^{-/-}$ mice). This in turn leads to a broader expression domain of Gsc and Hex, downstream targets of Nodal (Perea-Gomez et al., 2002). Single mutations in either have no obvious effect on the primitive streak mainly due to genetic redundancy (Meno et al., 1999; Belo et al., 2000). Lefty2, another Nodal antagonist, is expressed in the mesoderm in cells invaginating through the middle and posterior streak. *Lefty2* mutants have an enlarged primitive streak and an excess of mesoderm (Meno et al., 1999). Avian experiments have also confirmed that the hypoblast is able to inhibit ectopic primitive streak formation via Cerberus expression (Bertocchini and Stern, 2002). Together, these antagonists assist in positioning and regulating the size of the primitive streak.

Although Nodal signaling occurs via Smad2, streak formation is controlled by both Smad2-dependent and independent pathways. Experiments in which *Smad2* is deleted only from the epiblast has no effect on the formation of the primitive streak or on gastrulation movements. Instead, Smad2 signal transduction is required for the specification of axial mesendoderm precursors that give rise to the ADE and PCP mesoderm (Vincent et al., 2003). Evidence also suggests that Nodal is able to induce Bmp4 expression in the extra-embryonic ectoderm (Ben-Haim et al., 2006).

Why does the AVE secrete Nodal inhibitors as well as BMP and Wnt antagonists if regulating them is not essential for primitive streak formation?   Wnt antagonists expressed in the AVE include: mDkk1, Cer1, Sfrp1, and Sfrp5 (Kemp et al., 2005). Conversely, numerous Wnt pathway members are expressed in the posterior epiblast, the site of the future primitive streak including: Wnt2b, Wnt3, Wnt3a, and Fzd8 (review Pfister et al., 2007). In the chick, Wnt8C in conjunction with Vg1 is required to form the primitive streak (Skromne and Stern, 2002). By misexpressing Wnt8C in the mouse, another streak is created (Popperl et al., 1997). Wnt3a is expressed in the proximal epiblast in early pre-streak embryos before being localized to the posterior epiblast during gastrulation (Rivera-Perez and Magnuson, 2005). Along with Wnt2b, its expression overlaps with T marking the site of the future primitive streak (Kemp et al., 2005). Wnt3 and Eomesodermin are initially expressed in the proximal epiblast and later become confined to the posterior side (Liu et al., 1999; Russ et al., 2000). They are both essential for the formation of mesoderm as mutations in either fail to form a primitive streak and lack mesoderm and mesodermal markers such as Brachyury. Studies have also indicated that T expression is controlled by the Wnt pathway as Wnt response elements are present in the T promoter (Arnold et al., 2000; Yamaguchi et al., 1999). Not only do mice homozygous null for *Wnt3* lack a primitive streak but T expression is lost (Liu et al., 1999). Coincidently, the Wnt3 expression domain is adjacent to BMP4 expression in the ExE. Together with Nodal, these signals create a P-D gradient within the epiblast (Pfister et al., 2007). AVE signaling is therefore essential for the correct positioning of the primitive streak by restricting TGFβ/BMP and Wnt signals to the posterior but not for its formation (Liu et al., 1999; Robertson et al., 2003).

Gastrulation

Prior to the onset of gastrulation at E6.5, signals within the epiblast as well as from the extra-embryonic tissues determine the position of the primitive streak, the node, and the anterior primitive streak (APS). Next, cells in the epiblast begin to converge towards the posterior pole of the embryo. The epiblast then

thins and extends (*i.e.* epiboly) followed by the break-down of the basement membrane. Finally, cells undergo an epithelium-to-mesenchyme transition (EMT) as they migrate through the transient primitive streak leaving the epiblast (review Solnica-Krezel, 2005; Boyer and Thiery, 1993; Viebahn et al., 1995) (Figure 1-3, Figure 1-4).

In order for EMT to occur, it is necessary for the adherens junctions in these cells to loosen so that cells can delaminate and ingress through the streak (Lawson et al., 1999). The adherens junctions are controlled by interactions between E-Cadherin (*i.e.* E-Cad, uvomorulin, or Cdh1) and catenin. It has been shown that β-catenin links cadherins to the actin cytoskeleton of the adherens junctions (Nagafuchi et al., 2001). Down-regulating E-Cad allows the adherens junctions to loosen. During gastrulation, this is accomplished by Fgf8 activation of the repressor Snail1. Slug (*i.e.* Snail2), another Snail family member expressed in premigratory neural crest at E8.5, also has the ability to downregulate E-Cad but its own regulation relies on EGF and TCF/ β-catenin signaling (Batlle et al., 2000; Ciruna & Rossant, 2001; Cano et al., 2000; Conacci-Sorrell et al., 2003). The repression of cadherins by Slug/Snail or TCF/β-catenin complexes reduces cell adhesion but also permits nuclear accumulation of β-catenin and an activation of the Wnt pathway (Nelson et al., 2004). Eomes, induced by Nodal, is also able to inhibit E-Cad expression. Failure to downregulate E-Cad in *Eomes*$^{-/-}$ mice inhibits EMT and causes a bolus of cells to form in the primitive streak (Arnold et al., 2008).   Other molecules that play a role in these processes, such as Lulu (Epb4.1l5), helps to anchor the actin-myosin contractile machinery to the membrane and thereby allowing the rearrangements of epithelia that mediate embryonic morphogenesis, illustrating the vast number of players and interactions yet to be determined (Lee et al., 2007).

Components of the extracellular matrix (ECM) are equally important in gastrulation. As mesendodermal cells migrate from the streak, they must be able to migrate along the basal surface of the ectoderm without adhering to or being

incorporated into it. The ventral, lower basal surface of the ectoderm is covered by a basement membrane that is lost/breached in the primitive streak as gastrulation occurs. The molecules that regulate and assist in mesendoderm migration in the mouse have not been well characterized. Fibronectin, a component of the ECM, has been implicated; however, mesoderm cells migrate normally when it was inactivated in mouse embryos (Georges-Labouesse et al., 1996). Laminins, also part of the ECM, play a role in cell migration. Laminin 111 (*i.e.* Laminin $\alpha 1\beta 1\gamma 1$) and Laminin 511 (*i.e.* Laminin $\alpha 5\beta 1\gamma 1$) are both initially expressed at E3.5. When either the $\alpha 1$ of Laminin 111 (Yurchenco and Wadsworth, 2004; Eklbom et al., 2003) or the $\alpha 5$ of Laminin 511 (Miner et al., 1998; Champliaud et al., 2000) is mutated, embryos die at E5.5 or E16.5, respectively. This is due to the loss of architectural support for the basement membrane. Integrins are glycoproteins that mediate cell-to-cell and cell-to-ECM adhesion. To date, there are 17 α and 8 β subunits capable of forming 22 different heterodimers (Hynes et al., 1992; Darribere et al., 2000). In the mouse, $\alpha 5\beta 1$, $\alpha 6\beta 1$, and $\alpha v\beta 3$ are expressed continuously in pre- and peri-implantation embryos (Sutherland et al., 1993) and the integrin subunits $\beta 1$ and $\beta 3$ have been shown to mediate adhesion between mesoderm, fibronectin, and laminin in the primitive streak (Burdsal et al., 1993). *$\beta 1^{-/-}$* mice die at E3.5 due to inner cell mass degeneration (Fassler and Meyer, 1995) and failure of the primitive endoderm to migrate (Stephens et al., 1995).

Notochord/Neural Induction

Over the years, the mechanisms and factors that initiate neural induction have been studied widely. A simple mechanism has prevailed, in which inhibition of Bmp signaling is necessary for the formation of neural ectoderm; however, the molecules and signaling cascades involved are still unclear (Harland, 2000). It is thought that neural induction begins prior to gastrulation with the inhibition of Bmp transcription by Fgfs which then promote neural differentiation. In *Xenopus*, Wnts induce neural tissue in the posterior by blocking Bmp signaling (Baker et al., 1999). As gastrulation proceeds, factors from the node (*i.e.*

11

Noggin, Chordin, and Follistatin) then block BMP protein from binding to its receptor and assist in establishing the neural plate (Jessell and Sanes, 2000). Effector molecules, such as Geminin and Sox2 that are already expressed in the future neural plate may also play a role (Sasai et al., 1998). Although the node and its derivatives express other factors such as RA, Gsc, and Foxa2. Additional factors that may play pivotal roles during this process are continually identified (O'Shea et al., 2006; Emmett et al., 2009 in preparation; O'Shea lab data). Due to cross-talk between major signaling pathways, genetic redundancy, and the identification of new players in this process, much has yet to be determined about the regulation of neural induction.

The notochord forms as endodermal cells emerge from the node as a thin strip lying underneath the ventral midline of the neural ectoderm (Echelard et al., 1993). These cells are initially continuous with the endoderm in the dorsal wall of the foregut before segregating and folding off (Lewis et al., 2006). Several genes are expressed in the notochord including: Foxa2, Noggin, Chordin, and Follistatin, with Shh as the most prominent. Shh acts as a morphogen to induce distinct neural structures as well as to convey ventral identity along the neural tube and induce the floor plate (Jessell and Sanes, 2000). Mice null for *Shh* have many defects including a smaller diencephalon and midbrain, notochord degeneration, an absence of ventral structures along the neural tube, and holoprosencephaly (Ishibashi et al., 2002). Both Shh and Foxa2, expressed in the node and notochord, are not only induced by high levels of Nodal but that they are able to regulate the expression of each other during neural patterning of the spinal cord (Lupo et al., 2006) (Figure 1-5).

3. BMPs and their Inhibitors

The Bone Morphogenetic Proteins (BMPs) are a large subgroup of signaling molecules belonging to the Transforming growth factor beta (TGFβ) superfamily. Initially, they were discovered based on their ability to induce endochondral bone

formation (Urist et al., 1965) but have since then been implicated in numerous developmental processes including dorsoventral and anterior-posterior axis formation (Hogan et al., 1996; Mishina et al., 2003). In the Xenopus embryo, BMPs, in particular, BMP4, have the ability to directly induce epidermis and to ventralize mesoderm (Dale et al., 1992; Jones et al., 1992).

BMPs are secreted proteins that bind to heterodimeric receptors (type I and type II). Upon binding, the type II receptor phosphorylates the type I receptor leading to activated kinase activity and phosphorylation of downstream targets, the Smads (Wrana et al., 1994; Whitman et al., 1998; Heldin et al., 1997). Within the cell, Smads are phosphorylated, and partner with the common Smad, Smad4, translocate to the nucleus where they act as transcription factors and activate gene expression. To date, there are: nine ligands, seven type I and five type II receptors. In addition, there are three classes of Smads: receptor-regulated, mediator (co-Smads), and inhibitory. There is also receptor-mediated inhibition via BAMBIs (BMP and Activin membrane bound inhibitor) and ligand antagonists including Noggin, Chordin, Gremlin, Geminin, and Follistatin to name a few. This vast array of ligands, receptors, Smads, and inhibitory molecules expressed in various tissues and stages during development illustrate the complexity of the BMP signaling pathway and how developmental signals can be refined (Figure 1-6).

The expression of the type I and type II receptors varies temporally and spatially during development. To date, three type I and type II receptors are used in BMP signal transduction (Goumans et al., 2000). Bmpr-1a (ALK-3) is ubiquitously expressed in the embryo at the egg cylinder stage (de Wulf et al., 1995). Embryos with null mutations die between E7.5 and E9.5 and lack mesoderm (Mishina et al., 1995). Similarly, embryos lacking ActR-IA (ALK-2), which is expressed in the extra-embryonic endoderm during gastrulation, also die at E7.5 and fail to form mesoderm. However, they also show defects in primitive streak elongation and have abnormal visceral endoderm. Anterior-Posterior axis

formation is unaffected in these embryos (Gu et al., 1999); however, mice lacking *Bmpr-1b* (ALK-6) exhibit defects in cartilage formation partially due to the elevated Fgf signaling as BMPs are unable to attenuate the FGF/MAPK pathway (Yoon et al., 2006). Expression and null mutations in *Bmpr-2* closely resemble those of *Bmpr-1a* (Beppu et al., 2005). The ActR-IIA receptor is expressed in extra-embryonic and embryonic ectoderm as well as in the visceral endoderm, whereas the ActR-IIB receptor is expressed ubiquitously at E6.5 except in the VE (Mummery & Van Den Eijnden- Van Raaij, 1999). Single mutations in either lead to skeletal anomalies or L-R asymmetry and cardiac defects, respectively (Matzuk et al., 1995; Oh & Li, 1997), but loss of both results in embryonic death at E6.5 with a loss of mesoderm (Song et al., 1999). Interestingly, *ActR-IIA*^{-/-}; *ActR-IIB*^{+/-} mice have severe gastrulation defects and A-P mispatterning but *ActR-IIA*^{+/-}; *ActR-IIB*^{-/-} resemble *ActR-IA* single mutations (Song et al., 1999). To complicate matters, the Activin type IA, IIA, and IIB receptors are used in both Bmp and Activin signal transduction and there is significant cross-talk between additional signaling pathways including Wnt, FGF, Ca2+, Erk-MAPK, and JAK-STAT that rely on these receptors and Smads (von Bubnoff and Cho, 2001; Guo and Wang, 2009).   The vast redundancy makes it extremely difficult to tease out the individual roles for each receptor at various times and locations during development.

The mouse *Bmp4* gene is found on chromosome 14 and contains three exons encoding 408 amino acids. BMP4 is expressed at high levels in the extra-embryonic ectoderm and the primitive streak before and during gastrulation (Winnier et al., 1995; Lawson et al., 1999b). Embryos lacking BMP4 die between E6.5 and E9.5 (genetic background influences the time of death) and are characterized by abnormal mesoderm differentiation, developmental delay, and disorganized posterior structures (Winnier et al., 1995). Heterozygous (+/-) mice have kidney and urinary tract anomalies, fail to induce a lens, and lack primordial germ cells (Kulessa et al., 2002).   Tetraploid chimeras generated with Bmp4 null ES cells and wild-type tetraploid embryos have indicated that Bmp4 is essential

in allantois differentiation and the formation and survival of primordial germ cells in the epiblast (Fujiwara et al., 2001). Bmp4 coated beads placed in the neural tubes of chick embryos can lead to holoprosencephaly (Golden et al., 1999), inhibition of cell proliferation and increased cell death (Furuta et al., 1997), and a decrease in Shh expression in the CNS (Arkell et al., 1997). Bmp4 is also important in the formation of several organs and tissues including: kidney, lung (Bellusci et al., 1996), tooth (Vaahtokari et al., 1996), limb (Guha et al., 2002), hair (Kulessa et al., 2000), eye (Furuta et al., 1998), heart (Johansson et al., 1995), the developing telencephalon and its derivatives (Hebert et al., 2002), and otic vesicles (Kulessa et al., 2002).

Bmp2 and Bmp7 are expressed in the anterior mesoderm adjoining the prospective headfolds in the neural ectoderm. Bmp7 is also expressed during gastrulation in the node and axial mesoderm (Lyons et al., 1995; Arkell et al., 1997; Solloway et al., 1999). *Bmp2* null embryos gastrulate but the knock-out is lethal at E8.5 due to abnormal extra-embryonic development (Zhang et al., 1996), whereas *Bmp7* null embryos die shortly after birth due to kidney defects but also have eye abnormalities (Dudley et al., 1995; Luo et al., 1995). BMP-2 and -4 are involved in cardiac development including migration of neural crest cells into the outflow tract (Allen et al., 2001). While inhibition of BMP signaling is critical at neural induction to neuralize the ectoderm, additional factors which must be involved remain to be elucidated. BMPs are also regulated by the Wnt and FGF pathways (Harland, 2000), Erk-MAPK, JAK-STAT, Ca2+/Wnt, and TGFβ/Activin (von Bubnoff and Cho, 2001; Guo and Wang, 2009). Thus, other unknown BMP antagonists or additional mechanisms are likely involved in neural induction.

Bmp regulation is controlled intra- and extracellularly, producing a gradient which in turn generates various cell types and tissues. For example, high levels of Bmp in the dorsal neural tube promote differentiation of neural crest while low levels in the floor plate, where Shh expression is high, lead to motor neuron formation

15

(Jessell and Sanes, 2000). During neural induction, the ectoderm in the anterior region of the embryo begins to receive molecules secreted from the APS and its derivatives. These factors bind Bmps extracellularly preventing Bmp signaling and activation of downstream target genes that would convert the epiblast into epidermal ectoderm and its derivatives. Without this activation, neural ectoderm is established instead, the default pathway.

Noggin is one of a number of factors that is secreted from the node that plays a role in the induction and patterning of the neural ectoderm. The 26 kDa protein was first identified in *Xenopus* embryos when it rescued UV-light ventralized embryos and lead to excessive head development when expressed at high levels (Smith and Harland, 1992). Noggin was expressed at high levels in Spemann's organizer in gastrula stage embryos and later in the notochord and prechordal mesoderm of the neurula stage (Smith and Harland, 1992). Rather than inducing mesoderm, which generates neuralizing signals, Noggin has the ability to induce neural tissue directly (Lamb et al., 1993).

The single exon of the mouse *Noggin* gene is found on chromosome 11 and encodes a 232 residue, 25 kDa protein. During gastrulation in the mouse, Noggin is expressed in the node, notochord, and later in the dorsal neural tube and somites of the developing embryo (Valenzuela et al., 1995; McMahon et al., 1998). Homozygous null embryos exhibit neural tube closure defects, wide club-like limbs, shortened body axis, abnormal cartilage condensation, and die at birth (McMahon et al., 1998; Valenzuela et al., 1995). It is interesting to note that while Noggin is important for neural induction, it is not essential. However, it is required for the subsequent growth and patterning of the neural tube (McMahon et al., 1998) and cartilage morphogenesis (Brunet et al., 1998).

Noggin antagonizes signaling of key members of the TGFβ superfamily by binding to BMP 2, 4, and 7; thus, inhibiting their ability to bind with Type II receptors (Zimmerman et al., 1996). Noggin inhibition of Bmp signaling is

important in establishing the neural ectoderm versus the epidermal ectoderm (De Boer et al., 2005 in revision) as well as in later developing systems such as neural crest and somites (Sela-Donenfeld and Kalcheim, 1999), bone formation (Devlin et al., 2003), eye and retinal patterning (Sharov et al., 2003; Furtura et al., 1998), axon guidance (dorsal root ganglion, motor neurons, and cranial nerve VII) (Dionne et al., 2002), adult neurogenesis in the SVZ (Lim et al., 2000), and neuronal differentiation of ESCs (Gratsch and O'Shea, 2002).

Chordin is another potent antagonist of Bmp signaling. Located on chromosome 16, the gene contains 23 exons and encodes a 948 aa protein containing cysteine-rich binding domains (Piccolo et al., 1996). Single mutations in *Chordin* cause some embryos to die at E8.5 while others die later. Defects of the skull, vertebra, and cardiovascular system are produced. Mice also lack the thymus and parathyroid glands (Piccolo et al., 1996). Chordin is expressed in the APS and node, as well as in brain, lung, liver, and kidney suggesting multiple functions during organogenesis. When mutant embryos null for both *Chordin* and *Noggin* were examined, they displayed defects in the posterior neuropore and severe anterior defects which included the loss of the forebrain and optic placodes. Embryos also lacked dorsal mesendodermal tissues including the loss of the notochord. Left-right patterning was also abnormal. These data indicated that BMP antagonism from the node and its derivatives is required for anterior and posterior neuroectoderm differentiation (Bachiller et al., 2000; Anderson et al., 2002).

Follistatin, found on chromosome 13 and encoding 344 residues, was isolated based on its ability to suppress follicle-stimulating hormone (FSH) from the pituitary. It is expressed in the node, primitive streak, caudal ectoderm and mesoderm as well as in the adult brain, ovary, testis, bone marrow, and pituitary (review Patel et al., 1998; Albano et al., 1994). It has a particular affinity to Bmp7 (Matzuk et al., 1995). Null mutations are not as severe as single *Noggin* or *Chordin* mutations likely due to their overlapping functions, but embryos are

17

growth retarded and generally die postnatally due to respiratory failure. Abnormal skin and palate formation is often observed in these mice as well (Matzuk et al., 1995; Wu et al., 2003). Follistatin also antagonizes growth and differentiation factor 11 (GDF11) in olfactory epithelium and promotes neurogenesis (Wu et al., 2003).

Cerberus-like 1(Cer1 aka Cerberus related gene/Cerr1 and Cerberus homolog 1/Cer1), the mouse ortholog of *Xenopus* Cerberus and chick Caronte, is secreted from the AVE and is induced by Nodal/Smad2 activation of cells in the distal tip of the visceral endoderm prior to gastrulation (Shawlot et al., 2000; Belo et al., 1997). Located on chromosome 4, *Cer1* contains 2 exons. Its main function is to establish the A-P gradient in the embryo by inhibiting Bmps as well as nodal from the anterior region of the epiblast. When homozygous mice are generated, embryos are generally normal (Belo et al., 2000). This is not surprising considering the numerous factors secreted from the AVE that have overlapping function with Cer1.

Other extracellular BMP antagonists exist in the developing embryo but have not been well characterized. For example, in zebrafish, there are three *Noggin* genes, whereas there is only one in the mouse (Bauer et al., 1998) and human (Valenzuela et al., 1995). Several proteins with a strong homology to Chordin including splice variants have been identified in the mouse and human. These include Chordin-like (Neuralin-1), Chordin-like 1, Chordin-like 2, and Crim1. The function of Chordin-like is to inhibit BMPs in the neural plate and induce neural crest formation (Coffinier et al., 2001). Chordin-like 2 binds BMP4 during chondrocyte development (Nakayama et al., 2004). Finally, Crim1 is expressed in the floor plate of the neural tube at E9.0 and has a binding motif similar to Chordin (Kolle et al., 2000). Genes similar to *Follistatin* have also been linked to BMP inhibition (Follistatin-like 1 through 5) but their function to date has not been well characterized. *Gremlin* and *DAN* are two *Cerberus* related genes. Gremlin is yet another BMP antagonist whose role is in promoting osteoblast formation

(Gazzerro et al., 2005). It is also expressed in the apical ectodermal ridge (AER) along with Fgf4 and Shh and is able to regulate Shh/Fgf4 by antagonizing BMP repression of Fgf activity (Zuniga et al., 1999). DAN has been shown to bind to BMP2 but its role in mouse development has not been determined (Hsu et al., 1998; Dionne et al., 2001).

The search continues for genes that regulate the position of neural/epidermal boundary as well as those that maintain the expression of pan-neural genes in the neural plate prior to the onset of neuronal differentiation. One candidate, the 33 kDa protein Geminin was discovered in a *Xenopus* screen based on its ability to increase the size of the neural plate when overexpressed, with reductions in both neural crest and epidermal ectoderm (Kroll et al., 1998). Misexpression in the ectoderm suppressed BMP4 and converted future epidermis to neural tissue and induced early expression of neurogenin-related 1, an early proneural gene. The dominant-negative geminin prevented neural differentiation even within the neural plate. (Rogers et al., 2009; Kroll et al., 1998) Similar neural inducing activity has also been shown in chick (Linker et al., 2009; Papanayoutou et al., 2008) and Drosophila (Quinn et al., 2001).

Geminin is located on mouse chromosome 13 and includes seven exons encoding a 206 residue (33 kDa) protein. The Geminin protein includes an N-terminal domain which includes a destruction box and bi-partite nuclear localization signals (NLS) (Boos et al., 2006). The neck and C-terminal region contain the coiled-coil domain, glutamate and hydrophobic residues. The neuralizing domain of Geminin lies in the N-terminus while the cell-cycle control as well as *Hox* and Polycomb complex binding areas is found in the C-terminus (McGarry & Kirschner, 1998; Benjamin et al., 2004) (Figure 1-7).

Compelling evidence has implicated Geminin as a molecular switch between the cell-cycle and patterning during embryogenesis. Geminin has been shown to act as a transcriptional repressor by binding to Hox proteins directly or indirectly via

Polycomb complex members antagonizing their function (Luo et al., 2004; Luo & Kessel, 2004; Del Bene et al., 2004). In the chick, axial patterning was shifted anteriorly when Geminin was ectopically expressed (Luo et al., 2004). During Medaka eye development, Geminin binds directly to Six3 expressed in the proliferating marginal cells of the retina. Loss of *Geminin* increased cell proliferation and expanded optic vesicles, while overexpression of Geminin leads to smaller eyes and a small to non-existent forebrain. (Del Bene et al., 2004). As the binding region for the Hox/Polycomb proteins is in the same region as the binding of Cdt1, a licensing factor, there is competition between the two. When geminin is bound to Cdt1 during the S phase of the cell cycle, it prevents Cdt1 from forming a complex with the origin recognition complex (ORC), Cdc6, and minichromosomal maintenance complex (MCM).   As DNA replication has already begun, geminin prevents cells from re-replication. During the M phase, geminin is ubiquitinated and targeted for destruction (Luo and Kessel, 2004). Geminin was also found to prevent DNA re-replication after S phase (McGarry & Kirschner, 1998; Wohlschlegel et al., 2002).

The evidence to date strongly supports the assertion that expression of Geminin cause cells to switch from proliferation to differentiation. In the context of cancer, if Geminin is expressed in proliferating cells, using it as a tumor suppressor is very intriguing. Geminin is expressed in many solid tumors including lymphomas, renal cell carcinomas, breast cancers, and colon and rectal tumors (Wohlschlegel et al., 2002; Montanari et al., 2005; Obermann et al., 2005; Gonzalez et al., 2004; Dudderidge et al., 2005). However, when Geminin was overexpressed in U2OS cells (an osteosarcoma cell line) it was unable to block cell cycle progression (Wohlschlegel et al., 2002). These observations indicate that Geminin is unable to function as a tumor suppressor. Instead, we propose that Geminin may control the progression of epithelial cells to malignancy by regulating EMT. Loss of *Geminin* in embryos inhibits cell migration away from the primitive streak during gastrulation and overexpression in embryoid bodies

(EBs) causes widespread migration and loss of cellular adhesions (Emmett and O'Shea, 2009a in preparation/ Chapter Four; Slawny et al in preparation).

The role of Geminin in murine development has not been examined. When *Geminin* was deleted, embryos die at E3.5 (Blastocyst stage) due to failure of the inner cell mass to form correctly due to the excess amount of DNA present within the cells (endo-replication) (Hara et al., 2006; Gonzalez et al., 2006). Geminin is expressed as early as E1.5 but as maternal Geminin protein lingers until the four- to eight-cell stage; embryos do not begin to exhibit an abnormal morphology until this time. Geminin has been reported to be expressed in the developing nervous system at E12.5 (Kroll et al., 2007) and E15.5 (Spella et al., 2007), but detailed studies have not yet been reported.

Geminin has also been linked to several signaling pathways including Wnt and BMP. The *geminin* promoter contains binding motifs for Cdt1 (Luo and Kessel, 2004; Luo et al., 2004), Hox and Polycomb complexes (Del Bene et al., 2004), SWI/SNF members (Seo et al., 2005a; Seo et al., 2005b), and an AP4 (Kim et al., 2006). When the 5' sequence domains were analyzed, they revealed three Tcf and two Vent binding sites. In the Wnt pathway, activated β-catenin binds to Tcfs sites allowing transcription and promoting Geminin expression whereas Bmp signaling induces Vent1 and Vent2 which inhibit Geminin expression (Taylor et al., 2005). Overexpression of Geminin in the Wnt reporter mouse line (Mohamed et al., 2004) leads to an increase in Wnt signaling in the neural tube, neural crest, and somites (Emmett and O'Shea, 2009b in preparation) whereas shRNA targeting Geminin has stage specific effects on Wnt signaling: increasing signaling during gastrulation and decreasing signaling in regions of EMT and neural crest cell migration in E9 embryos (Emmett and O'Shea, 2009a/b in preparation). Geminin also inhibits Bmp expression from the neural plate in chick and *Xenopus* as overexpression or ectopically injected Geminin protein resulted in an expansion of the neural plate and markers such as Sox2 at the expense of the epidermal ectoderm (Papanayoutou et al., 2008; Kroll et al., 1998). In

addition, shRNA targeted to Geminin increases the Bmp4 expression domain at the edge of the neural plate and decreases the size of the neural crest population (Emmett and O'Shea, 2009a in preparation). In a differential-display analysis of control mESCs compared to those transfected with a Noggin expression construct, Geminin is upregulated by Noggin (O'Shea et al., 2006; O'Shea lab data). These data further support Geminin's role in inhibiting differentiation, as well as suggest a role in the regulation of Wnt and BMP signaling during development (Figure 1-8).

4. FGFs and WNTs

The Fibroblast growth factor (Fgf) family of secreted signaling molecules have extensive and diverse activities during development. Many of these genes are crucial for early embryo patterning, differentiation, cell proliferation, and cell migration, and are expressed in early signaling centers (review Itoh et al., 2007). However, even though many *Fgf* knockout mice die at embryonic or postnatal stages, many others have subtle phenotypes. This implies that either a particular Fgf is unimportant for that process/tissue or that other Fgfs or other factors compensate for their loss, such as Wnt and TGFβ family members. Currently, 22 Fgfs and 24 Fgf receptors (Fgfr) have been identified in the mouse. Signaling is activated by binding of the Fgf to its receptor, followed by phosphorylation of the receptor, thereby triggering several downstream pathways.

The most important Fgf in the early embryo is Fgf8. Although Fgf4 is expressed in the primitive streak, *Fgf4*^{-/-} embryos die shortly after implantation; thus, a role in gastrulation has been difficult to determine (Niswander and Martin, 1992). Fgf8 is expressed in the posterior region of the epiblast at the base of the allantois in pre-streak embryos and extends distally to the node at E7.5 (Crossley and Martin, 1995). As cells ingress through the primitive streak, Fgf8 is downregulated but induces expression of Snail1 which inhibits E-Cadherin

expression allowing EMT to occur (Ciruna and Rossant, 2001). At E8.5, Fgf8 is expressed at the midbrain/hindbrain boundary of the open neural tube as well as in the prechordal plate, the foregut endoderm, surface ectoderm, and lateral plate mesoderm. At E9.0, it marks the rostral limit of the neural plate, the commissural plate/anterior neural keel, the isthmus, the surface ectoderm covering the mandibular and maxillary prominences of branchial arch 1, and the developing limb bud (Sun et al., 1999). Mice homozygous null for *Fgf8* are embryonic lethal at E8 due to gastrulation defects as cells fail to migrate and accumulate at the streak (Sun et al., 1999). *Fgfr1*$^{-/-}$ mice also have gastrulation defects; however, the cells that fail to undergo EMT and accumulate, form ectopic neural tubes (Ciruna et al., 1997).

Fgfs also interact extensively with other signaling molecules during development. Fgfs downregulate Bmp expression in the neural domain of zebrafish allowing neural differentiation to occur (Wilson et al., 2000; Furthauer et al., 2004). They can also promote neural fate via a Bmp-independent pathway (Delaune et al., 2005; Linker et al., 2004), or mediate Bmp signaling during neural crest formation (LaBonne and Bronner-Fraser, 1998). They also indirectly regulate Wnt signaling in the primitive streak (Ciruna and Rossan,t 2001) and at the isthmus (Canning et al., 2007). Finally, they can influence left-right asymmetry as ectopic Fgf8 is able to induce expression of Nodal and Pitx2, an inhibitor of Lefty1, required for specification of right-side gene expression (Fischer et al., 2002). These data not only illustrate Fgfs complexity but that they have has context specific roles during development.

The Wnt pathway, consisting of over 100 genes is perhaps the most important system used to control progenitor cell expansion and lineage decisions (Cadigan and Nusse, 1997). One of the most essential is β -catenin. This gene has dual functions as it can form a stable complex with members of the cadherin family and participate in the formation of adherens junctions (Nelson et al., 2004), as well as activate downstream target genes of the Wnt pathway (Kemler et al.,

1993; review Grigoryan et al., 2008). Loss of *β-catenin* results in embryos that die prior to gastrulation due to a failure to form an A-P axis, mesoderm, and failure of head development (Haegel et al., 1995; Huelsken et al., 2000) indicating Wnt/ β -catenin signaling is necessary for early embryo patterning.

A number of Wnts also play a role in gastrulation. Wnt3a, expressed in the proximal epiblast in the early embryo before becoming sequestered to the posterior region by antagonists (*i.e.* mDkk1, Cer1) from the AVE, is one such molecule. Mice that are homozygous null for *Wnt3a* form ectopic neural tubes and have increased neural tissue at the expense of endoderm and mesoderm (Yoshikawa et al., 1997).

During neural patterning, Wnts are needed early for neural induction and patterning but must be inhibited later by BMPs for induction to occur. This has been illustrated by mutation of the Wnt co-receptors, Lrp5 and Lrp6, resulting in expansion of the anterior neuroectoderm (Kelly et al., 2004). mDkk1, a Wnt inhibitor expressed in the AVE, sensitizes the overlying ectoderm to neuralizing signals. Loss of mDkk1 prevents forebrain development (Mukhopadhyay et al., 2001). Wnt1 is expressed in the caudal midbrain adjacent to Fgf8 expression in the isthmus and is essential to maintain its identity (Canning et al., 2007). Loss of *Wnt1* yields embryos lacking a midbrain and anterior hindbrains by E9.5 (McMahon et al., 1992).

At gastrulation, cell proliferation, fate specification, and subsequent cell movements act in synergy to pattern and sculpt the developing embryo. The FGF, BMP, and Wnt pathways coordinate the signals required for cell movements (Solnica-Krezel, 2005). The most integral pathways for convergence and extension is the Wnt/PCP (planar cell polarity) which is essential for directly controlling cell movements in the embryo and regulating cell polarity within an epithelium (Myers et al., 2002). While convergent and extension is not considered to play a role in gastrulation movements in the mouse embryo, Wnt 1

and Wnt 11 signaling controls G proteins such as RhoA and Rac which control actin filaments (Habas et al., 2003) and Van Gogh-like 2 (Vangl2 aka Loop-tail 1/Lpp1) (Ciruna et al., 2006; Kibar et al., 2001; Keller et al., 2002; Wallingford et al., 2002). Vangl2 affects cell movements during neurulation. First, it prompts neural progenitors in the neural tube to converge at the midline. Second, as cells undergo mitosis, they lose their polarity. Vangl2 expression in the daughter cells allows them to re-polarizing and intercalate into the neuroepithelium. Loss of *Vangl2* disrupts the integration of these cells into the neuroepithelium illustrated by ectopic accumulations in the ventral neural tube and anterior neural keel leading to neural tube defects (Ciruna et al., 2006).

5. Hypothesis and Goals

During the development of the mammalian embryo, the genes that control the boundary between the neural and epidermal ectoderm and later convey neural identity are largely unknown. To test the hypothesis that BMP4 signaling sets the boundary between neural ectoderm and epidermal ectoderm as well as to identify novel BMP antagonists required in this process, a series of independent experiments have been completed. Two approaches test whether neural ectoderm can be expanded into the epidermal ectoderm domain: transgenic misexpression of noggin in the epidermal ectoderm (Chapter Two) and knock-down of BMP4 expression in the embryo via short hairpin RNAs (Chapter Three). Because the bi-functional protein Geminin was suggested to affect the amphibian neural plate via BMP signaling, the role of Geminin in post-implantation embryos was examined. Knock-down of Geminin alters neural ectoderm differentiation and lineage allocation at gastrulation (Chapter Four). This work has also identified a novel role for geminin in EMT and neural crest specification (Chapter Five). Unique genes involved in this process were identified using differential-display of RNAs from noggin overexpressing ESCs (Appendix One) and laser capture microdissection of signaling centers and their responding tissues followed by microarray analysis (Appendix Two).

In aggregate, these experiments demonstrate that, as in other species, Noggin-BMP4 signaling plays a critical role in setting the border of the neural/epidermal ectoderm. This work also elucidates the role of the Geminin gene/protein in this process and identifies novel genes involved in neural fate specification in the mouse embryo.   My research has contributed to the elucidation of the role these genes play in development, and also reveal novel approaches in understanding the genesis of birth defects of the nervous system.

Figure 1-1. Model illustrating how temporally and spatially distinct Nodal activities pattern the anterior-posterior axis.

E5.0. Nodal is expressed in a proximal ring of epiblast in response to signals from the   ExE (such as Bmp4).

E5.5. Nodal signaling maintains expression of ExE markers and amplifies its own expression throughout the epiblast and into the overlying VE. Nodal in the epiblast activates the Smad2 pathway in the VE, leading to the formation of the AVE and the expression of target genes such as Cer1 and Lefty1.

E6.0. Cer1 and Lefty1 from the AVE then feed back to downregulate Nodal expression in first the distal and then in the anterior epiblast after anterior displacement of the VE (gray arrows). As a consequence, Nodal expression becomes spatially restricted, resulting in primitive streak formation at the posterior end of the embryo.

E6.5. Anterior proximal epiblast cells migrate posteriorly (pink arrows) towards the primitive streak where they downregulate E-Cadherin, egress through the streak, giving rise to mesoderm and definitive endoderm (collectively referred to as the mesendoderm).

E7.0. Cer1 and Lefty1 from the precursors of the anterior primitive streak (APS) pattern the anterior-posterior axis of the streak, which will give rise to corresponding medial-lateral mesoderm populations. The AVE is displaced by mesendodermal cells migrating from the streak. The node forms from the APS and begins secreting the Bmp antagonists Noggin, Chordin, and Follistatin. (Modified from: Perea-Gomez et al., 2002; Brennan et al., 2001; Marikawa et al., 2006).

Post-implantation

E5.0 E5.5 E6.0 E6.5 E7.0

Extra-embryonic Ectoderm (ExE)

Epiblast (Embryonic Ectoderm)

Extra-embryonic Visceral Endoderm (ExEn)

Visceral Endoderm (VE)

ExE

Anterior Visceral Endoderm (AVE)

Proximal Epiblast

AVE

ExE

ExEn

AVE

Primitive Streak

ExEn

ExE

AVE

Allantois (Extra-embryonic Mesoderm)

Embryonic Mesoderm

VE

Node

Anterior Neural Ectoderm

Anterior Mesendoderm (AME)

Proximal

Anterior

Posterior

Distal

Legend:

Nodal

Bmps

Cer1, Lefty1

Path of AVE migration

Migration of cells during gastrulation

Path of Mesendoderm migration

28
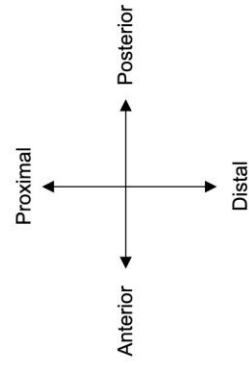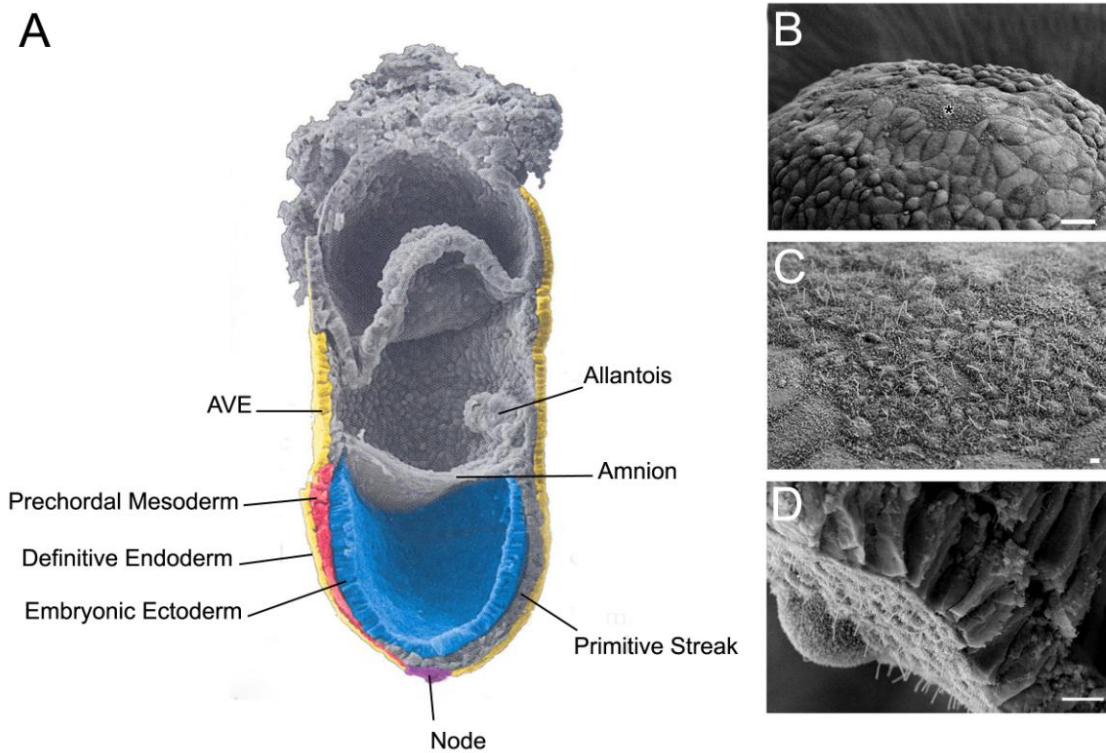
Figure 1-2. The Node.

A. Scanning electron microscropy image of the node. Germ layers are colored to represent: ectoderm = blue; mesoderm = red; endoderm = yellow; node = purple. Anterior is to the left.

B. SEM image of the node (*). The ventral view of the distal tip of the embryo. Anterior to the left. Scale = 20 μm.

C. Higher magnification of B. Note the ciliated cells. Scale = 2 μm.

D. A Higher magnificiation of the node in A. Ciliated, apically consticted ventral node cells lie beneath the columnar epithelium of the dorsal node. Scale = 5 μm. (Modified from: Sulik et al., 1994; Lee and Anderson, 2008)
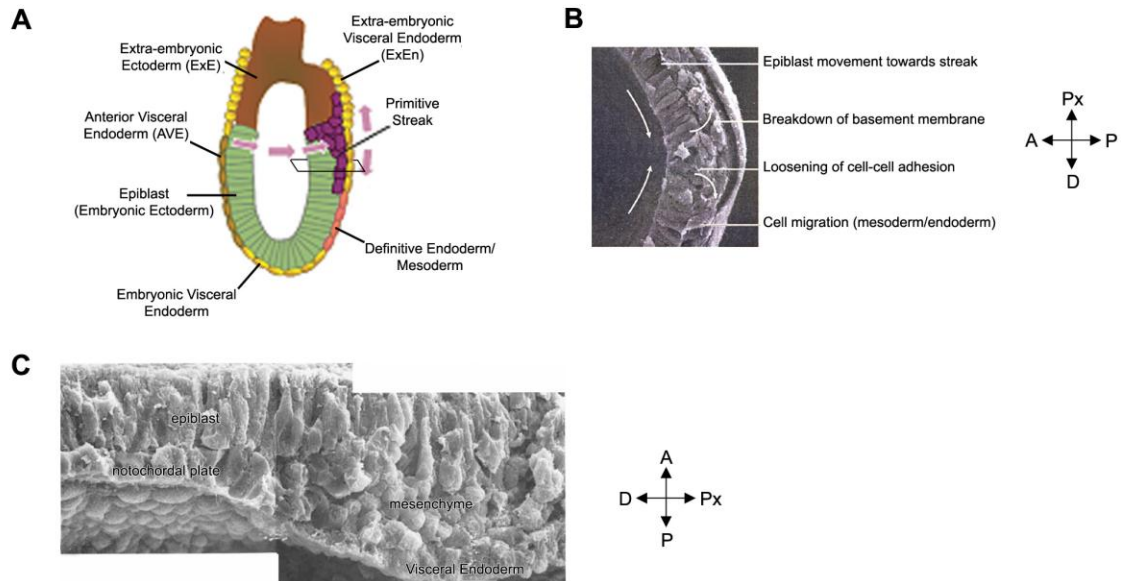
Figure 1-3. The primitive streak during gastrulation.

A. Schematic of an E6.5 embryo. Arrows indicate the movement of the epiblast cells to the primitive streak.

B. SEM view of the box in A. Epithelial cells in the epiblast converge towards the primitive streak where increasing levels of Nodal, Wnt3, and FGF8 influence cell behavior. The cells detach from the primitive streak, lose apical-basal cell polarity, and undergo rapid cytoskeletal rearragements that allow them to delaminate and migrate between the epiblast and overlying visceral endoderm. Arrows indicate cell movements.

C. Sagittal SEM view of the node at E7.5. Mesenchymal cells lie between the columnar cells of the epiblast and the visercal endoderm. The ciliated cells of the notochordal plate lie rostral to the primitive streak. Scale = 10 μm.
(Modified from: Sulik et al., 1994; Arnold and Robertson, 2009)
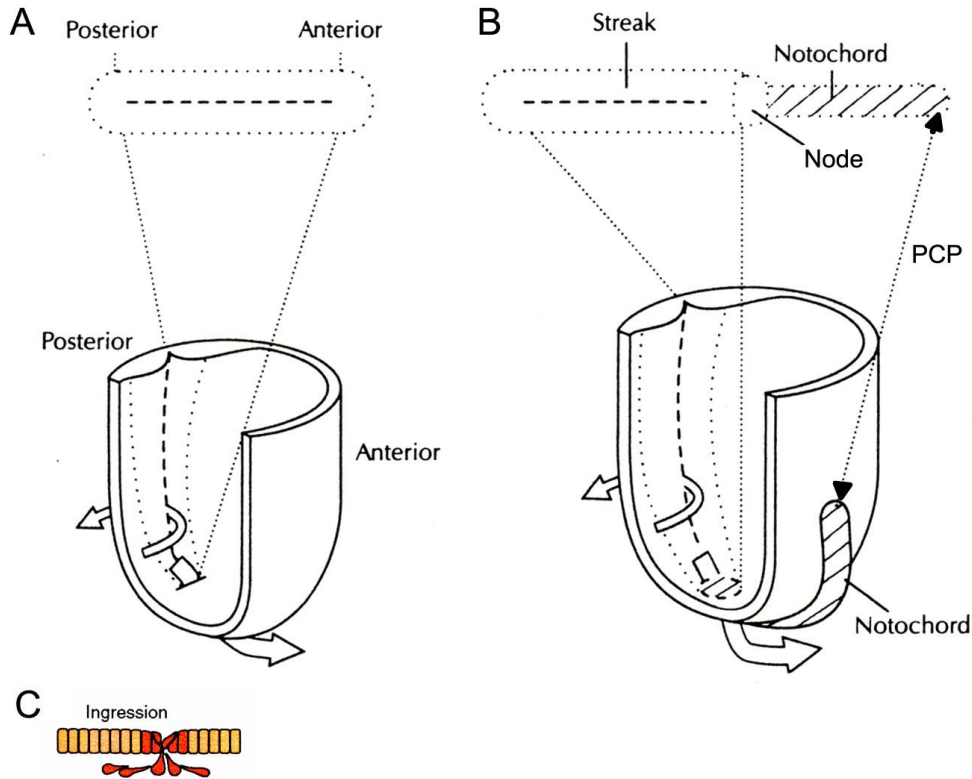
Figure 1-4. Schematic of gastrulation.

A. At E6.5, cells from the epiblast migrate posteriorly and ingress through the primitive streak. Newly formed mesoderm and endoderm displaces cells in an anterior direction.

B. E7.5, the node is well established and expresses signaling molecules such as Noggin, Chordin, Goosecoid, and Foxa2. The notochord with the prechordal plate at its rostral extreme lie underneath the neural plate and secrete Shh.

C. Schematic of cell ingression at the primitive streak.
(Modified from Solnica-Krezel, 2005)

Figure 1-5. The Notochord.

A. E7.5 embryo illustrating the prechordal plate, notochord, and node (arrow). The embryo is oriented with the ventral surface of the distal tip up. Anterior is towards the top. Arrow = node; p = prechordal plate. Scale = 50 μm.

B. Higher magnification of the boxed area in A. Small, ciliated cells comprising the prechordal plate and notochordal plate (node and notochord) migrate anteriorly underneath the epiblast (the neural plate and future neural tube). They are surrounded by visceral endoderm cells (en). Boxed area are cells in the notochord. Scale = 10 μm.

C. Schematic of the node and notochord at E7.0 and E7.5. Cells from the primitive streak migrate anteriorly giving rise to mesoderm and definitive endoderm.

D. A transverse section through an E8.5 embryo. Cells that will give rise to the notochord are initially continuous with endodermal cells forming the gut (arrow) and lie underneath the neural tube.   Dorsal is up; m= mesoderm; n = neural ectoderm; arrow = notochord. Scale = 50 μm.

E. As the neural tube closes, the mature notochord is formed as cells fold off in a dorsal direction from the wall of the gut and begin to secrete Shh (arrowhead). Along with Bmp4 expressed in the dorsal neural tube, Shh acts as a morphogen to pattern dorsal-ventral cell fate. Dorsal is up: m = mesoderm; n = neural tube; arrow = notochord. Scale = 50 μm. (Modified from Sulik et al., 1994; Yamanaka et al., 2007)

C

Ventral/posterior view

anterior ← right ↕ left → posterior

E7.0   E7.5

Lateral plate mesoderm
Paraxial mesoderm/Somite
Primitive streak
Prechordal plate/notochord
Node
area of node cells facing outside surface

D   dorsal ← right ↕ left → ventral

E
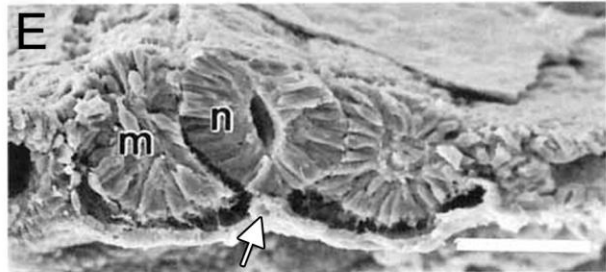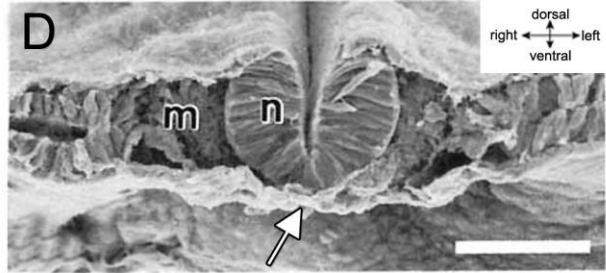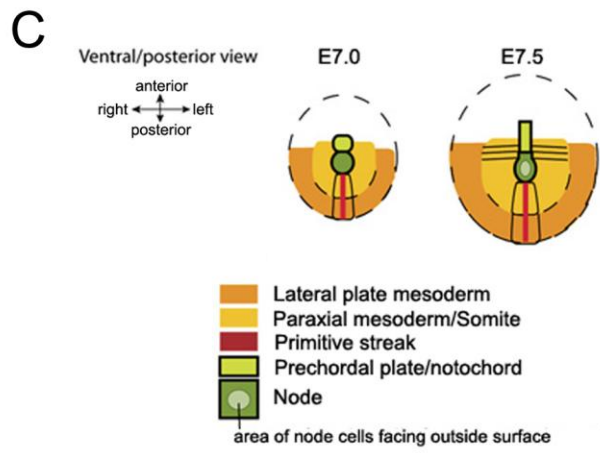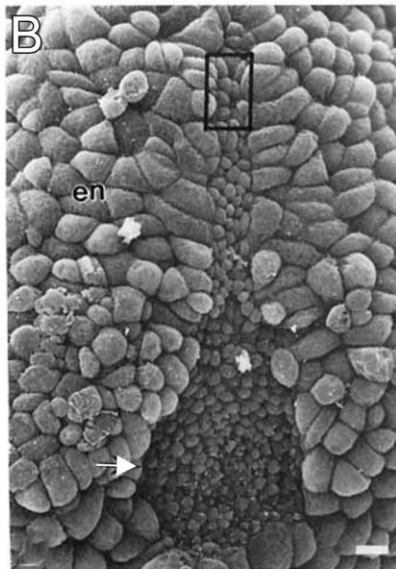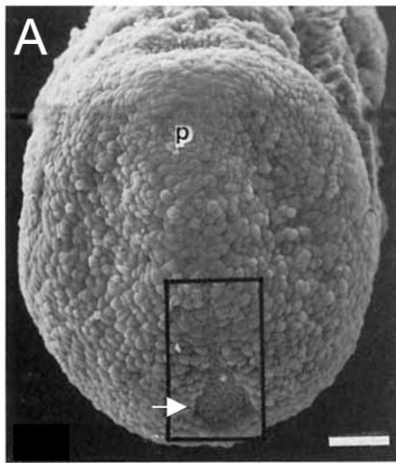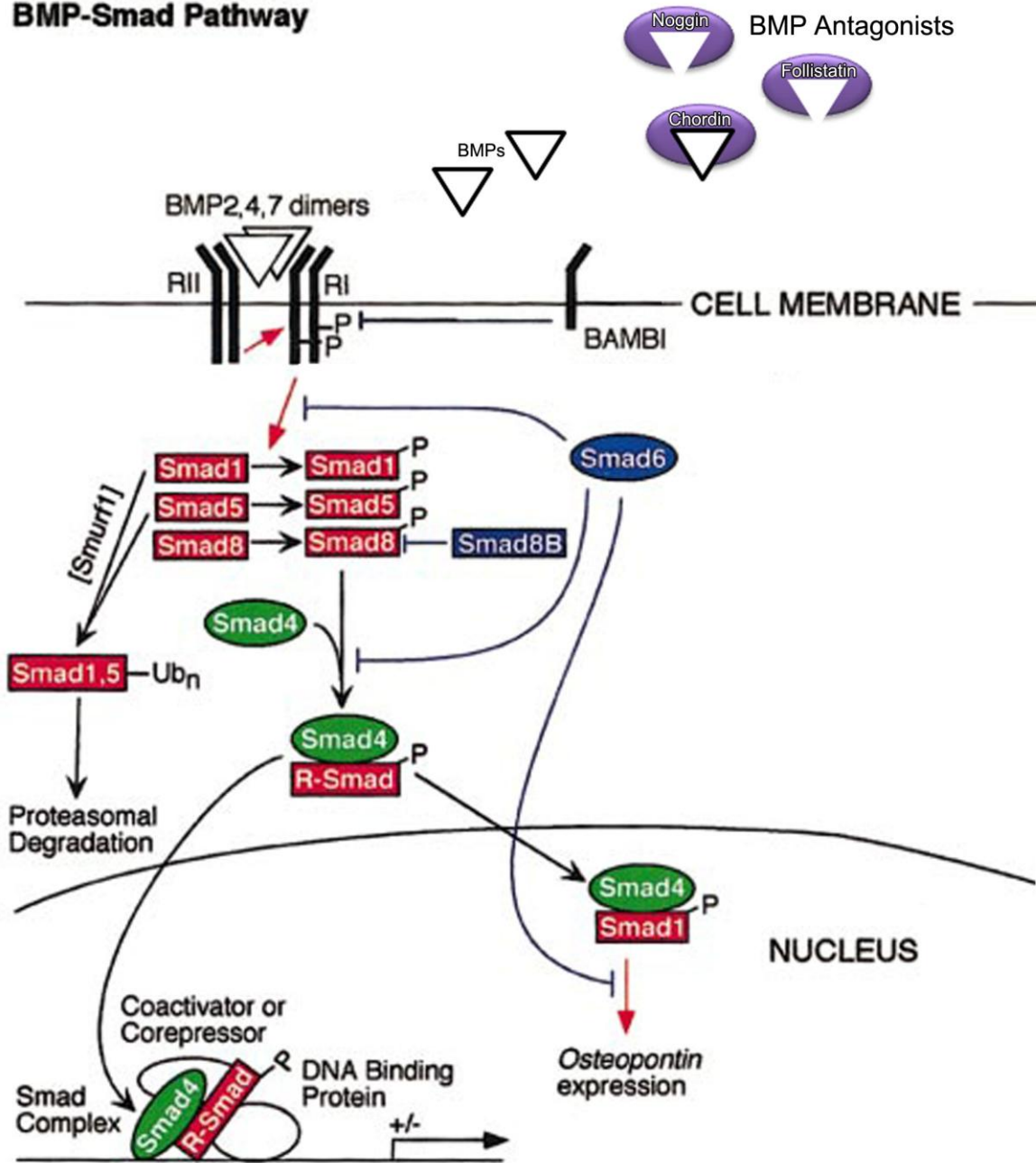
Figure 1-6. The BMP-Smad pathway.

Regulation of BMP signaling is modulated at three levels. Extracellular antagonists such as Noggin, Chordin, and Follistatin bind BMP ligands and prevent their subsequent association with type I and type II receptors. The pseudoreceptor BAMBI modulates BMP signaling at the cell membrane by binding to the type II receptor. Finally, inhibitor-Smads (Smad 6, 7, and 8) and Smurfs regulate intracellular signaling by preventing further Smad signaling and subsequent gene transcription of target genes. (Modified from: von Bubnoff and Cho, 2001; Balesman and Van Hul, 2002).
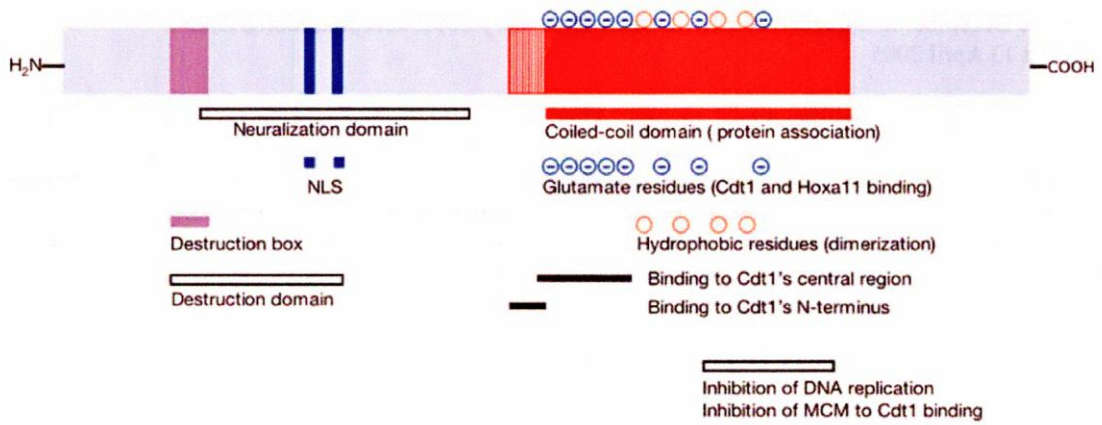
Figure 1-7. The structural and functional domains of Geminin.
(From Pitulescu et al., 2005)
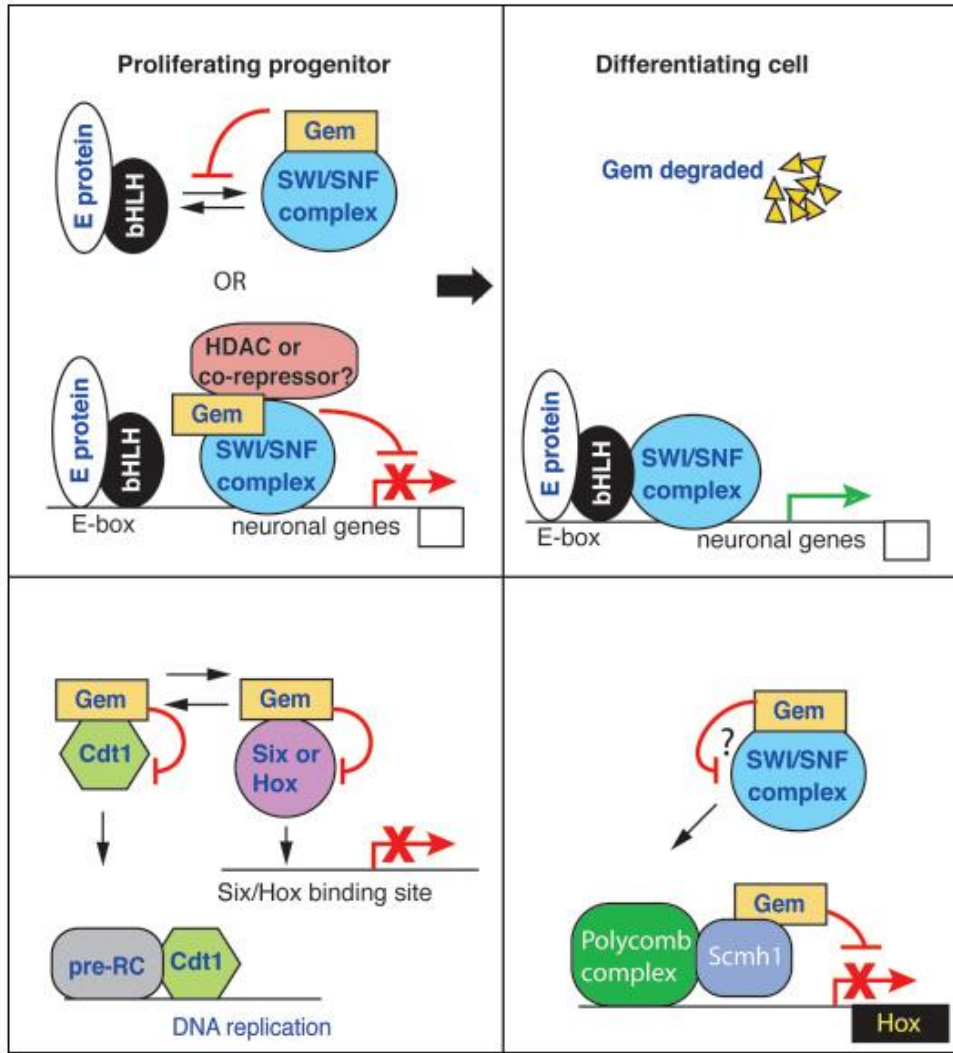
Figure 1-8. Geminin's roles during development.

A. Geminin expression found in proliferating neural progenitor cells can block coordinated activities of neural bHLH proteins and SWI/SNF.

B. Downregulation of Geminin levels occurs around the time of cell cycle exit, enabling bHLH/SWI/SNF complexes to activate target gene transcription.

C. Geminin can bind to Cdt1, Six3, or Hox transcription factors in a competetive manner by either antagonizing Hox/Six3-dependent transcription or Cdt1 assosication with pre-replication complexes.

D. Geminin can also negatively regulate *Hox* gene transcription by interacting with Polycomb proteins at Hox enhancers.
(From Seo and Kroll, 2006).

REFERENCES

Albano RM, Arkell R, Beddington RS, and Smith JC. 1994. Expression of inhibin subunits and follistatin during postimplantation mouse development: decidual expression of activin and expression of follistatin in primitive streak, somites and hindbrain. Development 120: 803-813.

Allen SP, Bogardi JP, Barlow AJ, Mir SA, Qayyum SR, Verbeek FJ, Anderson RH, Francis-West PH, Brown NA, and Richardson MK. 2001. Misexpression of noggin leads to septal defects in the outflow tract of the chick heart. Developmental Biology 235: 98-109.

Anderson RM, Lawrence AR, Stottmann RW, Bachiller D, and Klingensmith J. 2002. Chordin and noggin promote organizing centers of forebrain development in the mouse. Development 129: 4975-4987.

Ang and Rossant 1994. HNF-3 beta is essential for node and notochord formation in mouse development. Cell 78: 561-574.

Ang SL, Jin O, Rhinn M, Daigle N, Stevenson L, and Rossant J. 1996. A targeted mouse Otx2 mutation leads to severe defects in gastrulation and formation of axial mesoderm and to deletion of rostral brain. Development 122: 243:252.

Arkell R and Beddington RSP. 1997. BMP-7 influences pattern and growth of the developing hindbrain of mouse embryos. Development 124: 1-12.

Arnold SJ, Stappert J, Bauer A, Kispert A, Herrmann BG, and Kemler R. 2000. Brachyury is a target gene of the Wnt/ β -catenin signaling pathway. Mech Dev 91: 249-258.

Arnold SJ, Hofmann UK, Bikoff EK, and Robertson EJ. 2008. Pivotal roles for eomesodermin during axis formation, epithelium-to-mesenchyme transition and endoderm specification in the mouse. Development 135: 501-511.

Arnold SJ and Robertson EJ. 2009. Making a commitment: cell lineage allocation and axis patterning in the early mouse embryo. Nature Rev Mol Cell Biol 10: 91-103.

Bachiller D, Klingensmith J, Kemp C, Belo JA, Anderson RM, May SR, McMahon JA, McMahon AP, Harland RM, Rossant J, and De Robertis EM. 2000. The organizer factors Chordin and Noggin are required for mouse forebrain development. Nature 403: 658-661.

Baker JC, Beddington RS, and Harland RM. 1999. Wnt signaling in Xenopus embryos inhibits bmp4 expression and activates neural development. Genes Dev 13: 3149-3159.

Balemans W and Van Hul W. 2002. Extracellular regulation of BMP signaling in vertebrates: a cocktail of modulators. Dev Biol 250: 231-250.

Batlle E, Sancho E, Franci C, Dominguez D, Monfar M, Baulida J, and Garcia De Herreros A. 2000. The transcription factor snail is a repressor of E-cadherin gene expression in epithelial tumour cells. Nat Cell Biol 2: 84-89.

Bauer H, Meier A, Hild M, Stachel S, Economides A, Hazelett D, Harland RM, and Hammerschmidt M. 1998. Follistatin and noggin are excluded from the zebrafish organizer. Dev Biol 204: 488-507.

Beck SV, Le Good A, Guzman M, Ben Haim N, Roy K, Beermann F, and Constam DB. 2002. Extraembryonic proteases regulate Nodal signaling during gastrulation. Nature Cell Biol 4: 981-985.

Beddington RS and Robertson EJ. 1999. Axis development and early asymmetry in mammals. Cell 96: 195-209.

Bellusci S, Henderson R, Winnier G, Oikawa T, and Hogan BLM. 1996. Evidence from normal expression and targeted misexpression that bone morphogenetic protein-4 (Bmp-4) plays a role in mouse embryonic lung morphogenesis. Development 122: 1693-1702.

Belo JA, Bouwmeester T, Leyns L, Kertesz N, Gallo M, Follettie M, and De Robertis EM. 1997. Cerberus-like is a secreted factor with neutralizing activity expressed in the anterior primitive endoderm of the mouse gastrula. Mech Dev 68: 45-57.

Belo JA, Bachiller D, Agius E, Kemp C, Borges AC, Marques S, Piccolo S, and De Robertis EM. 2000. Cerberus-like is a secreted BMP and nodal antagonist not essential for mouse development. Genesis 26: 265-270.

Ben-Haim N, Lu C, Guzman-Ayala M, Pescatore L, Mesnard D, Bischofberger M, Naef F, Robertson EJ, and Constam DB. 2006. The nodal precursor acting via activin receptors induces mesoderm by maintaining a source of its convertases and BMP4. Dev Cell 11: 313-323.

Benjamin JM, Torke SJ, Demeler B, and McGarry TJ. 2004. Geminin has dimerization, Cdt1-binding, and destruction domains that are required for biological activity. J Biol Chem 279: 45957-45968.

Bennett D, Dunn LC, Spiegelman M, Artzt K, Cookingham J, and Schermerhorn E. 1975. Observations on a set of radiation-induced dominant T-like mutations in the mouse. Genet Res 26: 95-108.

Beppu H, Lei H, Bloch KD, and Li E. 2005. Generation of a floxed allele of the mouse BMP type II receptor gene. Genesis 41: 133-137.

Bertocchini F and Stern CD. 2002. The hypoblast of the chick embryo positions the primitive streak by antagonizing Nodal signaling. Dev Cell 3: 735-744.

Boos A, Lee A, Thompson DM, and Kroll KL. 2006. Subcellular translocation signals regulate Geminin activity during embryonic development. Biol Cell 98: 363-375.

Bouillet P, Oulad-Abdelghani M, Ward SJ, Bronner S, Chambon P, and Dolle P. 1996. A new mouse member of the Wnt gene family, mWnt8, is expressed during early embryogenesis and is ectopically induced by retinoic acid. Mech Dev 58: 141-152.

Boyer B and Thiery JP. 1993. Epithelium-mesenchyme interconversion as example of epithelial plasticity. APMIS 101: 257-268.

Brennan J, Lu CC, Norris DP, Rodriguez TA, Beddington RSP, and Robertson EJ. 2001. Nodal signaling in the epiblast patterns the early mouse embryo. Nature 411: 965-969.

Brunet LJ, McMahon JA, McMahon AP, and Harland RM. 1998. Noggin, Cartilage Morphogenesis, and Joint Formation in the Mammalian Skeleton. Science 280: 1455-1457.

Burdsal CA, Damsky CH, and Pedersen RA. 1993. The role of E-cadherin and integrins in mesoderm differentiation and migration at the mammalian primitive streak. Dev 118: 829-844.

Cadigan KM and Nusse R. 1997. Wnt signaling: a common theme in animal development. Genes Dev 15: 3286-3305.

Canning CA, Lee L, Irving C, Mason I, and Jones CM. 2007. Sustained interactive Wnt and FGF signaling is required to maintain isthmic identity. Dev Biol 305: 276-286.

Cano A, Perez-Moreno MA, Rodrigo I, Locascio A, Blanco MJ, del Barrio MG, Portillo F, and Nieto MA. 2000. The transcription factor snail controls epithelial-mesenchymal transitions by repressing E-cadherin expression. Nat Cell Biol 2: 76-83.

Champliaud MF, Virtanen I, Tiger CF, Korhonen M, Burgeson R, and Gullberg D. 2000. Posttranslational modifications and beta/gamma chain associations of human laminin alpha1 and laminin alpha5 chains: purification of laminin-3 from placenta. Exp Cell Res 259: 326-335.

Chesley P. 1935. Development of the short-tailed mutant in the house mouse. J Exp Zool 70: 429-459.

Ciruna BG, Schwartz L, Harpal K, Yamaguchi TP, and Rossant J. 1997. Chimeric analysis of fibroblast growth factor receptor-1 (Fgfr1) function: a role for FGFR1 in morphogenetic movement through the primitive streak. Development 124: 2829-2841.

Ciruna B and Rossant J. 2001. FGF signaling regulates mesoderm cell fate specification and morphogenetic movement at the primitive streak. Dev Cell 1: 37-49.

Ciruna B, Jenny A, Lee D, Mlodzik M, and Schier AF. 2006. Planar cell polarity signalling couples cell division and morphogenesis during neurulation. Nature 439: 220-224.

Coffinier C, Tran U, Larraín J, and De Robertis EM. 2001. Neuralin-1 is a novel Chordin-related molecule expressed in the mouse neural plate. Mech Dev 100: 119-122.

Collignon J, Varlet I, and Robertson EJ. 1996. Relationship between asymmetric nodal expression and the direction of embryonic turning. Nature 381: 155-158.

Conacci-Sorrell M, Simcha I, Ben-Yedidia T, Blechman J, Savagner P, Ben-Ze'ev A. 2003. Autoregulation of E-cadherin expression by cadherin-cadherin interactions: the roles of beta-catenin signaling, Slug, and MAPK. J. Cell Biol 163: 847.

Conlon FL, Lyons KM, Takaesu N, Barth KS, Kispert A, Herrmann B, and Robertson EJ. 1994. A primary requirement for Nodal in the formation and maintenance of the primitive streak in the mouse. Development 120: 1919-1928.

Crossley PH and Martin GR. 1995. The mouse Fgf8 gene encodes a family of polypeptides and is expressed in regions that direct outgrowth and patterning in the developing embryo. Development 121: 439-451.

Dale L, Howes G, Price BM and Smith JC. 1992. Bone morphogenetic protein 4: a ventralizing factor in early Xenopus development. Development 115: 573-585.

Darribère T, Skalski M, Cousin HL, Gaultier A, Montmory C, and Alfandari D. 2000. Integrins: regulators of embryogenesis. Biol Cell 92: 5-25.

Davidson BP, Kinder SJ, Steiner K, Schoenwolf GC, and Tam PP. 1999. Impact of node ablation on the morphogenesis of the body axis and the lateral asymmetry of the mouse embryo during early organogenesis. Dev Biol 211: 11-26.

De Boer LS, Gratsch TE, Premo AM, and O'Shea KS. 2005. Transgenic misexpression of noggin in the early postimplantation mouse embryo. Dev Dyn in revision.

De Souza FS and Niehrs C. 2000. Anterior endoderm and head induction in early vertebrate embryos. Cell Tissue Res 300: 207-217.

De Wulf N, Verscheren K, Lonnoy O, Moren A, Grimsby S, Vandespiegle K, Miyazono K, Huylebroeck D, and ten Dijke P. 1995. Distinct spatial and temporal expression patterns of two type I receptors for bone morphogenetic proteins during mouse embryogenesis. Endocrinology 136: 2652-2663.

Del Bene F, Tessmar-Raible K, and Wittbrodt J. 2004. Direct interaction of geminin and Six3 in eye development. Nature 427: 745-748.

Delaune E, Lemaire P, and Kodjabachian L. 2005. Neural induction in Xenopus requires early FGF signaling in addition to BMP inhibition. Development 132: 299-310.

Devlin RD, Du Z, Pereira RC, Kimble RB, Economides AN, Jorgetti V, and Canalis E. 2003. Skeletal Overexpression of Noggin Results in Osteopenia and Reduced Bone Formation. Endocrinology 144: 1972-1978.

Diez del Corral R and Storey RG. 2004. Opposing FGF and retinoid pathways: a signalling switch that controls differentiation and patterning onset in the extending vertebrate body axis. BioEssays 26: 857–869.

Diez del Corral R, Olivera-Martinez I, Goriely A, Gale E, Maden M, and Storey K. 2003. Opposing FGF and Retinoid Pathways Control Ventral Neural Pattern, Neuronal Differentiation, and Segmentation during Body Axis Extension. Neuron 40: 65–79.

Ding J, Yang L, Yan YT, Chen A, Desai N, Wynshaw-Boris A, and Shen MM. 1998. Cripto is required for correct orientation of the anterior-posterior axis in the mouse embryo. Nature 395: 702-707.

Dionne MS, Skarnes WC, and Harland RM. 2001. Mutation and analysis of Dan, the founding member of the Dan family of transforming growth factor beta antagonists. Mol Cell Biol 21: 636-643.

Dionne MS, Brunet LJ, Eimon PM, and Harland RM. 2002. Noggin is Required for Correct Guidance of Dorsal Root Ganglion Axons. Developmental Biology 251: 283-293.

Dudderidge TJ, Stoeber K, Loddo M, Atkinson G, Fanshawe T, Griffiths DF, and Williams GH. 2005. Mcm2, Geminin, and KI67 define proliferative state and are prognostic markers in renal cell carcinoma. Clin Cancer Res 11: 2510-2517.

Dudley AT, Lyons KM, and Robertson EM. 1995. A requirement for bone morphogenetic protein-7 during development of the mammalian kidney and eye. Genes Dev 9: 2795-2807.

Dufort D, Schwartz L, Harpal K, and Rossant J. 1998. The transcription factor HNF3beta is required in visceral endoderm for normal primitive streak morphogenesis. Development 125: 3015-3025.

Echelard Y, Epstein DJ, St-Jacques B, Shen L, Mohler J, McMahon JA, and McMahon AP. 1993. Sonic Hedgehog, a member of a family of putative signaling molecules, is implicated in the regulation of CNS polarity. Cell 75: 1417-1430.

Ekblom P, Lonai P, and Talts JF. 2003. Expression and biological role of laminin-1. Matrix Biol 22: 35-47.

Emmett LSD and O'Shea KS. 2009a. Geminin is required for gastrulation in the post-implantation mouse embryos. In preparation.

Emmett LSD and O'Shea KS. 2009b. Geminin controls EMT and neural crest specification in the mouse embryo. In preparation.

Emmett LSD, Belzyt CL, Schmoll S, and O'Shea KS. 2009. Identification of novel genes in the mouse embryo via laser capture microdissection. In preparation

Episkopou V, Arkell R, Timmons PM, Walsh JJ, Andrew RL, and Swan D. 2001. Induction of the mammalian node requires Arkadia function in the extraembryonic lineages. Nature 410: 825-830.

Fässler R and Meyer M. 1995. Consequences of lack of beta 1 integrin gene expression in mice. Genes Dev 9: 1896-1908.

Fischer A, Viebahn C, and Blum M. 2002. FGF8 acts as a right determinant during establishment of the left-right axis in the rabbit. Curr Biol 12: 1807-1816.

Fujiwara T, Dunn NR, and Hogan BL. 2001. Bone morphogenetic protein 4 in the extra-embryonic mesoderm is required for allantois development and the localization and survival of primordial germ cells in the mouse. PNAS 98: 13739-13744.

Furthauer M, Van Celst J, Thisse C, and Thisse B. 2004. Fgf signaling controls the dorsoventral patterning of the zebrafish embryo. Development 131: 2853-2864.

Furuta Y, Piston DW, and Hogan BLM. 1997. Bone morphogenetic proteins (BMPs) as regulators of dorsal forebrain development. Development 124: 2203-2212.

Furuta Y and Hogan BLM. 1998. BMP4 is essential for lens induction in the mouse embryo. Genes Dev 12: 3764-3775.

Gazzerro E, Pereira RC, Jorgetti V, Olson S, Economides AN, and Canalis E. 2005. Skeletal overexpression of gremlin impairs bone formation and causes osteopenia. Endocrinology 146: 655-665.

Georges-Labouesse EN, George EL, Rayburn H, and Hynes RO. 1996. Mesodermal development in mouse embryos mutant for fibronectin. Dev Dyn 207: 145-156.

Golden JA et al. 1999. Ectopic bone morphogenetic proteins 5 and 4 in the chicken forebrain lead to cyclopia and holoprosencephaly. PNAS 54: 623-634.

Gonzalez MA, Tachibana KE, Chin SF, Callagy G, Madine MA, Vowler SL, Pinder SE, Laskey RA, and Coleman N. 2004. Geminin predicts adverse clinical outcome in breast cancer by reflecting cell-cycle progression. J Pathol 204: 121.

Gonzalez MA, Tachibana KK, Adams DJ, van der Weyden L, Hemberger M, Coleman N, Bradley A, and Laskey RA. 2006. Geminin is essential to prevent endoreplication and to form pluripotent cells during mammalian development. Genes & Dev 20: 1880-1884.

Goumans MJ and Mummery C. 2000. Functional analysis of the TGFbeta receptor/Smad pathway through gene ablation in mice. Int J Dev Biol 44: 253-265.

Gratsch TE and O'Shea KS. 2002. Noggin and Chordin have distinct activities in promoting lineage commitment of mouse embryonic stem (ES) cells. Developmental Biology 245: 83-94.

Grigoryan T, Wend P, Klaus A, and Birchmeier W. 2008. Deciphering the function of canonical Wnt signals in development and disease: conditional loss- and gain-of-function mutations of β -catenin in mice. Genes & Dev 22: 2308-2341.

Gu Z, Nomura M, Simpson BB, Lei H, Feijen A, van den Eijnden-van Raaij J, Donahoe PK, and Li E. 1998. The type I activin receptor ActRIB is required for egg cylinder organization and gastrulation in the mouse. Genes and Dev 15: 844-857.

Gu Z, Reynolds EM, Song J, Lei H, Feijen A, Yu L, He W, MacLaughlin DT, Van Den Eijnden-Van Raaij J, Donahoe PK, and Li E. 1999. The type I serine/threonine kinase receptor ActRIA (ALK2) is required for gastrulation of the mouse embryo. Development 126: 2551-2561.

Guha U, Gomes WA, Kobayashi T, Pestell RG, and Kessler JA. 2002. In Vivo Evidence That BMP Signaling is Necessary for Apoptosis in the Mouse limb. Dev Biol 249: 108-120.

Guo X and Wang XF. 2009. Signaling cross-talk between TGF-beta/BMP and other pathways. Cell Res 19: 71-88.

Habas R, Dawid IB, He X. 2003. Coactivation of Rac and Rho by Wnt/Frizzled signaling is required for vertebrate gastrulation. Genes Dev 17: 295-309.

Haegel H, Larue L, Ohsugi M, Fedorov L, Herrenknecht K, and Kemler R. 1995. Lack of β -catenin affects mouse development at gastrulation. Development 121: 3529-3537.

Hara K, Nakayama KI, and Nakayama K. 2006. Geminin is essential for the development of preimplantation mouse embryos. Genes to Cells 11: 1281-1293.

Harland R. 2000. Neural Induction. Curr Opin Genet Dev 10: 357-362.

Hebert JM, Hayhurst M, Marks ME, Kulessa H, Hogan BLM, and McConnell SK. 2002. BMP ligands act redundantly to pattern the dorsal telencephalic midline. Genesis 35: 214-219.

Heldin CH, Miyazono K, and ten Dijke P. 1997. TGF-beta signaling from cell membrane to nucleus through SMAD proteins. Nature 390: 465-471.

Herrmann BG, Labiet S, Poustka A, King TR, and Lehrach H. 1990. Cloning of the T gene required in mesoderm formation in the mouse. Nature 343: 617-622.

Herrmann BG. 1991. Expression pattern of the Brachyury gene in whole-mount Twis/Twis mutant embryos. Development 113: 913-917.

Hermann BG. 1995. The mouse *Brachyury (T)* gene. Semin Dev Biol 6: 385-394.

Hogan BL. 1996. Bone morphogenetic proteins in development. Curr Opin Genet Dev 6: 432-438.

Hoodless PA, Pye M, Chazaud C, Labbe E, Attisano L, Rossant J, and Wrana JL. 2001. FoxH1 (Fast) functions to specify the anterior primitive streak in the mouse. Genes & Dev 15: 1257-1271.

Hsu DR, Economides AN, Wang X, Eimon PM, and Harland RM. 1998. The Xenopus dorsalizing factor gremlin identifies a novel family of secreted proteins that antagonize BMP activities. Mol Cell 1: 673-683.

Huelsken J, Vogel R, Brinkmann V, Erdmann B, Birchmeier C, and Birchmeier W. 2000. Requirement for β -catenin in anterior-posterior axis formation in mice. J Cell Biol 148: 567-578.

Hynes RO. 1992. Integrins: versatility, modulation, and signaling in cell adhesion. Cell 69: 11-25.

Ishibashi M and McMahon AP. 2002. A sonic hedgehog-dependent signaling relay regulates growth of diencephalic and mesencephalic primordia in the early mouse embryo. Development 129: 4807-4819.

Itoh N. 2007. The Fgf Families in Humans, Mice, and Zebrafish: Their Evolutional Processes and Roles in Development, Metabolism, and Disease. Biol Pharm Bull 30: 1819-1825.

Jessell TM and Sanes JR. 2000. Development: The decade of the developing brain. Curr Opin Neurobio 10: 599-611.

Johansson BM and Wiles MV. 1995. Evidence for involvement of activin A and bone morphogenetic protein 4 in mammalian mesoderm and haematopoietic development. Mol Cell Biol 15: 141-151.

Jones CM, Lyons KM, Lapan PM, Wright CV, and Hogan BL. 1992. DVR-4 (bone morphogenetic protein-4) as a posterior-ventralizing factor in Xenopus mesoderm induction. Development 115: 639-647.

Keller R. 2002. Shaping the vertebrate body plan by polarized embryonic cell movements. Science 298: 1950-1954.

Kelly OG, Pinson KI, and Skarnes WC. 2004. The Wnt co-receptors Lrp5 and Lrp6 are essential for gastrulation in mice. Development 131: 2803-2815.

Kemler R. 1993. From cadherins to catenins: cytoplasmic protein interactions and regulation of cell adhesion. Trends Genet 9: 317-321.

Kemp C, Willems E, Abdo S, Lambiv L, and Leyns L. 2005. Expression of all Wnt genes and their secreted antagonists during mouse Blastocyst and postimplantation development. Dev Dyn 233: 1064-1075.

Kibar Z, Underhill DA, Canonne-Hergaux F, Gauthier S, Justice MJ, and Gros P. 2001. Identification of a new chemically induced allele (Lp (m1Jus)) at the loop-tail locus: morphology, histology, and genetic mapping. Genomics 72: 331-337.

Kim MY, Jeong BC, Lee JH, Kee HJ, Kook H, Kim NS, Kim YH, Kim JK, Ahn KY, and Kim KK. 2006. A repressor complex, AP4 transcription factor and geminin, negatively regulates expression of target genes in nonneuronal cells.

Kispert A, Vainio S, Shen L, Rowitch DH, and McMahon AP. 1996. Proteoglycans are required for maintenance of Wnt-11 expression in the ureter tips. Development 122: 3627-3637.

Klingensmith J, Ang SL, Bachiller D, and Rossant J. 1999. Neural induction and patterning in the mouse in the absence of the node and its derivatives. Dev Biol 216: 535-549.

Kolle G, Georgas K, Holmes GP, Little MH, and Yamada T. 2000. CRIM1, a novel gene encoding a cysteine-rich repeat protein, is developmentally regulated and implicated in vertebrate CNS development and organogenesis. Mech Dev 90: 181-193.

Kroll KL, Salic AN, Evans LM, and Kirschner MW. 1998. Geminin, a neuralizing molecule that demarcates the future neural plate at the onset of gastrulation. Development. 125: 3247-3258.

Kroll KL. 2007. Geminin in embryonic development: coordinating transcription and the cell cycle during differentiation. Front Biosci 12:1395-1409.

Kulessa H, Turk G, and Hogan BLM. 2000. Inhibition of Bmp signaling affects growth and differentiation in the anagen hair follicle. EMBO journal 19: 6664-6674.

Kulessa H and Hogan BLM. 2002. Generation of a loxP Flanked Bmp4 [loxP-lacZ] Allele Marked by Conditional lacZ Expression. genesis 32: 66-68.

LaBonne C and Bronner-Fraser M. 1998. Neural crest induction in Xenopus: Evidence for a two-signal model. Development 125: 2403-2414.

Lamb TM, Knecht AK, Smith WC, Stachel SE, Economides AN, Stahl N, Yancopolous GD, and Harland RM. 1993. Neural Induction by the Secreted Polypeptide Noggin. Science 262: 713-718.

Lawson KA, Dunn NR, Roelen BA et al. 1999a. Bmp4 is required for the generation of primordial germ cells in the mouse embryo. Genes Dev 13: 424-436.

Lawson KA. 1999b. Fate mapping the mouse embryo. Int J Dev Biol 43: 773-775.

Lee JD, Silva-Gagliardi NF, Tepass U, McGlade CJ, and Anderson KV. 2007. The FERM protein Epb4.1I5 is required for organization of the neural plate and for the epithelial-mesenchymal transition at the primitive streak of the mouse embryo. Development 134: 2007-2016.

Lee JD and Anderson KV. 2008. Morphogenesis of the node and notochord: the cellular basis for the establishment and maintenance of left-right asymmetry in the mouse. Dev Dyn 237: 3464-3476.

Levine AJ and AH Brivanlou. 2007. Proposal of a model of mammalian neural induction. Dev Biol 308: 247-256.

Lewis SL and Tam PPL. 2006. Definitive endoderm of the mouse embryo: formation, cell fates, and morphogenetic function. Dev Dyn 235: 2315-2329.

Lim DA, Tramontin AD, Trevejo JM, Herrera DG, Garcia-Verdugo JM, and Alvarez-Buylla A. 2000. Noggin Antagonizes BMP Signaling to Create a Niche for Adult Neurogenesis. Neuron 28: 713-726.

Linker C and Stern CD. 2004. Neural induction requires BMP inhibition only as a late step and involves signals other than FGF and Wnt antagonists. Development 131: 5671-5681.

Linker C, De Almeida I, Papanayoutou C, Stower M, Sabado V, Ghorani E, Streit A, Mayor R, and Stern CD. 2009. Cell communication with the neural plate is required for induction of neural markers by BMP inhibition: evidence for homeogenetic induction and implications for Xenopus animal cap and chick explants assays. Dev Biol 327: 478-486.

Liu P, Wakamiya M, Shea MJ, Albrecht U, Behringer RR, and Bradley A. 1999. Requirement for Wnt3 in vertebrate axis formation. Nature Genet 22: 361-365.

Lowe LA, Yamada S, and Kuehn MR. 2001. Genetic dissection of nodal function in patterning the mouse embryo. Development 128: 1831-1843.

Lu CC, Brennan J, and Robertson EJ. 2001. From Fertilization to gastrulation: Axis formation in the mouse embryo. Curr Opin Genet Dev 11: 384-392.

Luo G, Hofman C, Bronchers AJ, Sohocki M, Bradley A, and Karsenty G. 1995. BMP-7 is an inducer of nephrogenesis and is also required for eye development and skeletal patterning. Genes Dev 9: 2808-2820.

Luo L and Kessel M. 2004. Geminin coordinates cell cycle and developmental control. Cell Cycle 3: 711-714.

Luo L, Yang X, Takihara Y, Knoetgen H, and Kessel M. 2004. The cell-cycle regulator geminin inhibits Hox function through direct and polycomb-mediated interactions. Nature 427: 749-753.

Lupo G, Harris WA and Lewis KE. 2006. Mechanisms of ventral patterning in the vertebrate nervous system. Nat Rev Neurosci 7: 103-114.

Luther WH. 1935. Entwicklungsphysiologische Untersuchungen am Forellenkeim: die Rolle des Organisationszentrums bei der Entstehung der Embryonalanlage. Biol Zentralbl 55: 114-137.

Lyons KM, Hogan BLM, and Robertson EJ. 1995. Colocalization of BMP7 and BMP2 RNAs suggests that these factors cooperatively mediate tissue interactions during murine development. Mech Dev 50: 71-83.

Marikawa Y. 2006. Wnt/ β -catenin signaling and body plan formation in mouse embryos. Semin Cell Dev Biol 17: 175-184.

Matzuk MM, Kumar TR, and Bradley A. 1995. Different phenotypes for mice deficient in either activins or activin receptor type II. Nature 374: 356-360.

McGarry TJ & Kirschner MW. 1998. Geminin, an inhibitor of DNA replication, is degraded during mitosis. Cell 93: 1043-1053.

McMahon AP, Joyner AL, Bradley A, and McMahon JA. 1992. The midbrain/hindbrain phenotype of Wnt1-/Wnt1- mice results from stepwise deletion of engrailed-expressing cells by 9.5 days postcoitum. Cell 69: 581-595.

McMahon JA, Takada S, Zimmerman LB, Fan CM, Harland RM, and McMahon AP. 1998. Noggin-mediated antagonism of BMP signaling is required for growth and patterning of the neural tube and somite. Genes & Development 12: 1438-1452.

Meno C, Gritsman K, Ohishi S, Ohfuji Y, Heckscher E, Mochida K, Shimono A, Kondoh H, Talbot WS, Robertson EJ, Schier AF, and Hamada H. 1999. Mouse Lefty2 and zebrafish antivin are feedback inhibitors of nodal signaling during vertebrate gastrulation. Mol Cell 4: 287-298.

Miner JH, Cunningham J, and Sanes JR. 1998. Roles for laminin in embryogenesis: exencephaly, syndactyly, and placentopathy in mice lacking the laminin alpha5 chain. J Cell Biol 143:1713-1723.

Mishina Y, Suzuki A, Ueno N, and Behringer RR. 1995. Bmpr encodes a type I bone morphogenetic protein receptor that is essential for gastrulation during mouse embryogenesis. Genes & Dev 6: 432-438.

Mishina Y. 2003. Function of bone morphogenetic protein signaling during mouse development. Front Biosci 8: 855-869.

Mohamed OA, Clarke HJ, and Dufort D. 2004. β -catenin Signaling Marks the Prospective Site of Primitive Streak Formation in the Mouse Embryo. Dev Dyn 231: 416-424.

Molotkova N, Molotkov A, Sirbu IO, and Duester G. 2005. Requirement of mesodermal retinoic acid generated by Raldh2 for posterior neural transformation. Mech Dev 122: 145-155.

Montanari M, Boninsegna A, Faraglia B, Coco C, Giordano A, Cittadini A, and Sgambato A. 2005. Increased expression of geminin stimulates the growth of mammary epithelial cells and is a frequent event in human tumors. J Cell Physiol 202: 215-222.

Morkel M, Huelsken J, Wakamiya M, Ding J, van de Wetering M, Clevers H, Taketo MM, Behringer RR, Shen MM, and Birchmeier W. 2003. Beta-catenin regulates Cripto- and Wnt3-dependent gene expression programs in mouse axis and mesoderm formation. Development 130: 6283-6294.

Mukhopadhyay M, Shtrom S, Rodriguez-Esteban C, Chen L, Tsukui T, Gomer L, Dorward DW, Glinka A, Grinberg A, Huang SP, et al. 2001. Dickkopf1 is required for embryonic head induction and limb morphogenesis in the mouse. Dev Cell 1: 423-434.

Mummery CL and Van Den Eijnden- Van Raaij AJ. 1999. Developmental tumours, early differentiation and the transforming growth factor beta superfamily. Int J Dev Biol 43: 693-709.

Myers DC, Sepich DS, and Solnica-Krezel L. 2002. Convergence and extension in vertebrate gastrulae: cell movements according to or in search of identity? Trends in Genet 18: 447-455.

Nagafuchi A. 2001. Molecular architecture of adherens junctions. Curr Opin Cell Biol 13: 600-603.

Nakayama N, Han CY, Cam L, Lee JI, Pretorius J, Fisher S, Rosenfeld R, Scully S, Nishinakamura R, Duryea D, Van G, Bolon B, Yokota T, and Zhang K. 2004. A novel chordin-like BMP inhibitor, CHL2, expressed preferentially in chondrocytes of developing cartilage and osteoarthritic joint cartilage. Development 131: 229-240.

Nelson WJ and Nusse R. 2004. Convergence of Wnt, β -Catenin, and Cadherin Pathways. Science 303: 1483-1487.

Niswander L and Martin GR. 1992. Fgf-4 expression during gastrulation, myogenesis, limb and tooth development in the mouse. Development 114: 755-768.

Norris DP, Brennan J, Bikoff EK, and Robertson EJ. 2002. The Foxh1-dependent autoregulatory enhancer controls the level of Nodal signals in the mouse embryo. Development 129: 3455-3468.

O'Shea KS, De Boer LS, Slawny NA, and Gratsch TE. 2006. Transplacental RNAi: Deciphering Gene Function in the Postimplantation-Staged Embryo. J Biomed Biotechnol 4: 18657.

Obermann EC, Eward KL, Dogan A, Paul EA, Loddo M, Munson P, Williams GH, and Stoeber K. 2005. DNA replication licensing in peripheral B-cell lymphoma. J Pathol 205: 318-328.

Oh SP and Li E. 1997. The signaling pathway mediated by the type IIB activin receptor controls axial patterning and lateral asymmetry in the mouse. Genes & Dev 11: 1812-1826.

Papanayotou C, Mey A, Birot AM, Saka Y, Boast S, Smith JC, Samarut J, and Stern CD. 2008. A mechanism regulating the onset of Sox2 expression in the embryonic neural plate. PLoS 6: e2.

Pappano WN, Scott IC, Clark TG, Eddy RL, Shows TB, and Greenspan DS. 1998. Coding sequence and expression patterns of mouse chordin and mapping of the cognate mouse chrd and human CHRD genes. Genomics 52: 236-239.

Patel K. 1998. Follistatin. Int J Biochem Cell Biol 30: 1087-1093.

Perea-Gomez A, Shawlot W, Sasaki H, Behringer RR, and Ang S. 1999. HNF3beta and Lim 1 interact in the visceral endoderm to regulate primitive streak formation and anterior-posterior polarity in the mouse embryo. Development 126: 4499-4511.

Perea-Gomez A, Rhinn M, and Ang SL. 2001b. Role of the anterior visceral endoderm in restricting posterior signals in the mouse embryo. Int J Dev Biol 45: 311-320.

Perea-Gomez A, Vella FDJ, Shawlot W, Oulad-Abdelghani M, Chazaud C, Meno C, Pfister V, Chen L, Robertson E, Hamada H, Behringer RR, and Ang SL. 2002. Nodal Antagonists in the Anterior Visceral Endoderm Prevent the Formation of Multiple Primitive Streaks. Developmental Cell 3: 745-756.

Pfister S, Steiner KA, and PP Tam. 2007. Gene expression pattern and progression of embryogenesis in the immediate post-implantation period of mouse development. Gene Exp Pat 7: 558-573.

Piccolo S, Sasai Y, Lu B, and De Robertis EM. 1996. Dorsoventral patterning in Xenopus: Inhibition of ventral signals by direct binding of Chordin to BMP-4. Cell 86: 589-598.

Pitulescu M, Kessel M, and Luo L. 2005. The regulation of embryonic patterning and DNA replication by geminin. Cell Mol Life Sci 62:1425-1433.

Pöpperl H, Schmidt C, Wilson V, Hume CR, Dodd J, Krumlauf R, and Beddington RS. 1997. Misexpression of Cwnt8C in the mouse induces an ectopic embryonic axis and causes a truncation of the anterior neuroectoderm. Development 124: 2997-3005.

Quinn LM, Herr A, McGarry TJ, and Richardson H. 2001. The Drosophila Geminin homolog: roles for Geminin in limiting DNA replication, in anaphase and in neurogenesis. Genes & Dev 15: 2741-2754.

Rhinn M, Dierich A, Shawlot W, Behringer RR, Le Meur M, and Ang SL. 1998. Sequential roles for Otx2 in visceral endoderm and neuroectoderm for forebrain and midbrain induction and specification. Development 125: 845-856.

Ribes V, Le Roux I, Rhinn M, Schuhbaur B and Dollé P. 2009. Early mouse caudal development relies on crosstalk between retinoic acid, Shh and Fgf signalling pathways. Development 136: 665-676.

Rivera-Perez JA and Magnuson T. 2005. Primitive streak formation in mice is preceded by localized activation of Brachyury and Wnt3. Dev Biol 288: 363-371.

Robertson EJ, Norris DP, Brennan J, and Bikoff EK. 2003. Control of early anterior-posterior patterning in the mouse embryo by TGFbeta signaling. Phil Trans R Soc Lond B Biol Sci 358: 1351-1357.

Rogers CD, Harafuji N, Archer T, Cunningham DD, and Casey ES. 2009. Xenopus Sox3 activates sox2 and geminin and indirectly represses Xvent2 expression to induce neural progenitor formation at the expense of non-neural ectodermal derivatives. Mech Dev 126: 42-55.

Russ AP, Wattler S, Colledge WH, Aparicio SA, Carlton MB, Pearce JJ, Barton SC, Surani MA, Ryan K, Nehls MC, Wilson V, and Evans MJ. 2000. Eomesodermin is required for mouse trophoblast development and mesoderm formation. Nature 404: 95-99.

Sasai Y. 1998. Identifying the missing links: genes that connect neural induction and primary neurogenesis in vertebrate embryos. Neuron 21: 455-458.

Sela-Donenfeld D and Kalcheim C. 1999. Regulation of the onset of neural crest migration by coordinated activity of BMP4 and Noggin in the dorsal neural tube. Development 126: 4749-4762.

Seo S, Herr A, Lim JW, Richardson GA, Richardson H, and Kroll KL. 2005a. Geminin regulates neuronal differentiation by antagonizing Brg1 activity. Genes & Dev 19: 1723-1734.

Seo S, Richardson GA, and Kroll KL. 2005b. The SWI/SNF chromatin remodeling protein Brg1 is required for vertebrate neurogenesis and mediates transactivation of Ngn and NeuroD. Development 132: 105-115.

Seo S and Kroll KL. 2006. Geminin's Double Life: chromatin connections that regulate transcription at the transition from proliferation to differentiation. Cell Cycle 5: 374-380.

Sharov AA, Weiner L, Sharova TY, Siebenhaar F, Atoyan R, Reginato AM, McNamara CA, Funa K, Gilchrest BA, Brissette JL, and Botchkarev VA. 2003. Noggin overexpression inhibits eyelid opening by altering epidermal apoptosis and differentiation. EMBO Journal 22: 2992-3003.

Shawlot W, Min Deng J, Wakamiya M, and Behringer RR. 2000. The cerberus-related gene, Cerr1, is not essential for mouse head formation. Genesis 26: 253-258.

Sheng G, dos Reis M, Stern CD. 2003. Churchill, a zinc finger transcriptional activator, regulates the transition between gastrulation and neurulation. Cell 115: 603–613.

Skromne I and Stern CD. 2002. A hierarchy of gene expression accompanying induction of the primitive streak by Vg1 in the chick embryo. Mech Dev 114: 115-118.

Smith WC and Harland RM. 1992. Expression cloning of noggin, a new dorsalizing factor localized to the Spemann organizer in Xenopus embryos. Cell 70, 829-840.

Solloway MJ and Robertson EJ. 1999. Early embryonic lethality in Bmp5; Bmp7 double-mutant mice suggests functional redundancy within the 60A subgroup. Development 128: 1753-1768.

Solnica-Krezel L. 2005. Conserved patterns of cell movements during vertebrate gastrulation. Curr Biol 15: 213-228.

Song J, Oh SP, Schrewe H, Nomura M, Lei H, Okano M, Gridley T, and Li E. 1999. The type II activin receptors are essential for egg cylinder growth, gastrulation and rostral head development in mice. Dev Biol 213: 157-169.

Sousa-Nunes R, Rana AA, Kettleborough R, Brickman JM, Clements M, Forrest A, Grimmond S, Avner P, Smith JC, Dunwoodie SL, and Beddington RSP. 2003. Characterizing Embryonic Gene Expression Patterns in the mouse using nonredundant sequence-based selection. Genome Res 13: 2609-2620.

Spella M, Britz O, Kotantaki P, Lygerou Z, Nishitani H, Ramsay RG, Flordellis C, Guillemot F, Mantamadiotis T, and Taraviras S. 2007. Licensing regulators Geminin and Cdt1 identify progenitor cells of the mouse CNS in a specific phase of the cell cycle. Neuroscience 147: 373-387.

Spemann H and Mangold H. 1924. Uber induktion can Embryonalanlagen durch Implantion artfremder Organisatoren. Arch mikrosk Anat EntwMech 100, 599-638.

Stephens LE, Sutherland AE, Klimanskaya IV, Andrieux A, Meneses J, Pedersen RA, and Damsky CH. 1995. Deletion of beta 1 integrins in mice results in inner cell mass failure and peri-implantation lethality. Genes Dev 9: 1883-1895.

Storey KG, Goriely A, Sargent CM, Brown JM, Burns HD, Abud HM, and Heath JK. 1998. Early posterior neural tissue is induced by FGF in the chick embryo. Development 125: 473-484.

Sulik, K Dehart DB, Iangaki T, Carson JL, Vrablic T, Gesteland K and Schoenwolf GC. 1994. Morphogenesis of the murine node and notochordal plate. Dev Dyn 201: 260-278.

Sun X, Meyers EN, Lewandoski M, Martin GR. 1999. Targeted disruption of Fgf8 causes failure of cell migration in the gastrulating mouse embryo. Genes Dev 13: 1834-1846.

Sutherland AE, Calarco PG, and Damsky CH. 1993. Developmental regulation of integrin expression at the time of implantation in the mouse embryo. Development 119: 1175-1186.

Tam and Loebel. 2007. Gene function in mouse embryogenesis: get set for gastrulation. Nat Rev Genet 8: 368-381.

Taylor JJ, Wang T, and Kroll KL. 2005. Tcf- and Vent-binding sites regulate neural-specific geminin expression in the gastrula embryo. Dev Biol 289: 494-506.

Thomas P and Beddington RS. 1996. Anterior primitive endoderm may be responsible for patterning the anterior neural plate in the mouse embryo. Curr Biol 6: 1487-1496.

Thomas PQ, Brown A, and Beddington RS. 1998. Hex: A homeobox gene revealing peri-implantation asymmetry in the mouse embryo and an early transient marker of endothelial cell precursors. Development 125: 85-94.

Urist MR. 1965. Bone: formation by autoinduction. Science 150: 893-899.

Vaahtokari A, Albert T, Jernvall J, Keranen S, and Thesleff I. 1996. The enamel knot as a signaling center in the developing mouse tooth. Mech Dev 54: 39-43.

Valenzuela DM, Economides AN, Rojas E, Lamb TM, Nunez L, Jones P, Ip NY, Espinosa R, Brannan CI, Gilbert DJ, Copeland NG, Jenkins NA, LeBeau MM, Harland RM, and Yancopoulos GD. 1995. Identification of mammalian noggin and its expression in the adult nervous system. J. Neuroscience 15: 6077-6084.

Varlet I, Collignon J, and Robertson EJ. 1997. Nodal expression in the primitive endoderm is required for specification of the anterior axis during mouse gastrulation. Development 124: 1033-1044.

Vermot J, Gallego Llamas J, Fraulob V, Niederreither K, Chambon P, and Dolle P. 2005. Retinoic acid controls the bilateral symmetry of somite formation in the mouse embryo. Science 308: 563-566.

Viebahn C. 1995. Epithelial-mesenchymal transformation during formation of the mesoderm in the mammalian embryo. Acta Anat 154: 79-97.

Vincent SD, Dunn NR, Hayashi S, Norris DP, and Robertson EJ. 2003. Cell fate decisions within the mouse organizer are governed by graded Nodal signals. Genes & Development 17: 1646-1662.

von Bubnoff A and Cho KW. 2001. Intracellular BMP signaling regulation in vertebrates: pathway or network? Dev Biol 239: 1-14.

Waddington CH. 1936. Organizers in Mammalian Development. Nature 138: 125.

Waddington CH. 1932. Experiments on the development of chick and duck embryos cultivated in vitro. Philos Trans R Soc Lond B Biol Sci 221: 179-230.

Waldrip WR, Bikoff EK, Hoodless PA, Wrana JL, and Robertson EJ. 1998. Smad2 signaling in extraembryonic tissues determines anterior-posterior polarity of the early mouse embryo. Cell 92: 797-808.

Wallingford JB, Fraser SE, and Harland RM. 2002. Convergent extension: the molecular control of polarized cell movement during embryonic development. Dev Cell 2: 695-706.

Weisberg E, Winnier GE, Chen X, Farnsworth CL, Hogan BL, and Whitman M. 1998. A mouse homologue of FAST-1 transduces TGFbeta superfamily signals and is expressed during early embryogenesis. Mech Dev 79: 17-27.

Whitman M. 1998. Smads and early developmental signaling by the TGFbeta superfamily. Genes Dev 12: 2445-2462.

Wilson SI, Graziano E, Harland R, Jessell TM, and Edlund T. 2000. An early requirement for FGF signaling in the acquisition of neural cell fate in the chick embryo. Curr Biol 20: 421-429.

Winnier G, Blessing M, Labosky PA, and Hogan BL. 1995. Bone morphogenetic protein-4 is required for mesoderm formation and patterning in the mouse. Genes Dev 9: 2105-2116.

Wohlschlegel JA, Kutok JL, Weng AP, and Dutta A. 2002. Expression of Geminin as a Marker of Cell Proliferation in Normal Tissues and Malignancies. Am J Path 161: 267-273.

Wotton D and Massague J. 2001. Smad transcriptional co-repressors in TGF beta family signaling. Curr Top Microbiol Immunol 254: 145-164.

Wrana JL, Attisano L, Weiser R, Ventura F, and Massague J. 1994. Mechanism of activation of the TGF-beta receptor. Nature 370: 341-347.

Wu HH, Ivkovic S, Murray RC, Jaramillo S, Lyons KM, Johnson JE, and Calof AL. 2003. Autoregulation of neurogenesis by GDF11. Neuron 37: 197-207.

Yamaguchi TP, Takada S, Yoshikawa Y, Wu N, and McMahon AP. 1999. T (Brachyury) is a direct target of Wnt3a during paraxial mesoderm specification. Genes Dev 13: 3185-3190.

Yamamoto M, Meno C, Sakai Y, Shiratori H, Mochida K, Ikawa Y, Saijoh Y, and Hamada H. 2001. The transcription factor FoxH1 (FAST) mediates Nodal signaling during anterior-posterior patterning and node formation in the mouse. Genes & Dev 15: 1242-1256.

Yamanaka Y, Tamplin OJ, Beckers A, Gossler A, and Rossant J. 2007. Live Imaging and Genetic Analysis of Mouse Notochord Formation Reveals Regional Morphogenetic Mechanisms. Dev Cell 13: 884-896.

Yoon BS, Pogue R, Ovchinnikov DA, Yoshii I, Mishina Y, Behringer RR, and Lyons KM. 2006. BMPs regulate multiple aspects of growth-plate chondrogenesis through opposing actions on FGF pathways. Development 133: 4667-4678.

Yoshikawa Y, Fujimori T, McMahon AP, and Takada S. 1997. Evidence that absence of Wnt-3a signaling promotes neuralization instead of paraxial mesoderm development in the mouse. Dev Biol 183: 234-242.

Yurchenco PD and Wadsworth WG. 2004. Assembly and tissue functions of early embryonic laminins and netrins. Curr Opin Cell Biol 16: 572–579.

Zhou X, Sasaki H, Lowe L, Hogan BL, and Kuehn MR. 1993. Nodal is a novel TGF-beta-like gene expressed in the mouse node during gastrulation. Nature 361: 543-547.

Zimmerman LB, DeJesus-Escobar JM, and Harland RM. 1996. The Spemann organizer signal noggin binds and inactivates Bone Morphogenetic Protein 4. Cell 86: 599-606.

Zúñiga A, Haramis AP, McMahon AP, and Zeller R. 1999. Signal relay by BMP antagonism controls the SHH/FGF4 feedback loop in vertebrate limb buds. Nature 401: 598-602.

Chapter 2

Transgenic Misexpression of Noggin in the
Early Postimplantation Mouse Embryo

ABSTRACT

Signaling molecules produced by the node including noggin, chordin, and follistatin appear to induce neural ectoderm by antagonizing BMP signaling in the embryonic ectoderm of the early embryo. To begin to tease out the roles of these factors in vivo, we have used transgenesis to misexpress noggin and abrogate BMP signaling in the early embryo. Expression was driven by the keratin 14 intermediate filament protein promoter, which we demonstrate is expressed surprisingly early in development at E6.5 in visceral endoderm and extraembryonic tissues. Transgenic embryos examined on E7.5 were characterized by cell death in the mesoderm and anterior embryonic endoderm, as well as by defects of axis formation. By E8.5, surviving transgenic embryos had widened neural plates, defects of neural tube closure and of axial rotation. In addition, there was a poor differentiation of the first branchial arch, and defects of the optic and otic placodes as well as the heart were commonly observed in transgenic embryos. Expression analysis of the pan-neural markers Sox2 and Sox3 in these embryos indicated that ectopic neural tissue differentiated at the expense of ectoderm. Although few animals examined postnatally carried the transgene, skeletal, tooth, and hair anomalies were present in these mice. This work demonstrates the critical role of BMP signaling in establishing the boundary between the neural and epidermal ectoderm, in the embryonic endoderm, and suggests a role in early axis formation and patterning.

KEY WORDS: bone morphogenetic proteins, differentiation, ectoderm, endoderm, gastrulation, induction, mesoderm, mouse embryo, neurulation, and noggin.

INTRODUCTION

Lineage restriction in the early mouse embryo occurs as compaction of the morula segregates cells destined to form the inner cell mass (ICM) to the center and trophoblast to the outside of the E2.5 embryo (Johnson and Ziomek, 1981), and possibly as early as the two cell stage (Piotrowska et al., 2001). The next major embryonic lineage differentiation event occurs several days later at gastrulation when cells in the primitive ectoderm move medially through the primitive streak, to form mesoderm and definitive (embryonic) endoderm. There has been considerable progress in understanding the molecular embryology of gastrulation, prompted by studies in Xenopus embryos, where signaling from the Nieuwkoop center establishes the dorsal lip of the blastopore (the functional analogue of the mouse node) as the major signaling center in the gastrula (Harland, 2000). In the mouse embryo, the node produces signaling molecules (noggin, chordin, follistatin) that inhibit the action of the bone morphogenetic proteins (BMPs) produced by the ectoderm, to induce and then pattern the neural ectoderm. A mouse Nieuwkoop has not yet been identified, although nodal signaling through FoxH1 appears to be responsible for establishing the mouse organizer (Hoodless et al., 2001; Yamamoto et al., 2001). Nodal signaling from the epiblast also promotes the formation of a second signaling center in the anterior visceral endoderm (AVE; Brennan et al., 2001). The AVE secretes additional signaling molecules including mouse dickkopf-1 (Mukhopadhay et al., 2001) and Cerberus-like (Belo et al., 1997) that induce and pattern the cephalic region of the embryo. Nodal signaling thus is critical in establishing the signaling centers in the early embryo, the strength of the nodal signal may also control cell fate decisions during gastrulation in the mouse (Vincent et al., 2003), as in the Xenopus embryo (Agius et al., 2000).

Local inhibition of BMP signaling in the ectoderm by secreted signaling molecules such as chordin (the vertebrate homolog of the drosophila short gastrulation gene) and noggin that bind BMPs in the extracellular space thereby preventing receptor activation, induce expression of early neural genes in the ectoderm (Balemans and van Hul, 2002). Although it is clear that the neuroepithelia/surface ectoderm boundary is controlled by BMP signaling (reviewed in Bally-Cuif and Hammerschmidt, 2004), the precise contribution of negative (BMP inhibition) and positive (Wnts, FGFs, and others) signaling in neural induction remains controversial.

Abrogation of BMP2/4 signaling in Bmpr1a conditional null embryos results in widely expanded neuroepithelial fields and reduced surface ectoderm (Davis et al., 2004); as in the current investigation where noggin misexpression widened the neural plate. Noggin or chordin null embryos of many species are characterized by reduced neuroepithelial fields, although in mouse embryos, null mutations of the noggin and chordin genes have not been informative in delineating their specific roles in neural induction, likely because they have overlapping functions, such that mutation of one gene appears not to affect neural induction, while ablation of two produces lethal phenotypes that affect both anterior and posterior regions of the neuraxis (McMahon et al., 1998; Bachiller et al., 2000; Anderson et al., 2002). Conversely, mutation of genes for members of the transforming growth factor beta superfamily: Bmp2 (Zhang and Bradley, 1996) Bmp4 (Winnier et al.,1995), Bmp7 (Dudley et al., 1995), activins (Vassalli et al., 1994; Matzuk et al., 1995) TGFβ1 (Shull et al., 1992; Dickson et al., 1995), BMP receptors Type 1 (Mishina et al., 1995, 1999, 2002; Gu et al., 1998, 1999; Oh et al., 2000), Type II (Beppu et al., 2000), or of the eight signal transducing Smad proteins; Smad 1 (Tremblay et al., 2001), Smad 5 (Chang et al., 1999, 2000), the common Smad 4 (Sirard et al., 1998), or of Smad protein cofactors such as Ecsit (Xiao et al., 2003) produce severe embryonic phenotypes and result in early lethality at implantation or egg cylinder stages of development

(reviewed in Zhao, 2002). Although gene targeting has established a critical role for this signaling family in development, early lethality has limited their usefulness in studying induction, patterning, and later developmental events, although many will be reconstructed using conditional gene targeting strategies.

A number of alternative approaches have been developed to alter signaling pathways in the early embryo, including injection of antisense oligonucleotides or morpholinos, RNA interference (RNAi), and gain of function approaches employing protein bound to beads, retroviral infection, and embryo electroporation. In the case of antagonistic signaling molecules, over-expression of one has often been interpreted as knock-down of the other (e.g., Anderson et al., 2002). Accordingly, BMP signaling has been abrogated by noggin mis-expression in a number of developing tissues. It has been possible to interfere with the BMP dependent process of interdigital cell death by placing noggin coated beads in the digital fields, and when placed at the tips of forming digital rays, severe digit truncations formed (Merino et al., 1998). Noggin protein added to headfold stage embryos in whole embryo culture inhibited the BMP4 dependent induction of nodal expression in the left lateral plate mesoderm and randomized left-right patterning (Fujiwara et al., 2002), noggin expressing CHO cells inhibited development of the chick semicircular canals (Geriach et al., 2000), and noggin coated beads transformed incisors to molars in E10 mouse mandibular explants (Tucker et al., 1998).

These tactics have the advantage of producing highly localized alterations in the microenvironment, but the extent of protein delivery from beads, and the extent of inhibition of protein by RNAi may be variable (or unknown), and are often impractical in the early post-implantation staged mouse embryo. Targeted misexpression of putative developmental control molecules in the mouse embryo can also be achieved by driving expression via and enhancer/promoter of a gene expressed in the tissue of interest using transgenesis. This approach has classically been employed in promoter analysis, where expression of a marker

60

such as β-galactosidase is controlled by sequentially deleted pieces of DNA, or "knock-in" to determine the ontogeny/pattern of expression of a particular gene. Targeted misexpression of putative regulatory genes to the ectoderm has been widely employed in *Xenopus* to determine if the gene is "sufficient" to convert ectoderm to another fate. Neuronal differentiation of epidermal ectoderm was observed by expressing NeuroD (Turner and Weintraub, 1994), Ngn1 (Olson et al., 1998), Geminin (Kroll et al., 1998), N-cadherin (Detrick et al., 1990), but not N-CAM (Kintner 1988), while misexpression of Foxd3 resulted in mesoderm differentiation (Hanna et al., 2002) in Xenopus embryos.

Transgenic misexpression has been employed less widely in the mouse embryo, but has produced striking phenotypes. For example, when the human β-actin promoter was used to overexpress chick Wnt8c, two primitive streaks and nodes formed, without secondary head structures (Popperl et al., 1997). Misexpression of Noggin via the *Msx2* gene promoter that is expressed in proliferative hair matrix cells produced mice with hair follicles that lacked external hairs due to the inhibition of differentiation of shaft hair cells (Kulessa et al., 2000), demonstrating a critical role of BMP signaling in controlling differentiation and stem cell number in this niche. Misexpression of BMP4 in the embryonic lung where it normally controls branching morphogenesis produced distended terminal buds and fluid filled sacs (Bellusci et al., 1996). Expression of BMP4 via the NSE promoter produced heterotopic bone formation similar to the fibrodysplasia ossificans progressive syndrome, which was prevented by mating with transgenic mice in which NSE drives expression of Noggin (Kan et al., 2004). When the intermediate filament gene keratin 14 (K14) promoter was employed to express noggin in the murine limb, the BMP dependent apoptosis required for digit formation was inhibited, and there was hyperinnervation of the skin; however, early gastrulation stages of development were not examined (Guha et al., 2002, 2004). Noggin misexpression in epidermal ectoderm has also been driven by the later keratin 5 (K5) promoter, reducing apoptosis and resulting in failure of epidermal differentiation specifically affecting eyelid opening (Sharov et al.,

2003). Thus, misexpression studies have been efficient in identifying unsuspected roles of genes not previously observed in the null embryos.

In the current investigation, we have employed the K14 promoter to express Noggin in the early embryo. K14 has previously been employed to express Sonic hedgehog (Shh) in the ectoderm, producing CNS, skeletal, and skin abnormalities (Oro et al., 1997). Expression of the keratin intermediate filament proteins occurs sequentially during development; previous published work indicated that K14 was expressed in the ectoderm as early as E9.5—the earliest time point examined in that investigation (Fuchs et al., 1994). We have determined that K14 is expressed as early as E6.5, suggesting that this promoter is active in directing gene expression surprisingly early in development. In the current investigation, we have expanded the noggin expression domain in the early embryo resulting in gastrulation defects and producing later embryos with broad neural plates, failure of neural tube closure, defects of axis formation, and of cardiac and branchial arch development. Not surprisingly, these results phenocopy many of the defects observed in the rare BMP4 null embryo that survives to the 20 somite stage (Lawson et al., 1999), conditional mutation of Bmpr1a in epiblast (Davis et al., 2004), and the defects we have observed in embryos following exposure to BMP4 RNAi on E6.75 (Gratsch el al., 2003).

MATERIALS AND METHODS

Noggin Expression Constructs.

Two Noggin expression vectors were developed for these studies. In the first, the K14 promoter was used to drive expression of noggin. A 1 kb noggin cDNA (containing the entire ORF) was amplified from genomic DNA (gDNA) with primers designed from Genebank accession #U79163, then ligated in place of the Shh coding region in the K14/Shh plasmid (Oro et al., 1997) to generate pK14/Nog (Figure 2-1 A). In order to monitor transgene expression in embryos,

the entire K14/noggin cassette (minus the polyA signal) was removed from pK14/Nog using an AseI/SacII digest and ligated into the promoterless pIRES2-EGFP vector (Figure 2-1 B, Clontech). Prior to injection, the expression cassettes were removed from the plasmid backbone by either an EcoRI/HindIII or AseI/AflIII digest.

Transgenesis.

Transgenic embryos were created by injecting the gel purified pK14/Nog transgenes into the pronuclei of donor embryos obtained from C57BL/6 superovulated females fertilized by (C57BL/6 x SJL) F1 males. Zygotes were transferred to donor mice (n=26) at the two-cell stage and harvested on E7.5, E8.5, or E9.5, or pregnant dams (n=8) allowed to deliver.

Analysis.

Embryos were dissected from the uterus, decidua, and membranes were removed; the ectoplacental cone and chorion were removed and used for PCR genotyping. Prior to fixation, light and EGFP fluorescence images of embryos were captured using a Leitz inverted fluorescence microscope to identify transgene carriers and to determine the extent of transgene expression. Embryos were then fixed in either 1% glutaraldehyde (resin sections and SEM) or 1.5% paraformaldehyde (PFA) (frozen sections) for 1 hour at room temperature, and then stored at 4°C in PBS. Selected control and transgenic embryos were then embedded in OCT for cryostat sectioning or were post-fixed in 1% osmium tetroxide, dehydrated, and embedded in araldite resin for sectioning at 1 micrometer. Additional embryos were dehydrated in serial dilutions of EtOH followed by hexamethyl-disilazane (HMDS) for SEM analysis. Dehydrated embryos were affixed to Cambridge mounts using double sided tape, sputter coated with gold-palladium, viewed, and digital images captured using an Amray 1000B scanning electron microscope.

An additional eight pregnant females were allowed to deliver and neonates genotyped and analyzed for evidence of external abnormalities. Transgene carriers were mated to determine their fertility and heritability of the transgene.

DNA/RNA Extraction and RT-PCR.

Expression of the endogenous keratin 14 mRNA was determined by RT-PCR with primers F-aatgccaatgtcctcctgca, R-tccacattgacgtctccacc (266 bp product) on RNAs obtained from control (CD-1) E6.5-E13.5 embryos. PCR conditions were: 94°C /50s, 58°C /1m, 72°C/1.5m for 40 cycles. To identify carriers of the transgenes, DNA and RNA were extracted from embryos, extraembryonic tissue, or tail biopsies using the Trizol reagent (ILT) according to the manufacturer's instructions. The presence of the first transgene was determined using primers (Figure 2-1 A I, ii): F-cccggtgctgtacgcgtgg, R-agtgggatctgtgtccacac (330 bp product), 92°C /1m, 60°C /1m; 72°C/2m for 25 cycles. To identify carriers of the second transgene, primers (Figure 2-1 B iii, iv) F-ccgcttttggccacgcta, R-ggttgtgccgcctttgca (600 bp product) were employed in PCR: 93°C /30s; 53°C/ 1m, 72°C/2m; for 40 cycles.

Immunohistochemistry.

To determine the pattern of expression of the endogenous keratin 14 protein, sagittal and transverse cryostat sections (10 micrometer) were cut through E6.5, E7.5, and E8.5 control and transgenic embryos. Non-specific antibody binding was blocked and sections exposed to primary antibody, mouse anti-keratin 14 Ab-1 (NeoMarkers, 1:100) for two hours at room temperature. Sections were washed, then exposed to secondary antibody conjugated to Cy3 (1:100) for 30 minutes. Slides were washed, coverslipped, and digital images captured using a Leitz Fluovert microscope then imported into Adobe Photoshop.

In situ hybridization.

Transverse cryostat sections were cut at ten microns using the cryojane system (Instrumedics) and collected on Starfrost slides. Sections were fixed in cold 4%

PFA for 1 hour prior to pretreatment consisting of: two 0.1% DEPC washes, a 3% H_2O_2 wash, proteinase K (1 µg/ml) treatment at RT, and equilibration in SSC. Antisense and sense probes for Noggin, Sox2, and Sox3 were DIG labeled (Roche) and applied to sections. Hybridization was carried out at 53°C for at least ten hours followed by a series of high stringency washes and a brief fixation at RT in 4% PFA. Slides were treated with Blocking solution (Roche) and then incubated with anti-DIG antibody (Roche) mixed with goat IgG (Jackson Labs) followed by incubation with biotinylated tyramide (Dako), then streptavidin-AP (Dako). After detection buffer, NBT/BCIP (Roche) solution was applied to yield a blue reaction product. Staining was stopped with a Tris-EDTA wash. Slides were stained with nuclear fast red (Dako), dehydrated, and coverslipped using CureMount (Instrumedics). Digital images were acquired using a Zeiss Axiophot microscope then imported into Adobe Photoshop to assemble plates.

The Noggin *in situ* probe was made by subcloning a 720 bp portion (nt 270-959) from the original 1 kb, cDNA into pBSSK. Plasmids were linearized using EcoRI or Apa I, purified, and probe synthesis carried out with T7 or T3 RNA polymerase in the presence of DIG-11-UTP (Roche). A Sox2 (accession # X94127) cDNA was amplified in PCR from gDNA using primers: F-ggggatcccggcaaccagaagaacagcc and R-gggaattcaaatccgaataaactccttccttg (restriction enzyme sites in bold) for 35 cycles at 94°C/30s, 57°C/1m, 72°C/2m to yield a 1.4 kb product. The purified product was digested with BamHI/EcoRI and ligated into pBSSK. A BamHI/AccI 776 bp fragment was subcloned into pBSSK to generate the template for Sox2 probe synthesis. A Sox3 (accession # 94125) cDNA was amplified in PCR with primers: F-ggggatccctgcaggcaagagtggcgcg and R-gggaattccgttccattgaccgcagtcc for 35 cycles at 94°C/30s, 53°C/1m, 72°C/2m to yield a 1 kb product. The purified product was digested with BamHI/EcoRI and ligated into pBSSK. A MluI/ApaI 671 bp fragment was then subcloned into pBSSK to generate the template for the Sox3 probe. The *in situ* probe for both Sox2 and Sox3 was generated using T3 and T7 primers in PCR,

purification, and transcript synthesis with T3 and T7 RNA polymerase in the presence of DIG RNA labeling mix.

Area measurements.

To determine the area occupied by neuroepithelium, surface ectoderm and mesenchyme, transverse sections through E8.5 and E9.5 embryos were stained lightly with nuclear fast red, and photographed at 10X. Digital images were opened in ImageJ (Sun Microsystems, Palo Alto, CA), and areas of: neuroepithelium, mesenchyme, and surface ectoderm measured. The length of the surface ectoderm was also determined, since it represented a very small percentage of the total area. At least three sections per embryo were measured and meaned. Mean areas from individual embryos were then averaged, and because there were small variations in the exact level of the sections between embryos, data were expressed as % of total area. Length of the surface ectoderm was set as 100% for control embryos, and K14-noggin embryos expressed as % of control. Data are expressed as mean $\pm$ sem, and significance of the observed differences evaluated using paired t-tests.

RESULTS

Keratin 14 expression.

Immunohistochemical localizations indicated that keratin 14 is expressed on E6.5 in the visceral endoderm surrounding the embryo (Figure 2-2 A, arrowhead), in the extraembryonic mesoderm, at high levels in the extraembryonic endoderm (Figure 2-2 A arrows). By E7.5, K14 was expressed in the embryonic ectoderm (Figure 2-2 B, arrowhead), and in the endoderm, at high levels in the extraembryonic endoderm (Figure 2-2 B, C, arrow), in the parietal endoderm, at lower levels in the allantois (A) and amnion (Figure 2-2 B, C, double arrows). This early expression suggests that the K14 promoter will successfully drive Noggin expression prior to and during the phases of embryonic development we wished to examine. In fact, in transgenic embryos, expression of EGFP (Figure

66

2-2 E) recapitulated the endogenous K14 expression (Figure 2-2 E). RT-PCR indicated that K14 was first detected at E6.5 and was expressed throughout gestation (Figure 2-2 F).

Transgene expression.

In the two separate rounds of transgenesis, embryos were examined on E7.5-E9.5, and eight females were allowed to deliver. From initial transfers to 26 females, 25 pregnancies resulted; two additional litters were entirely reabsorbed, producing 23 litters for analysis. The percentage of surviving embryos that carried the transgene was 89.3% on E7.5, 62.1% on E8.5 and on E9.5, and 17.9% of neonatal animals. Table 2-1 summarizes these data.

EGFP expression.

On E7.5 there was diffuse EGFP expression in transgene carriers in the region of the forming amnion, near the allantois, and in the visceral and embryonic endoderm (Figure 2-3 A, B), which mirrors the endogenous K14 expression. By E8.5, EGFP expression was seen in the allantois, the heart, ectoderm, and with intense expression in the embryonic endoderm (Figure 2-3 C, D). There was some variability in the intensity of expression of EGFP between transgenic embryos. By E9.5, the extent of EGFP expression in whole embryos was difficult to determine due to the thickness of the embryo. There was regionally intense fluorescence, for example in the tailbud region, in the ectoderm covering the cephalic neural tube, and in the otic pit. Sections of embryos prior to and following *in situ* hybridization indicated robust expression in the endoderm, and in the epidermal ectoderm (Figure 2-3 E, F). At E7.5, there was some autofluorescence in the ectoplacental cone in control embryos, but EGFP was not specifically expressed in any control embryo.

Embryo morphologies.

A spectrum of abnormalities was observed in transgenic embryos examined at the light level (Figure 2-4), or using scanning electron microscopy (Figure 2-5).

Embryos generated using either transgene exhibited a similar pattern of anomalies compared with non-transgenic littermates or with CD-1 control embryos. E7.5 control embryos had developed to the advanced primitive streak stage and headfolds with a mesenchymal core were forming. There was a well defined allantois that had not yet fused with the chorion, although the amniotic folds had typically closed. Embryos were expanded, with an even "U" shape; gastrulation was ongoing with mesoderm forming, with visceral endoderm being replaced by embryonic endoderm. Blood islands were present in the extraembryonic mesoderm of the visceral yolk sac and there was a well developed ectoplacental cone (Figure 2-4 A).

Transgene carriers (Figure 2-4 B) were often delayed in development typically having attained the primitive streak stage typical of an E7.0 rather than E7.5 day embryo. There were anomalies of axis formation in these embryos with an abnormally flattened and elongated ectodermal plate (Figure 2-4 B). The allantoic bud was often small and misoriented and there was poor demarcation of embryonic from extraembryonic tissues. There were often bulges of ectopic cells near the node as well (Figure 2-4 B, arrowhead).

By E8.5, control embryos had developed 8-14 somites and were in the process of "turning" (Figure 2-4 C). The headfolds were prominent, but neural fold fusion was still incomplete. Otic pits could be distinguished bilaterally from the surrounding ectoderm. The heart tube and the foregut pocket were also visible and well formed. The first branchial arch had developed and the second was beginning to form.

Transgenic embryos examined on E8.5 were delayed in development compared with control embryos having typically attained the 6-9 somite stage (Figure 2-4D, 5C). The neural folds in the future cervical region had often fused, but the neural tube in both anterior and posterior regions were widely open and everted over the surface ectoderm (Figure 2-4D, 2-5C). The first branchial arch was

beginning to form but often appeared hypoplastic (Figure 2-5C). There was a small cardiac bulge and poorly defined (or missing) otic pit (Figure 2-4D, 2-5C). The allantois was present, in some embryos much shorter than normal, the turning process was in progress, and many embryos exhibited poorly organized somites (Figure 2-5C).

By E9.5, non-transgenic embryos had developed 15-24 pairs of somites and had completed the turning process to adopt the fetal "C" shape (Figure 2-4E, 2-5A). The allantois had fused with the chorion and the amnion completely surrounded the embryos. The rostral neuropore had closed and the posterior neuropore was in the process of closing. The first and second branchial arches were present; the third was beginning to form. The forelimb buds and an irregularly beating heart were also present. Somites were well organized and the otic pit had closed/was closing.

Surviving transgene carriers were typically delayed in development; many still in the process of turning. They had typically developed 15-18 pairs of somites, the first and second arches were visible, although often small. There was a cardiac bulge and some embryos had developed a heartbeat; however, there were defects of cardiac rotation and development (Figure 2-4 F) in these embryos. The neural folds in the future fourth ventricle and posterior neuropore often remained widely open. The forelimb bud was just forming or absent in these embryos. Transgenic embryos that survived to E9.5 also exhibited anomalies of rotation that appear to have resulted from poor/delayed attachment of the allantois to the chorion. (Figure 2-4F, 2-5B).

Histological analyses.
Entire litters of E7.5 and E8.5 embryos were sectioned at one micrometer (araldite resin) or at ten micrometer (frozen sections), in sagittal or transverse planes. On E7.5 compared with control embryos (Figure 2-6 A, C, E), transgenic embryos (Figure 2-6 B, D, F) exhibited a number of characteristic anomalies.

Control embryos had a well developed headfold region; neuroepithelium surrounded a mesenchymal core supported by embryonic endoderm; the primitive streak directly opposite (Figure 2-6 A, C, E). The neuroepithelium was columnar and rested on an organized basement membrane, with mitotic figures present at the apical surface. In contrast, the headfold region of transgenic mice was wider and broad with a thickened neuroepithelium. The basal surface was often wavy and ectopic neural tissue was present often forming rosettes, and there was abnormal thickening of the ectoderm. The transgenic embryos were often characterized by turning abnormalities and defects of axis formation, with the primitive streak misoriented by 40-45 degrees from the midline.

There was a range in severity of the observed effects. In more severely affected embryos (Figure 2-6 G-I), the ectoderm was overgrown and disorganized, and there was a flattening of the neural plate. The ectoderm was often wavy rather than smooth, and exhibited many regions of rosetting with mitotic figures present throughout. Surprisingly, there was considerable, consistent cell death in the mesoderm, both in embryonic and in extraembryonic regions including the allantois. There was also very striking cell death at the node and forming notochordal plate. The mesoderm and the anterior embryonic endoderm were strikingly affected and pyknotic, with cells herniating from the embryo into the amniotic and yolk sac cavity. Posteriorly, the neuroepithelium and the squamous embryonic endoderm appeared morphologically normal; the columnar primitive endoderm exhibited its normal vacuolated appearance with prominent microvilli (Figure 2-6 I). With the exception of the amniotic fold that was thickened in some embryos and the allantois that exhibited significant mesodermal cell death, additional extraembryonic tissues did not appear to be affected.

Areal Measurements.

To obtain quantitative data on the area occupied by neuroepithelium and surface ectoderm, sequential transverse sections of control and K14-Noggin transgenic embryos were analyzed using ImageJ. Because the absolute level of each

section varied between embryos, data are expressed as a percentage of total section area (Figure 2-7). In wild type embryos examined on E8.5, the neuroepithelium was significantly smaller (20 $\pm$ 0.8%) proportion of the section area compared with the neuroepithelium in K14-Noggin embryos (26 $\pm$ 0.6% of the area). In wild-type embryos examined on E9.5, 27 $\pm$ 1.4% of the area of the embryo was composed of neuroepithelium, compared with 33 $\pm$ 0.7% in transgenic embryos.

There was a slight, non-statistically significant increase in the amount of mesenchyme in control embryos on both days, and a significant decrease in the length of the surface ectoderm in K14-Noggin transgenic embryos on E8.5; 63 $\pm$ 2.5 percent of control, while on E9.5, the length of the surface ectoderm in K14-Noggin transgenics was 40 $\pm$ 1.2% of control.

In situ Hybridization.
Noggin probes were employed to detect the presence of both endogenous and transgene driven Noggin mRNA in control and transgenic embryos from E7.5 to E9.5. To determine the extent of neural differentiation we used probes for Sox2 and Sox3. In prestreak embryos (E6.5), both Sox2 and Sox3 are expressed throughout the epiblast and in the extraembryonic ectoderm near the boundary between embryonic and extraembryonic tissues. After gastrulation, they are restricted to the anterior ectoderm (future neural plate) and the chorion (Wood and Episkopu, 1999). On E7.5, noggin was restricted in expression to the node of control embryos. Transgenic embryos exhibited expression of EGFP (Figure 2-8 A) and of Noggin mRNA (Figure 2-8 B) additionally in the embryonic endoderm, in the extraembryonic endoderm, and amnion. Interestingly, K14-Noggin expression also appeared to induce sox gene expression in endodermal tissues. By E8.5 in transgenic embryos, Noggin was expressed in the endoderm of the foregut and heart tube as well as in a dorsal region of epidermal ectoderm, where Sox2, Sox 3, and EGFP were also expressed (Figure 2-8 E-H). The possible neural characteristic of these epidermal cells is not yet known. Not

71

surprisingly, ectopic expression of Noggin in the embryonic endoderm of E8.5 was not sufficient to cause expression of Sox2 or Sox3 (Figure 2-8). At E9.5, the neural folds of transgenic embryos were everted over the surface ectoderm, which expressed Noggin, Sox2 and high levels of Sox3 (Figure 2-8 I). In wild type embryos on E9.5, Sox2 (J) and Sox3 mRNA was restricted to the neuroepithelium.

Transgenic neonates.

In the eight litters examined postnatally, only 17.9% of the neonates carried the transgene. Two were female, five male. These animals exhibited a number of anomalies including syndactyly (n=3), claw-like fusion of the digits (n=3), anomalies of teeth (molar fusions) and jaws (n=6), and of the facial region (n=4). Three had sparse, coarse fur. One severely affected female died soon after birth, the other was mated by no pregnancies resulted. Of the five male animals, only one was fertile but no transgenic offspring were produced by that male.

DISCUSSION

Noggin misexpression produced a spectrum of changes in postimplantation staged embryos, including defective endoderm and mesoderm differentiation at gastrulation, widening of the neural plate, abnormal development of the allantois and of axis formation, as well as skeletal defects. Previous gene targeting studies have identified a critical role for BMP4 in allantois development and primordial germ cell formation (Lawson, 1999; Fujiwara et al., 2001; Ying et al., 2001), in mesoderm differentiation, left-right asymmetry and heart looping (Winnier et al., 1999; Fujiwara et al., 2002).   The anomalies of endoderm differentiation observed in the current investigation suggest a role for BMP signaling in this process as well. Similar ectopic cells distal to the node and in the amniotic cavity were also observed in the BMP4 null embryos (Fujiwara et al., 2002); although it is possible that noggin misexpression inhibited signaling by other BMP family members expressed in this region. Defects of axial

72

mesendoderm differentiation were also present in embryos deficient in embryonic Bmpr1a (Davis et al., 2004).

Current evidence suggests that signaling molecules present in the microenvironment of the posterior primitive streak are responsible for allocating cells to somatic fates, to extraembryonic mesoderm, or to primordial germ cells (PGCs) (Saitou et al., 2002). Just prior to gastrulation (E6-E6.5), BMP4 is expressed in the extraembryonic ectoderm where it is required for the consolidation and initial differentiation of PGCs in the proximal region of the embryo. At E6.5, at the mid to late streak stage, BMP4 is responsible for the alignment and posterior migration of the PGCs (Lawson et al., 1999); Fujiwara et al., 2001), then at E6.75-E7, BMP4 is expressed in the extraembryonic mesoderm where its role appears to be in promoting survival and organized migration of the PGCs back into the embryo.

Careful study of the development of the allantois has demonstrated that BMP4 is expressed initially in the mesoderm lining the exocoelomic cavity, in the mesothelium covering the allantoic bud, and in the posterior amniotic fold. At the 6 somite stage, BMP4 is expressed throughout the allantois; by the 16 somite stage, BMP4 is present at the site of fusion of allantois and chorion (Down et al., 2004). Somewhat surprisingly, cytokeratins are also expressed in the allantois during its early development (Hashido et al., 1991; Downs et al., 2004; this study). At E6.5 and E7.5, K14 is expressed at high levels in the visceral endoderm, and at lower levels in the forming amnion and in the cells covering the allantois, where it would direct Noggin expression and inhibit BMP signaling. Expression of K14 in the allantois is downregulated after E8.5, (Downs et al., 2004; this study). Modulation of BMP activity in the allantois my explain the rotation defects and anomalies of tailbud development observed in the current investigation, since fusion of the allantois with the overlying chorion forms a stable pivot point for rotational movements that occur as the U shaped early embryo adopts the fetal C shape.

It is clear that BMP signaling plays a critical role in maintaining the PGC niche since embryos null for BMP4, for additional family members BMP2, BMP8b (Ying et al., 2000; Ying and Zhao, 2001), or for BMP signal transducing Smad proteins such as Smad 1 (Tremblay et al., 2001) or Smad 5 (Chang and Matsuk, 2001) have reduced numbers of primordial germ cells and exhibit varying degrees of defects of allantois development. These results are consistent with the reproductive failure observed in the few surviving adult transgene carriers observed in the current investigation and with recent observations that exposure of E6.75 embryos to small hairpin RNAs directed to Bmp4 result in failure of ovary and testis differentiation (Emmett et al., in preparation).

After gastrulation, BMP4 is expressed in the extraembryonic mesoderm derived from the epiblast and in the posterior primitive streak where it appears to regulate the development of left-right asymmetry in the embryo and thereby cardiac looping (Fujiwara et al., 2001). Restoration of BMP4 in the trophoblast-derived extraembryonic ectoderm by tetraploid rescue of BMP4 null embryos restored both the node and the anterior-posterior organization of the embryo, suggesting that the defects of axis organization and left-right asymmetry observed in the current study may result from the inhibition of BMP signaling in the extraembryonic ectoderm.

Tetraploid rescue of BMP4 null embryos also produced embryos with broad, wavy neural plates that failed to fuse, similar to those observed in the current investigation. These observations as well as similar axis elongation defects observed in embryos null for the Bmpr1a (Mishina et al., 1995) which transduces BMP4 signals, as well as in the BMP4 null embryos themselves (Winnier et al., 1995), suggest that BMP4 present in the epiblast and embryonic ectoderm is required for neural ectodermal differentiation and neurulation. Like the E8.5 embryos in the current investigation, embryos null for Bmpr1a exhibited similar defects in ectodermal organization and stratification of the neural ectoderm

74

(Mishina et al., 1995), while embryos mosaic for Bmpr1a activity have expanded neuroepithelium at the expense of surface ectoderm (Davis et al., 2004).

The unsuspected expression of K14 in the visceral endoderm significantly complicated analysis of the transgenic phenotype, as signals from the extraembryonic endoderm influence both patterning and the organization of the early embryo, particularly the induction and patterning of the mesoderm. Interestingly, the organization of the visceral endoderm itself appeared normal, but as cells from the primitive streak replaced visceral endoderm with embryonic endoderm, there was widespread cell death in both the mesoderm where BMP signals are required (Lawson et al., 1999) as well as the anterior (but not posterior) embryonic endoderm. Specification of epiblast cell fate at gastrulation is thought to be determined largely by the relative position of cells within the epiblast, with extraembryonic mesoderm forming first followed by embryonic mesoderm and endoderm (Lawson, 1999). Signaling by TGFβ superfamily members is critically involved in this process, as demonstrated by the multiple gastrulation, neural induction, and patterning defects in null embryos (reviewed in Zhao, 2002). There appears to be considerable "cell mixing" of epiblast cells at gastrulation, suggesting that the local microenvironment, is critical in determining cell fate (e.g., Tremblay et al., 2000). Gene targeting experiments have demonstrated that signaling by Nodal and Smad2 is required to specify the anterior mesendoderm (Tremblay et al., 2000); Vincent et al., 2003). Embryos lacking the common Smad, Smad4 have deficiencies in endoderm formation and fail to express T (Sirard et al., 1998), like the Bmpr1a (Mishina et al., 1995) and BMP4 (Winnier et al., 1995) null embryos resulting from a primary growth deficiency in the embryonic ectoderm (Sirard et al., 1998), although in the conditional Bmpr1a embryos there is an expansion of mesendoderm (Davis et al., 2004). These results and others in which genes expressed in the visceral endoderm, particularly Foxh1 (Duncan et al., 1997) were deleted, have demonstrated and essential role for endoderm derived signals in mesoderm specification at gastrulation. Although Noggin/Chordin double null embryos

75

exhibited marked deficiencies in the formation of anterior embryonic ectoderm (Bachiller et al., 2000), the current investigation suggests that local inhibition of BMP signaling at gastrulation may alter the allocation of cells to the definitive endoderm, and consistent with the known requirement of BMP4 for mesoderm differentiation, results in widespread apoptosis of mesodermal cells and of anterior embryonic endoderm. Similar observations were recently made in 20 somite BMP4 null embryos where there was an irregular boundary at the endoderm transition zone, and cells piled up near the node. As in the current investigation, the posterior amniotic cavity of BMP4$^{-/-}$ embryos also contained ectopic mesodermal and endodermal cells and clumps of misdirected cells were present near the node (Lawson et al., 1999). These observations are also reminiscent of FGF8 null embryos where mesodermal cells fail to migrate normally through the primitive streak and fill the amniotic cavity (Sun et al., 1999). Although these results support a role for BMP signaling in mesoderm specification at gastrulation, its role in endoderm differentiation and survival remains to be further determined.

The keratin 14 promoter has previously been employed to develop other transgenic mice (Oro et al., 1997; Guha et al., 2002, 2004; Plikus et al., 2004); however, these mice did not exhibit the early phenotype observed in the current investigation, possibly due to genetic variation between strains, transgene copy number, and/or functional redundancy with BMP2 and BMP8b (Ying and Zhao, 2001). Early expression of RCAS-noggin in the chick embryo produced similar widespread early lethality, however (Pizette and Niswander, 1999). BMP4 gene deletion was lethal prior to gastrulation on an inbred background (C56Bl/6 x CBA) (Winnier et al., 1995), but embryos survive to the 20 somite stage when maintained on a Black Swiss background (Lawson et al., 1999). Given its unsuspected early expression in the extraembryonic endoderm and mesoderm, the allantois and later in the embryonic endoderm, K14 might be useful in driving expression of other signaling molecules to these regions of the early embryo.

BMPs play multiple roles in the development of bone and cartilage (Canalis et al., 2003). Interestingly, mice in which K14 was employed to drive noggin expression developed syndactyly and polydactyly on an outbred background, but similar "lobster claw" type digital defects and distal reductions formed on the Fvb inbred strain (Guha et al., 2002) employed in the current investigation, and resulted in the loss of the nail bed on the Black background (Plikus et al., 2004).

Failure of differentiation of lateral somites was previously observed in both the noggin$^{-/-}$ embryos (Brunet et al., 1998), and following RCAS-Noggin injection into the chick limb bud (Capdevila and Johnson, 1998). The tooth abnormalities observed in the current investigation have not previously been reported in the noggin transgenic mice. Tucker et al (1998) observed that in explants cultures, noggin misexpression converted incisor teeth to molars, with a variety of intermediate tooth forms. BMP4 is normally expressed in patches in the early oral epithelium where it may control the spacing of teeth by inducing genes such as Msx1 which specify prospective incisor fate; misexpression of Noggin in the oral epithelium clearly affected incisor growth and likely influenced tooth spacing and the molar fusions observed here.

Much has been learned recently of the roles of these molecules in controlling cell fate decisions in the microenvironment of stem cell populations including; primordial germ cells (Saitou et al., 2002), the tooth germ (Tucker et al., 1998), hair follicle (Kulessa et al., 2000), and neural stem cells (Lim et al., 2000), where there is a constant association between BMP expression, cell proliferation and general stem cell maintenance (Ying et al., 2003), while inhibition of BMP signaling e.g., by Noggin expression promotes differentiation (Lim et al., 2000; Gratsch and O'Shea, 2002) and inhibits cell proliferation. Increasing evidence suggests a similar local control of cell fate decisions at gastrulation between mesoderm and ectoderm, with genes such as Churchill controlling the allocation of epiblast to mesoderm (Sheng et al., 2003). The ectoderm is then sensitized to BMP signals by the expression of Sip1 (Van de Putte et al., 2003) or Geminin

(Kroll et al., 1998), induction of a neural phenotype by the BMP inhibitors Noggin, Chordin; (Harland, 2000), followed by the expression of neurogenic genes. Not surprisingly, the microenvironmental signals that control cell type specification at gastrulation appear to be similar to those that maintain other stem cell populations in the embryo and the adult (Watt and Hogan, 2000).

ACKNOWLEDGEMENTS:

This chapter represents the contents of an article in revision:

De Boer LS, Gratsch TE, Premo AM, and O'Shea KS. 2005. Transgenic
    misexpression of Noggin in the early post-implantation mouse embryo. Dev
   Dyn.
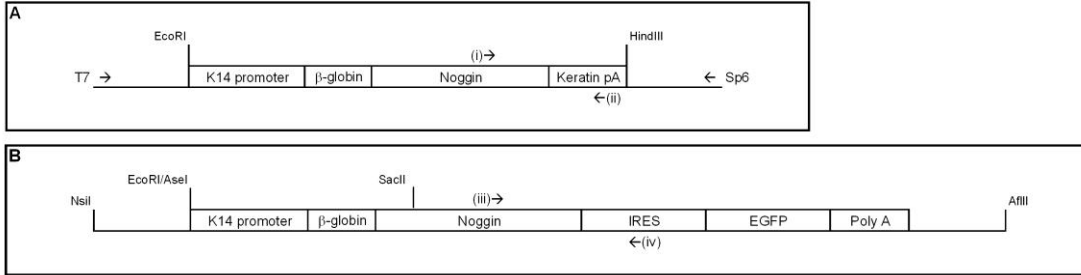
Figure 2-1. **K14-noggin expression constructs.**

A. K14 promoter driving Noggin expression.

B. Includes a fluorochrome reporter, EGFP.

Figure 2-2. Keratin 14 expression.

A-E. Immunohistochemical localization of K14 in sagittal sections of embryos on E6.5 and E7.5. **A.** On E6.5, K14 is expressed in the embryonic endoderm (arrowhead), and at particularly high levels in the extraembryonic endoderm (arrows) at the embryonic-extraembryonic boundary. At this stage, expression was higher in the posterior endoderm (double arrows) compared with the anterior endoderm. **B,C.** On E7.5, K14 was expressed at high levels in the extraembryonic endoderm (arrows) and embryonic endoderm (arrowhead), in cells overlying the allantois and within the allantoic bud (A), in the amnion (double arrows) and in the chorion. Parietal endoderm (PE) cells attached to the Reichert's membrane at the distal region of the embryo also expressed K14. **D,E.** Transverse sections through the anterior neural folds in an E8.5 transgenic embryo illustrating the considerable overlap in expression of endogenous K14 (D) and K14-driven EGFP (E) in surface ectoderm (double arrows) and endoderm (arrowheads). Anterior is oriented to the left in all figures, but D,E. E = embryonic ectoderm, EPC = ectoplacental cone, A = allantois, NE = neuroepithelium, M = mesenchyme. Scale bars A,B = 200 micrometers, C-E = 100 micrometers.

F. RT=PCR was carried out on RNA isolated from E6.5 to E13.5 staged embryos to determine the onset of keratin 14 (K14) expression (266 bp product) compared with β-actin (560 bp).
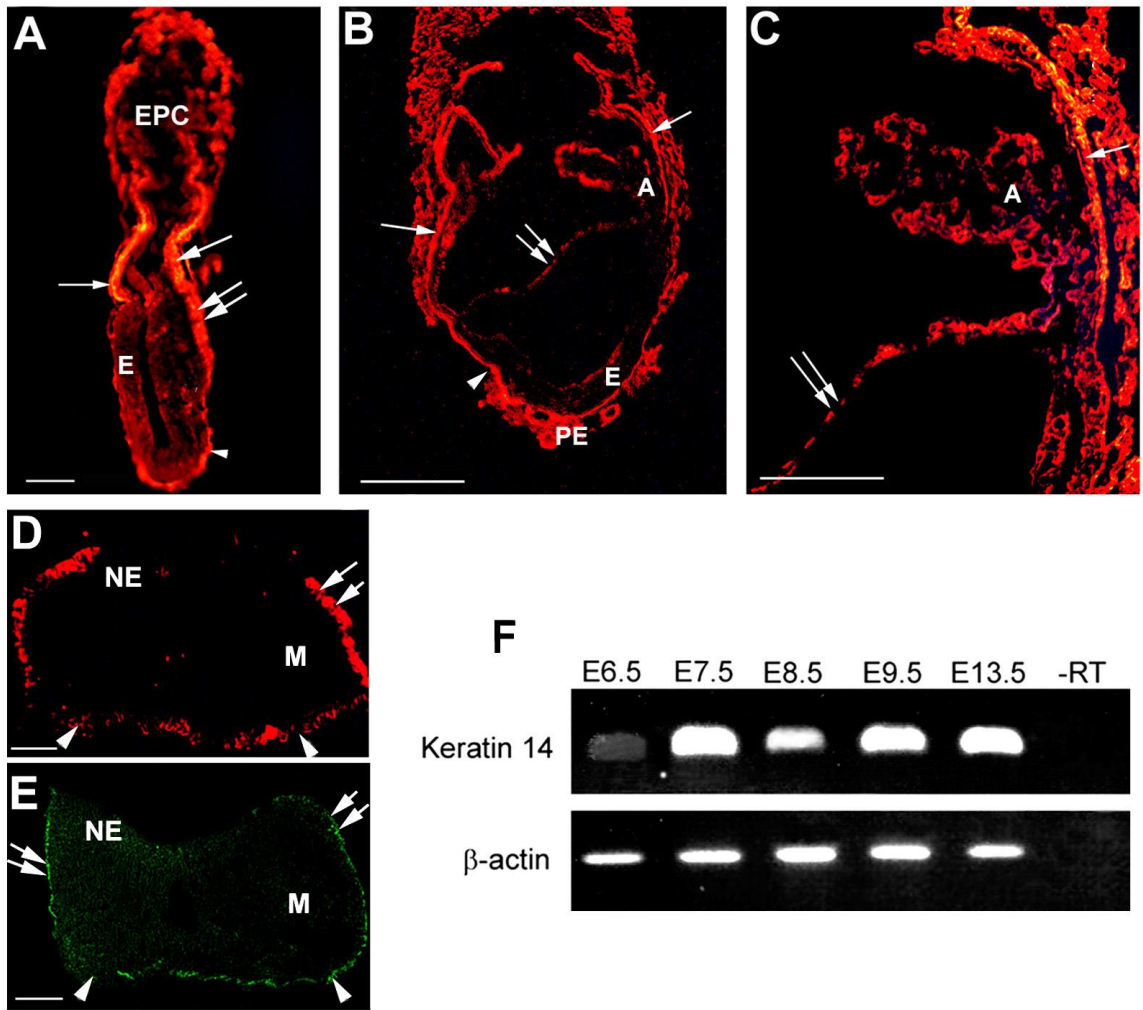
Figure 2-3. EGFP expression in transgenic embryos.

The expression of EGFP was analyzed using epifluorescence microscopy of whole embryos (A,C), and in sections (B,D-F).

A, B. At E7.5, EGFP was expressed at high levels in the extraembryonic endoderm (A, arrows) surrounding the ectoplacental cone (EPC), and at lower levels in the embryonic endoderm (arrowheads). EGFP was also present in the allantois, and at low levels in the embryonic ectoderm (E) at this stage. The embryos is A,B are oriented with anterior toward the left.

C, D. At E8.5, there was low EGFP expression throughout the embryo. The arrow in C indicates the foregut pocket just below the forming headfolds. EGFP was expressed in the primitive and embryonic endoderm (D, arrowheads), in the allantois (A) and in the ectoderm (E).

E, F. On E9.5, EGFP was expressed at high levels in the surface (epidermal) ectoderm (SE), but not in the neuroepithelium (NE) of the closing neural folds, or in the mesenchyme (Mes). Control embryos and sections were negative for EGFP expression (not shown). Bars = 200 micrometers
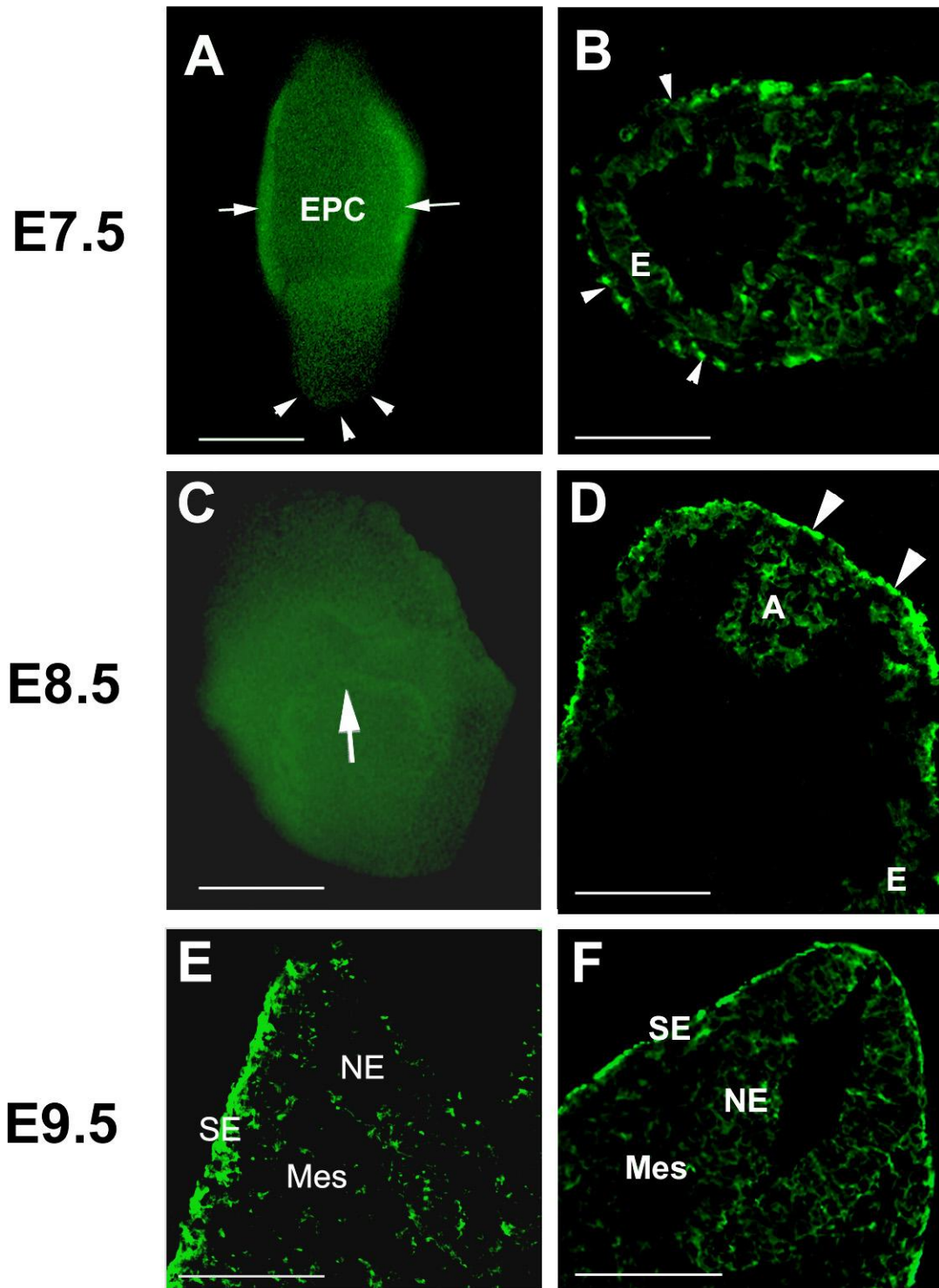
Figure 2-4. Morphologies of transgenic embryos.

Phase-contrast images of control (A,C,E) and transgenic (B,D,F) embryos on EF7.5 (A,B), E8.5 (C,D), and E9.5 (E,F). Transgenic embryos were uniformly developmentally delayed compared to controls.

A,B. Side views of E7.5 embryos. Compared with control embryos (A), the earliest observable difference at E7.5 in K14 noggin transgenic embryos was the poor demarcation between embryonic and extraembryonic regions (arrow, A). In transgenic embryos (B), there were abnormalities of anterior-posterior elongation of the embryo, and cells extruded near the node (arrowhead).

C,D. Dorsolateral views of E8.5 embryos. By E8.5, the neural folds (NF) had fused in the future cervical region in control embryos (C), but were often widely open in K14-noggin embryos (D). The allantois (A) was highly differentiated in controls, and often rudimentary in K14-noggin transgenics. H = heart.

E, F. Side views of E9.5 embryos. Control embryos (E) had completed the turning process, well organized optic (OV) and otic vesicles had formed, the first (1) branchial arch was present and the second arch was forming. In K14-noggin transgenic embryos (F), there were rotational anomalies of the heart (H), the optic vesicles were mis-oriented and there were anomalies of rotation of the tailbud region (arrow). Anterior is oriented toward the left in all figures. EPC = ectoplacental cone, NF = neural folds, H = heart, OV = optic vesicle, 1 = first branchial arch. Scale bars = 500 micrometers.
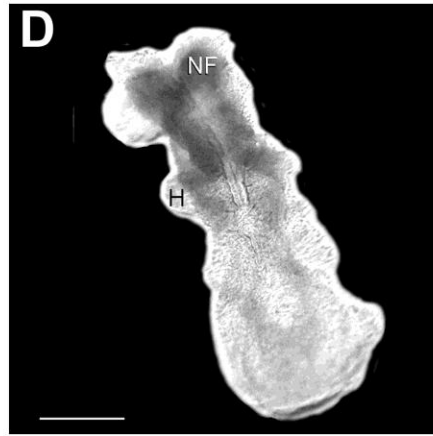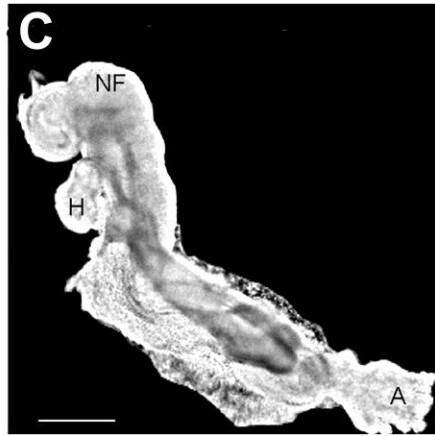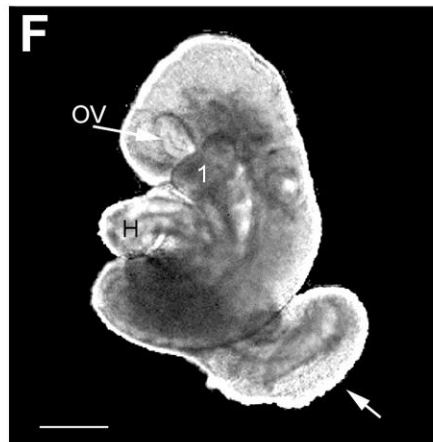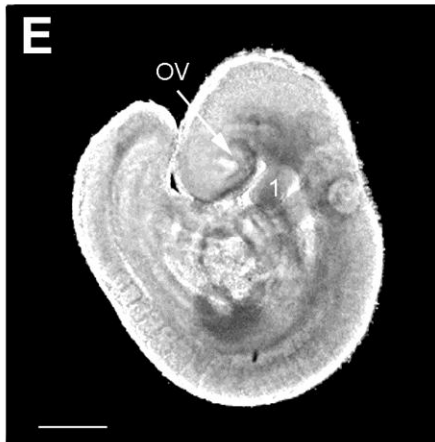
Control **K14-noggin**

E7.5
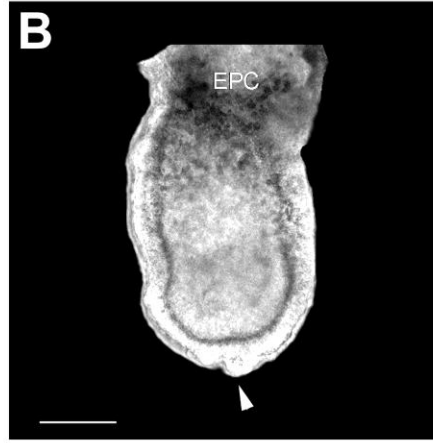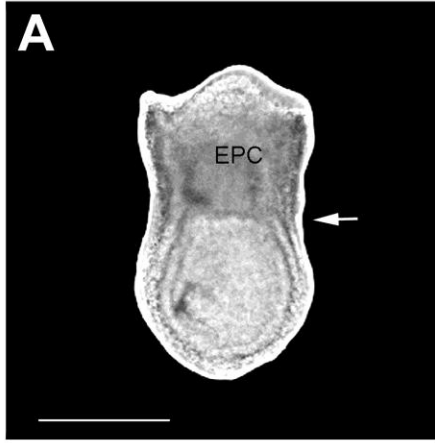
E8.5

E9.5
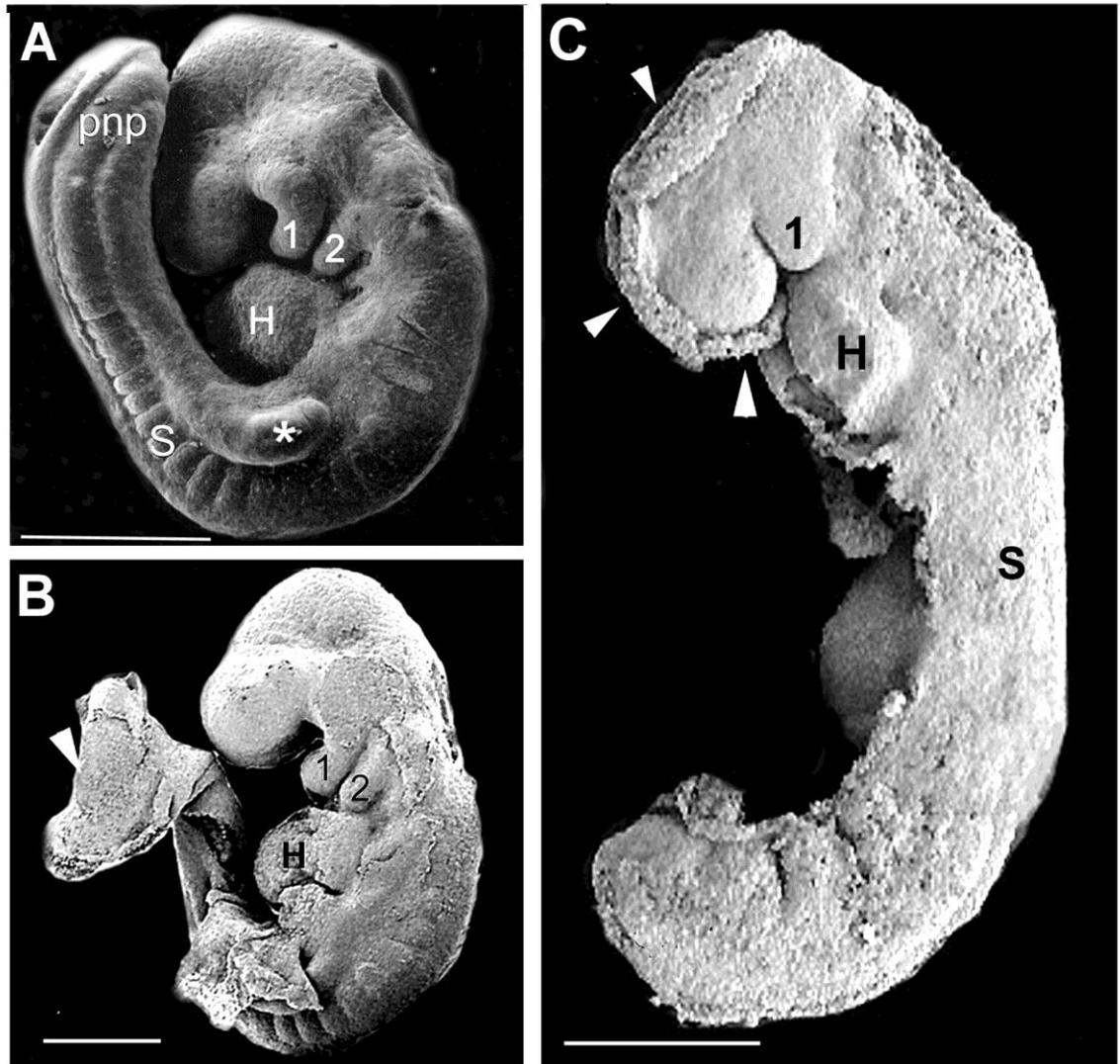
Figure 2-5. Scanning electron microscopy

SEM images of control (A) and transgenic (B,C) embryos on E8.5 (C) and on E9.5 (A,B), illustrating the morphological alterations typical of transgenic embryos (B,C). In control embryos (A), the neural folds have nearly closed throughout the cephalic region, remaining open in the posterior neuropore (pnp). Somites (S) are highly organized, the first (1) and second (2) branchial arches, heart (H) and forelimb buds (*) are characteristically well formed. At this stage, many transgenic embryos had begun, but not completed the turning process, as the posterior portion of the embryo was abnormally rotated (arrowhead, B). In many transgenic embryos, forelimb bud development was delayed (B,C). On E8.5 in K14-noggin transgenic embryos, the neural folds had typically failed to fuse in the cephalic region, remaining everted over the surface ectoderm (arrowheads, C). Somites (S) were poorly organized and the first branchial arch (1) was small and unsegmented. Scale bars = 500 micrometers. Anterior is toward the left.

Figure 2-6. Histological analysis of E7.5 embryos.

Schematic diagram illustrating the level of the transverse sections (after Kaufman, 1992); anterior left.

**A-F.** Transverse one micron resin sections through control (A,C,E) and K14-noggin transgenic (B,D,F) embryos, anterior is down. In the control embryo, the primitive streak (PS) region is located directly opposite (bar) the headfolds, unlike the K14-Noggin embryo in which the primitive streak is mis-oriented at approximately 145° from the headfolds. Although the K14-noggin embryo is sectioned at a slight angle, in this and other K14-Noggin embryos, there is considerable stratification of the neuroepithelium in the headfold region (NE arrow, D). At lower axial levels, there are large aggregates of cells present in the endoderm (arrow in F). PS = primitive streak, NE = neuroepithelium, Mes = mesenchyme.

G-I. Sagittal sections of K14-Noggin transgenic embryos, anterior left. G. In this embryo, the neuroepithelium (NE) is abnormally stratified, there are cells outside the node (double arrows) and within the amniotic cavity, and there is widespread cell death in the mesoderm (Mes), and in the anterior embryonic endoderm. The amnion (A), and posterior embryonic endoderm (single arrow G,H) and the embryonic ectoderm are not affected. H is a higher magnification view of G, illustrating the extruded cells near the node. The morphology of the embryonic endoderm posterior to the node is normal and squamous (single arrows G,H). I. Another E7.5 embryo illustrating that at the junction between extra- and embryonic regions of the primitive endoderm (ExEn) appears viable, although there is widespread cell death in embryonic and extraembryonic mesoderm extending into the allantois and in the covering mesendodermal cells. A = amnion, NE = neuroepithelium, ExEn = extraembryonic endoderm, EE = embryonic ectoderm, Mes = mesenchyme. Anterior is oriented to the left in each figure. Bars A-G = 200 micrometers; H, I 100 = micrometers.
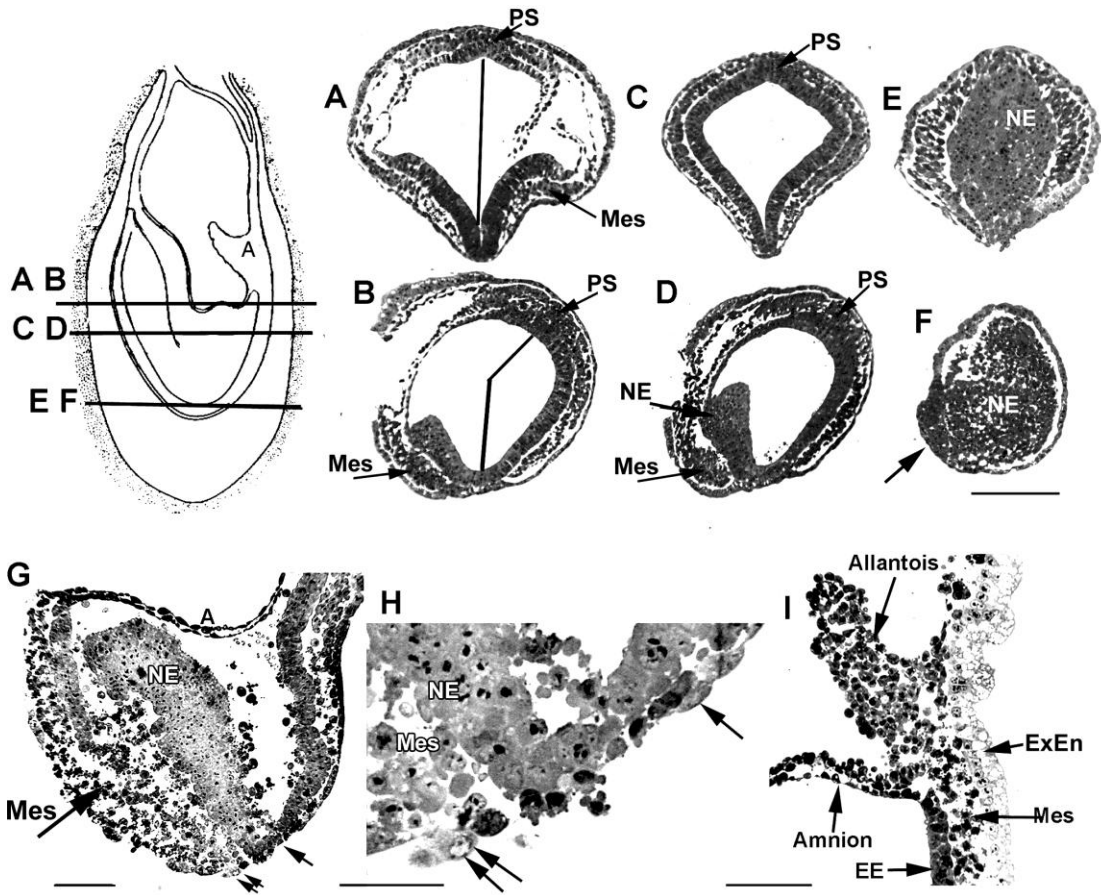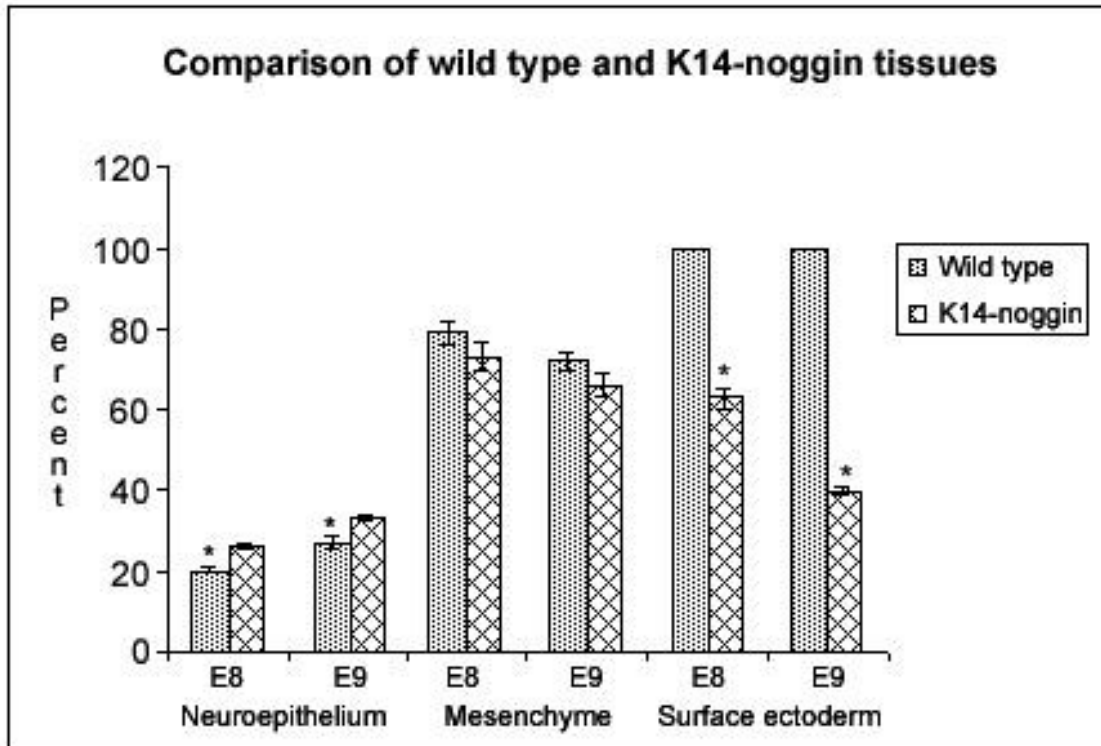
Figure 2-7. Mean areas of wild-type and K14-noggin transgenic tissues.

The average area of the neuroepithelium was significantly greater in transgenic embryos on both E8.5 and E9.5. The area of mesenchyme was slightly reduced in transgene carriers, while the mean length of the surface ectoderm was significantly reduced in K14-Noggin transgenic embryos on both days. * = wild type significantly less than K14-Noggin, $p \leq 0.01$. ** = wild type significantly greater that K14-Noggin, $p \leq 0.01$.
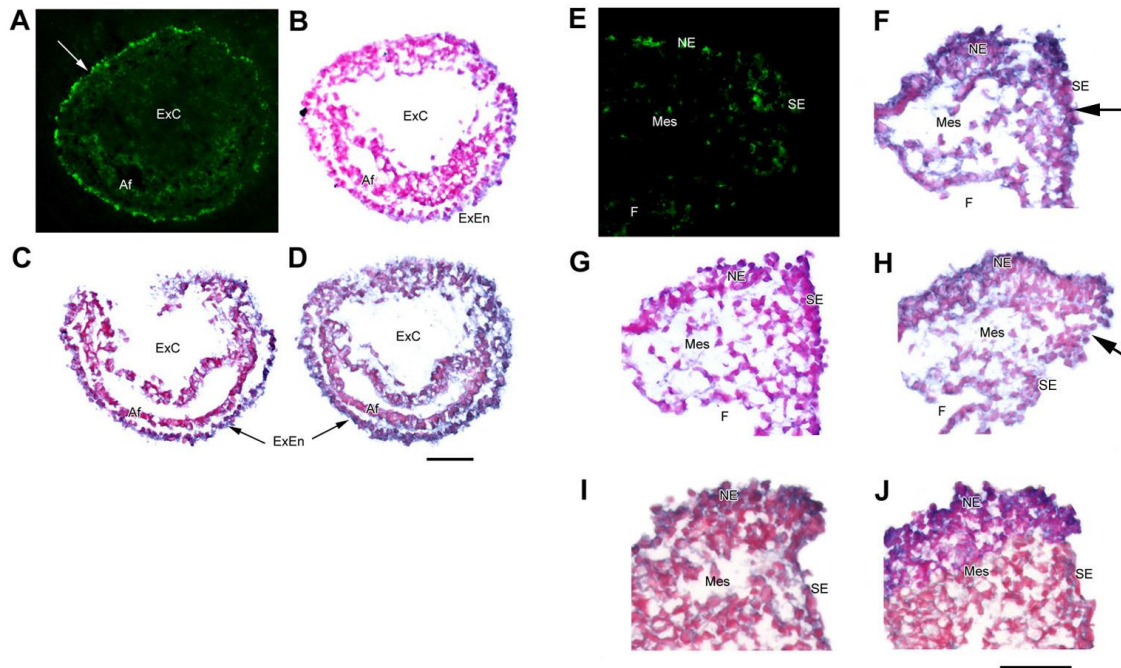
Figure 2-8. *In Situ* **hybridization analysis.**

In E7.5 transgenic embryos (**A-D**), EGFP expression (A) was driven to the extraembryonic endoderm (arrow) and at lower levels in the amniotic fold (Af), as is the expression of noggin (B). Somewhat surprisingly, Sox2 (C), and Sox3 (D) were expressed in these regions as well. ExC = exocoelomic cavity, ExEn = extraembryonic endoderm, Af = posterior amniotic fold.

E-G. Sequential transverse sections through and E8.5 transgenic embryo illustrating high magnification views of the headfold region. E. EGFP was expressed in the surface ectoderm (SE). Sox3 (F), and Sox2 (G), are normally expressed in the neuroepithelium at this stage and Sox3 expression particularly, was also driven by the transgene in the surface ectoderm (arrow).

H. Transverse section of another E8.5 transgenic embryo illustrating the expression of Sox3 mRNA in the neuroepithelium, extending laterally in the SE field (arrow).

I. An early E9.5 transgenic embryo illustrating the everted neural folds and high expression of Sox2 mRNA in the neuroepithelium and dorsal portion of the surface ectoderm.

J. Transverse section through the anterior neural folds of an early E9.5 wild type embryo illustrating the normal expression in of Sox2 in the neuroepithelium, not extending into the surface ectoderm. NE = neuroepithelium, SE = surface ectoderm, F = foregut, Mes = mesenchyme. Bars = 100 micrometers.

Day	Litters	Decidual Swellings	Reabsorptions	Living Embryos (%)	Transgenic Embryos (%)
7.5	5	54	26	28 (51.9)	25 (89.3)
8.5	6	64	35	29 (45.3)	18 (62.1)
9.5	6	65	36*	29 (44.6)	18 (62.1)
Post-natal	8	--	--	39 (17.9)	7 (17.9)
Totals:	25	183	61	125 (68.3)	68 (54.4)

* indicates 2 entire litters

Table 2-1. Summary of transgenic embryos.

REFERENCES

Agius E, Oelgeschlager M, Wessely O, Kemp C, De Robertis EM. 2000. Endodermal Nodal-related signals and mesoderm induction in Xenopus. Develop 127: 1173-1183.

Anderson RM, Lawrence AR, Stottmann RW, Bachiller D, Klingensmith J. 2002. Chordin and noggin promote organizing centers of forebrain development in the mouse. Develop 129: 4975-4987.

Bachiller D, Klingensmith J, Kemp C, Belo JA, Anderson RM, May SR, McMahon JA, McMahon AP, Harland RM, Rossant J, DeRobertis EM. 2000. The organizer factors chordin and noggin are required for mouse forebrain development. Nature 403: 658-661.

Balemans W, van Hul W. 2002. Extracellular regulation of BMP signaling in vertebrates: a cocktail of modulators. Dev Biol 250: 231-250.

Bally-Cuif L, Hammerschmidt M. 2003. Induction and patterning neuronal development and its connection to cell cycle control. Curr Opin Neurobiol 13: 16-25.

Bellusci S, Henderson R, Winnier G, Oikawa T, Hogan BL. 1996. Evidence from normal expression and targeted misexpression that bone morphogenetic protein (Bmp-4) plays a role in mouse embryonic lung morphogenesis. Develop 122: 1693-1702.

Belo JA, Bouwmeester T, Lenys L, Kertesz N, Gallo M, Follettie M, DeRobertis EM. 1997. Cerberus-like is secreted factor with neuralizing activity expressed in the anterior primitive endoderm of the mouse gastrula. Mech Dev 68, 45-57.

Beppu H, Kawabata M, Hamamoto T, Chytil A, Minowa O, Noda T, Miyazono K. 2000. BMP type II receptor is required for gastrulation and early development of mouse embryos. Dev Biol 221: 249-258.

Brennan J, Lu CC, Norris DP, Rodriguez TA, Beddington RSP, Robertson EJ. 2001. Nodal signaling in the epiblast patterns the early mouse embryo. Nature 411: 965-969.

Canalis E, Economides AN, Gazzerro E. 2003. Bone morphogenetic proteins, their antagonists, and the skeleton. Endo Rev 24: 218-235.

Capdevila J, Johnson RL. 1998. Endogenous and ectopic expression of noggin suggests a conserved mechanism for regulation of BMP function during limb and somite patterning. Dev Biol 197: 205-217.

Chang H, Matzuk MM. 2001. Smad5 is required for mouse primordial germ cell development. Mech Dev 104: 61-67.

Chang H, Huylebroeck D, Verschueren K, Guo Q, Matzuk MM, Zwijsen A. 1999. Smad5 knockout mice die at mid-gestation due to multiple embryonic and extraembryonic defects. Develop 126: 1631-1642.

Chang H, Zwijseen A, Vogel H, Huylebroeck D, Matzuk MM. 2000. Smad5 is essential for left right asymmetry in mice. Dev Biol 219: 71-78.

Davis S, Miura S, Hill C, Mishina Y, Klingensmith J. 2004. BMP receptor IA is required in the mammalian embryo for endodermal morphogenesis and ectodermal patterning. Dev Biol 270: 47-63.

Detrick RJ, Dickey D, Kintner CR. 1990. The effects of N-cadherin misexpression on morphogenesis in Xenopus embryos. Neuron 4: 493-506.

Dickson MC, Martin JS, Cousins FM, Kulkarni AB, Karisson S, Akhurst RJ. 1995. Defective haematopoiesis and vasculogenesis in transforming growth factor-beta 1 knock out mice. Develop 121: 1845-1854.

Downs KM, Hellman ER, McHugh J, Barrickman K, Inman KE. 2004. Investigation into a role for the primitive streak in development of the murine allantois. Develop 131: 37-55.

Dudley AT, Lysons KM, Robertson EJ. 1995. A requirement for bone morphogenetic protein-7 during development of the mammalian kidney and eye. Genes Dev 9: 2795-2807.

Duncan SA, Nagy A, Chan W. 1997. Murine gastrulation requires HNF-4 regulated gene expression in the visceral endoderm: tetraploid rescue of Hnf-4 -/- embryos. Develop 124: 279-287.

Fuchs E. 1994. Epidermal differentiation and keratin gene expression. Princess Takamatsu Symposia. 24: 290-302.

Fujiwara T, Dehart DB, Sulik KK, Hogan BLM. 2002. Distinct requirements for extra-embryonic and embryonic bone morphogenetic protein 4 in the formation of the node and primitive streak and coordination of left-right symmetry in the mouse. Develop 129: 4685-4696.

Fujiwara T, Dunn NR, Hogan BLM. 2001. Bone morphogenetic protein 4 in the extraembryonic mesoderm is required for allantois development and the localization and survival of primordial germ cells in the mouse. Proc Natl Acad Sci USA 98: 13739-13744.

Geriach LM, Hutson MR, Germiller JA, Nguyen-Luu D, Victor JC, Barald KF.
2000. Addition of the BMP4 antagonist, noggin, disrupts avian inner ear
development. Develop 127: 45-54.

Gratsch TE, DeBoer LS, O'Shea KS. 2003. RNA inhibition of BMP-4 gene
expression in post-implantation mouse embryos. genesis 37: 12-17.

Gratsch TE, O'Shea KS. 2002. Noggin and chordin have distinct activities in
promoting lineage commitment of mouse embryonic stem (ES) cells. Dev
Biol 245: 83-94.

Gu Z, Nomura M, Simpson BB, Lei H, Fijen A, van den Eijinden-van Raaij J,
Donahoe PK, Li E. 1998. The type I Activin receptor ActRIB is required for
egg cylinder organization and gastrulation in the mouse. Genes Dev 12:
844-857.

Gu Z, Reynolds EM, Song J, Lei H, Feijen A, Yu L, He W, MacLaughlin DT, van
den Eijinder-vanRaaij J, Donahoe PK, Li E. 1999. The type I serine-
threonine kinase receptor ActRIA (ALK2) is required for gastrulation of the
mouse embryo. Develop 126: 2551-2561.

Guha U, Gomes WA, Kobayashi T, Pestell RG, Kessler JA. 2002. In vivo
evidence that BMP signaling is necessary for apoptosis in the mouse limb.
Dev Biol 249: 108-120.

Guha U, Gomes WA, Samanta J, Gupta M, Rice FL, Kessler JA. 2004. Target-
derived BMP signaling limits sensory neuron number and the extent of
peripheral innervations in vivo. Develop 131: 1175-1186.

Hanna LA, Foreman RK, Tarasenko IA, Kessler DS, Labosky PA. 2002.
Requirement for Foxd3 in maintaining pluripotent cells of the early mouse
embryo. Genes & Dev 16: 2650-2661.

Harland R. 2000. Neural induction. Curr Opin Genet Dev 10: 357-362.

Hashido K, Morita T, Matsushiro A, Nozaki M. 1991. Gene expression of
cytokeratin endo A and endo B during embryogenesis and in adult tissues of
mouse. Exp Cell Res 192: 203-212.

Hoodless PA, Pye M, Chazaud C, Labbe E, Attisano L, Rossant J, Wrana JL.
2001. FoxH1 (Fast) functions to specify the anterior primitive streak in the
mouse. Genes & Dev 15: 1257-1271.

Johnson MH, Ziomek CA. 1981. The foundation of two distinct cell lineages
within the mouse morula. Cell 24: 71-80.

Kan L, Hub M, Gomes WA, Kessler JA. 2004. Transgenic mice overexpressing BMP4 develop a fibrodysplasia ossificans progressive (FOP)-like phenotype. Amer J Pathol 165: 1107-1115.

Kaufman MH. 1992. The Atlas of Mouse Development. London: Academic Press.

Kintner C. 1988. Effects of altered expression of the neural cell adhesion molecule, N-CAM, on early neural development in Xenopus embryos. Neuron 1: 545-555.

Kroll KL, Salic AN, Evans LM, Kirschner MW. 1998. Geminin, a neuralizing molecule that demarcates the future neural plate at the onset of gastrulation. Develop 125: 3247-3258.

Kulessa H, Turk g, Hogan BL. 2000. Inhibition of Bmp signaling affects growth and differentiation in the anagen hair follicle. EMBO J 19: 6664-6674.

Lawson KA. 1999. Fate mapping the mouse embryo. Int J Dev Biol 43: 773-775.

Lawson KA, Dunn NR, Roelen BAJ, Zeinstra LM, Davis AM, Wright CVE, Korving JPWFM, Hogan BLM. 1999. Bmp4 is required for the generation of primordial germ cells in the mouse embryo. Genes & Dev 13: 424-436.

Lim DA, Tramontin AD, Trevejo JM, Herrrera DG, Garcia-Verdugo JM, Alvarez-Buylla A. 2000. Noggin antagonizes BMP signaling to create a niche for adult neurogenesis. Neuron 28: 713-726.

Matzuk MM, Kumar TR, Vassalli A, Bickenbach JR, Roop DR, Jaenisch R, Bradley A. 1995. Functional analysis of activins during mammalian development. Nature 374: 354-356.

McMahon JA, Takada S, Zimmerman LB, Fan CM, Harland RM, McMahon AP. 1998. Noggin-mediated antagonism of BMP signaling is required for growth and patterning of the neural tube and somite. Genes & Dev 12: 1438-1452.

Merino R, Ganan Y, Marcias D, Economides AN, Sampath KT, Hurle JM. 1998. Morphogenesis of digits in the avian limb is controlled by FGFs, TGFβs, and noggin through BMP signaling. Dev Biol 200: 35-45.

Mishina Y, Suzuki A, Ueno N, Behringer RR. 1995. Bmpr encodes a type I bone morphogenetic protein receptor that is essential for gastrulation during mouse embryogenesis. Genes & Dev 9: 3027-3037.

Mishina Y, Crombie R, Bradyley A, Behringer RR. 1999. Multiple roles for Activin-like kinase-2 signaling during mouse embryogenesis. Dev Biol 213: 314-326.

Mishina Y, Hanks MC, Miura S, Tallquist MD, Behringer RR. 2002. Generation of Bmpr/Alk-3 conditional knockout mice. Genesis 32: 69-72.

Mukhopadhay M, Shtrom S, Rodriguez-Esteban C, Chen L, Tsukui T, Gomer L, Dorward DW, Glinka A, Grinberg A, Huang SP, Niehrs C, Belmonte JC, Westphal H. 2001. Dickkopf1 is required for embryonic head induction and limb morphogenesis in the mouse. Dev Cell. 1: 423-434.

Oh SP, Seki T, Goss KA, Imamura T, Yi Y, Donahoe PK, Li L, Miyazono K, ten Dijke P, Kim S, Li E. 2000. Activin receptor-like kinase 1 modulates transforming growth factor-beta 1 signaling in the regulation of angiogenesis. Proc Natl Acad Sci USA 97: 2626-2631.

Olson EC, Schinder AF, Dantzker JL, Marcus EA, Spitzer NC, Harris WA. 1998. Properties of ectopic neurons induced by Xenopus neurogenin 1 misexpression. Mol Cell Neurosci 12: 281-299.

Oro AE, Higgins KM, Hu Z, Bonifas JM, Epstein EH Jr. Scott MP. 1997. Basal cell carcinomas in mice overexpressing sonic hedgehog. Science 276: 817-821.

Piotrowska K, Wianny F, Pedersen RA, Zernicka-Goetz M. 2001. Blastomeres arising from the first cleavage division have distinguishable fates in normal mouse development. Develop 128: 3739-3748.

Pizette S, Abate-Shen C, Niswander L. 2001. BMP controls proximodistal outgrowth, via induction of the apical ectodermal ridge, and dorsoventral patterning in the vertebrate limb. Develop 128: 4463-4474.

Plikus M, Wang WP, Liu J, Wang X, Jiang TX, Chuong CM. 2004. Morpho-regulation of ectodermal organs. Integument pathology and phenotypic variations in K14-noggin engineered mice through modulation of bone morphogenic protein pathway. Am J Pathol 164: 1099-1114.

Popperl H, Schmidt C, Wilson V, Hume CR, Dodd J, Krumlauf R, Beddington RS. 1997. Misexpression of Cwnt8C in the mouse induces an ectopic embryonic axis and causes a truncation of the anterior neuroectoderm. Develop 124: 2997-3005.

Saitou M, Barton SC, Surani MA. 2002. A molecular programme for the specification of germ cell fate in mice. Nature 418: 293-300.

Sharov AA, Weiner L, Sharova TY, Siebenhaar F, Atoyan R, Reginato AM, McNamara CA, Funa K, Gilchrest BA, Brissette JL, Botchkarev VA. 2003. Noggin overexpression inhibits eyelid opening by altering epidermal apoptosis and differentiation. The EMBO J 22: 2992-3003.

Sheng G, dos Reis M, Stern CD. 2003. Churchill, a zinc finger transcriptional activator, regulates the transition between gastrulation and neurulation. Cell 115: 603-613.

Shull MM, Ormsby I, Kier AB, Pawlowski S, Diebold RJ, Yin M, Allen R, Sidman C, Proetzel G, Calvin D. 1992. Targeted disruption of the mouse transforming growth factor-beta 1 gene results in multifocal inflammatory disease. Nature 359: 693-699.

Sirard C, de la Pompa JL, Elia A, Itie A, Mirtsos C, Cheung A, Hahn S, Wakeham A, Schwartz L, Kern SE, Rossant J, Mak TW. 1998. The tumor suppressor gene Smad4/Dpc4 is required for gastrulation and later for anterior development of the mouse embryo. Genes & Dev 12: 107-119.

Sun X, Meyers EN, Lewandoski M, Martin GR. 1999. Targeted disruption of Fgf8 causes failure of cell migration in the gastrulating mouse embryo. Genes Dev 13: 1834-1846.

Tremblay KD, Hoodless PA, Bikoff EK, Robertson EJ. 2000. Formation of the definitive endoderm in mouse is a Smad 2-dependent process. Develop 127: 3079-3090.

Tremblay KD, Dunn NR, Robertson EJ. 2001. Mouse embryos lacking Smad1 signals display defects in extra-embryonic tissues and germ cell formation. Develop 128: 3609-3621.

Tucker AS, Matthews KL, Sharpe PT. 1998. Transformation of tooth type induced by inhibition of BMP signaling. Science 282: 1136-1138.

Turner DL, Weintraub H. 1994. Expression of achaete-scute homolog 3 in Xenopus embryos converts ectodermal cells to a neural fate. Genes Dev 8: 1434-1447.

Van de Putte T, Maruhashi M, Francis A, Nelles L, Kondoh H, Huylebroeck d, Higashi Y. 2003. Mice lacking Zfhx1b, the gene that codes for Smad interacting protein 1, reveal a role for multiple neural crest cell defects in the etiology of Hirschsprung disease-mental retardation syndrome. Am J Hum Genet 72: 465-470.

Vassalli A, Matzuk MM, Gardner HA, Lee KF, Jaenisch R. 1994. Activin/inhibin beta B subunit gene disruption leads to defects in eyelid development and female reproduction. Genes & Dev 8: 414-427.

Vincent SD, Dunn NR, Hayashi S, Norris DP, Robertson EJ. 2003. Cell fate decisions within the mouse organizer are governed by graded nodal signals. Genes Dev 17: 1646-1662.

Warren SM, Brunet LJ, Harland RM, Economides AN, Longaker MT. 2003. The BMP antagonist noggin regulates cranial suture fusion. Nature 422: 625-629.

Watt FM, Hogan BL. 2000. Out of Eden: Stem cells and their niche. Science 287: 1427-1430.

Wilson SI, Rydstrom A, Trimborn T, Willert K, Nusse R, Jessell TM, Edlund T. 2001. The status of Wnt signaling regulates neural and epidermal fates in the chick embryo. Nature 411" 325-330.

Winnier G, Blessing M, Labosky PA, Hogan BL. 1995. Bone morphogenetic protein-4 is required for mesoderm formation and patterning in the mouse. Genes & Dev 9: 2105-2116.

Wood HB, Episkopou V. 1999. Comparative expression of the mouse Sox1, Sox2 and Sox3 genes from pre-gastrulation to early somite stages. Mech Dev 86: 197-201.

Xiao C, Shim J-h, Kluppel M, Zhang SS-M, Dong C, Flavell RA, Fu X-Y, Wrana JL, Hogan BLM, Ghosh S. 2003. Ecsit is required for Bmp signaling and mesoderm formation during mouse embryogenesis. Genes & Dev 17: 2933-2949.

Yamaguchi TP, Takada S, Yoshikawa Y, Su N, McMahon AP. 1999. T (Brachyury) is a direct target of Wnt3a during paraxial mesoderm specification. Genes & Dev 13: 3185-3190.

Yamamoto M, Meno C, Sakai Y, Shiratori H, Mochida K, Ikawa Y, Saijoh Y, Hamada H. 2001. The transcription factor FoxH1 (FAST) mediates Nodal signaling during anterior-posterior patterning and node formation in the mouse. Genes & Dev 15: 1242-1256.

Ying QL, Nichols J, Chambers I, Smith A. 2003. BMP induction of Id proteins suppresses differentiation and sustains embryonic stem cell self-renewal in collaboration with STAT3. Cell115: 281-92.

Ying Y, Liu X-M, Marble A, Lawson KA, Zhao G-Q. 2000. Requirement of Bmp8b for the generation of primordial germ cells in the mouse. Mol Endo 14: 1053-1063.

Ying Y, Qi X, Zhao G-Q. 2001. Induction of primordial germ cells from murine epiblasts by synergistic action of BMP4 and BMP8B signaling pathways. Proc Natl Acad Sci USA 98: 7858-7862.

Ying Y, Zhao G-Q. 2001. Cooperation of endoderm-derived BMP2 and extraembryonic ectoderm derived BMP4 in primordial germ cell generation in the mouse. Dev Biol 232: 484-492.

Yoshikawa Y, Fujimori T, McMahon AP, Takada S. 1997. Evidence that absence of Wnt3a signaling promotes neuralization instead of paraxial mesoderm development in the mouse. Dev Biol 183: 234-242.

Zhang H, Bradley A. 1996.   Mice deficient for BMP2 are nonviable and have defects in amnion/chorion and cardiac development. Develop 122: 2977-2986.

Zhao G-Q. 2002. Consequences of knocking out BMP signaling in the mouse. Genesis 35: 43-56.

Chapter 3

RNA Inhibition of BMP-4 Gene Expression in Postimplantation Mouse Embryos

SUMMARY

Short, hairpin RNA (shRNA) directed against bone morphogenetic protein 4 (Bmp-4) was delivered to early postimplantation staged mouse embryos via tail vein injection of pregnant dams. As early as 24h postinjection, embryos expressed a DsRed marker and later exhibited defects of neural fold elevation and closure and of cardiac morphogenesis. Immunohistochemical analysis of sectioned embryos indicated that Bmp-4 protein was depleted and gene expression analysis indicated there was a reduction in Bmp-4 mRNA and an upregulation of the Bmp-4 antagonists, noggin and chordin, in embryos exposed to the shRNA, but not in control embryos. There was no change in the expression of Gata4, brachyury, or claudin6 in RNAi exposed embryos, indicating that RNA silencing was specific to Bmp-4 rather than producing widespread gene inhibition. Delivery of shRNA to embryos has the potential to specifically knockdown the expression of developmentally essential genes and to rescue gene mutations, significantly decreasing the time required to analyze the function(s) of individual genes in development.

INTRODUCTION

Gene targeting in the mouse embryo has produced tremendous insights into gene function during development (Doetschmann e*t* al., 1987; Thomas and Capecchi, 1987). Although gene deletion is considered to be the gold standard,

generation of targeted mutant mice is a tedious process and problematic if the targeted gene produces an embryonic lethal phenotype. Other approaches such as using morpholino antisense oligonucleotides have also been developed to disrupt gene expression in embryos, but have not been widely employed because of problems with toxicity, nonspecific effects, and the short life of the morpholino (Siddall e*t* al., 2002). Over the last few years, there have been tremendous advances in sequence-specific gene silencing using RNA interference techniques (Paddison and Hannon, 2002). The phenomenon was identified in *Caenorhabditis* elegans, where it was noted that the control RNA (sense RNA) also downregulated gene expression. It was initially thought that this was an aberrant cellular event, but it is now clear that this process is an innate method employed by many organisms to control gene expression. In addition, RNA interference is now recognized as a powerful tool to produce gene silencing. When introduced into cells, small interfering RNAs (siRNA), or RNAs expressed as short hairpins (shRNA), efficiently target and cause degradation of the cognate RNAs (Paddison and Hannon, 2002).

Posttranscriptional gene silencing by RNAi has been employed extensively in C. elegans (Fire et al., 1998) and more recently in mammalian cells (Elbashir et al., 2001; Brummelkamp et al., 2002; Yang et al., 2001, 2002). siRNAs have been expressed in mouse embryos by electroporation or injection of preimplantation staged embryos (Grabarek et al., 2002; Wianny and Zernicka-Goetz, 2002), and in postimplantation embryos via exoutero surgery and regional electroporation (Calegari et al., 2002). Transgenic expression of siRNA has also recently been achieved by electroporation of ES cells followed by chimera formation (Carmell et al., 2003; Rubinson et al., 2003), or following tetraploid aggregation (Kunath et al., 2003), which produced embryos that expressed shRNA to Rasa 1 and phenocopied the Rasa1 null mouse. Others have injected fertilized eggs with shRNA plasmids (Hasuwa et al., 2002) or transduced two-cell embryos with lentiviral vectors expressing shRNAs (Tiscornia et al., 2003) and observed stable, heritable gene knockdown. RNA interference has the advantages that

individual genes or combinations can be targeted, multiple regions of the same transcript can be targeted, and the RNAi can be constitutively expressed to produce long-term gene suppression. If delivered to pregnant animals, the length of time required to assess gene function could be greatly reduced compared with conventional germ line mutagenesis strategies. Unlike gene targeting using siRNA in ES cells, this approach allows targeting of genes expressed in the trophoblast and yolk sac—structures that are not normally formed from ES cells, as well as genes involved in growth and maintenance of the ES cells themselves. In addition, the timing of the delivery of the shRNA can be precisely controlled to target the stage of interest, making it a powerful approach to study genes whose loss of function produces early embryonic lethality. Finally, different levels of RNA silencing (Hemann et al., 2003) produced by targeting different regions of the transcript may be effective in generating hypomorphic alleles and in teasing out gene structure/function relationships.

In this investigation, we delivered shRNA targeted to bone morphogenetic protein 4 (Bmp-4) mRNA (Figure 3-1) to early postimplantation staged mouse embryos using tail vein injection. Rather than co-injection of a reporter plasmid with separate siRNAs (Calegari et al., 2002; Miyagishi and Taira, 2002; Ya et al., 2002), a single vector was designed in which DsRed was expressed from the CMV promoter and constitutive expression of Bmp-4i was controlled by the mouse RNA polymerase III U6 promoter (Miyagishi and Taira, 2002; Ya et al., 2002). Unlike high-pressure tail vein injection designed to open capillaries and deliver an siRNA to adult tissues (Lewis et al., 2002), we employed low-pressure injection to deliver the shRNA, with the goal of examining the effects of Bmp-4 gene knockdown during early postimplantation stages of embryonic development.

Embryonic day (E) 6.5 time pregnant mice were injected via the tail vein with either pCS2/Red (control) or pCS2/Red/Bmp-4i (pBmp4i), and sacrificed after 24 h, 48 h, 72 h, and 8 days (E14.5) postinjection. As early as 24 h postinjection,

embryos expressed DsRed (Figure 3-2A), with expression persisting over the next 72 h, extending to E14.5 (Figure 3-2C). Within an individual litter, there was some variation between embryos in their expression of the DsRed marker: a majority (64%) of the embryos examined expressed DsRed with no preference for a particular day of gestation. Controls expressed DsRed within all tissues in the embryo (Figure 3-2G) and no morphological abnormalities were observed in these embryos. Bmp-4i exposed embryos exhibited a number of morphological alterations, including defects of neural tube closure consisting of a failure of neural fold elevation in the cephalic region (Figure 3-2B), rachischisis, a truncated posterior axis, and occasionally a small allantois. The first branchial arch was often hypoplastic and defects of cardiac looping were also evident. These phenotypes appeared to reflect hypomorphic behavior of the lethal phenotype previously observed in germline targeted Bmp-4 null embryos (Fujiwara et al., 2001, 2002; Hebert et al., 2003). It would be of considerable interest to examine primordial germ cell differentiation in these embryos since the expression of genes such as fragilis that are involved in specification of primordial germ cells also appear to be affected by Bmp-4 expression levels (Lawson et al., 1999; Saitou et al., 2002). Interestingly, maternal tissues expressed variable levels of the DsRed marker, as observed previously (Lewis et al., 2002). There was constant high expression in liver, pancreas, spleen, and heart, and variable expression in skin and striated muscle, while brain never expressed DsRed.

To determine if Bmp-4 protein expression was affected in the shRNA exposed embryos, immunohistochemical analyses were carried out on sectioned embryos (Figure 3-3). Unlike control embryos that expressed high levels of Bmp-4 in the surface ectoderm (Figure 3-3E,F), there was very little Bmp-4 protein in the shRNA-exposed embryos (Figure 3-3A–D). Scattered Bmp-4 immunoreactivity was present in the surface ectoderm of embryos on E8.5 and E9.5; by E14.5 there was little expression in the CNS, lung, or epidermal ectoderm. The function of the Bmp-4 hairpin was also assessed by comparison of Bmp-4 expression in control (pCSRed) and pBmp-4i embryos using RT-PCR. The expression of Bmp-

4 mRNA was diminished 4 –8-fold in embryos that received the Bmp-4i cassette (Figure 3-4, lane 1) compared to pCSRed control embryos. Importantly, expression of the DsRed or Bmp-4i cassettes did not affect global transcriptional regulation as expression of an endoderm marker Gata4 (Figure 3-4, lane 6), Brachyury (T), a mesoderm marker (Figure 3-4, lane 7), claudin6, an ectoderm marker (Figure 3-4, lane 8), and β-actin, a positive control (Fig3-4, lane 9), were similar in both groups, indicating that the shRNA silenced Bmp-4 specifically rather than producing widespread gene inhibition. Interestingly, mRNA for the Bmp-4 antagonists, chordin and noggin, was upregulated in Bmp-4i exposed embryos (4-fold and 12-fold, respectively) (Figure 3-4, lanes 2 and 3). Musashi1, a marker of primitive neuroepithelium, was strikingly upregulated in the presence of Bmp-4i by 30-fold (Figure 3-4, lane 4). Nodal, a downstream target of Bmp-4 was unexpectedly up-regulated 3-fold (Figure 3-4, lane 5), possibly releasing control over L-R-asymmetry in the embryo.

These results demonstrate for the first time the systemic delivery and expression of shRNA directed to a gene critical in the development of postimplantation mouse embryos. The results phenocopy many of the characteristics of the Bmp-4 gene targeted embryos and identify alterations in the expression of target genes. Although it is not yet known if this approach will be successful later in development after placental development is more complete, this potential limitation might be overcome by early injection of plasmids in which expression of the RNAi is controlled by an inducible promoter. The use of RNAi to study gene function in development has many advantages including: precise control of gene knockdown at a specific stage of embryonic development, the ability to target multiple genes without complicated breeding regimens, to attempt gene rescue, and in the long term to treat genetic, prenatal conditions.

MATERIALS AND METHODS

Construction of cDNA Expression Vectors

A BamHI/XbaI fragment that contained the DsRed coding region was removed from pDsRed2-1 (ClonTech, Palo Alto, CA) and ligated into the first MCS of pCS2 (Turner and Weintraub, 1994) to generate pCS2/Red. The mouse U6 promoter (GenBank X06980) was PCR amplified from genomic DNA and cloned into the EcoRI and BamHI sites in pBS SK (Stratagene, La Jolla, CA) to yield pSKU6. An RNAi hairpin was designed to target nt 305–323 of the Bmp-4 mRNA (GenBank X56848) and ligated downstream of the U6 promoter in pSKU6 (Figure 3-1). The final vector pCS2/Red/Bmp-4i was constructed by removing the U6/BMP-4i cDNA from the SK using NotI and KpnI followed by ligation of this cDNA into the second MCS of pCS2/Red to yield pCS2/Red/Bmp-4i (pBmp-4i). Plasmid preparations for injections were prepared with the Qiagen (Chatsworth, CA) Maxi Prep Kit.

Tail Vein Injections

Plasmids (10 µg) were diluted in Ringer's solution and injected into the tail vein of unanesthetized, time pregnant (E6.5; plug day = E0.5) mice (CD-1, Charles River, Portage, MI) in a volume of 250 µl, using a 23 G butterfly needle anda1cc syringe. At least 10 mice were injected per replicate experiment (n = 4 replicates). Over 398 embryos from a total of 32 pregnant females were ex-amined. Mice were sacrificed at 24 h, 48 h, 72 h, and 8 days (E14.5) postinjection. Embryos were removed from the uterus and membranes and examined using epifluorescence microscopy to determine the extent of DsRed expression. Embryos were then either processed for histological analysis, SEM, or RNA extraction. Additional maternal tissues: spleen, liver, kidney, lung, heart, striated muscle, skin, and brain were removed 72 h postinjection and embedded in OCT. Frozen sections were cut and examined using epifluorescence to determine the pattern of expression of the DsRed marker.

105

Immunohistochemical localization of Bmp-4 protein was carried on 10 μm thick frozen sections of embryos. Sections were fixed briefly, washed, blocked, then exposed to anti-Bmp-4 antibodies (1:50, Santa Cruz Biotechnology, sc-6896, Santa Cruz, CA) followed by secondary antibodies conjugated to FITC. Sections were examined and photographed using epifluorescence microscopy and digital images imported to PhotoShop (Adobe Systems, Mountain View, CA) to construct illustrations.

RT-PCR Analysis of Gene Expression

RNA was extracted from E8.5 and E9.5 embryos with Trizol (ILT), DNAsed, and quantified. Approximately 10–12 embryos were recovered per litter and combined in a single Trizol aliquot for extraction. One control and two Bmp-4i-exposed litters were examined for each experiment. The RT-PCR was done in triplicate for each embryo pool. The RNAs (1 μg) served as templates in oligo dT primed reverse transcription (RT) reactions, then 1/10 of the reaction was used as a template in PCR with gene-specific primers. The optimal number of PCR cycles was determined for each primer pair to ensure amplification in the linear range (Gratsch, 2002). General PCR conditions were 94°/3 min, 94°/30 sec–1 min, 51–60°/1 min, 72°/2 min for 25–35 cycles, and a final extension of 72°/7 min.

PCR primers

β-actin, F-aaccctaaggccaaccgtg, and R-caggattccatacccaagaagg (498 bp, 22 cycles); Bmp-4, F-ctcccaagaatcatggactg and R-aaagcagagctctcactggt (468 bp, 32 cycles); Noggin, F-cccggtgctgtacgcgtgg and R-gcaggaacacttacactcg (250 bp, 29 cycles); Chordin, F-accaacgcagtagagacctccc and R-ggggtagcaggaatggtgtg (901 bp, 30 cycles); DsRed, F- tcaccgagttcatgcgcttca and R-cgttgtgggaggtgatgtccagct (593 bp, 30 cycles); Mushashi 1, F-ttccaagccacgacctacgc and R- ggagcgagagaagagacaaggtctg (638 bp, 30 cycles); nodal, F- atttgccagacagaagccaac and R- tcctccacaatcatgtccttg (312 bp, 20 cycles); Brachyury, F- agaaagaaacgaccacaaagatg and R- atttatttattttttcccttgtcc

106

(729 bp, 33 cycles); Claudin 6, F- gataggaactccaagtctcgt and R-tgggacagatgtagaatagca (287 bp, 29 cycles); Gata4, F- ccgagcaggaatttgaagagg and R- gcctgtatgtaatgcctgcg (469 bp, 35 cycles). The PCR products were electrophoresed in 1.5% agarose/EtBr gels and photographed in a UV light box. For semiquantitative analyses, the gels were scanned, then analyzed using a Lab Works 4.0 (Cybergenetics, Pittsburgh, PA) densitometry program.
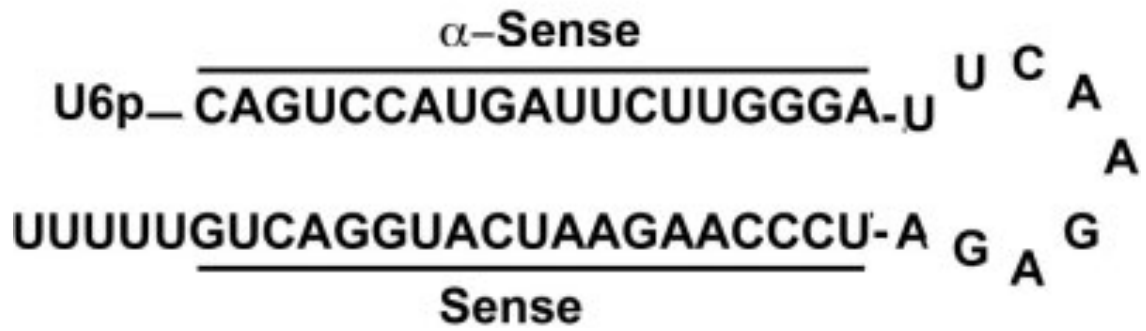
ACKNOWLEDGMENTS

This chapter represents the contents of a published article:

Gratsch TE, De Boer LS, and O'Shea KS. 2003. RNA inhibition of BMP-4 Gene Expression in Postimplantation Mouse Embryos. genesis 37: 12-17.

Predicted stem loop

α–Sense

U6p— CAGUCCAUGAUUCUUGGGA-U ᵁ ᶜ ᴬ
                                    ᴬ
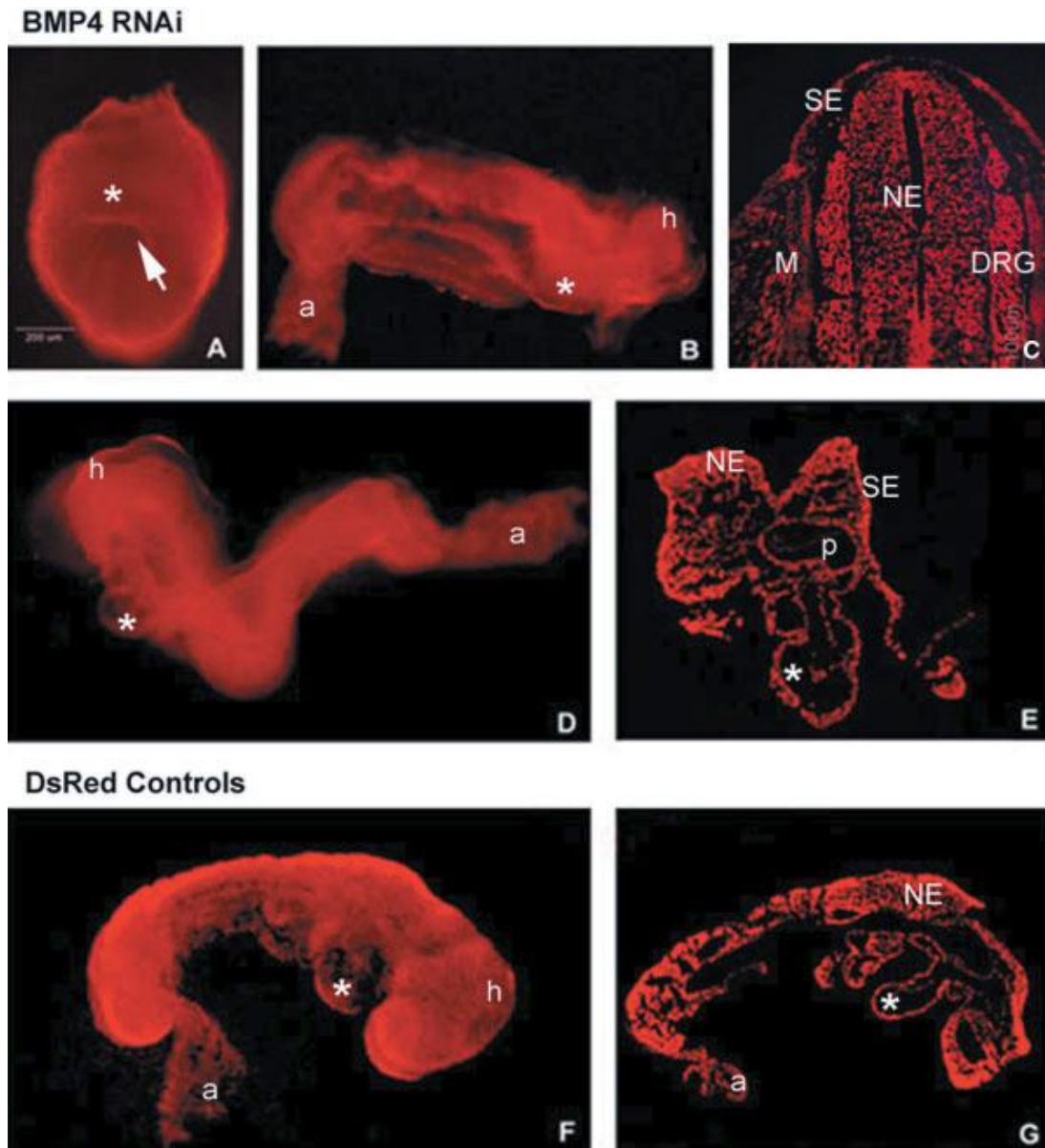UUUUUGUCAGGUACUAAGAACCCU-A ᴳ ᴳ
                          ᴬ
Sense

Figure 3-1. **Predicted stem loop**

Schematic of the predicted hairpin structure containing the antisense and sense regions that target the Bmp4 gene, and a 9 bp loop.

BMP4 RNAi

DsRed Controls

Figure 3-2. Expression of Bmp-4i or DsRed control.

Embryos were isolated onE7.5 (**A**), E8.5 (**B,D–G**), or E14.5 (**C**) of gestation from pregnant females injected on gestation E6.5 with Bmp-4i (**A–E**) or DsRed control plasmid (**F,G**). As early as 24 h postinjection, the DsRed marker was expressed in E7.5 embryos (**A**) and was uniformly distributed throughout sectioned embryos examined on E14.5 (**C**) or on E8.5 (**E,G**). Embryos exposed to Bmp-4i exhibited defects of neural fold elevation and closure (**B**), turning and cardiac rotation (**B,D,E**), compared with morphologically normal control embryos (**F,G**). Asterisks indicates the cardiac region; arrow in **A**, the foregut pocket. a = allantois; h = headfolds; SE = surface ectoderm; NE = neuroepithelium; M = forming myotome; DRG = dorsal root ganglion; p = pharynx.

109

Figure 3-3. Immunohistochemical localization of Bmp-4 protein in embryos exposed to pBmp-4i (A-D), and DsRed control embryos (E,F).

Phase contrast micrographs (**A,C,E**) illustrate the organization of the surface ectoderm (SE) and underlying neuroepithelium (NE). The neural folds are collapsed in this early somite embryo (E8.5, **A,B**) obliterating much of the mesenchyme. There was no immunoreactivity for Bmp-4 in the surface ectoderm, where it is normally expressed; with slight expression in the midline (arrow) and in the endoderm surrounding the pharynx (P). By E9.5 (**C,D**), the neural folds had not yet closed in many of the Bmp-4i-exposed embryos, and there was only slight scattered staining of Bmp-4 (arrows) in the surface ectoderm (SE). Control embryos exhibited normal neural tube closure and strong immunoreactivity for Bmp-4 in the surface ectoderm (**E,F**).
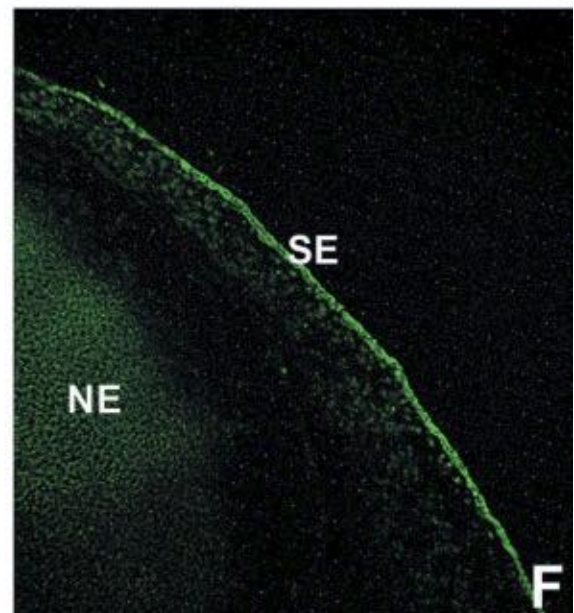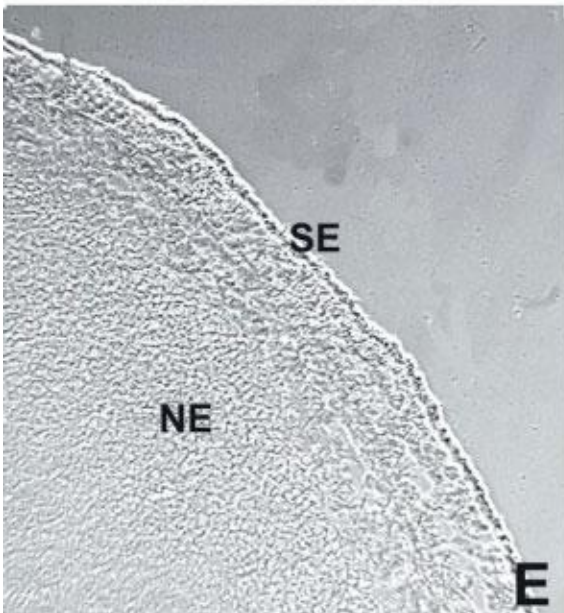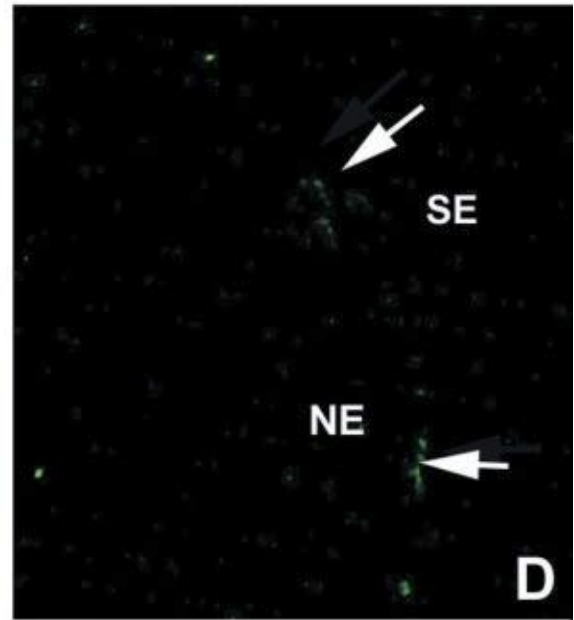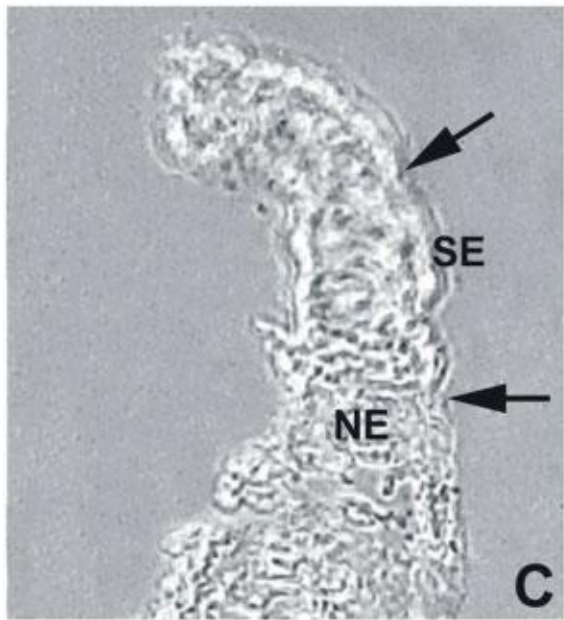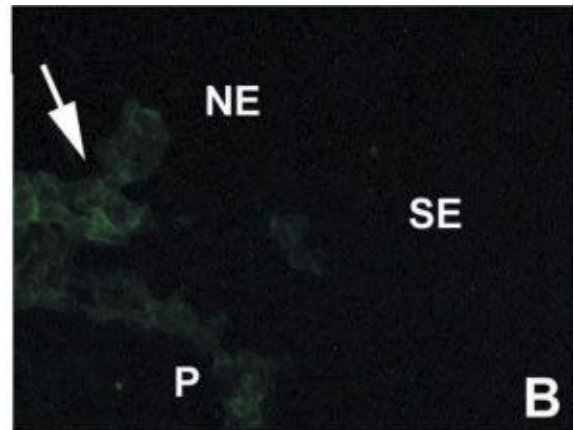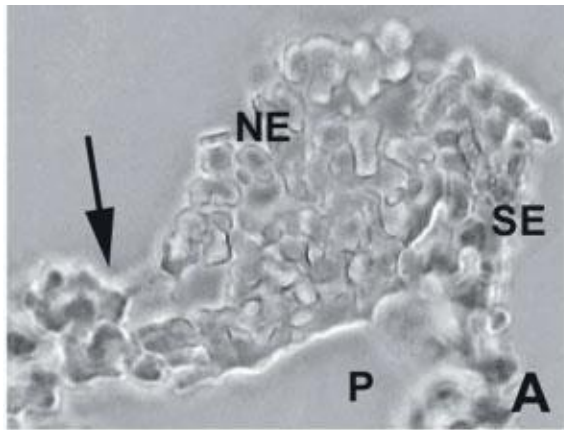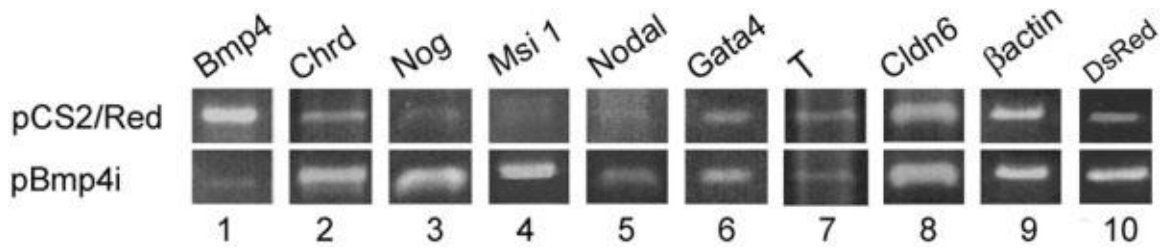
Figure 3-4. RT-PCR analysis of gene expression in pCS2/Red control and pBmp-4i-exposed embryos.

RNA was isolated from embryos on E8.5 of gestation and RNA (1 μg) was reverse-transcribed in the presence of oligo-dT and PCR with gene-specific primers was performed as described in Materials and Methods. The PCR products were electrophoresed in 1.5% agarose ethidium bromide gels. Expression of Bmp-4 decreased following exposure to Bmp-4i (lane 1). The expression of the Bmp-4 antagonists, Chordin and Noggin, as well as Musashi1 and Nodal, are upregulated in the Bmp-4i embryos (lanes 2–5). Gata4, an endoderm marker, Brachyury (T), a marker of mesoderm, Claudin 6 (Cldn6), a marker of early epidermal ectoderm, and β-actin expression were unchanged between controls and pBmp-4i-exposed embryos (lanes 6–9). DsRed expression was slightly higher in Bmp-4i embryos compared with controls (lane 10).

112

REFERENCES

Brummelkamp TR, Bernards R, Agami R. 2002. A system for stable expression of short interfering RNAs in mammalian cells. Science 296:550–553.

Calegari F, Haubensak W, Yang D, Huttner WB, Buchholz F. 2002. Tissue-specific RNA interference in post-implantation mouse embryos with endoribonuclease-prepared short interfering RNA. Proc Natl Acad Sci USA 99:14236–14240.

Carmell MA, Zhang L, Conklin DS, Hannon GJ, Rosenquist TA. 2003. Germline transmission of RNAi in mice. Nat Struct Biol 10:91–92.

Doetschman T, Gregg RG, Maeda N, Hooper ML, Melton DW, Thompson S, Smithies O. 1987. Targeted correction of a mutant HPRT gene in mouse embryonic stem cells. Nature 330:576–578.

Elbashir SM, Harborth J, Lendeckel W, Yalcin A, Weber K, Tuschl T. 2001. Duplexes of 21-nucleotide RNAs mediate RNA interference in cultured mammalian cells. Nature 411:494–498.

Fire A, Xu S, Montgomery MK, Kostas SA, Driver SE, Mello CC. 1998. Potent and specific genetic interference by double-stranded RNA in *Caenorhabditis elegans*. Nature 391:806–811.

Fujiwara T, Dunn NR, Hogan BL. 2001. Bone morphogenetic protein 4 in the extraembryonic mesoderm is required for allantois development and the localization and survival of primordial germ cells in the mouse. Proc Natl Acad Sci USA 98:13739–13744.

Fujiwara T, Dehart DB, Sulik KK, Hogan BLM. 2002. Distinct requirements for extra-embryonic and embryonic bone morphogenetic protein 4 in the formation of the node and primitive streak and coordination of left-right asymmetry in the mouse. Development 129:4685–4696.

Grabarek JB, Plusa, B, Glover DM, Zernicka-Goetz M. 2002. Efficient delivery of dsRNA into zona-enclosed mouse oocytes and preimplantation embryos by electroporation. genesis 32:269–276.

Gratsch TE. 2002. RT-PCR analyses of differential gene expression in ES derived neural stem cells. In: Zigova T, Sanberg P, Sanchez-Ramos J, editors. Neural stem cells. Totowa, NJ: Humana Press. 198:197–212.

Hasuwa H, Kaseda K, Einarsdottir T, Okabe M. 2002. Small interfering RNA and gene silencing in transgenic mice and rats. FEBS Lett 532:227–230.

Hebert JM, Hayhurst M, Marks ME, Kulessa H, Hogan BLM, McConnell SK. 2003. BMP ligands act redundantly to pattern the dorsal telencephalic midline. genesis 35:214–219.

Hemann MT, Fridman JS, Zilfou JT, Hernando E, Paddison PJ, Cordon-Cardo C, Hannon GJ, Lowe SW. 2003. An epi-allelic series of p53 hypomorphs created by stable RNAi produces distinct tumor phenotypes in vivo. Nat Genet 33:396–400.

Kunath T, Gish G, Lickert H, Jones N, Pawson T, Rossant J. 2003. Transgenic RNA interference in ES cell-derived embryos recapitulates a genetic null phenotype. Nat Biotech 21:559–561.

Lawson KA, Dunn NR, Roelen BA, Zeinstra LM, Davis AM, Wright CV, Korving JP, Hogan BL. 1999. Bmp4 is required for the generation of primordial germ cells in the mouse embryo. Genes Dev 13: 424–436.

Lewis DL, Hagstrom JE, Loomis AG, Wolff JA, Herweijer H. 2002. Efficient delivery of siRNA for inhibition of gene expression in postnatal mice. Nat Genet 32:107–108.

Miyagishi M, Taira K. 2002. U6 promoter-driven siRNAs with four uridine 3' overhangs efficiently suppress targeted gene expression in mammalian cells. Nat Biotech 20:497–500.

Paddison PJ, Hannon GJ. 2002. RNA interference: the new somatic cell genetics? Cancer Cell 2:17–23.

Rubinson DA, Dillon CP, Kwiatkowski AV, Sievers C, Yang L, Kopinja J, Rooney DL, Ihrig MM, McManus MT, Gertler FB, Scott ML, van Parijs L. 2003. A lentivirus-based system to functionally silence genes in primary mammalian cells, stem cells and transgenic mice by RNA interference. Nat Genet 33:401–406.

Saitou M, Barton SC, Surani MA. 2002. A molecular programme for the specification of germ cell fate in mice. Nature 418:293–300.

Siddall LS, Barcroft LC, Watson AJ. 2002. Targeting gene expression in the preimplantation mouse embryo using morpholino antisense oligonucleotides. Mol Reprod Dev 63:413–421.

Thomas KR, Capecchi, MR. 1987. Site-directed mutagenesis by gene targeting in mouse embryo-derived stem cells. Cell 51:503–512.

Tiscornia G, Singer O, Ikawa M, Verma IM. 2003. A general method for gene knockdown in mice by using lentiviral vectors expressing small interfering RNA. Proc Natl Acad Sci USA 100:1844 –1848.

Turner DL, Weintraub H. 1994. Expression of achaete-scute homolog 3 in Xenopus embryos converts ectodermal cells to a neural fate. Genes Dev 8:1434–1447.

Wianny F, Zernicka-Goetz M. 2000. Specific interference with gene function by double-stranded RNA in early mouse development. Nat Cell Biol 2:70 –75.

Yu J-Y, DeRuiter SL, Turner DL. 2002. RNA interference by expression of short-interfering RNAs and hairpin RNAs in mammalian cells. Proc Natl Acad Sci USA 99:6047–6052.

Yang S, Tutton S, Pierce E, Yoon K. 2001. Specific double-stranded RNA interference in undifferentiated mouse embryonic stem cells. Mol Cell Biol 21:7807–7816.

Yang D, Buchholz F, Huang Z, Goga A, Chen C-Y, Brodsky FM, Bishop JM. 2002. Short RNA duplexes produced by hydrolysis with *Escherichia coli* RHase III mediate effective RNA interference in mammalian cells. Proc Natl Acad Sci USA 99:9942–9947.

Chapter 4

Geminin is Required for Gastrulation in Postimplantation Mouse Embryos

INTRODUCTION

The epiblast of the early mouse embryo is patterned by multiple signaling molecules that first establish the proximal-distal (Nodal and BMP)(Brennan 2001) followed by the anterior-posterior axis (dickkopf-1 and cerberus-like 1) by limiting TGFβ, Wnt, and FGF signaling to the posterior region of the embryo (Mukhopadhay et al., 2001; Belo et al., 1997). These signals establish the correct location and formation of the node (Beddington and Robertson, 1999) and the primitive streak (Lawson et al., 1991) and ensure that coordinated cell movements occur (*i.e.* displacement of the anterior visceral endoderm) (Weber et al., 1999).

At the onset of gastrulation, cells in the posterior pole of the epiblast divide and move medially in the primitive streak, a process that appears to be determined largely by nodal signaling (Vincent et al., 2003). High levels of nodal, Bmp, and canonical Wnt signaling (reviews Beddington and Robertson, 1999; Tam and Loebel, 2007) combine to control the initial differentiation of endoderm and mesoderm from the epiblast. Subsequent cell rearrangements and epithelial-mesenchymal transition (EMT) depend on loss of adherens junctions which is caused by the FGF-mediated induction of the Snail1 gene and the subsequent down-regulation of Cadherin-1 (E-cadherin) and expression of genes involved in cell migration as well as endoderm and mesoderm lineages (Cano et al., 2000; Lawson et al., 1999). The remaining ectoderm is patterned by BMPs and BMP

116

inhibitors (Harland, 2000), although it appears that additional molecules must be involved in the early differentiation of the ectoderm in the mammalian embryo.

One candidate previously identified based on its ability to affect the size of the *Xenopus* neural plate (Kroll et al., 1998), is the 33 kDa protein Geminin (McGarry & Kirschner, 1998). Geminin expression is induced by Noggin and Chordin and is inhibited by BMP signaling (Kroll et al., 1998; Taylor et al., 2005). Overexpression of Geminin expands and knock-down of Geminin reduces the size of the neural ectoderm (Kroll et al., 1998). Geminin may act as a switch between proliferation and differentiation of many tissues (Del Bene et al., 2004; Luo et al., 2004; Luo & Kessel, 2004; Quinn et al., 2001) as well as certain cancers (Wohlschlegel et al., 2002; Xouri et al., 2004; Gonzalez et al., 2004; Montanari et al., 2005; Dudderidge et al., 2005; Obermann et al., 2005). It has been shown to control neuronal differentiation by antagonizing Brg1 (Seo et al., 2005a), and to bind and control the expression of Hox and Six transcription factors (Luo et al., 2004; Del Bene et al., 2004; Seo et al., 2005b). Geminin also controls cell-cycle progression via its association with Cdt1 (McGarry & Kirschner, 1998; Tachibana et al., 2006). Despite its provocative role in *Xenopus*, the expression and role of Geminin during development of the mammalian embryo is unknown. Loss of Geminin leads to embryonic lethality at E3.5 (blastocyst stage) of development (Hara et al., 2006; Gonzalez et al., 2006) due to an over-replication of DNA in the inner cell mass (ICM) leading to apoptosis and preventing study of its role in later development.

In the current investigation, Geminin expression was analyzed in the developing mouse embryo from the onset of neural induction (E6.5) through gastrulation to neural tube closure and neural crest migration (E9.5). Consistent with the ability of Noggin and Chordin to induce its expression, Geminin is initially expressed in a strip of cells on the dorsal surface of the embryo on E6.5. As neural induction and gastrulation proceed, Geminin is expressed in the neural plate as well as in the posterior region of the epiblast where the primitive streak is forming. Extra-

117

embryonic tissues and the epidermal ectoderm surrounding the neural plate lack geminin. During later stages of development, it is present in most embryonic tissues with notable exceptions of the heart and epidermal ectoderm. Geminin is expressed at high levels in the neural ectoderm and in the cells that will give rise to the neural crest.

To determine its role in early development, we employed specific shRNAs to knock-down Geminin expression in early post-implantation mouse embryos. Reduction in Geminin expression interfered with gastrulation movements, EMT was disrupted, and cells failed to migrate through the node and primitive streak producing defects in the neural tube, notochord, and closure of the body wall. Interestingly, as Geminin expression decreased, both Wnt and BMP4 expression were ectopically expressed suggesting that geminin may be a multifunctional modulator of early lineage differentiation.

MATERIALS & METHODS

DNA delivery

To knock-down Geminin expression in early post-implantation staged embryos, E6.0 ICR time pregnant dams (Harlan) or E6.0 time pregnant dams containing a transgene with six TCF/Lef sites driving β-gal (Mohamed et al., 2004) were injected via the tail-vein with 5 μg of two shRNAs targeting Geminin or scrambled hairpin control shRNA constructs (O'Shea et al., 2006; Supplemental Figure S4-1) in a total of 150 μl Ringer's solution. Injections were carried out as previously described (Gratsch et al., 2003).

We also targeted Geminin by injecting a shRNA targeting Geminin or scrambled (control) shRNA transgene into one pronucleus of fertilized oocytes, (C57BL/6 X SJL)F2 (carried out by the University of Michigan Transgenic Animal Core; Supplemental Figure S4-1) which were transferred to pseudopregnant dams. Mice were sacrificed at E7.0 to E9.0 of development.

<u>Tissue analysis</u>

Mice were sacrificed by cervical dislocation on E7.0 to E9.0 and embryos dissected from the decidua and membranes. Digital images of individual embryos were obtained using a Leitz-inverted fluorescence microscope and imported into Adobe Photoshop to assemble figures.

For alkaline phosphatase staining, horseradish peroxidase staining (HRP), whole-mount immunohistochemistry (IHC), and whole mount *in situ* hybridization (WISH) embryos were fixed for 10 minutes in 2% paraformaldehyde at room temperature. Embryos for WISH were dehydrated in a graded series of MeOH: PBS Tween washes and stored at –20°C. RNAse-free reagents/conditions were used for these embryos.

Embryos for scanning electron microscopy (SEM) were fixed in 1% glutaraldehyde in phosphate buffer for 30 minutes. Embryos were washed and stored at 4 °C in PBS. They were then dehydrated in a series of graded alcohols, washed twice in hexamethyldisilazane (HMDS), and allowed to air dry. Embryos were oriented on SEM stubs, sputter coated with gold palladium, and examined in an Amray 1910 SEM.

Embryos to be analyzed by quantitative PCR (QRT-PCR) were placed in Trizol reagent for RNA extraction.

E9.0 embryos to be analyzed by western blotting were placed in RIPA/7X Complete buffer (Roche) and stored at –20 °C. A 25 5/8G needle was used to homogenize the tissue prior to protein quantification using the Bradford assay.

For frozen sections, fixed embryos were embedded in OCT, frozen in 2-methylbutane in dry ice, and sectioned at 10 μm.

Quantitative RT-PCR

To minimize variations in gene expression due to differences in developmental stages, control embryos were carefully grouped into four developmental stages: stage 1 – primitive streak (E7.0) to 4-5 somites; stage 2 – 5 to10 somites; stage 3 – 10 to 12 somites; stage 4 – 12 to 25 somites. In addition, blastocyst, E11, E13, E15, and E17 staged embryos were collected. RNAs from all stages were pooled and used to develop a reference set.

RNA was also extracted from individual stage 3 and stage 4 embryos exposed to either geminin shRNA (n=7 and n=30, respectively) or scrambled shRNA (n=10 and n=22, respectively) and reverse transcribed (1 μg RNA with random nonamers). QRT-PCR was performed on cDNAs using iQ SYBR green supermix (BioRad) in a BioRad iCycler. β-actin was used as a reference gene for all pair-wise comparisons. Lineage genes examined included: Axin2, Bmp4, Brachyury, Foxa2, Geminin, Neurogenin-1, and Sox3. All analyses were run in triplicate. Sequences are provided in Supplemental Table 4-1.

Embryos with a coefficient of variation (CV) greater than 3.0 % were excluded from additional analysis. Ct values of the scrambled shRNA (control) embryos were averaged to yield an overall mean Ct for each target gene and an average Ct for the reference gene (β -actin). These values were used as the reference for all embryos exposed to Geminin shRNA. The Pfaffl method was used to generate fold changes (Pfaffl et al., 2001). To examine the effects of Geminin knock-down on lineage gene expression, we employed linear regression analysis.

Statistical Analysis

To determine the relationship between Geminin knock-down and target gene expression, we carried out regression analyses on QRT-PCR data from individual embryos. Analysis was done using SPSS, significance assessed using f ratio.

Immunohistochemisty/ Alkaline Phosphatase staining/ HRP staining/X-gal staining

Embryos were fixed, blocked in 2% non-fat dry milk/0.1% Triton-X/PBS for 2 hours, and incubated in primary antibody overnight at 4°C. After an additional 5 hours of blocking, appropriate secondary antibody was added and embryos incubated overnight at 4 °C. Primary antibodies included: Foxa2 (1:1000, Millipore #07-633), Sox3 (1:2000, from MW Klymkowsky, Denver, CO), E-cadherin (1:500, BD #610181), or TuJ1 (1:200, Covance #MMS-435P), secondary antibodies were conjugated to Cy3, Alexa-488 (1:1000), or HRP (1:200, Jackson Immunoresearch Laboratories). Propidium Iodide (1:1000, Sigma #P4864) or Hoechst 33258 (1:1000, Sigma #861405) was added to sections to identify nuclei. For the alkaline phosphatase staining, embryos were rinsed twice for 10 minutes in 1x detection buffer followed by staining with NBT/BCIP. Embryos detected with HRP were washed in 0.1%BSA with 0.1% PBS tween for 10 minutes followed by detection with DAB. X-gal staining was carried out following: (www.sanger.ac.uk/genetrap/) using X-gal (20 μg/μl ILT #15520-034). 0.02% ipegal and 0.01% deoxycholate were added to wash and staining buffers to increase penetration. Images were captured using an Olympus Bx-51, Leica dissecting scope, Leitz Fluovert, and/or a Zeiss 541 confocal microscope.

Western Blotting

Individual E9.0 embryos exposed to scrambled or Geminin shRNA were placed in RIPA/ 7X complete buffer and stored at -20°C until use. Protein was quantified using the Bradford reagent (BioRad) in a BioRad spectrophotometer. 10 μg of protein in 2X Lamelli buffer with β-mercaptoethanol was run on a 10% Tris-HCl (15 wells) polyacrylamide gel (BioRad). Protein was transferred to PVDF membranes, blocked in 5% non-fat dry milk/0.2% Tween-100/PBS then incubated in primary antibody overnight at 4 °C: anti-Geminin (1:1000, Santa Cruz sc-13015) and anti-β-actin (1:20,000, Sigma #A 1978). Membranes were

washed then secondary antibodies (rabbit anti-HRP, 1:2000 and mouse anti-HRP 1:20,000 both from Jackson Immunoresearch) were added for 1 hour at room temperature followed by additional washes in blocking buffer. Membranes were washed thoroughly in TBS/0.1 % Tween-100 followed by detection in luminol (Supersignal west pico chemiluminescent substrate, Thermo Scientific) and exposure to film for 1 minute.   Band intensity was determined using a BioRad ChemiDoc.

In Situ Hybridization

Embryos were rehydrated in a series of graded MeOH: PBS Tween-100 washes prior to proteinase K treatment (5 minutes for E7.0 to E8.5 embryos and 10 minutes for E9.0). Whole mount *in situ* hybridization was carried out following (Wilkinson and Nieto; 1993). Probes were generated using T3 or T7 polymerase and DIG-11-UTP labeling kit (Roche). A 412 bp Geminin probe was generated by linearizing pSK using BsAI and transcribing with T3 polymerase (NM_020567 nt 564 to 976). The 751 bp Brachyury probe was first linearized from pSK by Xho 1 and transcribed using T3 (NM_009309 nt 476 to 1227). Additional probes used were obtained to: Bmp4 (Gong et al., 2003), Engrailed-2 (Davis et al., 1988), Shh (Echelard et al., 1993), Fgf8 (Crossley et al., 1995), Msx2 (Jowett et al., 1993), Snail1 (Cano et al., 2000), and Nodal (Fischer et al., 2002). Detection was carried out using α-DIG-AP and NBT/BCIP (Roche). After visual examination and photography, embryos were embedded in OCT, sectioned, examined, and photographed using brightfield microscopy.

RESULTS

Geminin is expressed in the epiblast and neural ectoderm of early post-implantation staged embryos.

 We employed *in situ* hybridization on E7.5, E8.5, and E9.5 staged embryos to determine the pattern of expression of Geminin mRNA.   At E7.5, consistent with

studies in *Xenopus* (Kroll et al., 1998) and chick (Papanayotou et al., 2008), Geminin mRNA was expressed throughout the epiblast and in the neural ectoderm, whereas expression terminated sharply at the boundary with the epidermal ectoderm (arrow, Figure 4-1 A, B, C). Geminin was also expressed the posterior region of the embryo in the primitive streak (Figure 4-1 A, C), and was present in the dorsal, but not ventral layer of the node (Figure 4-1A, B arrowheads). Extra-embryonic tissues including the amnion, allantois, chorion, and ectoplacental cone failed to express geminin at any stage of development examined (Figure 4-1). At E8.5, Geminin was expressed strongly throughout the neural ectoderm (Figure 4-1D-F) and was absent from the epidermal ectoderm (arrows in Figure 4-1 D, E, F), endoderm and the heart. It was expressed at particularly high levels in the closing posterior neuropore (Figure 4-1D, F). At E9.5, Geminin mRNA was present throughout the neural ectoderm (Figure 4-1G-I). In the neural tube, Geminin mRNA was subnuclear as revealed by propidium iodide staining (Figure 4-1I). Geminin continued to be restricted from both the epidermal ectoderm and apex of the neural folds at this stage as well (Figure 4-1I).

To examine the expression of Geminin at additional stages of development, we collected carefully staged embryos for RNA extraction and QRT-PCR analysis. As Geminin was previously reported to be expressed in the blastocyst (Gonzalez et al., 2006; Hara et al., 2006), we used this as the reference point for all comparisons. Geminin was expressed at all stages examined (Figure 4-1K) from early egg cylinder (stage 1) embryos peaking at E8.0/E8.5 (stage 3), declining until E13, then increasing with differentiation of various tissue types.

Expression of Geminin mRNA and protein are down-regulated in Geminin shRNA exposed embryos.

We used QRT-PCR and western blot analysis to determine the degree of Geminin mRNA and protein knock-down in embryos exposed to shRNA. RNAs

were extracted from individual Stage 3 and Stage 4 embryos and subjected to QRT-PCR analysis using β-actin as a control.   Although there was a range in knock-down, the average reduction in Geminin RNA was significantly different (approximately 7-fold decrease, $p \leq 0.001$) from embryos exposed to the scrambled shRNA (Supplemental Figure 4-3A).   For western blot analysis, protein was extracted from stage 4 embryos (n = 22) with β-actin used to standardize protein loading. Values were averaged and showed a significant ($p \leq$ 0.001) decrease, an average reduction of 42% compared to normalized scrambled shRNA embryos, in expression of Geminin protein in shRNA exposed embryos compared to controls (Supplemental Figure 4-3B).   Individual embryos exhibited a range in Geminin protein level from normal, heterozygote levels, to virtually no protein compared to control embryos (Supplemental Figure 4-3C).   A value of the tail-vein technique is that it produces a graded knock-down in expression similar to an allelic series and a corresponding range of phenotypes within a litter (Supplemental Figure S4-3D).   Also, the numbers of affected embryos is higher than obtained with traditional methods of knock-down (Supplemental Figure S4-2 G-I).

Geminin is required in the epiblast for axis elongation.

To determine the role of Geminin in post-implantation development, we delivered shRNA constructs targeting Geminin via two methods: tail-vein injection and pronuclear injection (Supplemental Figure S4-1). Both result in the loss of Geminin protein; however, the tail-vein approach allows control of the stage of development at the time of exposure to the shRNA. By delivering the shRNAs on E6.0, we bypassed the requirement for Geminin on E3.5 (Gonzalez 2006; Hara 2006), yielding more than 70% affected embryos.   Pronuclear injection resulted in pre-implantation loss, with surviving embryos (18 %) exhibiting less knock-down and less severe morphologies (Supplemental Figure S4-2G-I). E7.0 embryos exposed to Geminin shRNA via the tail-vein exhibited severe axis elongation abnormalities. Not only did they fail to expand proximally-distally but

also in the anterior—posterior axis. By E7.0 control embryos had well-organized headfolds, and an expanded amniotic cavity (Supplemental Figure S4-2A). Geminin shRNA exposed embryos (Supplemental Figure S4-2D) failed to elongate, the node was positioned anteriorly, and they were developmentally delayed. By E8.5, compared with control embryos in which the neural folds were elevating and beginning to fuse in the trunk region (Supplemental Figure S4-2B), the axis elongation defect was more severe in shRNA exposed embryos; the anterior and posterior neuropores were small and widely open (Supplemental Figure S4-2E). By E9.5, the neural tube has typically closed in the cephalic region of control embryos (Supplemental Figure S4-2C), while embryos exposed to the shRNA were often characterized by open, everted headfolds affecting both the forebrain and midbrain (arrows, Supplemental Figure S4-2F). The first branchial arch was also small and abnormally oriented in shRNA exposed embryos (Supplemental Figure S4-2F). Surviving embryos carrying the hairpin shRNA express DsRed (Supplemental Figure S4-2F) or EGFP (Supplemental Figure S4-2I).

Geminin is required for gastrulation movements and formation of the definitive endoderm.

At gastrulation, epiblast cells delaminate from the primitive ectoderm to form mesoderm and intercalate and replace the primitive endoderm (PE) with embryonic (definitive) endoderm (DE). Since the primitive endoderm is composed of flattened, unspecialized cells, compared with the microvilli covered, smaller cells of the embryonic endoderm, it is possible to monitor the progress of gastrulation by examining the position of the boundary between these two cell types. As gastrulation proceeds, the boundary normally progresses from distal to proximal eventually terminating at its post-gastrulation position in the extra-embryonic region (Figure 4-2A, asterisk; 2E, arrows). In Geminin knock-down embryos, this boundary fails to migrate proximally (Figure 4-2B, F arrows), although the cells at the boundary appear normal.

Horseradish peroxidase (HRP) activity is normally found at high levels in the primitive ectoderm (Bielinska et al., 1999; Chen et al., 1994) (Figure 4-2C, arrow). However, in Geminin shRNA embryos, HRP expression is extended more distally compared to controls (Figure 4-2D, arrow). At the beginning of gastrulation when cells are moving toward and involuting through the primitive streak, a group of proximal epiblast cells in direct contact with the extra-embryonic ectoderm where BMP4 is expressed at high levels, form primordial germ cells (PGCs) (Lawson et al., 1999; Chiquoine et al., 1954; Ginsburg et al., 1990). PGCs express a number of markers including tissue non-specific alkaline phosphatase (TN-AP), which is specific for PGCs from E7 to E14 (Ginsburg et al., 1990; Hahnel et al., 1990). In control E7.5 embryos, a group of alkaline phosphatase positive PGC are located at the base of the allantois (Figure 4-5D). In contrast, the entire epiblast is positive for alkaline phosphatase in Geminin shRNA exposed embryos (Figure 4-5H). Since this population of cells is responsive to Bmp4 signaling, these data and expansion of the Bmp4 expression domain in shRNA embryos suggest that by down-regulating Geminin in the epiblast, Bmp4 expression is expanded and converts the epiblast into a region which may be permissive for PGC differentiation. Targeted deletion of Eomes results in a similar failure of differentiation of the definitive endoderm. In these embryos the expression of AFP, which normally marks the boundary between primitive and definitive endoderm, also continues to be expressed in the PE surrounding the embryo (Arnold et al., 2008).

Compared with control embryos (Figure 4-2A, E), both the foregut and hindgut pockets remain widely open in shRNA treated embryos (Figure 4-2B, F), likely due to the lack of definitive endoderm and failure of morphogenetic movements required for body wall closure. The notochord is also more prominent in affected embryos (Figure 4-2F) than in controls (Figure 4-2E). Foxa2, a marker of endoderm, highlights the widely open foregut pocket in shRNA embryos (Figure 4-5F) compared with the control (Figure 4-5B), and the widened floorplate and

126

notochord. QRT-PCR indicate that compared with individual control embryos, Foxa2 is slightly increased (Table 4-2). Both the proximal-distal as well as anterior-posterior axes were shortened in Geminin shRNA embryos (Figure 4-2B), which is particularly obvious in the anterior shortening of the neuraxis in this embryo (Figure 4-2B). These embryos also illustrate the presence of a well formed foregut pocket in control embryos (Figure 4-2A), compared with the shRNA embryo (Figure 4-2B).

Loss of Geminin produces defects of the node.

In control embryos, the node is a bi-layered structure consisting of small ciliated cells on its ventral surface, surrounded by flattened endoderm (Figure 4-3A). The node has a slightly concave appearance when viewed in sagittal sections (Figure 4-3C) with the number of cells at the distal tip decreasing as it moves towards the primitive streak (Figure 4-3A, black arrowhead). As the node regresses, newly formed endodermal cells replace it (Figure 4-3A). When Geminin expression is down-regulated, the node forms a deep, concave pit (Figure 4-3B, black arrowhead) with a bolus of mis-migrated cells behind it (Figure 4-3B, white arrowheads). The node is mis-positioned anteriorly and condensed, and fails to regress normally as illustrated by Foxa2 expression (Figure 4-3D, arrowhead). The bi-layer organization of the node is also disrupted (Figure 4-3F, asterisk); however, Nodal, which is expressed in the crown cells surrounding the node, is normal (Figure 4-3E and 3F arrows).

Geminin is required for posterior patterning of the embryo.

To understand the molecular basis of the gastrulation defect, we examined the expression of markers of the primitive streak, notochord, and mesoderm. Compared to controls (Figure 4-4A) where Fgf8 is expressed in its characteristic pattern in the primitive streak, Geminin shRNA embryos failed to express Fgf8 at this stage of development (Figure 4-4B). Snail1 is a downstream target of Fgf8

required for down-regulation of E-cadherin (Cano et al., 2000). In control embryos, Snail1 is expressed in the primitive streak (Figure 4-4C) whereas loss of Geminin results in loss of Snail1 expression in these embryos (Figure 4-4D). Snail1 is required to inhibit E-cadherin expression in the primitive streak for proper EMT to occur. In control embryos, E-cad expression is reduced in the primitive streak (Figure 4-4F, arrow); however, not only is there an aggregate of cells in the primitive streak of Geminin shRNA embryos, but E-cad expression fails to be down-regulated (Figure 4-4H). Brachyury, a marker of mesoderm in the primitive streak and node (Figure 4-4I), had a wider expression domain in shRNA embryos (Figure 4-4J) likely due to the failure of proximal elongation resulting in a broader embryo. This also persist at E9.0 were expression of Brachyury is normally restricted to the ectoderm (Supplemental Figure S4-5B') is expanded to include the underlying mesenchyme and gut epithelium of Geminin exposed embryos (Supplemental Figure S4-5F'). Wnt signaling is normally tightly restricted to the primitive streak (Figure 4-4K, M); however, Wnt signaling was expanded into the ectoderm and mesoderm in geminin shRNA embryos (Figure 4-4L, N). This ectopic Wnt signaling could be explained by the observation that Geminin can inhibit Wnt signaling in the epiblast. The primitive streak region itself, which is normally composed of a single layer of epiblast cells from which mesoderm and endoderm delaminate (Figure 4-4E), was also abnormally organized in shRNA exposed embryos, where multiple layers of epiblast were folded over single layers of mesoderm and endoderm (Figure 4-4G, arrow). These data support the conclusion that Geminin is required at gastrulation for EMT, lineage differentiation and axis elongation.

Anterior regions of the embryo are mispatterned in Geminin shRNA embryos.

Cells that migrate through the node that will give rise to form the anterior endoderm and mesoderm, fail to do so in shRNA embryos. Shh, which is expressed in the notochord (Figure 4-5A) is lost or severely decreased in the anterior region of Geminin shRNA embryos, (Figure 4-5E). Lack of Shh signaling

to the overlying neural tube results in failure of formation of the floorplate, lack of a medial hinge point, and expansion of the ventral neural ectoderm. At later stages of development, this results in an abnormally widened ventral neural tube and defects of neural tube closure (Supplemental Figure S4-5L, M). The loss of Shh expression from the notochord also fails to induce liver bud expression of Shh (Supplemental Figure S4-5N) in contrast to control embryos (Supplemental Figure S4-5K).

The early expression domain of Bmp4 in the extra-embryonic ectoderm and epidermal ectoderm in control embryos (Figure 4-5C) was expanded in shRNA embryos, particularly at the surface ectoderm/neural ectodermal boundary (Figure 4-5G). This was also identified in the regression analysis of QRT-PCR data indicating that Bmp4 expression increases (p $\leq$ 0.598) as Geminin decreases. This is also consistent with the suggestion that Geminin inhibits Bmp4 expression in the neural plate (Kroll et al., 1998, Seo et al., 2005a, our *in situ* data), and suggest that Bmp4 (and Nodal) is expressed at sufficient levels to position the node, but absent Geminin in the neural ectoderm, the Bmp4 expression domain in the epidermal ectoderm is expanded as was previously observed in *Xenopus* (Kroll et al., 1998).

Geminin is required for neural crest differentiation.

The striking lack of Geminin expression at the crest of the neural folds suggests a possible role in EMT by neural crest cells as well. (Supplemental Figure S4-4D arrows). In control embryos, Snail1 is expressed by forming neural crest cells (Supplemental Figure S4-4A) while Msx2, which is expressed by migrating neural crest is present at the boundary between neural ectoderm and epidermal ectoderm in the headfolds (Supplemental Figure S4-4B). In Geminin shRNA exposed embryos, Snail1 is strikingly absent (Supplemental Figure S4-4E), and Msx2 strongly down regulated (Supplemental Figure S4-4F). At the SEM level, the cephalic neural folds of control embryos are elevated, approaching in the

dorsal midline (Supplemental Figure S4-4C), unlike Geminin shRNA exposed embryos, where the neural ectoderm is folded and the neural folds are widely splayed (Supplemental Figure S4-4G). At the neural/surface ectoderm boundary, neural crest cells undergo epithelial to mesenchymal transition, leave the NE to migrate into the mesenchyme (Supplemental Figure S4-4H). In Geminin shRNA embryos, cells at the border region are disorganized, rounded, lack polarity and leading processes (Supplemental Figure S4-4I). These data suggest that Geminin plays a critical role in neural crest cell migration and/or differentiation, which may involve either mis-specification of the population or failure of EMT.

Geminin is required for the normal development of the midbrain & craniofacial region.

 By E8.5, the neural folds in the midbrain and hindbrain have elevated and are beginning to approximate in the midline (Figure 4-6A, B, E). Embryos in which geminin expression is down-regulated are characterized by axis elongation defects that affect both the anterior and posterior regions of the neuraxis (Figure 4-6G, H, K). The anterior neuropore is widely expanded and often fails to close in the midline (Figure 4-6B, U). Because many of the closure abnormalities affected the midbrain-hindbrain region, we examined the expression of Engrailed-2, which is present in the posterior hindbrain and in rhombomere 1 of the hindbrain in control embryos (Figure 4-6F). In experimental embryos, Engrailed-2 expression was strikingly reduced in the midbrain but not in rhombomere 1 (Figure 4-6L), suggesting a role for Geminin in development and patterning of the midbrain. The commissural plate, the most rostral part of the neural tube, is not only widened but a severe loss of Fgf8 expression here as well as in the first branchial arch is observed in Geminin shRNA embryos (Supplemental Figure S4-5G, inset in G, H) compared to controls (Supplemental Figure S4-5C, inset in C, D). Expression in the isthmus and developing limb bud were unaffected. Shh expression is also mispatterned along the length of the

neural tube with prominent defects in the diencephalon of affected embryos (Supplemental Figure S4-5L, M white arrows) compared to controls (Supplemental Figure S4-5I, J white arrows).

Delivery of Geminin shRNA to pregnant dams carrying a transgene containing six copies of TCF/Lef binding sites driving expression of β-gal (Wnt indicator mice), indicated that expression of activated β -catenin was strikingly down-regulated in cranial regions, particularly in the neural crest migratory pathway to the first branchial arch, as well as in cells located in the posterior neuropore (Figure 4-6K, arrowhead) compared to control embryos (Figure 4-6E). Axin2, a downstream target of Wnt signaling was also decreased (Table 4-2, $p \leq 0.409$) in QRT-PCR analysis of individual Geminin shRNA embryos. This suggests a role for Geminin in both neural crest formation and migration, and in modulating the Wnt pathway as well.

Geminin controls differentiation of neural progenitor cells.

Prior evidence suggested that Geminin may act as a switch between proliferation of neural progenitors and differentiation of immature neurons (Seo et al., 2005a, b). In control embryos, Sox3 is strongly expressed in neural progenitors throughout the early neural ectoderm (Figure 4-6M-O). As predicted, expression of Sox3 was reduced in geminin shRNA embryos (Figure 4-6S-U) whereas TuJ1, a marker of immature neurons (Figure 4-6P-R), was prematurely activated and expanded (Figure 4-6V-X). QRT-PCR for Sox3 ($p \leq 0.51$) and Neurogenin-1 ($p \leq 0.515$) on individual embryos confirms these results (Table 4-2).

DISCUSSION

The current investigation is the first to examine the expression and identify a novel role for Geminin during gastrulation in the post-implantation staged mouse embryo. Geminin is expressed throughout the epiblast, where it is required for

proper migration from the primitive streak and node. Cells leaving the primitive streak were able to form mesoderm and endoderm but failed to migrate anteriorly, producing embryos that failed to elongate in both the proximodistal and anterior-posterior axis. The notochord was incomplete and often interrupted resulting in a loss of Shh expression and failure of the floorplate to form. At later stages, we observed several neural tube defects including: open anterior and posterior neuropores, everted headfolds, mispatterning along the neural tube, and reductions in neural crest cells. The border between the neural and epidermal ectoderm was also affected as Bmp4 expression increased with the loss of Geminin in embryos. The Wnt signaling domain in the posterior epiblast was also expanded supporting a previously anticipated role for Geminin in inhibiting both BMPs and Wnts during gastrulation. Embryos exposed to Geminin shRNA exhibited premature neuronal differentiation (TuJ1+) at the expense of the neural precursor population (Sox3+). Geminin had previously been suggested to specify the neural ectoderm by inhibiting BMP signaling (Kroll et al., 1998), cell cycle regulation, and controlling neurogenesis (Luo et al., 2004; Del Bene et al., 2004; Seo et al., 2005a, b). Geminin knock out was lethal at E3.5, precluding analysis of its role in post-implantation development (Hara et al., 2006; Gonzalez et al., 2006). To avoid the early requirement for Geminin, we employed a technique which allowed us to deliver shRNAs targeting Geminin to pregnant dams on E6.0.

Geminin is required for EMT at gastrulation.

During gastrulation, epiblast cells delaminate and migrate from the primitive streak forming definitive endoderm and mesoderm (Tam and Loebel, 2007). In Geminin knock-down embryos, cells left the streak but formed a disorganized accumulation of cells posterior to the node and at the base of the streak. As a result, the PE was not replaced by DE, fewer cells passed through the node to form the prechordal plate and notochord, which produced axis elongation defects. In Geminin knock-down embryos, the expression of both Fgf8 and

Snail1 in the primitive streak was reduced, indicating that Geminin expression in the epiblast may regulate cell migration via induction of Fgf8, Snail1, and/or down-regulation of E-cadherin.

Control over EMT is maintained by a cascade of signaling factors that control the expression of E-cadherin (review Yang, 2008). Fgf signaling through FGFR1 induces expression of the transcriptional repressor Snail1 which binds to an E2-box element in the E-cadherin promoter and inhibits expression of E-cadherin (Cano et al., 2000). In embryos null for Fgf8 (Sun et al., 1999), FGFR1 (Yamaguchi et al., 1994), or Snail1 (Carver et al., 2001) EMT is disrupted. The Nodal target gene Eomes is required for EMT but appears to function at a different step in the pathway as Eomes$^{-/-}$ embryos fail to down-regulate E-cadherin but mesoderm formation, as indicated by Fgf8 and Snail1, is unaffected (Russ et al., 2000). E-cadherin inhibition alone is unable to induce EMT as overexpression of Geminin in epithelial cells conveys invasive properties to the cells, but they are unable to migrate (Llorens et al., 1998). Eomes null mice also fail to elongate in the A-P axis as cells fail to migrate away from the streak and thus axial mesoderm tissue fails to form (Arnold et al., 2008).

Cells in the primitive streak of Geminin shRNA embryos were able to ingress, change apical-basal polarity, and form mesoderm but many failed to migrate, similar to the situation in *Snail1$^{-/-}$* embryos (Carver et al., 2001). Consistent with this observation, expression of Brachyury, a marker of early mesoderm, was slightly elevated, indicating that the loss of Geminin did not inhibit mesoderm differentiation. In addition, embryos with mutations in genes such as Activin βa and βb (Matzuk et al., 1995) and MesP1 (Saga et al., 1996) also show abnormal EMT but do not affect mesoderm formation. How they may control/affect E-cadherin remains to be determined.

Bmp4 is required for the formation of the node and primitive streak as well as the specification of mesoderm (Fujiwara et al., 2002). Mouse embryos lacking either

Bmp4 or its type I receptor, Bmpr1A, lack mesoderm while overexpression of Bmp4 induces it (Lawson et al., 1999; Mishina et al., 1995; Thomsen et al., 1997). Expression of Bmp4 in the epidermal ectoderm is also required for the induction of neural crest cells which form in a region juxtaposed between the neural and non-neural ectoderm (review Sauka-Spengler and Bronner-Fraser, 2008; Liem et al., 1995). Wnts and FGFs have also been implicated in neural crest induction and specification but if and when they interact with BMPs is still debated (Patthey et al., 2009; Steventon et al., 2009; review Jones and Trainor, 2005).

In the amphibian embryo, over-expression of Geminin inhibits Bmp4 expression in the neural ectoderm (Kroll et al., 1998; Papanayotou et al., 2008), suggesting that it may control neural crest cell differentiation, migration, number, etc. In addition, other factors influence neural crest migration such as the notochord, which is inhibitory (Stern et al., 1991) and the non-canonical Wnt pathway through RhoA activation (Carmona-Fontaine et al., 2008). In the mouse embryo, Geminin is expressed in the neural ectoderm of E7.0 embryos with particularly strong expression in cells at the boundary between the neural and epidermal ectoderm (Figure 4-1C). As Geminin is reduced in shRNA exposed embryos, the Bmp4 expression domain is expanded into cells adjacent to the neural plate as well as in cells at the base of the allantois suggesting that Geminin is required for Bmp inhibition in these regions. In later embryos, we observed a striking decrease in the formation of neural crest cells as indicated by the loss of Msx2 and Snail1 expression as well as of Wnt signaling. It has alternatively been suggested that Wnts from the mesoderm are required to inhibit Bmps for neural crest formation (Steventon et al., 2009), and that neural crest cells form only in the absence of Wnt signaling (Patthey et al., 2009). Our data not only suggest that tight regulation of both Bmp and Wnt signaling is required for neural crest induction, but it may rely on Geminin. Geminin could also affect migration through interaction/inhibition of the non-canonical Wnt pathway but as neural

crest cells fail to form in Geminin shRNA embryos, alternative approaches will be necessary.

Geminin is required for the formation of definitive endoderm.

As gastrulation proceeds, the first cells to emerge from the streak form the node, notochord, and definitive endoderm (DE) (Beddington and Robertson, 1999). DE cells emerging from the primitive streak migrate distally and displace the AVE anteriorly (Vincent et al., 2003). Recent evidence suggests that VE cells may remain associated with the underlying epiblast that intercalate and form the gut endoderm (Kwon et al., 2008). The endodermal cells of the foregut are the first to emerge from the streak with mid- and hindgut progenitors emerging later as the primitive streak regresses posteriorly (Fukuda et al., 2005). In Geminin targeted shRNA embryos, definitive endoderm was specified in a dosage dependent manner, but failed to intercalate with and replace the primitive endoderm. This was illustrated by the presence of ciliated primitive endodermal cells in the distal region of the embryo in SEM, and by the uptake of HRP in primitive endodermal cells (Bielinska et al., 1999; Chen et al., 1994). In these embryos, the foregut pocket formed, but was wider and deeper than in controls. At later stages, the hindgut pocket remained widely open with the lateral edges of the gut tube failing to fuse.   Msx2, which is expressed in the intermediate mesoderm in both somatopleure and splanchnopleure, was strikingly reduced in Geminin targeted embryos. Although *Msx2* null mice exhibit defects in craniofacial, skin, and mammary tissues, mice are viable and are able to reproduce largely from the compensatory role of Msx1. However, double *Msx1*^{-/-};*Msx2*^{-/-} mutants have ventral body wall defects including the inability of the abdominal wall to close (Ogi et al., 2005). This is similar to *Sox17*^{-/-} embryos which fail to displace the visceral endoderm, (Kanai-Azuma et al., 2002), and *Smad2*^{-/-} embryos in which definitive endoderm contributes to the ADE but not the hindgut (Tremblay et al., 2000).

Ventral body wall closure defects are also present in embryos with mutations in Pitx2 due to a failure to form endoderm (Liu and Martin, 2001; Lu and Martin, 1999). Abnormal body wall closure is also observed in FLRT3 mutant mice (Egea et al., 2008). FLRT3 is a transmembrane protein required in the AVE to prevent ectopic EMT and mesoderm induction by maintaining basement membrane integrity. In Geminin shRNA exposed embryos, some definitive endoderm is formed and migrates, but whether the body wall defects are a primary result of a failure in endoderm lineage differentiation and/or migration, or whether elongation of the embryo driving the purse string-like closure of the gut tube also fails in these embryos is currently unresolved.

Geminin is required to restrict PGC specification to the distal epiblast.

There was widespread alkaline phosphatase staining of the epiblast of Geminin shRNA embryos. Tissue Non-specific Alkaline Phosphatase (TN-AP) is the only AP expressed at this stage, and is normally restricted to the primordial germ cell (PGC) population on E7 to E14 (Hahnel et al., 1990). Loss of Smad 5 in embryos results in ectopic AP and Oct4 expression suggesting that the epiblast is converted into a region competent to form PGCs (Bosman et al., 2006). These studies suggest that Geminin may similarly be required to restrict BMP expression posterior epiblast. Whether Geminin can regulate downstream Bmp target genes required for PGC differentiation remains to be determined.

Geminin regulates Wnt signaling during gastrulation.

To determine if Geminin interacts with the Wnt signaling pathway, the Geminin shRNAs were also delivered to homozygous time pregnant reporter mice that contain six copies of TCF/LEF driving expression of β-gal (Mohamed et al., 2004). We observed an anterior expansion of Wnt signaling in the epiblast and mesenchyme but not the endoderm in Geminin shRNA embryos compared with

controls. In later embryos, however, Wnt signaling was severely reduced in the somites and prospective neural crest along the entire length of the neural tube. Geminin has been shown to act as a transcriptional repressor in several contexts (*i.e.* Cdt1, Hoxb9, and Six3). Additionally, the *Geminin* promoter has been shown to contain Tcf and Vent binding sites which are able to mediate Wnt and Bmp signaling, respectively, in *Xenopus* embryos (Taylor et al., 2005). It is also plausible that geminin could interact with Smads in the nucleus as Hox proteins are able to form complexes with Geminin as well as Smads (*i.e.* Smad4-Hoxc9) (Zhou et al., 2007). In fact, until recently, Wnt target gene activation was thought to occur only when β -catenin was bound to TCF/LEFs (Stadel 2006; Parker 2007). Depending on the cell type, in now appears that β -catenin binding to TCF/LEFs can also be inhibitory (Piepenburg et al., 2000; Theisen et al., 2007; Blauwkamp et al., 2008). Our data suggest that at gastrulation, Geminin is required to restrict Wnt signaling to the primitive streak while later in development Geminin plays a role in specifying the neural crest.

During gastrulation, Wnt signaling is restricted to the primitive streak where Wnts are required for the formation of mesoderm and endoderm (Tam and Loebel, 2007). Upon activation of Wnt signaling, β -catenin accumulates and translocates to the nucleus where it binds to TCF/LEFs and activates expression of downstream target genes (review Roose and Clevers, 1999). Not only are TCF1, 3, 4, and LEF1 expressed in various spatial and temporal patterns during development but mutations in TCF3 lead to ectopic nodes and notochords; *TCF1*^{-/-}; *LEF1*^{-/-} mice have ectopic neural tubes; and *TCF1*^{-/-}; *TCF4*[/-] embryos have caudal truncations and hindgut defects (Galceran et al., 1999, Gregorieff et al., 2004, Merrill et al., 2004). Using the 6x Wnt reporter mice, our data indicate Wnt signaling increases in the primitive streak at E7.0 but has marked reduction in the neural crest at E9.0. It is possible that Geminin is interacting with one or TCFs in various times and tissues. At E6.5, only TCF3 is expressed throughout the epiblast and extra-embryonic tissues. At E7.5, although it is still expressed ubiquitously, a gradient of expression with higher levels in the anterior is

observed (Korinek et al., 1998). In contrast, TCF1 and LEF1 are both widely expressed in a posterior to anterior gradient with high levels in mesoderm, lower levels in ectoderm, and loss of expression in endoderm (Oosterwegel et al., 1993; Mayer et al., 1997). At later stages, TCF3 is in the anterior neuroectoderm whereas TCF1 and LEF1 are in the lateral plate mesoderm, mesenchyme of the branchial arches, and in patches in and around the neural tube where neural crest form (Oosterwegel et al., 1993). Given this information, Geminin could potentially bind to TCF3 at gastrulation and either TCF1 or LEF1 in the neural crest.

Geminin is required for formation of the notochord and induction of the floorplate.

The prechordal plate, at the rostral extreme of the neural tube *i.e.* the commissural plate, and the notochord not only induce formation of the floor plate but they convey dorsal/ventral patterning to the neural tube by secreting Shh (Echelard et al., 1993; Ericson et al., 1996). In control embryos, Shh from the prechordal plate maintains Fgf8 expression in the commissural plate while Bmp4 from the dorsal neural tube inhibits its expression (Ohkubo et al., 2002). Geminin shRNA embryos are characterized by disruptions in and poor organizion of the notochord and prechordal plate; Shh and Fgf8 expression are reduced. Absent inductive signals, the floor plate and commissural plate failed to form, resulting in a widened neural tube. This prevented the neural folds from bending toward the dorsal midline resulting in an eversion of the neuroepithelium at both the anterior and posterior neuropores. The notochord also plays a role in axis elongation (review Beddington and Robertson, 1999) which is strikingly inhibited in our embryos.

The endoderm of the digestive tract also requires signals from the notochord for specification and induction of organs along its length (Grapin-Botton and Melton, 2000). We observed that Shh normally expressed in the diverticulum of the liver was absent in Geminin shRNA embryos. In addition, specification of the dorsal

pancreas requires Hoxb9 and Pdx1 expression from the endoderm and notochord (Li et al., 1999; Harrison et al., 1999). As Geminin has been shown to directly bind to Hoxb9 in chick embryos and inhibit its expression (McGarry and Kirschner, 1998) it is likely that the pancreas and other endodermal organs may be affected by the loss of Geminin signaling either directly (*i.e.* repression by Geminin is lifted) or indirectly (*i.e.* failure of notochord formation and lack of downstream signals).

Geminin links cell cycle progression and neural differentiation.

In Geminin shRNA targeted embryos, the population of proliferative Sox3+ neural progenitor cells was severely decreased, while there was premature differentiation of TuJ1+ neurons compared to control embryos. There was also a strong negative correlation in Geminin expression and Ngn-1 identified using QRT-PCR of individual embryos. This indicates that Geminin is necessary to maintain the proliferative neural precursor population as when cells lose Geminin they appear to differentiate prematurely.

The ability to coordinate both cell cycle progression and differentiation suggests that Geminin may have a role controlling in the switch from rapidly proliferating progenitors to immature neurons (Luo and Kessel, 2004; Del Bene et al., 2004). This is consistent with the presence Geminin in proliferating neural progenitors and with its subsequent down-regulation as cells differentiate into immature neurons (Seo et al., 2005a, b). In addition to Cdt1, Geminin can bind to Polycomb complexes mediating *Hox* gene regulation or SWI/SNF complexes which regulate bHLH gene expression (Del Bene et al., 2004; Seo et al., 2005a, b). These events occur during G2 when cells make a fate choice between proliferation and differentiation. While Geminin was initially identified based on its neuralizing activity (Kroll et al., 1998), it has also been shown to play a critical role in preventing chromosomal duplication during the S phase (McGarry and Kirschner, 1998) and promoting proper cytokinesis (Nakuci et al., 2006). During

S-phase of the cell cycle, Geminin is bound to Cdt1 (a licensing factor), preventing Cdt1 from forming a complex with the origin recognition complex (ORC) and thereby inhibiting re-replication of the DNA. At G2, Geminin is uncoupled from Cdt1 and is subsequently inactivated by ubiquitination during the M-phase (Luo et al., 2004; Luo and Kessel, 2004; Saxena et al., 2005). In fact, Geminin null embryos died at E3.5 due to over-reduplication of DNA (Hara et al., 2006; Gonzalez et al., 2006).

Geminin is expressed in a number of solid tumors including renal cell carcinomas, breast cancers, colon and rectal tumors (Wohlschlegel et al., 2002; Montanari et al., 2005; Obermann et al., 2005; Gonzalez et al., 2004; Dudderidge et al., 2005). Recently, EMT has been proposed to cause the progression of epithelial carcinomas to malignancy (Doble and Woodgett, 2007).   While overexpression of Geminin in these cells was unable to inhibit cell proliferation (Wohlschlegel et al., 2002) the role of EMT in these cells was not examined. Our data suggest that Geminin may control EMT as loss of Geminin (current investigation) prevents and overexpression in EBs (Slawny et al in preparation) promotes EMT.

Tail vein delivery of shRNAs down-regulates target gene expression in post-implantation staged embryos.

Delivery of shRNAs targeting Geminin via pronuclear injection largely recapitulated the requirement for Geminin in the ICM as few affected (transgenic) embryos survived to E7.5 (Supplemental Figure S4-2) (Hara et al., 2006; Gonzalez et al., 2006). Although the lethality was stated to occur via over-duplication errors, given our observations that Geminin is required for EMT at gastrulation, it also seems possible that a down-regulation of E-cadherin expression required for compaction of the morula may have played a role in stage specific differentiation. Since Geminin expression was strongly up-regulated during early post-implantation development (Figure 4-1K), we wished

to examine its role in gastrulation and neurulation and avoid pre-implantation lethality. We therefore delivered shRNAs targeting Geminin to pregnant dams on E6.0. A number of factors including DNAs have been delivered via the maternal circulation, with long-term expression in the embryonic compartment. This approach is most effective in achieving long-time gene expression (reporter genes) and knock-down when delivered during early peri-implantation development (O'Shea et al., 2006). This produces a range in knock-down allowing correlation between genotype and phenotype and analysis of the many factors that act as a gradient *i.e.* BMP, Nodal.

Geminin is required at multiple stages of development.

It is widely accepted that signaling cascades are re-utilized in multiple contexts in patterning numerous tissues during development. Like Fgf8, which is present in the primitive streak then re-expressed in the isthmus (mid-hindbrain patterning zone), or Eomes which is critically involved in primitive streak formation early and later in the subventricular zone, Geminin is expressed in the primitive streak, ventricular zone of the neural epithelium, isthmus, and later in the SVZ where it may again play a role in lineage differentiation of proliferative progenitor C cells to neuroblasts.

Our data identify a previously unsuspected role of the bi-functional protein Geminin in gastrulation where it appears to control lineage specification and EMT and later to control cell cycle and neural differentiation. Since the development of nearly every organ system requires a similar switch in proliferation driven by cell cycle, it is likely that Geminin may play a role in the switch from precursor to proliferative progenitors in multiple tissues/phases of development.

ACKNOWLEDGMENTS

Figure 4-1. Geminin expression in the early postimplantation embryo

Whole mount *in situ* hybridization localization of Geminin mRNA was carried out on embryos isolated on E7.5 (A-C), E8.5 (D-F), and E9.5 (G-J) of gestation.

A-C. E7.5 Embryos. A. Side view (anterior, left) of an E7.5 embryo illustrating the strong expression of Geminin mRNA in the neural ectoderm of the headfolds and primitive streak. There was no expression in the endoderm or forming mesoderm at this stage, or in extra-embryonic tissues including the allantois (A) and yolk sac. B. Anterior view. Geminin is expressed at high levels in the neural ectoderm (double arrow), but is notably absent from the node (arrowhead) and epidermal ectoderm (dashed lines, arrow). C. Transverse section through an E7.5 embryo illustrating the cytoplasmic (subnuclear) localization of Geminin mRNA in the neural ectoderm in both the headfolds (Hf) terminating at the epidermal ectoderm (asterisks) and primitive streak (PS).

D-F. E8.5 Embryos. D. Side view (anterior, left) shows the lack of Geminin mRNA in the heart (H), allantois (A) and epidermal ectoderm (arrow), although Geminin is strongly expressed in the adjacent neural ectoderm. E. Ventral/Anterior view illustrates strong expression in the neural ectoderm of the headfolds and cervical neural tube (double arrow), and absence from the epidermal ectoderm (arrow). F. Dorsal view of the posterior neural tube (NT) and headfolds illustrating the strong expression of Geminin in the neural ectoderm, unlike mesoderm, surface ectoderm and allantois (A).

G-I. E9.5 Embryos. G. Geminin continues to be expressed at high levels in the neural ectoderm and otic vesicles (ov), but is absent from the heart (H), with low levels of expression beginning in the endoderm. H. Dorsal view illustrating expression throughout the neural ectoderm (NE) in the dorsal midline. I. Transverse section through the neural tube (NT) of an E9.5 embryo illustrating the presence of Geminin mRNA subjacent to the nuclei in the stratifying neural ectoderm. Geminin is not expressed in mesoderm or surface ectoderm (arrow) at this stage of development. Inset illustrates propidium iodide (orange) nuclear stain. J. Side view (cephalic, left) of an E9.5 embryo exposed to Geminin shRNA, illustrating the lack of Geminin mRNA, and characterized by multiple defects of the cephalic neural tube (arrow) and branchial arches. K. Quantitative RT-PCR was performed on cDNAs from carefully staged, pooled, wild-type embryos from Blastocyst to E17 stages of development. For the analysis, expression at the Blastocyst stage was used as the reference (fold change = 1.0). Geminin expression peaks at Stage 2 (5-10 somites) and decreases until E13, before spiking again at E15. Data are expressed as mean $\pm$ SD. All scale bars = 200 μm with the exception of: C and I where bars = 100 μm, and I' = 50 μm.
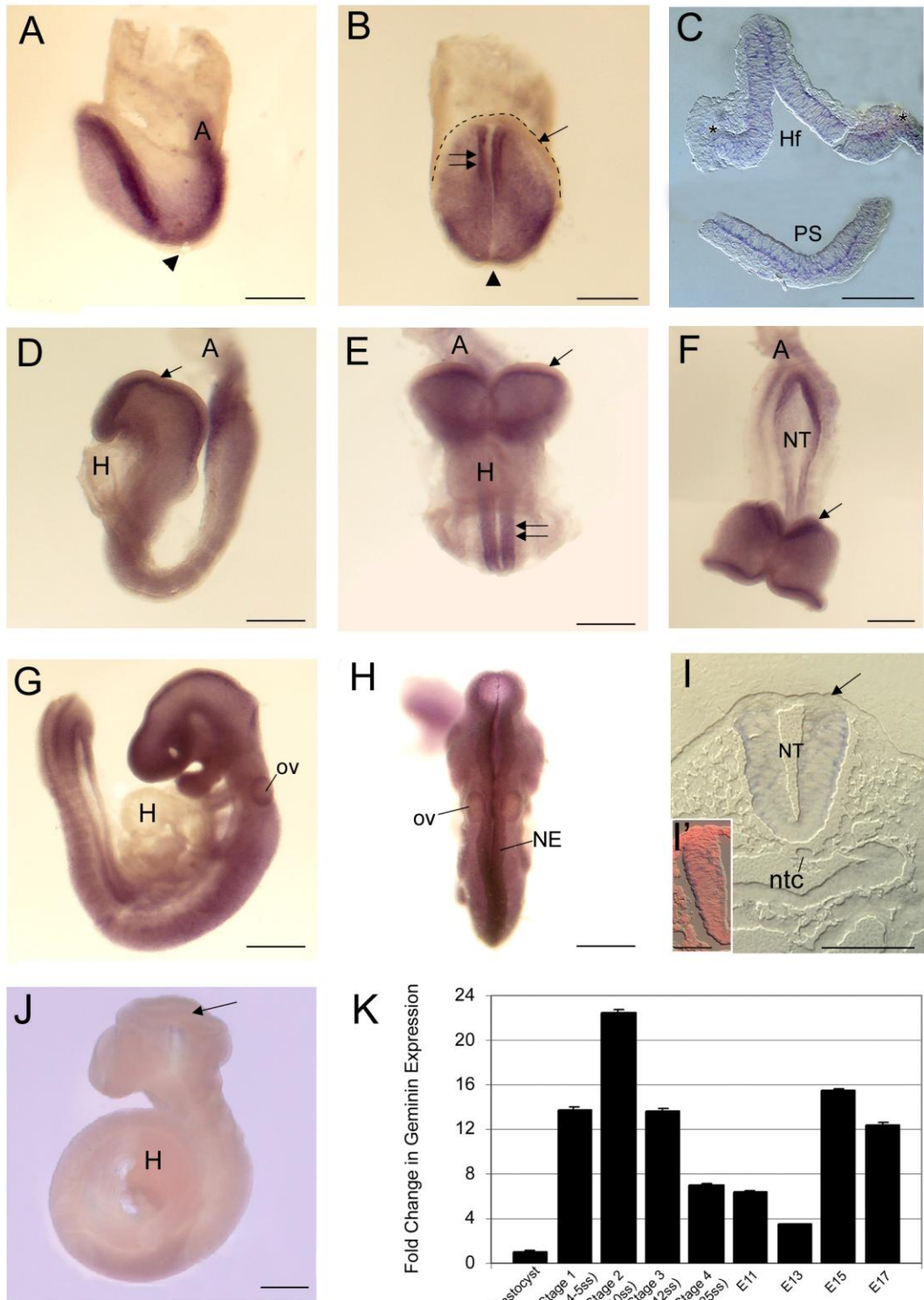
Figure 4-2. Geminin is required for gastrulation.

A,B. Side views of embryos (anterior to left) exposed to scrambled shRNA (A) or Geminin shRNA (B) on E7.5 of gestation visualized using SEM. As the primitive endoderm (PE) is replaced by embryonic endoderm (DE) at gastrulation, the surface morphology of the cells changes from a ciliated to a flattened, non-ciliated epithelium (A, inset. Dashed line indicates border). The progression of gastrulation can therefore be monitored by the gradual shift of this boundary from distal to proximal (D, P). In Geminin shRNA exposed embryos (B), where gastrulation movements are inhibited, the replacement of ciliated primitive endoderm by embryonic endoderm is abrogated, and the embryo fails to expand.

C,D. On E7.5, Horseradish-peroxidase (HRP) is used to stain primitive endoderm . HRP is expressed in the primitive endoderm in control embryos (C), but is further extended distally in embryos exposed to Geminin shRNA (D). Arrows indicate the PE/DE border. Anterior is to the left.

E,F. Anterior aspect of control (E) and Geminin shRNA (F) embryos viewed using SEM. Compared with control embryos (E), the foregut pocket is widely open and deeper in Geminin shRNA embryos (F), the notochord (N) is prominent and the headfolds are abnormally formed. In addition, the PD/DE boundary has not moved distally (arrows), the node failed to regress and often had a concave morphology (arrowheads).

Arrowheads = node, Hf = headfolds, Scale bars = 200 μm (C,D, G,H), 100 μm (A,B,E,F) and 10 μM (inset in A).

Control   shRNA

A   B

C   D

E   F
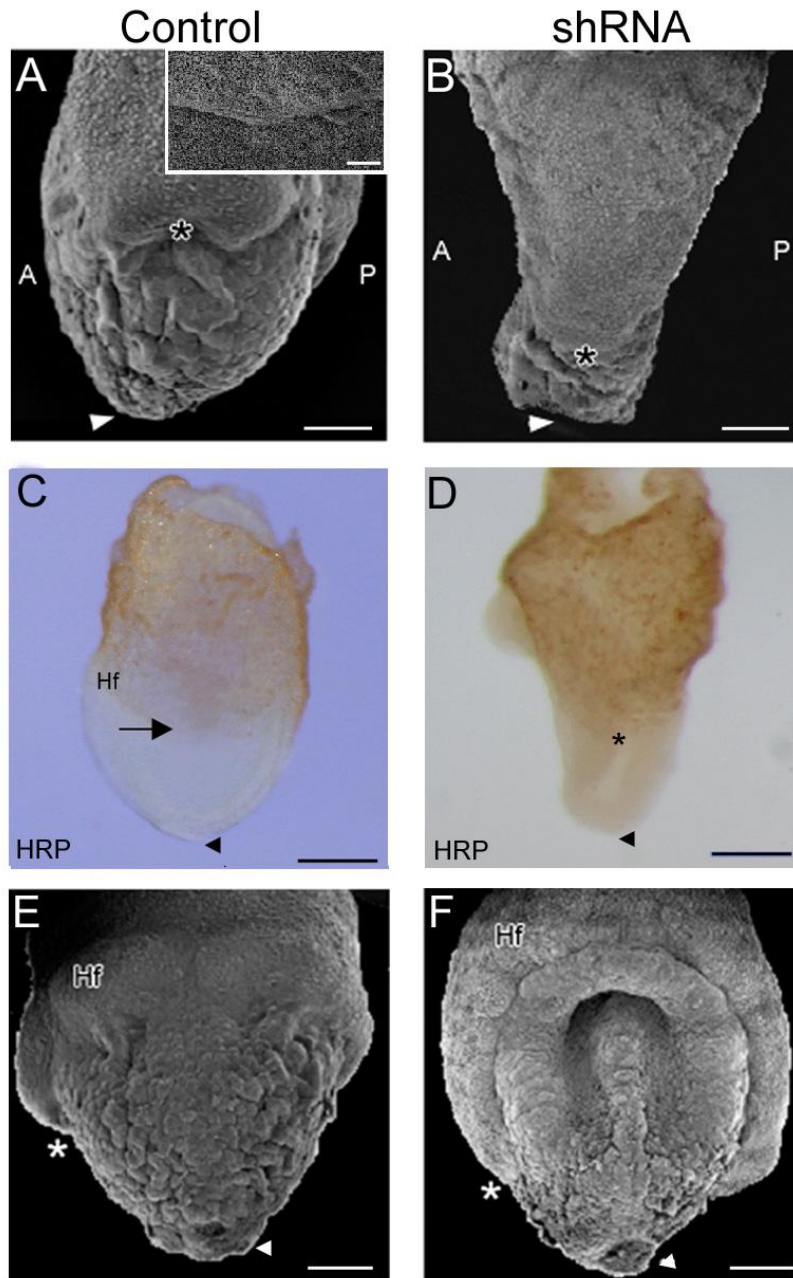
Figure 4-3. Alterations at the Node.

To examine the morphology of the node, E7.5 embryos exposed to scrambled shRNA (A,C,E) or Geminin shRNA (B,D,F) were analyzed using SEM, immunohistochemical localization of Foxa2 (C,D), and *in situ* hybridization localization of Nodal (E,F).

A,B. Ventral SEM views of the node with anterior oriented toward the top. Compared with the control (A) where a stripe of ciliated cells (black arrowhead) is surrounded by flattened endoderm (VE) that will eventually enclose the node, the morphology of the node was consistently abnormal following Geminin knock-down (B). Midline cells were ciliated, but the node often took on a concave, rather than flattened organization. At the posterior extent of the node near the primitive streak cells often piled up forming ectopic aggregates (white arrowheads).

C,D. Mid-sagittal sections of E7.5 control (C) and an embryo exposed to Geminin shRNA (D) illustrating the expression of the endoderm marker Foxa2 (brown reaction product). In control embryos, Foxa2 was expressed in the single layered node, and in the anterior endoderm extending into the headfold region (Hf) of the embryo. Geminin knock-down embryos failed to elongate normally, the foregut pocket in the headfold region did not invaginate normally, and the neural folds in the headfolds were not elevated. In these embryos, Foxa2 expression in the node was expanded, and the node (arrowhead) itself abnormally thickened. PS = Primitive streak.

E,F. Transverse sections through the node of control (E) and Geminin shRNA exposed embryos (F) illustrating the normal expression of Nodal in the crown cells surrounding the node (arrows) this region. In the knock-down embryo, the node lacks its normal bi-layered organization.

Scale bars = 200 μm (C,D), 100 μm (A,B,E,F).

148
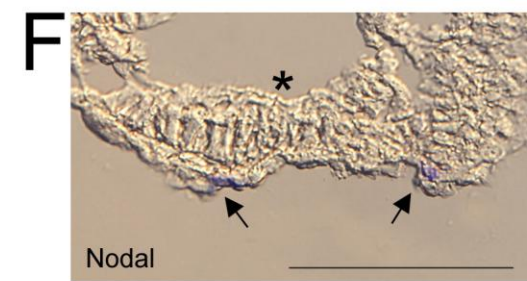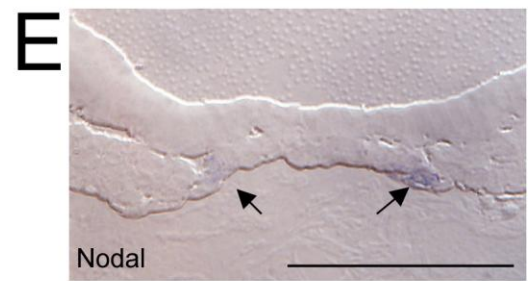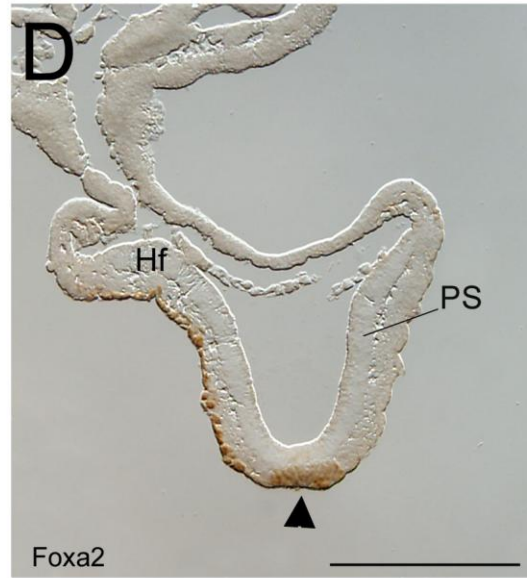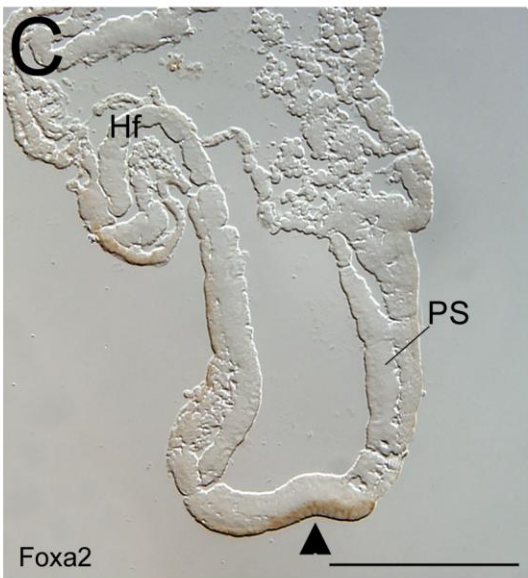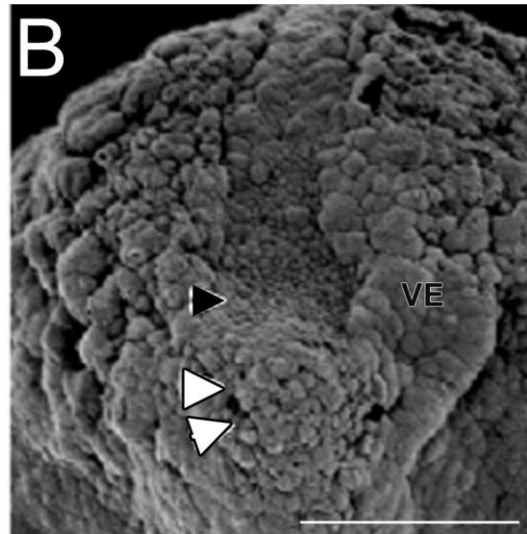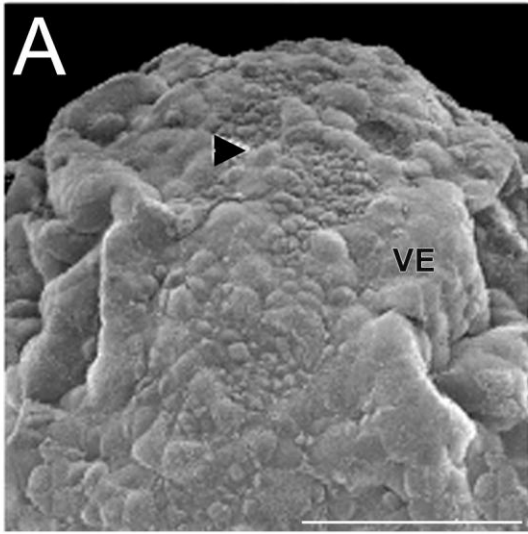
Figure 4-4. Organization of the primitive streak.

A,B. Side views of E7.5 embryos processed for whole mount *in situ* hybridization localization of Fgf8 mRNA. In embryos exposed to scrambled shRNA (A) Fgf8 is expressed in the primitive streak extending to the base of the allantois. Expression of Fgf8 in Geminin shRNA exposed embryos is absent at E7.5 (B). This embryo is also smaller than the control and axis elongation is impaired.

C,D. Sagittal views of E7.5 embryos illustrating WISH localization of Snail1 in control (C) and Geminin shRNA exposed embryos (D). While there is a stripe of Snail1 expression at the base of the allantois (A) to the primitive streak (PS) of controls embryos, Snail1 expression is undetected in affected embryos.

E,G. Transverse SEM images through the primitive streak of scrambled (E) and Geminin (G) shRNA exposed embryos illustrating an abnormal aggregation of cells (arrow) that would normally delaminate from the ectoderm to form mesoderm and endoderm. E = ectoderm; M = mesoderm; En = Endoderm.

F,H. Transverse sections through the primitive streak of scrambled (F) and Geminin (H) shRNA exposed embryos illustrating E-cad expression in the primitive streak. E-cad is down-regulated in control embryos (F) but remains expressed in the aggregate of cells in Geminin knock-down embryos (H). Dapi marks nuclei. Arrowhead = primitive streak.

I-J. Posterior views of E7.5 embryos illustrating WISH localization of Brachyury in control (I) and Geminin shRNA exposed embryos (J). There is a tight stripe of Brachyury expression in the control primitive streak (PS) and lateral expansion of Brachyury expression in the Geminin knock-down embryo. This embryo did not elongate in the AP axis. Mesoderm at the node is more intense in affected embryos due to the aggregate of cells (arrowhead).

K-N. Wnt indicator mice were exposed to scrambled shRNAs (K) or Geminin shRNA (L), then reacted with X-gal to identify sites of active Wnt signaling (β-gal+) and sectioned (M, N). In control embryos, active signaling is largely restricted to the primitive streak (K), while in embryos exposed to Geminin shRNA (L), control of Wnt signaling was disregulated, and β-gal reaction product was present at high levels in the primitive streak (PS), but also in the mesenchyme (m) and endoderm (En) of the E7.5 embryo (N). Anterior is to the left in E, F. Transverse sections with Anterior at top in M, N.

Scale bars = 200 μm (A-D, I-N); 100 μm (E-H).
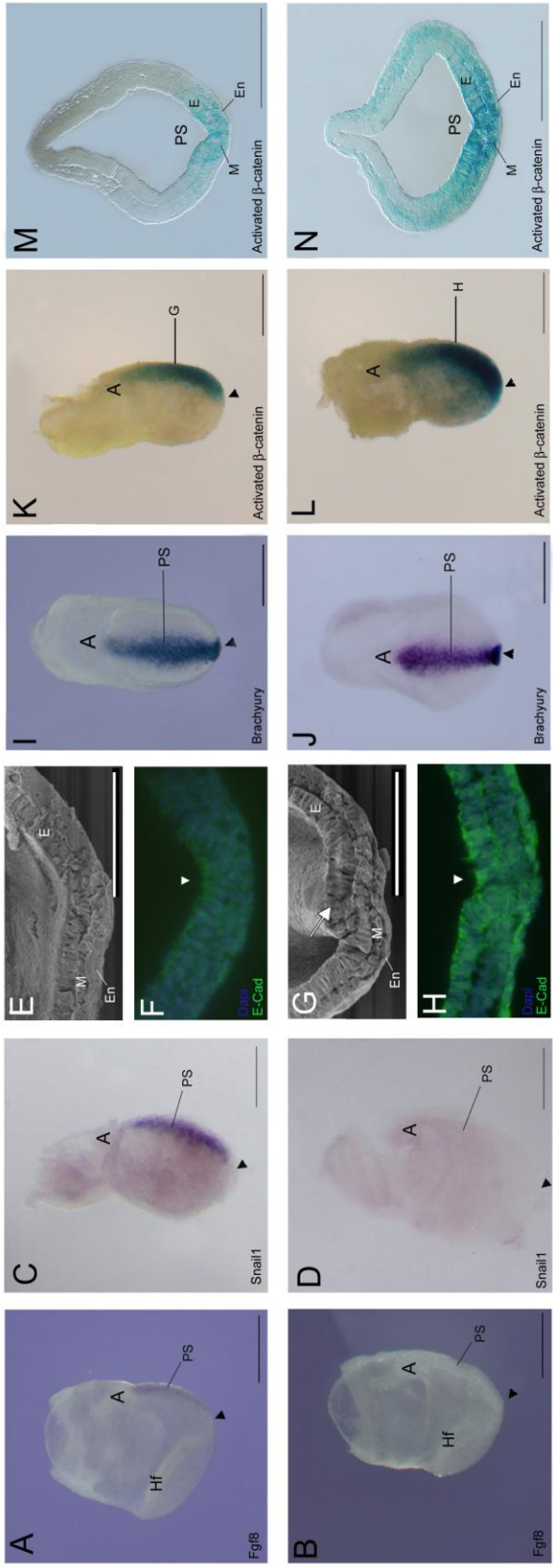
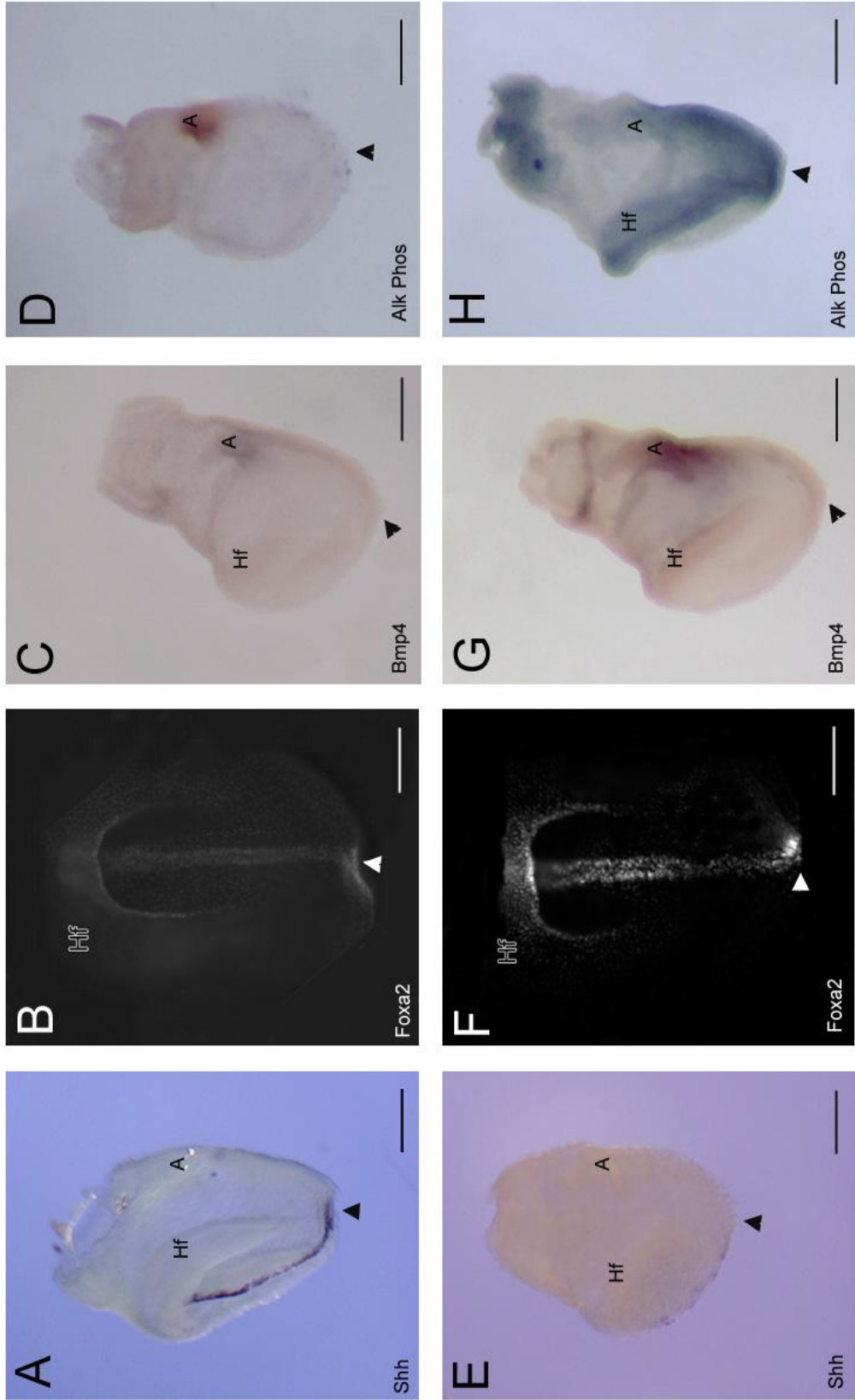**Figure 4-5. Geminin is required for anterior patterning.**

A,E. Sagittal view, with anterior to the left, of embryos exposed WISH for Shh. In control embryos (A), Shh is expressed in a stream of mesendodermal cells extending from the node to the headfolds in cells that will give rise to the notochord. In Geminin shRNA embryos (E), Shh expression is significantly reduced.

B,F. Whole mount immunohistochemical localization of the endoderm marker Foxa2 highlights the edges of the closing foregut pocket and notochord in anterior views of control embryos (B), and illustrates the widely open foregut region and wide notochord in Geminin shRNA exposed embryos (F). Node = white arrowhead; Hf = headfolds.

C,G. WISH localization of Bmp4 in control (C) and shRNA targeted embryos (I). Bmp4 expression is normal in the epidermal ectoderm surrounding the neural plate with intense expression at the base of the allantois (A) in control embryos (G). Expression increases in experimental embryos particularly around the neural plate (G). Anterior is to the left. Hf = headfolds; node = arrowhead.

D,H. Alkaline phosphatase is expressed in the forming primordial germ cells at the base of the allantois (A) of E7.5 control embryos (D). In embryos exposed to Geminin shRNA (H), widespread AP staining is found throughout the epiblast. Anterior is to the left. Hf = headfolds; node = arrowhead.

Scale bars = 200 μm for all embryos.

A — Shh
B — Foxa2
C — Bmp4
D — Alk Phos
E — Shh
F — Foxa2
G — Bmp4
H — Alk Phos

152

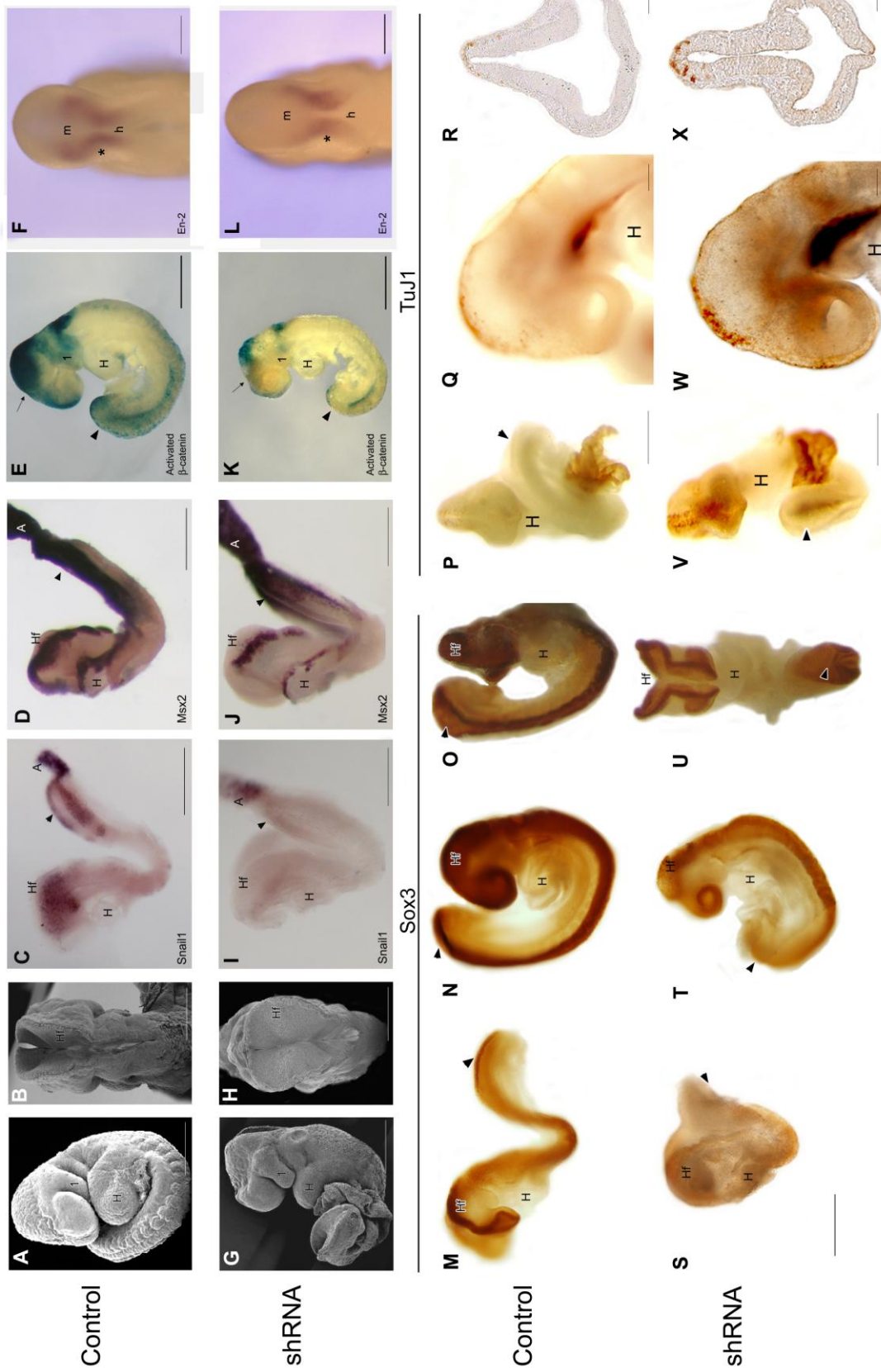**Figure 4-6. Geminin is required for patterning the cephalic region.**

A-B, G-H. SEM analysis of control embryos on E9.0 indicated that the neural tube was expanded and closed in the forebrain and midbrain (A), but remained open in the hindbrain region (B). The first branchial arch (1) had elongated and the heart and somites were visible on the lateral surface of the embryo (A). In embryos exposed to Geminin shRNA however, the embryonic axis was strikingly shortened, the posterior neuropore (pnp) region widely open, and the embryos often exhibited axial turning defects (G). The first branchial arch (1) was consistently reduced in size, and the neural tube failed to fuse throughout the cephalic region (H). A, G are sagittal views with ventral to the left. B, H are dorsal views. Hf = headfolds; H = heart; 1 = first branchial arch; pnp = posterior neuropore.

C-D, F, I-J, L. Whole-mount *in situ* hybridization localization of Snail1 (C,I), Msx2 (D, J), and Engrailed-2 (F, L) on control (C, D, F) and Geminin targeted (I, J, L) embryos. Embryos exposed to scrambled shRNA, En-2 was expressed in its normal domain in the caudal hindbrain and rhombomere 1 (F). In Geminin knock-down embryos, En-2 was expressed normally in rhombomere 1, but was reduced in the mesencephalon domain that will form the inferior and superior colliculi (L).

E,K. To determine if Wnt signaling was affected, scrambled shRNAs (E) or shRNA targeting Geminin (K) were delivered to pregnant Wnt reporter mice containing 6 Tcf/Lef sites. In control embryos, Wnt signaling was active (blue reaction product) in the cephalic region, in the neural crest cells migrating to the first branchial arch (1), and in the posterior region of the embryo of E9.0 embryos. In embryos exposed to Geminin shRNA, Wnt signaling was drastically affected, remaining in the midbrain, hindbrain, and posterior neuropore (K, arrowhead). Anterior is to the left. 1 = first branchial arch; H = heart; arrowhead = posterior neuropore; arrow = cephalic flexure between the prosencephalon and diencephalon.

M-X. Immunohistochemisty was used to detect changes in Sox3 (M-O, S-U) and TuJ1 (P-R, V-X) expression. Compared with control embryos (M-O), expression of Sox3, a marker of neural precursors, was strikingly reduced as Geminin decreases (S-U). Conversely, expression of TuJ1, which is restricted to immature neurons, it is up-regulated in the knock-down embryos (V-X) compared to controls (P-R). Sagittal views with anterior to the left (M, N, Q, S, T, W); Ventral views (O, P, U, V); Coronal sections (R, X). H = heart; Hf = headfolds; arrowhead = posterior neuropore.

Scale bars = 200 μm (A-Q, S-W); 100 μm (R, X).

Control

shRNA

F En-2

L En-2

Activated β-catenin

Activated β-catenin

Snail1

Msx2

Snail1

Msx2

Sox3

TuJ1

Control

shRNA

154

|	Forward	Reverse
Axin2	CTGTGGGTTGGTTGTGACAG	ACGTACGGTGTAGCCTTTGG
β-actin	ACCCCTAAGGCCAACCGTG	ATGGCTACGTACATGGCTG
Bmp4	CTCCCAAGAATCATGGACTG	TCAGGTATCAAACTAGCATGGC
Brachyury	CCCTGCACATTACACACCAC	ACAGGTGTCCACGAGGCTATGA
Foxa2	GTGGCCTAAGCGAGCTAAAGG	GGGTGGTTGAAGGCGTAATG
Geminin	ATTGCTGTCTGTGAGTCCGAG	CGGGTCCCTTCAAATCGT
Neurogenin-1	GTGGCATCACCACTCTCTGA	GAAAGGAGAAAAGGGGATCG
Sox3	CACAACTCCGAGATCAGCAA	GTCCTTCTTGAGCAGCGTCT

Table 4-1. QRT-PCR primers

Correlation Matrix

		Geminin R	Sox3 R	Ngn1 R	Foxa2 R	Bmp4 R	Brachyury R	Axin2 R
Correlation	Geminin R	1	-0.051	0.515	0.255	0.598	-0.306	0.409
	Sox3 R	-0.051	1	0.068	0.378	-0.323	-0.063	-0.062
	Ngn1 R	0.515	0.068	1	0.396	0.449	-0.381	0.65
	Foxa2 R	0.255	0.378	0.396	1	-0.1	-0.135	0.046
	Bmp4 R	0.598	-0.323	0.449	-0.1	1	0.056	0.262
	Brachyury R	-0.306	-0.063	-0.381	-0.135	0.056	1	-0.218
	Axin2 R	0.409	-0.062	0.65	0.046	0.262	-0.218	1

Table 4-2. Regression analysis.

QRT-PCR was analyzed on individual geminin shRNA exposed embryos using SPSS, significance assessed using f ratio.
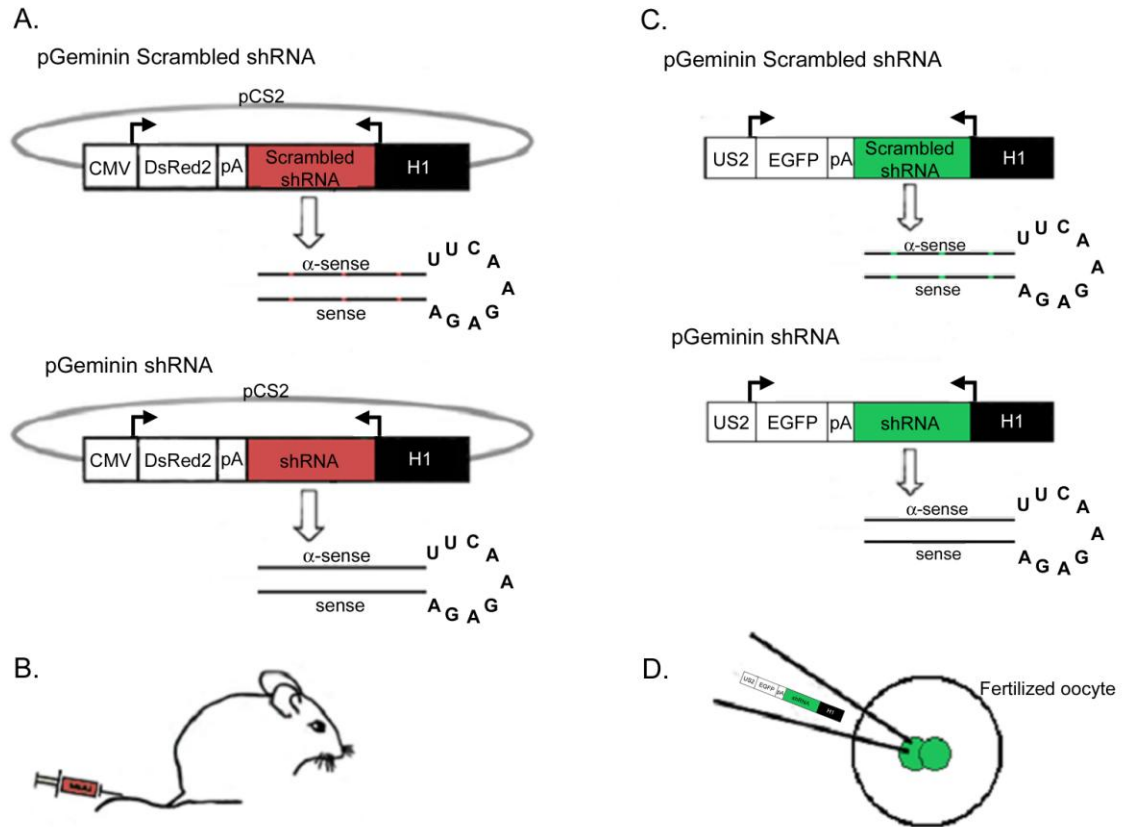
**Supplemental Figure S4-1. Geminin targeting constructs.**

Two different strategies were employed to knock-down Geminin expression. In the first, an shRNA construct was injected into the tail vein of pregnant dams on E6.5 of gestation (**A,B**). In the second approach, an shRNA transgene was injected into one pronucleus of fertilized eggs (**C,D**). As a control we used scrambled shRNAs which differed from the shRNA targeting Geminin by three nucleotide substitutions. The US2 promoter drove EGFP expression in transgenic embryos (C), while the CMV promoter drove expression of DsRed2 for the tail vein experiments (A).

Supplemental Figure S4-2. Geminin is required for axis elongation, closure of the anterior neural folds and branchial arch morphogenesis.

Embryos exposed to scrambled shRNAs (**A-C**), to Geminin shRNA via tail-vein injection (**D-F**), or by pronuclear injection (**G-H**) were analyzed using light and epifluorescence microscopy on E7.5 (A,D,G), E8.5 (B,E,H) and E9.5 (C,F,I) of gestation.

Compared with control embryos that had well formed headfolds (Hf) and had expanded in the proximal-distal axis (A), embryos exposed to shRNA targeting Geminin were developmentally delayed and failed to elongate normally (D). Compared with control embryos (B) on E8.5, Geminin shRNA exposed embryos (E) not only failed to elongate, but were characterized by defects of the turning process, and occasionally exhibited focal hemorrhages (C). By E9.5 the neural tube had closed throughout the cephalic region in control embryos (C). In Geminin shRNA embryos (F) there were often severe neural tube defects that affected both the midbrain and forebrain (arrows). In addition, the first branchial arches (1) were shifted anteriorly and failed to elongate normally.

Although transgenic embryos often failed to develop into the postimplantation period, surviving transgene positive embryos commonly exhibited defects of axis elongation and node morphogenesis (G), turning and neural tube closure (H). Many of the transgene positive embryos that survived to E9.5 were morphologically fairly normal, although they did express EGFP (I). Epifluorescence microscopy indicated that DsRed or EGFP was expressed in embryos carrying the shRNA constructs. Anterior is to the left in all embryos. Scale bars = 100 μm (A,D,G) and 500 μm (B,E,H), 200 μm (C,F,I). A = allantois, H = heart; 1 = first branchial arch; EPC = ectoplacental cone. Arrowheads = node; arrows in F = everted neural ectoderm.
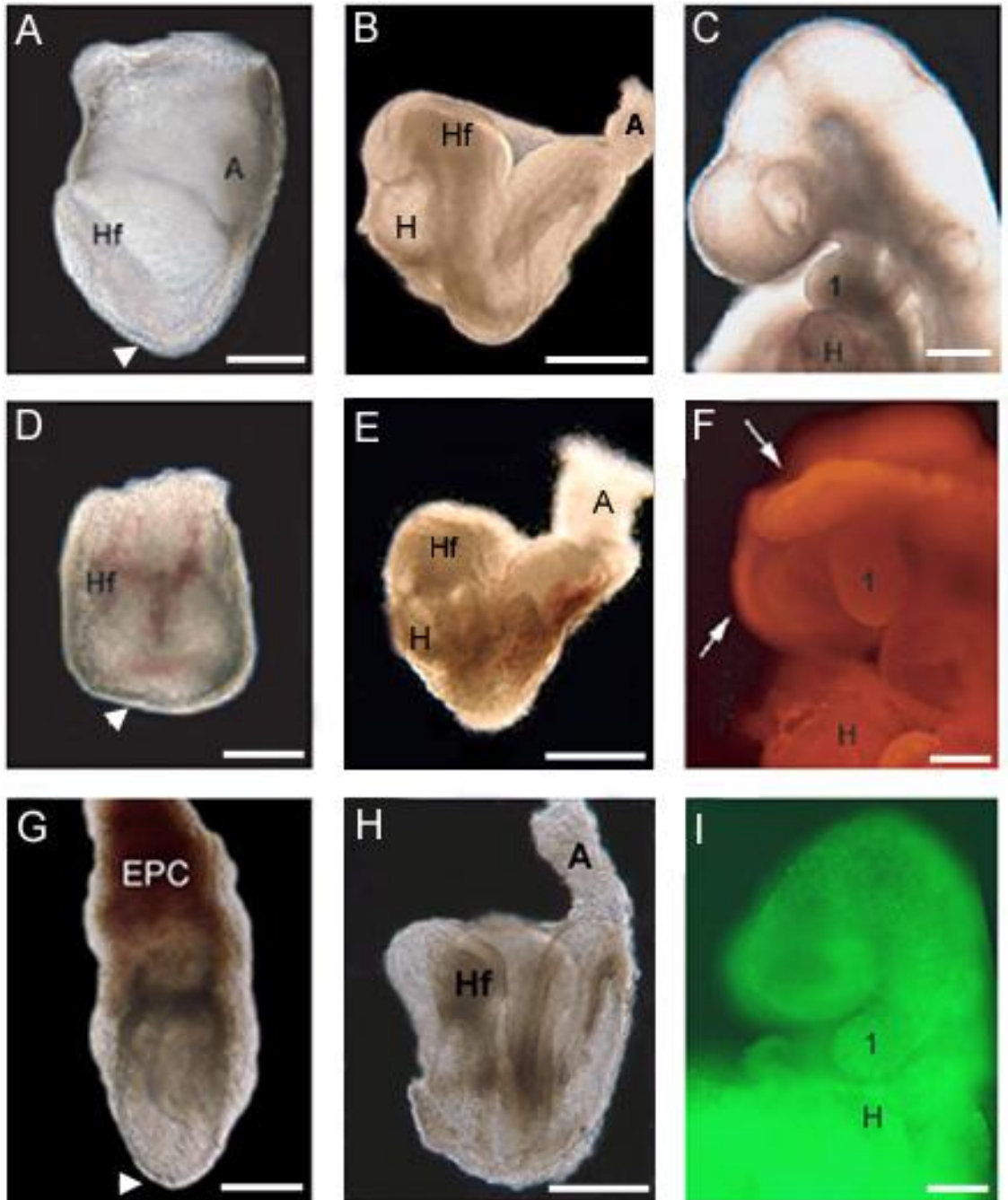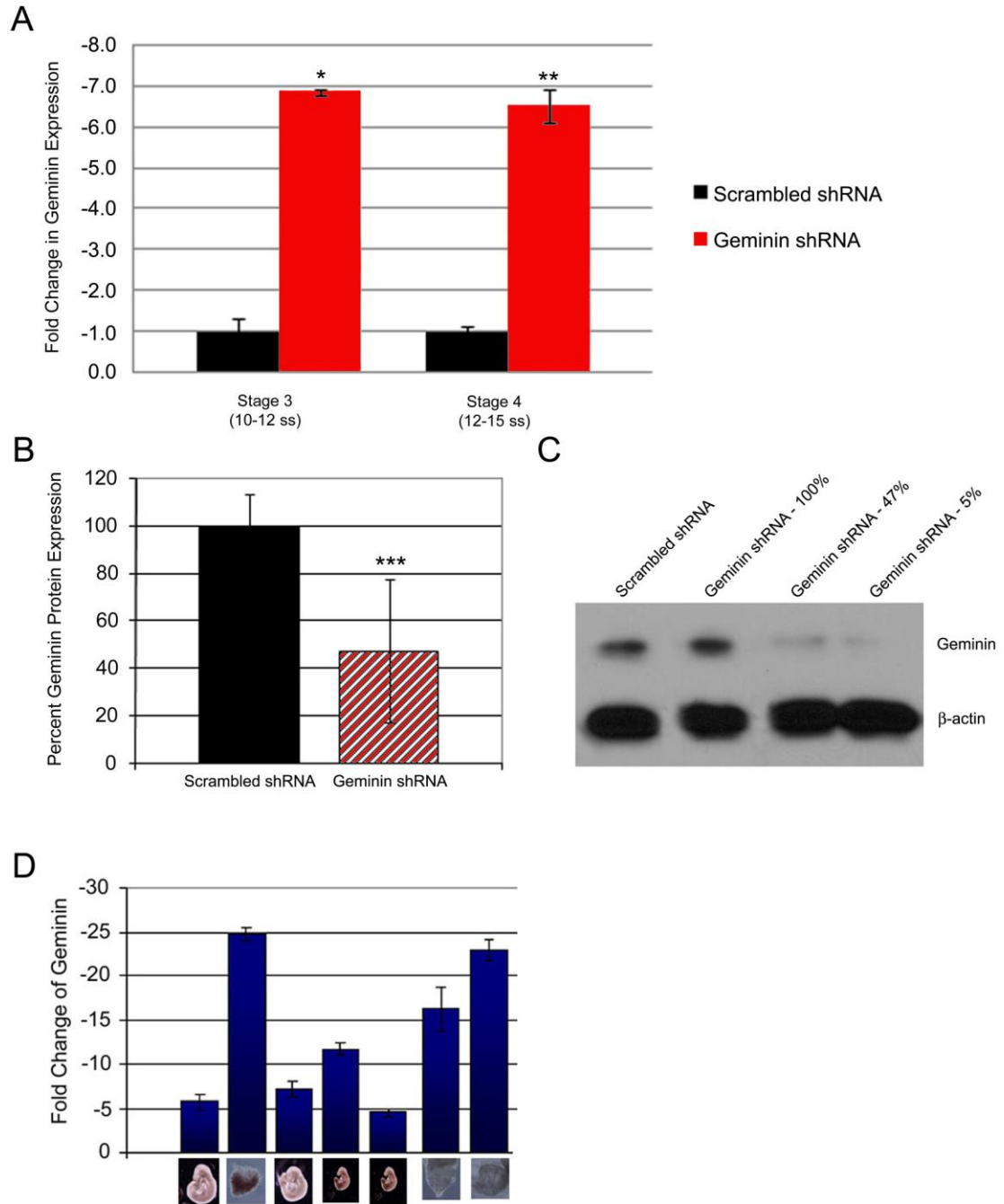
Supplemental Figure S4-3. Geminin expression is significantly reduced in Geminin shRNA embryos.

A. Geminin mRNA expression was analyzed using Quantitative RT-PCR in individual scrambled shRNA and Geminin shRNA exposed embryos. Expression levels were then averaged and control expression (scrambled shRNA exposed embryos) set at -1.0 for comparison with RNAs from Geminin shRNA exposed embryos. Data are represented as mean fold change $\pm$ SD. * = $p \leq 0.001$, ** = $p \leq 0.001$.

B. Quantitative analysis of Geminin protein expression in individual control and Geminin shRNA exposed embryos. Protein was extracted from individual embryos (n= two litters) of scrambled shRNA and individual embryos (n= three litters) of Geminin shRNA embryos. Western blotting was carried out and Geminin expression standardized relative to b-actin. Expression in control embryos was averaged and set at 100%. Mean expression of Geminin in Geminin shRNA exposed embryos was 47% of control, *** = $p \leq 0.001$, t= 2.9 x 10^{-5}.

C. Western blot illustrating the range in Geminin protein expression in four individual embryos. Geminin shRNA exposed embryos had a range in expression from 100% (*i.e.* normal levels) to nearly complete knock-down (5%).

D. Geminin mRNA expression from one Geminin shRNA exposed litter was analyzed using QRT-PCR and compared to scrambled shRNA embryos (Ct = -1.0 for comparision).
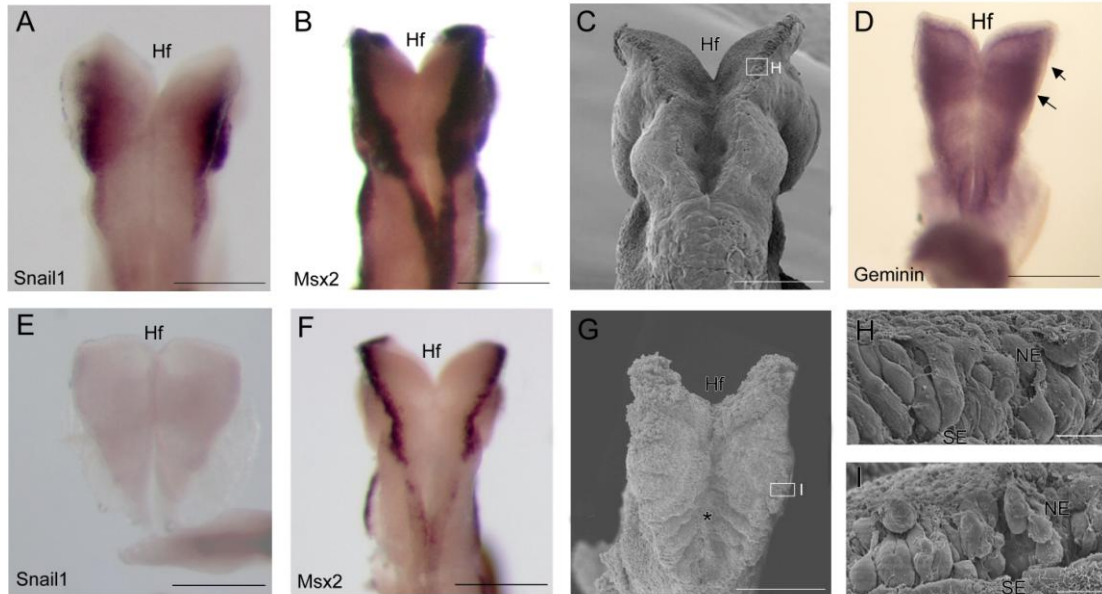
Supplemental Figure S4-4. Geminin alters neural crest restricted gene expression.

To examine the Geminin's role in neural crest migration and differentiation, embryos exposed to scrambled shRNAs (A-D,H) and embryos exposed to shRNA targeting Geminin (E-G,I) were processed for WISH localization of Geminin (D), the EMT marker Snail1 (A,E), or the neural crest marker Msx2 (B,F). Both Snail1 and Msx2 were strikingly downregulated in Geminin knockdown embryos (E,F), compared with controls (A,B). Geminin is expressed throughout the hindbrain neural ectoderm, but is absent at its junction with the epidermal ectoderm (double black arrows).

When analyzed using SEM, the headfolds of control embryos (C) were elevating and a population of neural crest cells could be seen at the border of the epidermal ectoderm and neural ectoderm (white boxes). In the Geminin shRNA embryos (G), the headfolds were widely open and infolded (*). Boxed areas in C,G illustrate neural crest cells at higher magnification (H,I). The neural crest in controls were organized and polarized (H), unlike the rounded unattached cells present in the Geminin embryos (I). Scale bars = 200 μm (A-B, D, E-F), 100 μm (C,G), 10 μm (H,I). Hf = headfolds; NE = neural ectoderm; SE = surface/epidermal ectoderm; double arrows = epidermal/neural ectoderm border; * = infolding of neural tube.

Supplemental Figure S4-5. Embryos that survive to E8.75-E9.0 are mispatterned

A,E. SEM views of the closing posterior neuropore (pnp) in control (A) and Geminin shRNA exposed embryos (E) illustrating its mis-shapen, widely open appearance.

B,B',F,F'. Brachyury expression in control embryos (B) was restricted to the ectoderm of the regressing streak in controls (B'). Expression was not only in the ectoderm but was also expressed in the underlying mesenchyme and gut epithelium in the shRNA exposed embryos (F,F'). B, F are sagittal views with anterior to left. B',F' are transverse sections through pnp of B,F as indicated by the asterisk with dorsal at top. H = heart; 1 = first branchial arch; pnp = posterior neuropore; g = gut; a = aorta.

C,D,G,H. WISH localization of Fgf8 mRNA found normally in the commissural plate (cp), isthmus (i), surface ectoderm of the first branchial arch (1), posterior neuropore (black arrowhead), and developing limb bud in control embryos (C,D). In Geminin knock-down embryos (G,H), not only is the anterior neuropore wider, but they fail to fuse at the future commissural plate (cp) (G, inset). Fgf8 expression is lost at the commissural plate (G and black arrow in H), but in the anterior ectoderm of the first branchial arch (black arrow in H). Expression in the isthmus (i), limb bud, and posterior neuropore appears to be normal (H) compared to scrambled shRNA exposed embryos. Ventral views in C,G; sagittal view with anterior to left in D, H; transverse sections though C,G as indicated by the asterisk in the insets with ventral at top. Hf = headfolds; H = heart; 1 = first branchial arch; i = isthmus; cp = commissural plate.

I-N. *in situ* hybridization of Shh in E8.75 (I,L) and E9.0 (J-K, M-N) embryos illustrates Shh is normally expressed in the floor plate of the neural tube and in the notochord/chordamesoderrm of the diencephalon (white arrow, I,J). In experimental embryos, expression in the diencephalons is disrupted (white arrow L,M) and expression domain is widened in the posterior region (black arrowheads in L, M). Expression is lost in the floor plate, but is expanded into the endoderm of the gut tube. By E9.0 expression remains low throughout the embryonic axis; and absent from the liver bud (N, white arrowhead in M), compared with the control (K, white arrowhead in J). Anterior is to the left in I,J, L,M; K,N are sagittal sections of J,M, respectively with ventral to the left. Lv = liver bud; H = heart; Hf = headfolds; 1 = first branchial arch; white arrows = expression in diencephalon; white arrowheads = expression in liver bud; black arrowheads = expression in posterior neuropore.

Scale bars = 200 μm (B-D, F-H, I-J, L-M); 100 um (A,E,B',F',insets in C and G,K,N).
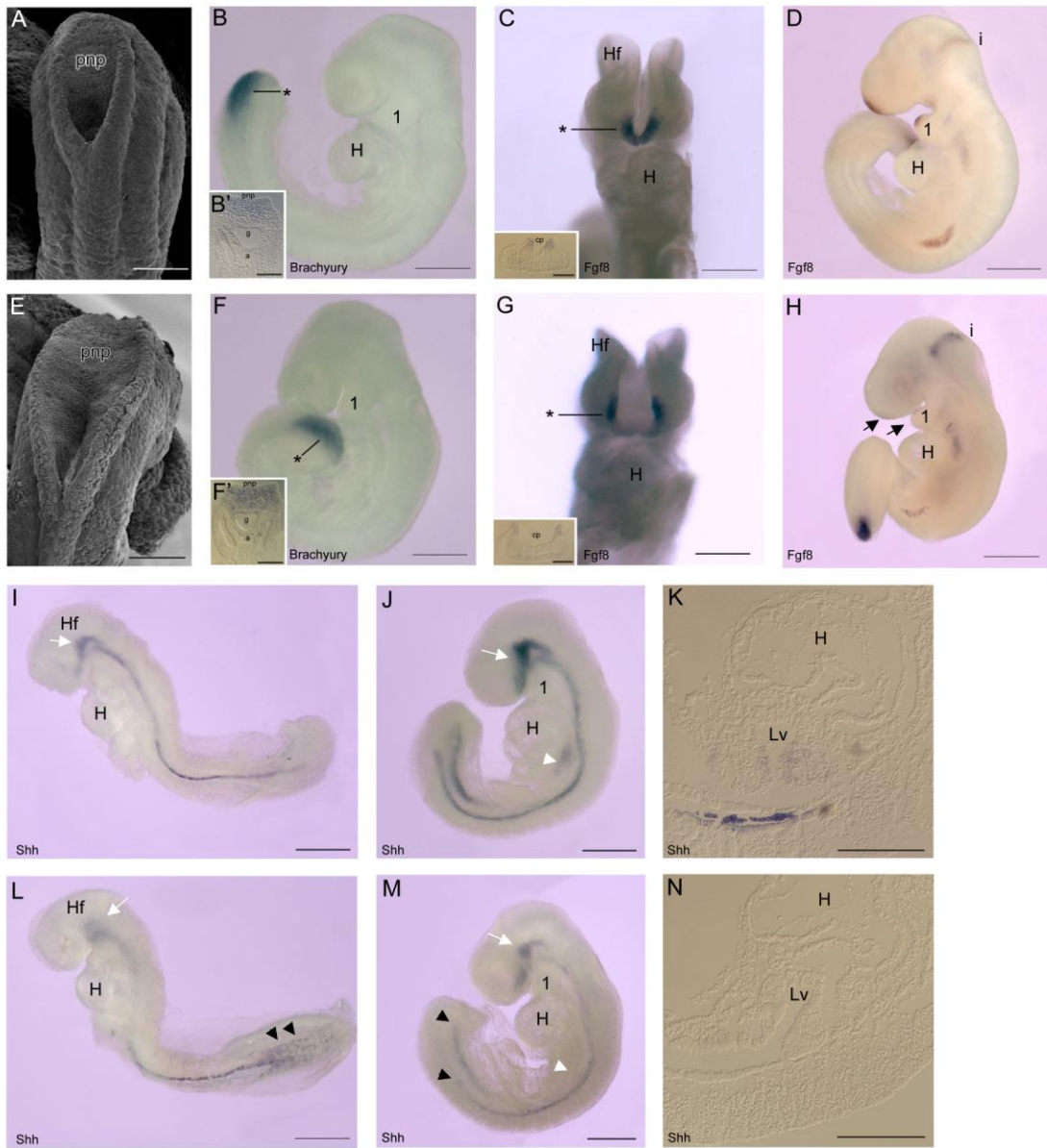
REFERENCES

Arnold SJ, Hofmann UK, Bikoff EK, and Robertson EJ. 2008. Pivotal roles for eomesodermin during axis formation, epithelium-to-mesenchyme transition and endoderm specification in the mouse. Development 135: 501-511.

Beddington RS and Robertson EJ. 1999. Axis development and early asymmetry in mammals. Cell 96: 195-209.

Belo JA, Bouwmeester T, Leyns L, Kertesz N, Gallo M, Follettie M, and De Robertis EM. 1997. Cerberus-like is a secreted factor with neutralizing activity expressed in the anterior primitive endoderm of the mouse gastrula. Mech Dev 68: 45-57.

Bensoussan V, Lallemand Y, Moreau J, Cloment CS, Langa F, and Robert B. 2008. Generation of an Msx2-GFP condidtional null allele. Genesis 46: 276-282.

Bielinska M, Narita N, and Wilson DB. 1999. Distinct roles for visceral endoderm during embryonic mouse development. Int J Dev Biol 43:183-205.

Blauwkamp TA, Chang MV, and Cadigan KM. 2008. Novel TCF-binding sites specify transcriptional repression by Wnt signalling. EMBO J 27:1436-1446.

Bosman EA, Lawson KA, Debruyn J, Beek L, Francis A, Schoonjans L, Huylebroeck D, and Zwijsen A. 2006. Smad5 determines murine amnion fate through the control of bone morphogenetic protein expression and signalling levels. Development 133: 3399-3409.

Brennan J, Lu CC, Norris DP, Rodriguez TA, Beddington RSP, and Robertson EJ. 2001. Nodal signaling in the epiblast patterns the early mouse embryo. Nature 411: 965-969.

Cano A, Perez-Moreno MA, Rodrigo I, Locascio A, Blanco MJ, del Barrio MG, Portillo F, and Nieto MA. 2000. The transcription factor snail controls epithelial-mesenchymal transitions by repressing E-cadherin expression. Nat Cell Biol 2: 76-83.

Carmona-Fontaine C, Matthews HK, Kuriyama S, Moreno M, Dunn GA, Parsons M, Stern CD, and Mayor R. 2008. Contact inhibition of locomotion in vivo controls neural crest directional migration. Nature 456: 957-961.

Carver EA, Jiang R, Lan Y, Oram KF, and Gridley T. 2001. The mouse snail gene encodes a key regulator of the epithelial-mesenchymal transition. Mol Cell Biol 21:8184-8188.

Chen WS, Manova K, Weinstein DC, Duncan SA, Plump AS, Prezioso VR, Bachvarova RF, and Darnell JE Jr. 1994. Disruption of the HNF-4 gene, expressed in visceral endoderm, leads to cell death in embryonic ectoderm and impaired gastrulation mouse embryos. Genes Dev 8: 2466-2477.

Chiquoine AD. 1954. The identification, origin, and migration of the primordial germ cells in the mouse embryo. Anat Rec 118:135-146.

Crossley PH and Martin GR. 1995. The mouse Fgf8 gene encodes a family of polypeptides and is expressed in regions that direct outgrowth and patterning in the developing embryo. Development 121: 439-451.

Davis CA, Noble-Topham SE, Rossant J, Joyner AL. 1988. Expression of the homeo box-containing gene En-2 delineates a specific region of the developing mouse brain. Genes Dev 2: 361-371.

Del Bene F, Tessmar-Raible K, and Wittbrodt J. 2004. Direct interaction of geminin and Six3 in eye development. Nature 427: 745-748.

Doble BW and Woodgett JR. 2007. Role of Glycogen synthase kinase-3 in cell fate and epithelial-mesenchymal transitions. Cell Tiss Organ 185: 73-85.

Dudderidge TJ, Stoeber K, Loddo M, Atkinson G, Fanshawe T, Griffiths DF, and Williams GH. 2005. Mcm2, Geminin, and Kl67 define proliferative state and are prognostic markers in renal cell carcinoma. Clin Cancer Res 11: 2510-2517.

Echelard Y, Epstein DJ, St-Jacques B, Shen L, Mohler J, McMahon JA, and McMahon AP. 1993. Sonic Hedgehog, a member of a family of putative signaling molecules, is implicated in the regulation of CNS polarity. Cell 75: 1417-1430.

Egea J, Erlacher C, Montanez E, Burtscher I, Yamagishi S, Hess M, Hampel F, Sanchez R, Rodriguez-Manzaneque MT, Bösl MR, Fässler R, Lickert H, and Klein R. 2008. Genetic ablation of FLRT3 reveals a novel morphogenetic function for the anterior visceral endoderm in suppressing mesoderm differentiation. Genes Dev 22: 3349-3362.

Fischer A, Viebahn C, and Blum M. 2002. FGF8 acts as a right determinant during establishment of the left-right axis in the rabbit. Curr Biol 12: 1807-1816.

Fujiwara T, Dehart DB, Sulik KK, and Hogan BL. 2002. Distinct requirements for extra-embryonic and embryonic bone morphogenetic protein 4 in the formation of the node and primitive streak and coordination of left-right asymmetry in the mouse. Development 129: 4685-4696.

Fukuda K and Kikuchi Y. 2005. Endoderm development in vertebrates: fate mapping, induction and regional specification. Develop Growth Differ 47: 343-355.

Galceran J, Fariñas I, Depew MJ, Clevers H, and Grosschedl R. 1999. Wnt3a-/--like phenotype and limb deficiency in Lef1(-/-)Tcf1(-/-) mice. Genes Dev 13: 709-717.

Ginsburg M, Snow MH, McLaren A. 1990. Primordial germ cells in the mouse embryo during gastrulation. Development 110: 521-528.

Gong SG, Guo C. 2003. Bmp4 gene is expressed at the putative site of fusion in the midfacial region. Differentiation 71: 228 -236.

Gonzalez MA, Tachibana KE, Chin SF, Callagy G, Madine MA, Vowler SL, Pinder SE, Laskey RA, and Coleman N. 2004. Geminin predicts adverse clinical outcome in breast cancer by reflecting cell-cycle progression. J Pathol 204: 121.

Gonzalez MA, Tachibana KK, Adams DJ, van der Weyden L, Hemberger M, Coleman N, Bradley A, and Laskey RA. 2006. Geminin is essential to prevent endoreplication and to form pluripotent cells during mammalian development. Genes & Dev 20: 1880-1884.

Grapin-Botton A and Melton DA. 2000. Endoderm development: from patterning to organogenesis. Trends Genet 16: 124-130.

Gratsch TE and O'Shea KS. 2002. Noggin and Chordin have distinct activities in promoting lineage commitment of mouse embryonic stem (ES) cells. Developmental Biology 245: 83-94.

Gregorieff A, Grosschedl R, and Clevers H. 2004. Hindgut defects and transformation of the gastro-intestinal tract in Tcf4(-/-)/Tcf1(-/-) embryos. EMBO J 23: 1825-1833.

Hahnel AC, Rappolee DA, Millan JL, Manes T, Ziomek CA, Theodosiou NG, Werb Z, Pedersen RA, and Schultz GA. 1990. Two alkaline phosphatase genes are expressed during early development in the mouse embryo. Development 110:555-564.

Hara K, Nakayama KI, and Nakayama K. 2006. Geminin is essential for the development of preimplantation mouse embryos. Genes to Cells 11: 1281-1293.

Harland R. 2000. Neural Induction. Curr Opin Genet Dev 10: 357-362.

Harrison KA, Thaler J, Pfaff SL, Gu H, and Kehrl JH. 1999. Pancreas dorsal lobe agenesis and abnormal islets of Langerhans in Hlxb9-deficient mice. Nat Genet 23: 71-75.

Jones NC and Trainor PA. 2005. Role of morphogens in neural crest cell determination. J Neurobiol 64: 388-404.

Jowett AK, Vainio S, Ferguson MWJ, Sharpe PT, and Thesleff I. 1993. Epithelial-mesenchymal interactions are required for msx 1 and msx 2 gene expression in the developing murine molar tooth. Development 117: 461-470.

Kanai-Azuma M, Kanai Y, Gad JM, Tajima Y, Taya C, Kurohmaru M, Sanai Y, Yonekawa H, Yazaki K, Tam PP, and Hayashi Y. 2002. Depletion of definitive gut endoderm in Sox17-null mutant mice. Development 129:2367-2379.

Korinek V, Barker N, Willert K, Molenaar M, Roose J, Wagenaar G, Markman M, Lamers W, Destree O, and Clevers H. 1998. Two members of the Tcf family implicated in Wnt/beta-catenin signaling during embryogenesis in the mouse. Mol Cell Biol 18: 1248-1256.

Kroll KL, Salic AN, Evans LM, and Kirschner MW. 1998. Geminin, a neuralizing molecule that demarcates the future neural plate at the onset of gastrulation. Development. 125: 3247-3258.

Kwon GS, Viotti M, and Hadjantonakis AK. 2008. The endoderm of the mouse embryo arises by dynamic widespread intercalation of embryonic and extraembryonic lineages. Dev Cell 15:509-520.

Lawson KA, Dunn NR, Roelen BA et al. 1999. Bmp4 is required for the generation of primordial germ cells in the mouse embryo. Genes Dev 13: 424-436.

Li H, Arber S, Jessell TM, and Edlund H. 1999. Selective agenesis of the dorsal pancreas in mice lacking homeobox gene Hlxb9. Nat Genet 23:67-70.

Liem KF Jr, Tremml G, Roelink H, Jessell TM. 1995. Dorsal differentiation of neural plate cells induced by BMP-mediated signals from epidermal ectoderm. Cell 82: 969-979.

Liu C, Liu W, Palie J, Lu MF, Brown NA, and Martin JF. 2002. Pitx2c patterns anterior myocardium and aortic arch vessels and is required for local cell movement into atrioventricular cushions. Development 129: 5081-5091.

Liu C, Liu W, Lu MF, Brown NA, and Martin JF. 2001. Regulation of left-right asymmetry by thresholds of Pitx2c activity. Development 128:2039-2048.

Llorens A, Rodrigo I, López-Barcons L, Gonzalez-Garrigues M, Lozano E, Vinyals A, Quintanilla M, Cano A, and Fabra A. 1998. Down-regulation of E-cadherin in mouse skin carcinoma cells enhances a migratory and invasive phenotype linked to matrix metalloproteinase-9 gelatinase expression. Lab Invest 78:1131-1142.

Luo L and Kessel M. 2004. Geminin coordinates cell cycle and developmental control. Cell Cycle 3: 711-714.

Luo L, Yang X, Takihara Y, Knoetgen H, and Kessel M. 2004. The cell-cycle regulator geminin inhibits Hox function through direct and polycomb-mediated interactions. Nature 427: 749-753.

Matzuk MM, Kumar TR, and Bradley A. 1995. Different phenotypes for mice deficient in either activins or activin receptor type II. Nature 374: 356-360.

Mayer K, Hieronymus T, Castrop J, Clevers H, and Ballhausen WG. 1997. Ectopic activation of lymphoid high mobility group-box transcription factor TCF-1 and overexpression in colorectal cancer cells. Int J Cancer 72: 625-630.

McGarry TJ & Kirschner MW. 1998. Geminin, an inhibitor of DNA replication, is degraded during mitosis. Cell 93: 1043-1053.

Merrill BJ, Pasolli HA, Polak L, Rendl M, García-García MJ, Anderson KV, and Fuchs E. 2004. Tcf3: a transcriptional regulator of axis induction in the early embryo. Development 131:263-274.

Mishina Y, Suzuki A, Ueno N, and Behringer RR. 1995. Bmpr encodes a type I bone morphogenetic protein receptor that is essential for gastrulation during mouse embryogenesis. Genes & Dev 6: 432-438.

Mohamed OA, Clarke HJ, and Dufort D. 2004. β-catenin Signaling Marks the Prospective Site of Primitive Streak Formation in the Mouse Embryo. Dev Dyn 231: 416-424.

Montanari M, Boninsegna A, Faraglia B, Coco C, Giordano A, Cittadini A, and Sgambato A. 2005. Increased expression of geminin stimulates the growth of mammary epithelial cells and is a frequent event in human tumors. J Cell Physiol 202: 215-222.

Mukhopadhyay M, Shtrom S, Rodriguez-Esteban C, Chen L, Tsukui T, Gomer L, Dorward DW, Glinka A, Grinberg A, Huang SP, et al. 2001. Dickkopf1 is required for embryonic head induction and limb morphogenesis in the mouse. Dev Cell 1: 423-434.

Nakuci E, Xu M, Pujana MA, Valls J, and ElShamy WM. 2006. Geminin is bound to chromatin in G2/M phase to promote proper cytokinesis. Int J Biochem Cell Biol 38: 1207-1220.

O'Shea KS, De Boer LS, Slawny NA, and Gratsch TE. 2006. Transplacental RNAi: Deciphering Gene Function in the Postimplantation-Staged Embryo. J Biomed Biotechnol 4: 18657.

Obermann EC, Eward KL, Dogan A, Paul EA, Loddo M, Munson P, Williams GH, and Stoeber K. 2005. DNA replication licensing in peripheral B-cell lymphoma. J Pathol 205: 318-328.

Ogi H, Suzuki K, Ogino Y, Kaminura M, Miyado M, Ying X, Zhang Z, Shinohara M, Chen Y, and Yamada G. 2005. Ventral Abdominal Wall Dysmorphogenesis of Msx1/Msx2 Double-Mutant Mice. Anat Record Part A 284A: 424–430.

Ohkubo Y, Chiang C, and Rubenstein JL. 2002. Coordinate regulation and synergistic actions of BMP4, SHH and FGF8 in the rostral prosencephalon regulate morphogenesis of the telencephalic and optic vesicles. Neuroscience 111: 1-17.

Oosterwegel M, van de Wetering M, Timmerman J, Kruisbeek A, Destree O, Meijlink F, and Clevers H. 1993. Differential expression of the HMG box factors TCF-1 and LEF-1 during murine embryogenesis. Development 118: 439-448.

Papanayotou C, Mey A, Birot AM, Saka Y, Boast S, Smith JC, Samarut J, and Stern CD. 2008. A mechanism regulating the onset of Sox2 expression in the embryonic neural plate. PLoS 6: e2.

Parker DS, Ni YY, Chang JL, Li J, and Cadigan KM. 2008. Wingless signaling induces widespread chromatin remodeling of target loci. Mol Cell Biol 28:1815-1828.

Patthey C, Edlund T, and Gunhaga L. 2009. Wnt-regulated temporal control of BMP exposure directs the choice between neural plate border and epidermal fate. Development 136: 73-83.

Piepenburg O, Vorbrüggen G, and Jäckle H. 2000. Drosophila segment borders result from unilateral repression of hedgehog activity by wingless signaling. Mol Cell 6:203-209.

Pfaffl MW. 2001. A new mathematical model for relative quantification in real-time RT-PCR. Nucleic Acids Res 29: e45.

Quinn LM, Herr A, McGarry TJ, and Richardson H. 2001. The Drosophila Geminin homolog: roles for Geminin in limiting DNA replication, in anaphase and in neurogenesis. Genes & Dev 15: 2741-2754.

Roose J and Clevers H. 1999. TCF transcription factors: molecular switches in carcinogenesis. Biochim Biophys Acta 1424:M23-M37.

Russ AP, Wattler S, Colledge WH, Aparicio SA, Carlton MB, Pearce JJ, Barton SC, Surani MA, Ryan K, Nehls MC, Wilson V, and Evans MJ. 2000. Eomesodermin is required for mouse trophoblast development and mesoderm formation. Nature 404: 95-99.

Saga Y, Hata N, Kobayashi S, Magnuson T, Seldin MF, and Taketo MM. 1996. MesP1: a novel basic helix-loop-helix protein expressed in the nascent mesodermal cells during mouse gastrulation. Development 122:2769-2778.

Sauka-Spengler T and Bronner-Fraser M. 2008. A gene regulatory network orchestrates neural crest formation. Nat Rev Mol Cell Biol 9: 557-568.

Saxena S and Dutta A. 2005. Geminin-Cdt1 balance is critical for genetic stability. Mut Res 569: 111-121.

Seo S, Herr A, Lim JW, Richardson GA, Richardson H, and Kroll KL. 2005a. Geminin regulates neuronal differentiation by antagonizing Brg1 activity. Genes & Dev 19: 1723-1734.

Seo S, Richardson GA, and Kroll KL. 2005b. The SWI/SNF chromatin remodeling protein Brg1 is required for vertebrate neurogenesis and mediates transactivation of Ngn and NeuroD. Development 132: 105-115.

Stern CD, Artinger KB, and Bronner-Fraser M. 1991. Tissue interactions affecting the migration and differentiation of neural crest cells in the chick embryo. Development 113:207-216.

Steventon B, Araya C, Linker C, Kuriyama S, and Mayor R. 2009. Differential requirements of BMP and Wnt signalling during gastrulation and neurulation define two steps in neural crest induction. Development 136: 771-779.

Sun X, Meyers EN, Lewandoski M, Martin GR. 1999. Targeted disruption of Fgf8 causes failure of cell migration in the gastrulating mouse embryo. Genes Dev 13: 1834-1846.

Tachibana KK, Gonzalez MA, and Coleman N. 2005. Cell-cycle-dependent regulation of DNA replication and its relevance to cancer pathology. J Path 205: 123-129.

Tam and Loebel. 2007. Gene function in mouse embryogenesis: get set for gastrulation. Nat Rev Genet 8: 368-381.

Taylor JJ, Wang T, and Kroll KL. 2006. Tcf- and Vent-binding sites regulate neural-specific geminin expression in the gastrula embryo. Dev Biol 289: 494-506.

Theisen H, Syed A, Nguyen BT, Lukacsovich T, Purcell J, Srivastava GP, Iron D, Gaudenz K, Nie Q, Wan FY, Waterman ML, and Marsh JL. 2007. Wingless directly represses DPP morphogen expression via an armadillo/TCF/Brinker complex. PLoS One 2: e142.

Tremblay KD, Hoodless PA, Bikoff EK, and Robertson EJ. 2000. Formation of the definitive endoderm in mouse is a Smad2-dependent process. Development 127: 3079-2090.

Vincent SD, Dunn NR, Hayashi S, Norris DP, and Robertson EJ. 2003. Cell fate decisions within the mouse organizer are governed by graded Nodal signals. Genes & Development 17: 1646-1662.

Weber RJ, Pedersen RA, Wianny F, Evans MJ, and Zernicka-Goetz M. 1999. Polarity of the mouse embryo is anticipated before implantation. Development 126: 5591-5598.

Wohlschlegel JA, Kutok JL, Weng AP, and Dutta A. 2002. Expression of Geminin as a Marker of Cell Proliferation in Normal Tissues and Malignancies. Am J Path 161: 267-273.

Xouri G, Lygerou Z, Nishitani H, Pachnis V, Nurse P, and Taraviras S. 2004. Cdt1 and geminin are down-regulated upon cell-cycle exit and are over-expressed in cancer-derived cell lines. Eur J Biochem 271: 3368-3378.

Yamaguchi TP, Harpal K, Henkemeyer M, and Rossant J. 1994. fgfr-1 is required for embryonic growth and mesodermal patterning during mouse gastrulation. Genes Dev 8:3032-3044.

Yang J and Weinberg RA. 2008. Epithelial-Mesenchymal Transition: At the crossroads of Development and Tumor Metastasis. Dev Cell 14: 818-829.

Zhou B. 2007. Structural studies of geminin-hox and smad-hox complexes. http://hdl.handle.net/1783.1/3159.

Chapter 5

Geminin Controls EMT and Neural Crest Specification in the Mouse Embryo

INTRODUCTION

The vertebrate neural crest is a transient population of multipotent cells that forms at the border between neural ectoderm and epidermal cells in vertebrate embryos. Considerable evidence suggests that Fgf, notch, Wnt and BMP signals are involved in neural crest induction, expansion and lineage differentiation (Basch et al., 2004), and it appears that Wnt signaling and Bmp inhibition is required early, while later NC differentiation requires activation of both pathways (Steventon et al., 2009). How these pathways converge remains controversial, but control of a common promoter such as Msx (Hussein et al., 2003) has been suggested as one possible mechanism. Another candidate whose promoter contains both vent and Tcf/Lef sites is the *Geminin* gene (Taylor et al., 2005). Experiments in *Xenopus* have demonstrated that over-expression of Geminin expands, and knock-down reduces the size of the neural plate (Kroll et al., 1998), suggesting that Geminin may play an important role in defining the position of the neural plate border. Geminin has been suggested to direct neurogenesis by controlling cell-cycle exit, (Seo et al., 2005) and/or inhibiting BMP signaling (Rogers et al., 2009), but its role in post-implantation development has been difficult to study due to the early lethality of knock-out mice (Hara et al., 2006; Gonzalez et al., 2006). Here we show that geminin is expressed at the neural plate boundary in the early epiblast, but is strikingly absent from this region during neural crest migration. Our results demonstrate that Geminin expression in the neural ectoderm determines the extent of neural crest cell migration; over-

expression of Geminin expands the neural plate and the neural crest cell population, while knock-down reduces neural crest cell number. Wnt signaling was expanded and Bmp4 reduced in embryos exposed to a Geminin expression construct. Conversely, shRNAs targeting Geminin caused a loss of these markers and down-regulated Wnt signaling. Our results demonstrate the cell autonomous role of geminin during neural crest formation in the mouse embryo.

METHODS

Mice

E6.0 time-pregnant dams from either ICR strain mice (Harlan) or mice carrying six copies of a TCF/LEF binding site linked to LacZ (Mohamed et al., 2004) were employed. Embryos were harvested on E8.5, E8.75, and E9.0.

DNA delivery

Tail-vein injections were performed as previously described (Gratsch et al., 2003). Knock-down of Geminin using shRNAs was carried out (O'Shea et al., 2006; Emmett and O'Shea, 2009). To over-express Geminin, 20 μg of plasmid in to a final volume of 300 μl in Ringer's solution was injected into the tail-vein of E6.0 pregnant dams. The US2 promoter was employed to drive expression of Geminin cDNA and EGFP (Supplemental Figure 5-1). Controls received scrambled shRNA constructs.

Whole-mount *in situ* hybridization/SEM/X-gal staining

 Whole-mount *in situ* hybridization was performed as previously described (Emmett and O'Shea, 2009) using digoxigenin-labeled RNA riboprobes to Snail1 (Cano et al., 2000), Msx2 (Jowett et al., 1993) and Geminin (Emmett and O'Shea, 2009).

Embryos for SEM were fixed in 1% glutaraldehyde in phosphate buffer and subsequently dehydrated in a series of graded alcohol washes followed by two rinses in hexamethyl-disilazane (HDMS).

X-gal staining was carried out following: www.sanger.ac.uk/genetrap/ using X-gal (20 mg/ml ILT #13320-034). In addition, 0.02% ipegal and 0.01% deoxycholate were added to the wash and staining buffers to increase penetration. Embryos were photographed before and after cyrosectioning at 10 μm.

RESULTS AND DISCUSSION

QRT-PCR analysis demonstrates that Geminin is expressed in the blastocyst, peaks at the 10-12 somite stage of development, decreasing on E13, and increasing as individual organ systems differentiate (Emmett and O'Shea, 2009). Geminin is expressed in the anterior neural folds at a region between the neural ectoderm and epidermal ectoderm on E7 of development, later Geminin is present within the neural ectoderm, but is strikingly absent from the neural crest, epidermal ectoderm, the heart, the endoderm and extraembryonic tissues (Emmett and O'Shea, 2009). Delivery of shRNA to pregnant dams on E6.0 followed by analysis of embryos at 10-12 and 12-15 somites, resulted in mean fold decreases in Geminin mRNA of 7 and 6 fold respectively, (p < 0.001), and an average protein expression of 42% (t= 2.9 x 10^{-5}).

Geminin is normally expressed throughout the neural ectoderm and absent in the epidermal ectoderm, heart, and extra-embryonic tissues at E8.5 (Figure 5-1a). shRNA targeted embryos lost Geminin expression (Figure 5-1b) whereas delivery of a Geminin cDNA increased levels of Geminin mRNA (Figure 5-1c) confirming successful transgene delivery. mRNA levels illustrated by *in situ* hybridization were confirmed by QRT-PCR of individual Geminin shRNA and Geminin overexpressing embryos compared (Figure 5-1d).

In control embryos on E9 of gestation, the cephalic neural folds are elevated and beginning to meet in the dorsal midline of the hindbrain, midbrain and forebrain regions (Figure 5-2a, d, g). In contrast, embryos in which Geminin expression was reduced were characterized by the presence of widely everted neural folds extending throughout the cephalic region, and poorly invaginated optic vesicles

175

(Figure 5-2b, e, h). Conversely, over-expression of Geminin produced overgrowth of the neural folds, infolding and wide eversion over the epidermal ectoderm. Neuroepithelial cells were rounded (Figure 5-2c, f, j). These data support the suggestion that Geminin is involved in specifying the edges of the neural ectoderm (Kroll et al., 1998, Papanayotou et al., 2008), and maintaining neural progenitor proliferation. Given its provocative expression at the border of the early neural plate, we examined Geminin dosage effects on neural crest cells (NCC).

Combinatorial signaling by Wnt, Bmp and Fgfs leads to the induction of genes such as Msx2 which specify neural crest (Sauka-Spengler and Bronner-Fraser, 2008). Emigration of NCC from the neural tube then requires disassembly of adherens junctions and up-regulation of receptors for extracellular matrix components present in the mesenchyme. This is process is initiated by Fgf induction of Snail1 expression which represses expression of E-cadherin in these cells (Cano et al., 2000), which can then undergo an epithelial to mesenchymal transformation (EMT). To determine if neural crest restricted gene expression is affected in these embryos, we performed *in situ* hybridization using Msx2 and Snail1. In control embryos, Snail1 is expressed at the border of the neural ectoderm and epidermal ectoderm; with high expression in the cephalic and posterior trunk regions where neural crest cell migration is ongoing (Figure 5-3a, b). With Geminin down-regulation, Snail1 expression is reduced, (Figure 5-3c, d), whereas Snail1 increases as the levels of Geminin are elevated (Figure 5-3e,f). Similar results were observed for Msx2 expression. In control embryos, Msx2 is present in presumptive neural crest cells with a higher level of expression at the posterior neuropore (Figure 5-4a, b). Msx2 is not as strongly affected in Geminin shRNA embryos (Figure 5-4c, d) as Snail1, likely due to its earlier expression compared with Snail1. In contrast, Msx2 expression is significantly increased in Geminin over-expressing embryos (Figure 5-4e, f) corresponding to the higher levels of Geminin mRNA. Expression of Msx2 in the somatopleure and splanchnopleure, which can affect body wall closure, is also

significantly reduced (Figure 5-4d) or up-regulated (Figure 5-4f) when Geminin mRNA is either decreased or increased, respectively.

In control E9.0 embryos, activated β-catenin is expressed along the length of the dorsal neural tube; at particularly high levels in the midbrain and rhombencephalon (Figure 5-5a, d, g). In Geminin shRNA embryos, Wnt signaling is severely reduced in the neural tube with slight expression remaining in the neural crest pathway to the first branchial arch and in the posterior neuropore (Figure 5-5b, e, h). Over-expression produces the reciprocal results – expression of activated β-catenin is elevated throughout the neural tube extending into the first branchial arch (Figure 5-5c, f, i). Although the anterior (arrows) and posterior (arrowheads) neuropores are wide and fail to close in both experimental groups, over-expression of Geminin expands the neural tissue and the neural folds are everted over the surface ectoderm (Figure 5-5c, f, i). In knock-down embryos, Bmp4 expression is expanded compared with controls (Emmett and O'Shea, 2009), indicating that Geminin not only affects both Wnt and Bmp signaling but proliferation and differentiation of the neural ectoderm as well.

These results indicate a critical role for Geminin in EMT required for neural crest migration, and likely other regions of the embryo, and suggest a mechanism by which Geminin over-expression increases tumorgenicity and metastasis. Several birth defects have also been traced back to the neural crest. DiGeorge syndrome (DGS) is characterized by hypocalcemia, thymic hypoplacia, cleft palates, and defects of the outflow tract of the heart (Chieffo et al., 1997). Mutations in Msx2 can lead to craniosynostosis type 2 (CRS2) as indicated by defects in skull malformations, seizures, and the cerebellum (Li et al., 1993). Both defects are due to impaired migration of neural crest cells to the branchial arches. Given the changes in the neural crest population as Geminin expression is either reduced or up-regulated, it would not be surprising to find effected embryos with similar abnormalities. Additionally, the notochord is inhibitory to

neural crest cells (Stern et al., 1991). As the cells that comprise the notochord not only are mispatterned but lose expression of Shh in Geminin shRNA targeted embryos (Emmett and O'Shea, 2009 in preparation), migratory defects in neural crest cells could also be attributed to changes in dorsal-ventral signaling. Further evaluation is necessary to determine if geminin's role is only for the specification of neural crest or if it controls neural crest migration by regulating EMT.

ACKNOWLEDGEMENTS

These results will be submitted for publication with LSD Emmett and KS O'Shea as authors.
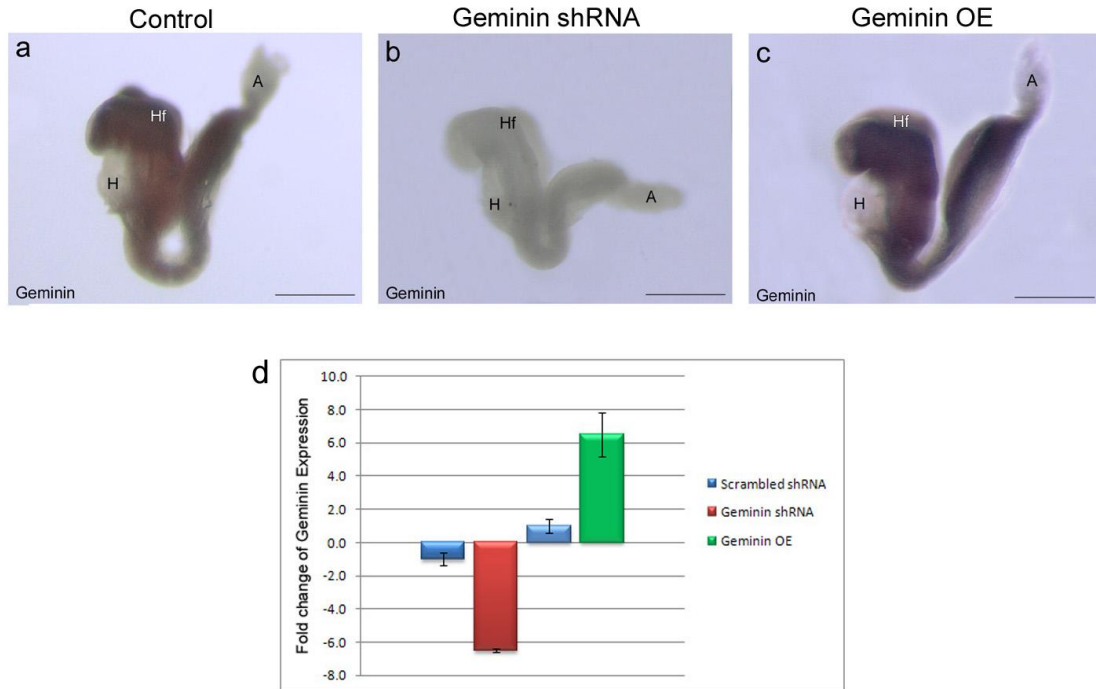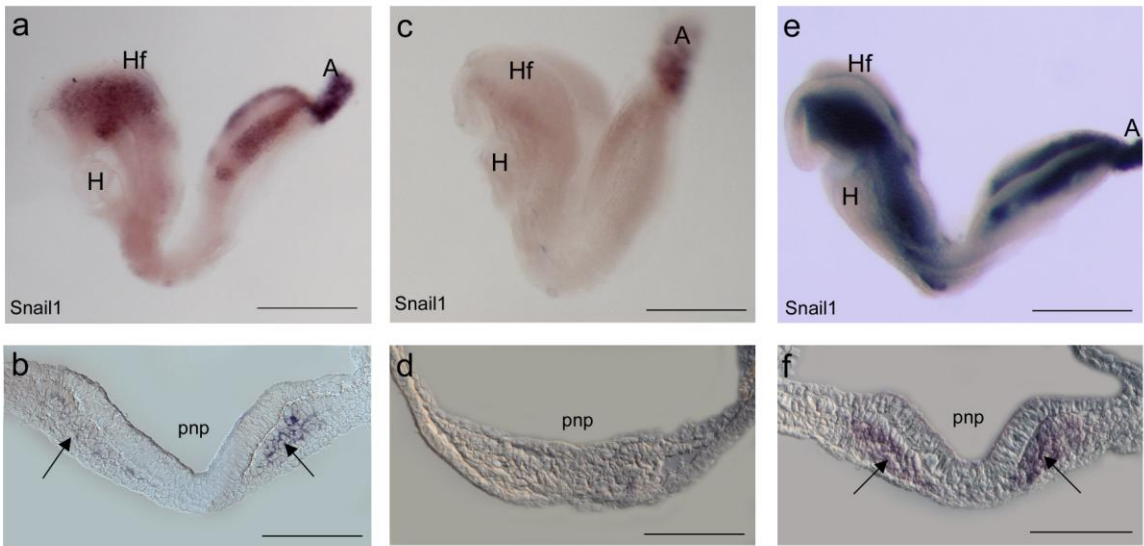
Figure 5-1. *In situ* **hybridization of Geminin.**

The levels of Geminin mRNA in E8.5 embryos was evaluated in control (**a**), knock-down (**b**), and over-expressing (**c**) embryos. In all embryos, Geminin was absent in heart, epidermal ectoderm, and extra-embryonic tissues. Geminin was unable to be detected in embryos exposed to Geminin shRNAs (**b**) whereas an increase in expression compared to controls was observed in embryos exposed to Geminin cDNA (**c**). In experimental embryos (**b, c**), defects in axis elongation, open and expanded anterior/posterior neuropores, and lack of segmentation (*i.e.* somites) were indicated. (**d**). Changes in Geminin mRNA levels with either exposure to Geminin shRNA or Geminin overexpression were validated with QRT-PCR compared to scrambled (control) embryos. A= allantois; H = heart; Hf = headfolds. Scale = 200 μm. Anterior is to the left.

179
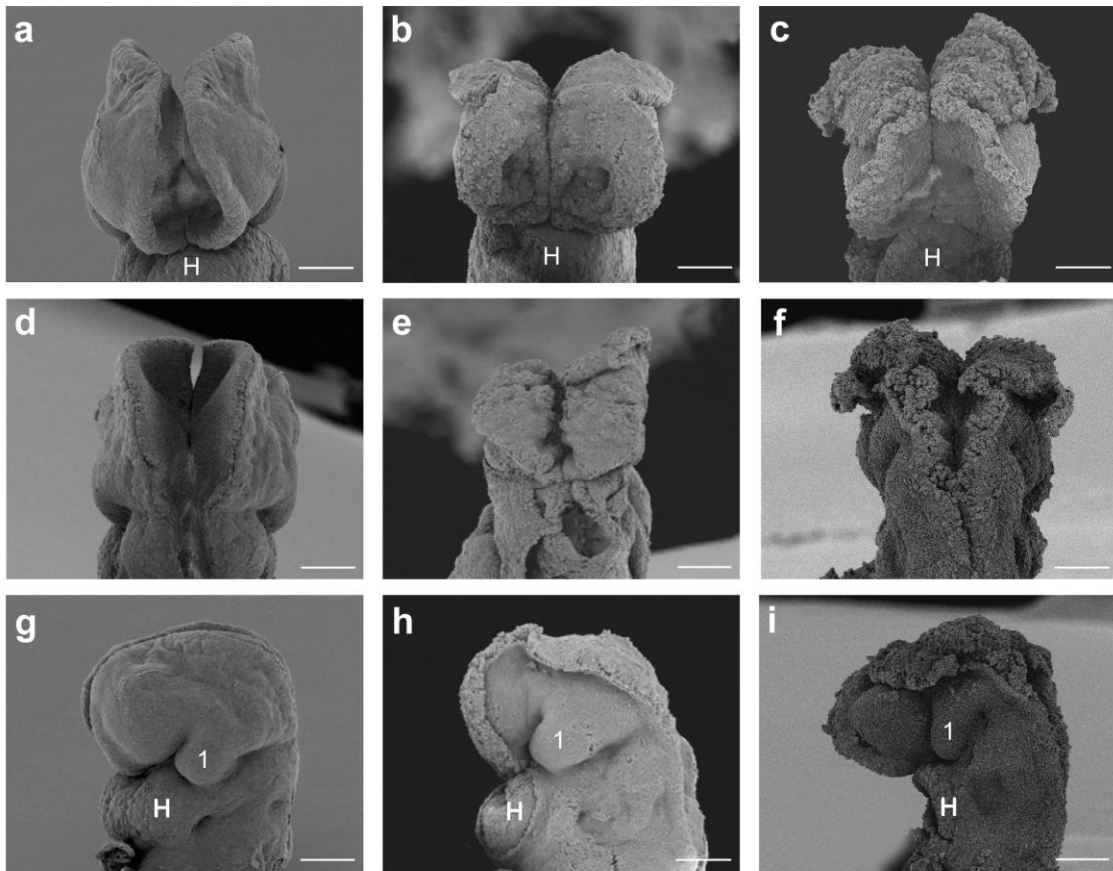
Figure 5-2. Geminin controls proliferation and closure of the neural folds.

SEM analysis of scrambled control (**a, d, g**), Geminin shRNA (**b, e, h**), and
Geminin over-expressing (**c, f, i**) embryos reveals neural tube closure defects
which result when Geminin expression levels change. Coronal (**a-c**), dorsal (**d-f**),
and sagittal (**g-i**) views of E9.0 embryos. Although loss of Geminin produces
everted neural tissue (**b, e, h**), the headfolds are flattened, and individual cells
are not rounded compared to controls (**a, d, g**). Over-expression of Geminin
leads to an expansion of neural tissue which everts over the surface ectoderm (**c,
f, i**). Anterior-posterior axis elongation is also compromised when Geminin
expression is changed. Scale bars = 100 μm. H = heart; 1 = first branchial arch.

Figure 5-3. Geminin controls expression of Snail1 involved in EMT and neural crest specification.

In situ hybridization localization of Snail1 reveals the expression of in cranial neural crest cells of controls (**a, b**), while there is a loss of neural crest cells in embryos exposed to the shRNA (**c, d**), and an increased number of NCC is detected in over-expressing embryos (**e, f**). The domain of Snail1 expression is significantly expanded in not only the cranial neural tube but throughout the trunk (**e, f**). Sagittal views with anterior to the left (**a,c,e**) and transverse sections through the posterior neuropore with anterior at the top (**b,d,f**). Scale bars = 200 μm (**a,c,e**); 100 μm (**b,d,f**) A = allantois; H = heart; Hf = headfolds; pnp = posterior neuropore; arrows = Snail1 expression in the mesenchyme.

181
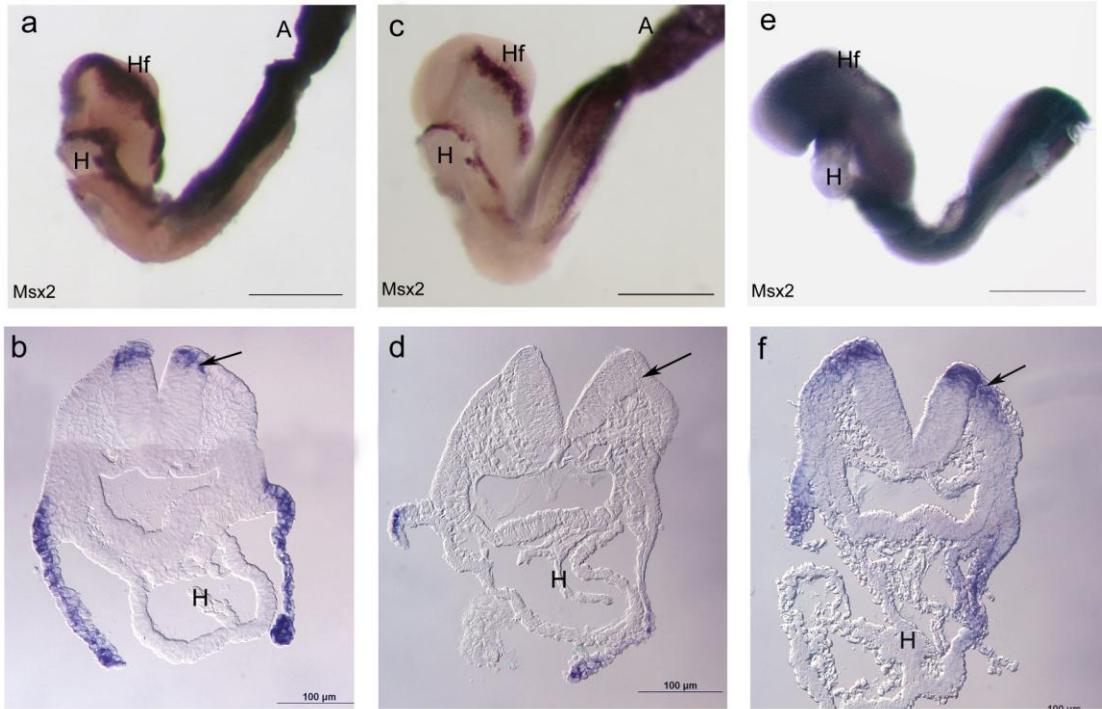
Figure 5-4. Geminin controls expression of Msx2 involved in neural crest specification and body wall closure.

In situ hybridization localization of Msx2 reveals the expression of in cranial neural crest cells of controls (**a, b** (arrow)), while there is a loss of neural crest cells in embryos exposed to the shRNA (**c, d** (arrow)), and an increased number of NCC is detected in over-expressing embryos (**e, f** (arrow)). The domain of Msx2 expression is significantly expanded in not only the cranial neural tube but throughout the trunk specifically in the somatopleure and splanchnopleure (**e, f**). Sagittal views with anterior to the left (**a,c,e**) and transverse sections with anterior at the top (**b,d,f**). Scale bars = 200 μm (**a,c,e**); 100 μm (**b,d,f**) A = allantois; H = heart; Hf = headfolds; pnp = posterior neuropore; arrows = Msx2 expression in the NCC of the neural tube.

Figure 5-5. Wnt signaling is strongly affected by Geminin dosage.

Expression of activated β-catenin in control (**a, d, g**), Geminin shRNA (**b, e, h**), and Geminin over-expressing embryos (**c, f, i**). **a-c**, sagittal views, **d-f** dorsal views, and **g-i** coronal sections through the forebrain of E9.0 embryos after X-gal staining. Compared with controls (**a, d, g**), down-regulation of Geminin leads to a reduction of Wnt signaling and neural tissue (**b, e, h**) whereas over-expression causes an increase in activated β-catenin expression and an expansion of neural tissue (**c, f, i**). Scale bars = 200 μm (**a-f**); 100 μm (**g-i**). H = heart; Hf = headfolds; 1 = first branchial arch; arrows = anterior neuropore; arrowheads = posterior neuropore.

REFERENCES

Basch ML, Garcia-Castrol MI, and Bronner-Fraser M. 2004. Molecular mechanisms of neural crest induction. Birth Defects Res C Embryo Today 72: 109-123.

Cano A, Perez-Moreno MA, Rodrigo I, Locascio A, Blanco MJ, del Barrio MG, Portillo F, and Nieto MA. 2000. The transcription factor snail controls epithelial-mesenchymal transitions by repressing E-cadherin expression. Nat Cell Biol 2: 76-83.

Chieffo C, Garvey N, Gong W, Roe B, Zhang G, Silver L, Emanuel BS, Budar, ML, 1997. Isolation and characterization of a gene from the DiGeorge chromosomal region homologous to the mouse Tbx1 gene. Genomics 43: 267-277.

Emmett LSD and O'Shea KS. 2009. Geminin is required for gastrulation in post-implantation mouse embryos. In preparation.

Gonzalez MA, Tachibana KK, Adams DJ, van der Weyden L, Hemberger M, Coleman N, Bradley A, and Laskey RA. 2006. Geminin is essential to prevent endoreplication and to form pluripotent cells during mammalian development. Genes & Dev 20: 1880-1884.

Gratsch TE and O'Shea KS. 2002. Noggin and Chordin have distinct activities in promoting lineage commitment of mouse embryonic stem (ES) cells. Developmental Biology 245: 83-94.

Hara K, Nakayama KI, and Nakayama K. 2006. Geminin is essential for the development of preimplantation mouse embryos. Genes to Cells 11: 1281-1293.

Hussein SM, Duff EK, and Sirard C. 2003. Smad4 and beta-catenin co-activators functionally interact with lymphoid-enhancing factor to regulate graded expression of Msx2. J Biol Chem 278: 48805-14.

Jowett AK, Vainio S, Ferguson MWJ, Sharpe PT, and Thesleff I. 1993. Epithelial-mesenchymal interactions are required for msx 1 and msx 2 gene expression in the developing murine molar tooth. Development 117: 461-470.

Kroll KL, Salic AN, Evans LM, and Kirschner MW. 1998. Geminin, a neuralizing molecule that demarcates the future neural plate at the onset of gastrulation. Development. 125: 3247-3258.

Li X, Ma L, Snead M, Haworth I, Sparkes R, Jackson C, Warman M, Mulliken J, Maxson R, Muller U, and Jabs E. 1993. A mutation in the homeodomain of the MSX2 gene in a family affected with craniosynostosis, Boston type. Am. J. Hum. Genet. 53 (suppl.): A213 only.

Mohamed OA, Clarke HJ, and Dufort D. 2004. β-catenin Signaling Marks the Prospective Site of Primitive Streak Formation in the Mouse Embryo. Dev Dyn 231: 416-424.

O'Shea KS, De Boer LS, Slawny NA, and Gratsch TE. 2006. Transplacental RNAi: Deciphering Gene Function in the Postimplantation-Staged Embryo. J Biomed Biotechnol 4: 18657.

Papanayotou C, Mey A, Birot AM, Saka Y, Boast S, Smith JC, Samarut J, and Stern CD. 2008. A mechanism regulating the onset of Sox2 expression in the embryonic neural plate. PLoS 6: e2.

Rogers CD, Harafuji N, Archer T, Cunningham DD, and Casey ES. 2009. Xenopus Sox3 activates sox2 and geminin and indirectly represses Xvent2 expression to induce neural progenitor formation at the expense of non-neural ectodermal derivatives. Mech Dev 126: 42-55.

Sauka-Spengler T and Bronner-Fraser M. 2008. A gene regulatory network orchestrates neural crest formation. Nat Rev Mol Cell Biol 9: 557-568.

Seo S, Richardson GA, and Kroll KL. 2005b. The SWI/SNF chromatin remodeling protein Brg1 is required for vertebrate neurogenesis and mediates transactivation of Ngn and NeuroD. Development 132: 105-115.

Stern CD, Artinger KB, and Bronner-Fraser M. 1991. Tissue interactions affecting the migration and differentiation of neural crest cells in the chick embryo. Development 113: 207-216.

Steventon B, Araya C, Linker C, Kuriyama S, and Mayor R. 2009. Differential requirements of BMP and Wnt signaling during gastrulation and neurulation define two steps in neural crest induction. Development 136: 771-779.

Taylor JJ, Wang T, and Kroll KL. 2005. Tcf- and Vent-binding sites regulate neural-specific geminin expression in the gastrula embryo. Dev Biol 289: 494-506.

Chapter 6

Summary and Future Directions

During development, the neural plate which will give rise to neural ectoderm requires the absence of BMP signaling for its formation. This is achieved by numerous extracellular and intracellular factors activated by the FGF, Wnt, and/or TGFβ pathways expressed in the epiblast and extra-embryonic tissues (Harland, 2000; Stern et al., 2005). Surrounding the neural plate is the epidermal ectoderm which has active BMP signaling. The juxtaposition of these two tissues is where the future neural crest will form; thus, tight regulation of signaling between the neural and epidermal ectoderm is necessary. Our hypothesis is that BMP antagonism sets the boundary between the neural and epidermal ectoderm. To test the role of BMP signaling and its antagonists during neural induction, through either loss of BMP4 or misexpression of an antagonist in mouse embryos, we found that neural ectoderm expanded at the expense of the epidermal ectoderm. Additionally, embryos with transgenic misexpression of Noggin or loss of Bmp4 expression by shRNAs had severe neural tube defects including an expansion of neural ectoderm. This confirms a critical role for BMP antagonism in setting the border between the neural and epidermal ectoderm.

Numerous factors that regulate BMP antagonism have been identified but perturbation is largely inconclusive for several reasons. First, many have compensatory actions such as Noggin and Chordin, as individual knock-outs are unable to completely inhibit BMP signaling (Valenzuela et al., 1995; McMahon et al., 1998; Piccolo et al., 1996; Bachiller et al., 2000; Anderson et al., 2002). Second, many BMP inhibitors have other functions such as FGFs that not only inhibit Bmp RNA prior to gastrulation, but are required for the formation of

mesoderm (Wilson et al., 2000; Furthauer et al., 2004; Crossley and Martin, 1995). Furthermore, several large scale differential screens have identified new molecules that are either able to inhibit BMPs (*i.e. Geminin*) (Kroll et al., 1998) or are potential antagonists as they are expressed at a time and place where BMP inhibition is necessary (*i.e.* m8708a22, p7822b53, and/or t8130b59) (Sousa-Nunes et al., 2003) but their functions have yet to be elucidated. Thus, the second aim of our research was to identify and characterize novel BMP antagonists. Previously, Geminin was shown to play a role in the neural plate of *Xenopus* (Kroll et al., 1998) and chick (Papanayotou et al., 2008; Linker et al., 2009) but its activity during mouse development was not well characterized. In subsequent work, we confirmed a role for Geminin in BMP antagonism/neural induction, and identified its function during gastrulation and neural crest formation. In embryos exposed to shRNAs targeting Geminin, we observed an increase in Bmp4 expression around the neural plate as well as in the posterior epiblast at the base of the allantois. Geminin shRNA embryos were also found to have severe neural tube defects and aggregates of cells within the primitive streak and posterior to the node. As these embryos resembled mutants that failed to undergo EMT (*i.e. Fgf8* and *Snail1* null mice), it was concluded that Geminin was necessary for the proper completion of EMT. We also characterized its role in neural crest development by using Geminin shRNAs and an overexpressing Geminin construct to decrease or increase the levels of Geminin, respectively. Neural crest cells form at the border between neural and epidermal ectoderm where Geminin is expressed, and they undergo EMT during migration away from the neural tube. Loss of *Geminin* leads to the decrease in expression of neural crest markers such as Snail1 and Msx2, whereas overexpression, increased them. These findings have significant implications that are not limited to developmental biology but extend to cancer biology. Although Geminin is able regulate the cell-cycle, it is unable to inhibit proliferation when overexpressed (Wohlschlegel et al., 2002). If Geminin controls EMT by regulation of an adhesion molecule such as E-cadherin, the progression of

epithelial cells to malignancy could be disrupted. Further work is required to assess its role in cancer but the preliminary results are promising.

Since Geminin was identified in a large scale screen to find cDNAs that could expand the *Xenopus* neural plate; we wanted to identify other novel BMP antagonists. This was accomplished by using two vastly different techniques: differential-display of Noggin overexpressing ESCs and laser capture microdissection (LCM) of E7.25 embryos. Not only did we identify over a thousand differentially expressed genes in ESCs upregulated with noggin but several were expressed in and around the node. Preliminary findings from embryos exposed to shRNAs of a few select ESTs revealed their requirement in early development as targeted embryos had numerous defects when examined at E7 to E9. Although this work is published (O'Shea et al., 2006), there are literally hundreds of possible candidates yet to be evaluated. For example, *in situ* hybridization of EST 493-4 at E7.5 showed expression around the node in the crown cells and primitive streak. shRNAs to EST 493-4 have been made and are awaiting injection and evaluation. Hundreds of genes were also identified by LCM. Whereas differential-display pulled out either stem-cell like genes or noggin induced, we obtained information for the entire embryo by using LCM. Tissues collected included: induced versus non-induced neural ectoderm, posterior versus anterior; AVE versus primitive streak versus node; and epiblast versus visceral endoderm. Further work is necessary to validate targets obtained from microarray analysis; however, once complete, we will be able to select targets for further study. In addition, these data will also be used in conjunction with microarray analyses conducted on various ESC lines from the lab for *in vivo* versus *in vitro* comparisons of gene expression profiles. For instance, we have microarray data from Neurogenin-1 overexpressing mESCs (Velkey and O'Shea in revision) and both Geminin and dominant-negative TCF overexpressing cell lines (Slawny et al., 2009 in preparation). The ability to compare various ESCs to specific regions within an embryo provides a powerful tool for teasing out the genes involved during embryogenesis.

Tail-vein technique as a tool to study gene function.

The gold standard for studying the loss- or gain- of function analyses during mouse embryogenesis is achieved by creating transgenic mice by pronuclear injection or by generating mouse lines using genetically manipulated ES cells by homologous recombination. Over the last few years, siRNAs have been employed more extensively during mammalian development by electroporation (Grabarek et al., 2002; Soares et al., 2005) or injection (Wianny and Zernicka-Goetz, 2002; Cao et al., 2005) into pre-implantation staged embryos as well as by the generation of tetraploid chimeras (Kunath et al., 2003).

To evaluate BMP4 antagonism, we have employed traditional methods to generate three transgenic and two knock-out mouse lines with the assistance of the Transgenic Animal Core. Although, we were able to glean valuable data from these mice, each line had its own limitiations. Not only is it rather expensive to generate and maintain the mouse lines, but quite time consuming until sufficient numbers of F1 progeny are obtained for analyses. On average, mice gestate 18 days and take an additional six weeks for maturation.   Chimeras are first generated then outbred in order to produce F1 progeny containing the mutation. Our first attempt at creating a *Geminin* gene-trapped mouse line produced chimeras but was unable to generate *Geminin* F1 offspring as the ES cells used to produce the chimeras had chromosomal anomalies which prevented their contribution to the germ line. Although we were able to successfully obtain *Geminin* F1 mice and begin analysis, we were unsuccessful in collecting homozygous null embryos from E7.0 onward. During this stage in our research, two papers were published illustrating the lethality of *Geminin* knock-out embryos at E3.5 (Hara et al., 2006; Gonzalez et al., 2006). As we had generated a gene-trapped line which contained a LacZ reporter, we used this line to monitor Geminin expression during shRNA exposure. Unfortunately, the LacZ insert was unable to produce viable protein for detection.

The three transgenic mice lines generated, while informative, were also problematic. In general, the number of embryos collected that contained the transgene at E7.0 to E9.0, our timepoints for analyses, was quite low. For example, out of 194 embryos collected, only 35 were carriers for the Geminin shRNA transgene (18%) and even fewer exhibited abnormalities (Supplemental Figure 4-2). This is a primary limitation of pronuclear injection as insertion into regulatory elements, low copy insertion, or early lethality such as geminin at E3.5, makes obtaining enough embryos for further study difficult.

As we wanted to evaluate the role novel BMP antagonists posed during early embryo patterning, an alternative approach for loss- and gain-of-function analyses was necessary. Especially in light of the numerous factors that are able to compensate for loss of function (*i.e. Noggin* and *Chordin*). RNAi has been used extensively for gene suppression in recent years particularly with short interfering (siRNAs) (Elbashir et al., 2001) and short hairpin RNAs (shRNAs) which are able to convey long-term gene suppression (Yu et al., 2002). RNAi can be used to produce hypomorphs and different levels of RNA silencing can be achieved by targeting various regions of the transcript (Hemann et al., 2003). Initially, Lewis et al were able to show positive EGFP expression in liver cells when mice were injected via the tail-vein with an EGFP expressing construct (Lewis et al., 2001). With these observations, we created a shRNA construct targeting a gene of interest *i.e.* Bmp4 with a fluorochrome color marker (DsRed) to inject into the tail-vein of pregnant dams (O'Shea and Gratsch lab data). If successful, we could evaluate potential candidates quickly and would avoid early embryo lethality, since these injections would bypass the early requirement of gene expression prior to implantation. To date, our lab has used tail-vein injection to successfully knock-down expression of several developmentally regulated genes such as Wnts, BMPs, Nanog, BMP antagonists, as well as novel ESTs (Gratsch et al., 2003; O'Shea et al., 2006; Emmett and O'Shea, 2009a/b in preparation; Emmett lab data; Slawny lab data). This has been extremely useful as we were able to quickly obtain sufficient numbers of effected embryos and to

screen for genes that may be required for embryo patterning. We have also used tail-vein injection to deliver a Geminin expression construct for gain-of-function analyses (Emmett and O'Shea, 2009b in preparation). Additionally, we have observed long-lasting expression of the shRNAs in 5-week post-natal F1 mice (lab data from Emmett and Morell) providing even greater possibilities of using tail-vein injections to pregnant dams without traditional transgenesis.

The Venn diagram of the embryo.

As illustrated in Figure 6-1, the expression domains of the early embryo resemble a Venn diagram. The expression of one gene may induce formation of a specific cell type but when expressed with another factor, the identity of the tissue can be changed. For example, the overlapping expression of Nodal, Wnt3, Wnt3a, Bmp4, Fgf8, Cer1, and Spry2 induces cells at the anterior most region of the embryo to become the node and notochord (Pfister et al., 2007; Dunn et al., 2001), whereas the expression of high levels of Bmp4, Stella, and Fragilis in the proximal epiblast induce primordial germ cell formation (reference?). In addition, the downstream effectors of signal transduction such as the Smads (TGFβ superfamily) and TCF/LEFs (canonical Wnt pathway) can have differential spatial-temporal expression as well. TCF3 is initially expressed in an anterior to posterior gradient in all tissues at E7.5, is restricted to the anterior neuroectoderm at E8.5, and is lost by E10.5 (Korinek et al., 1998). Conversely, TCF1 is expressed in a posterior to anterior gradient with high levels in mesoderm, intermediate in ectoderm, and no expression detected in the endoderm at E7.5. In E9.5, expression is in the forelimbs, lateral plate mesoderm, branchial arches, and in patches in and around the neural tube where neural crest cells form (Oosterwegel et al., 1993). TCF4 is initially expressed at E10.5 and continues to be expressed in the CNS at later times in development (Korinek et al., 1998). These data not only illustrate how unique patterning events and tissue types emerge during embryogenesis but shows how complex an already dynamic structure the embryo is.

Inhibition of BMP signaling has been considered the default pathway in neural induction which leads to the eventual formation of neural tissue (Harland, 2000; Stern et al., 2005; Levine and Brivanlou, 2007). However, how this is accomplished, where signals are inhibited, and the factors that accomplish this are still unknown. While the node secretes BMP antagonists such as Noggin and Chordin, embryos with loss of either gene or a functional node are still able to form neural tissue (Valenzuela et al., 1995; McMahon et al., 1998; Piccolo et al., 1996; Klingensmith et al., 1999; Ding et al., 1998). The identification of other genes expressed in the node may also regulate BMP signaling but many are still largely uncharacterized (Sousa-Nunes et al., 2003; O'Shea lab data). The data obtained from our lab thus far has illustrated the tight control and regulation that is required by antagonizing BMP signaling at the border of the epidermal/neural ectoderm for proper formation and closure of the neural tube as well as other novel genes that not only play a role in BMP inhibition but have other functions as well.
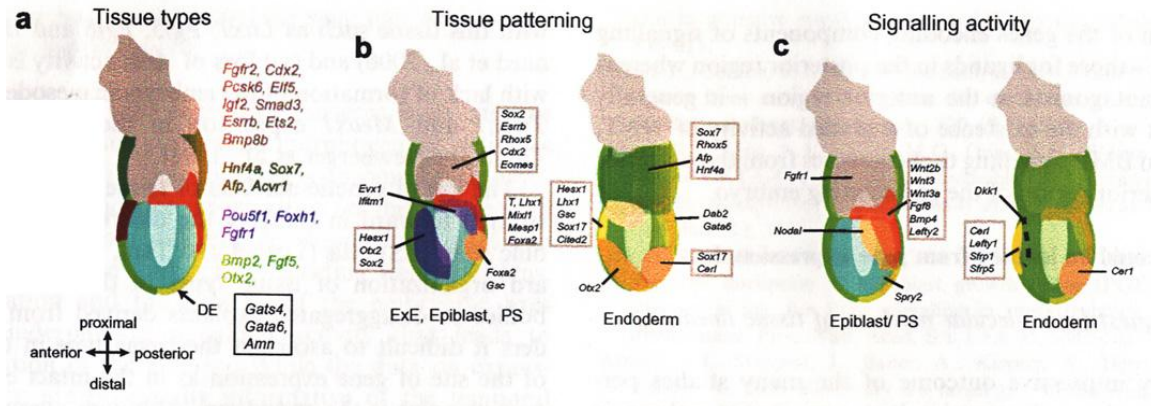
Figure 6-1. Schematic illustrating the overlapping expression patterns at gastrulation.

A. Genes that are expressed in each tissue type: gray = trophectoderm; green = embryonic visceral endoderm (VE); brown = AVE; dark green = extra-embryonic visceral endoderm (ExEn); yellow = definitive endoderm; orange = primitive streak and mesoderm; blue = epiblast.

B. Patterns of gene expression which reveal tissue patterning.

C. Patterns of gene expression illustrating the regionalization of transcripts encoding components of signaling cascades in the ExEn, epiblast, and VE.

(From Pfister 2007)

REFERENCES

Anderson RM, Lawrence AR, Stottmann RW, Bachiller D, and Klingensmith J. 2002. Chordin and noggin promote organizing centers of forebrain development in the mouse. Development 129: 4975-4987.

Bachiller D, Klingensmith J, Kemp C, Belo JA, Anderson RM, May SR, McMahon JA, McMahon AP, Harland RM, Rossant J, and De Robertis EM. 2000. The organizer factors Chordin and Noggin are required for mouse forebrain development. Nature 403: 658-661.

Cao W, Hunter R, Strnatka D, McQueen CA, and Erickson RP. 2005. DNA constructs designed to produce short hairpin, interfering RNAs in transgenic mice sometimes show early lethality and an interferon response. Journal of Applied Genetics 46: 217–225.

Crossley PH and Martin GR. 1995. The mouse Fgf8 gene encodes a family of polypeptides and is expressed in regions that direct outgrowth and patterning in the developing embryo. Development 121: 439-451.

Ding J, Yang L, Yan YT, Chen A, Desai N, Wynshaw-Boris A, and Shen MM. 1998. Cripto is required for correct orientation of the anterior-posterior axis in the mouse embryo. Nature 395: 702-707.

Dunn NR and Hogan BLM. 2001. How does the mouse get its trunk? Nat Genet 27: 351-352.

Elbashir SM, Harborth J, Lendeckel W, Yalcin A, Weber K et al. 2001. Duplexes of 21-nucleotide RNAs mediate RNA interference in cultured mammalian cells. Nature 411: 494-498.

Emmett LSD and O'Shea KS. 2009a. Geminin is required for gastrulation in post-implantation mouse embryos. In preparation.

Emmett LSD and O'Shea KS. 2009b. Geminin controls EMT and neural crest specification in the mouse embryo. In preparation.

Furthauer M, Van Celst J, Thisse C, and Thisse B. 2004. Fgf signaling controls the dorsoventral patterning of the zebrafish embryo. Development 131: 2853-2864.

Gonzalez MA, Tachibana KK, Adams DJ, van der Weyden L, Hemberger M, Coleman N, Bradley A, and Laskey RA. 2006. Geminin is essential to prevent endoreplication and to form pluripotent cells during mammalian development. Genes & Dev 20: 1880-1884.

Grabarek JB, Plusa B, Glover DM, and Zernicka-Goetz M. 2002. Efficient delivery of dsRNA into zona-enclosed mouse oocytes and preimplantation embryos by electroporation. Genesis 32: 269–276.

Gratsch TE and O'Shea KS. 2002. Noggin and Chordin have distinct activities in promoting lineage commitment of mouse embryonic stem (ES) cells. Developmental Biology 245: 83-94.

Hara K, Nakayama KI, and Nakayama K. 2006. Geminin is essential for the development of preimplantation mouse embryos. Genes to Cells 11: 1281-1293.

Harland R. 2000. Neural Induction. Curr Opin Genet Dev 10: 357-362.

Hemann MT, Fridman JS, Zilfou JT, Hernando E, Paddison PJ, Cordon-Cardo C, Hannon GJ, and Lowe SW. 2003. An epi-allelic series of p53 hypomorphs created by stable RNAi produces distinct tumor phenotypes in vivo. Nat Genet 33: 396–400.

Klingensmith J, Ang SL, Bachiller D, and Rossant J. 1999. Neural induction and patterning in the mouse in the absence of the node and its derivatives. Dev Biol 216: 535-549.

Korinek V, Barker N, Willert K, Molenaar M, Roose J, Wagenaar G, Markman M, Lamers W, Destree O, and Clevers H. 1998. Two members of the Tcf family implicated in Wnt/beta-catenin signaling during embryogenesis in the mouse. Mol Cell Biol 18: 1248-1256.

Kroll KL, Salic AN, Evans LM, and Kirschner MW. 1998. Geminin, a neuralizing molecule that demarcates the future neural plate at the onset of gastrulation. Development. 125: 3247-3258.

Kunath T, Gish G, Lickert H, Jones N, Pawson T, and Rossant J. 2003. Transgenic RNA interference in ES cell-derived embryos recapitulates a genetic null phenotype. Nature Biotechnology 21: 559–561.

Levine AJ and Brivanlou AH. 2007. Proposal of a model of mammalian neural induction. Dev Biol 308: 247-256.

Lewis DL, Hagstrom JE, Loomis AG, Wolff JA, and Herweijer H. 2001. Efficient delivery of siRNA for inhibition of gene expression in postnatal mice. Nat Genet 32: 107-108.

Linker C, De Almeida I, Papanayoutou C, Stower M, Sabado V, Ghorani E, Streit A, Mayor R, and Stern CD. 2009. Cell communication with the neural plate is required for induction of neural markers by BMP inhibition: evidence for homeogenetic induction and implications for Xenopus animal cap and chick explants assays. Dev Biol 327: 478-486.

McMahon JA, Takada S, Zimmerman LB, Fan CM, Harland RM, and McMahon AP. 1998. Noggin-mediated antagonism of BMP signaling is required for growth and patterning of the neural tube and somite. Genes & Development 12: 1438-1452.

Oosterwegel M, van de Wetering M, Timmerman J, Kruisbeek A, Destree O, Meijlink F, and Clevers H. 1993. Differential expression of the HMG box factors TCF-1 and LEF-1 during murine embryogenesis. Development 118: 439-448.

O'Shea KS, De Boer LS, Slawny NA, and Gratsch TE. 2006. Transplacental RNAi: Deciphering Gene Function in the Postimplantation-Staged Embryo. J Biomed Biotechnol 4: 18657.

Papanayotou C, Mey A, Birot AM, Saka Y, Boast S, Smith JC, Samarut J, and Stern CD. 2008. A mechanism regulating the onset of Sox2 expression in the embryonic neural plate. PLoS 6: e2.

Pfister S, Steiner KA, and Tam PPL. 2007. Gene expression and progression of embryogenesis in the immediate post-implantation period of mouse development. Gene Expr Pat 7: 558-573.

Piccolo S, Sasai Y, Lu B, and De Robertis EM. 1996. Dorsoventral patterning in Xenopus: Inhibition of ventral signals by direct binding of Chordin to BMP-4. Cell 86: 589-598.

Soares ML, Haraguchi S, Torres-Padilla ME, et al. 2005. Functional studies of signaling pathways in peri-implantation development of the mouse embryo by RNAi. BMC Developmental Biology 5: 28 e-pub.

Sousa-Nunes R, Rana AA, Kettleborough R, Brickman JM, Clements M, Forrest A, Grimmond S, Avner P, Smith JC, Dunwoodie SL, and Beddington RSP. 2003. Characterizing Embryonic Gene Expression Patterns in the mouse using nonredundant sequence-based selection. Genome Res 13: 2609-2620.

Stern CD. 2005. Neural induction: old problem, new findings, yet more questions. Development 132: 2007-2021.

Valenzuela DM, Economides AN, Rojas E, Lamb TM, Nunez L, Jones P, Ip NY, Espinosa R, Brannan CI, Gilbert DJ, Copeland NG, Jenkins NA, LeBeau MM, Harland RM, and Yancopoulos GD. 1995. Identification of mammalian noggin and its expression in the adult nervous system. J. Neuroscience 15: 6077-6084.

Velkey JM and O'Shea KS. Neurogenin 1 expression in mouse embryonic stem cells produces growth factor-sensitive neural progenitors. In revision.

Wilson SI, Graziano E, Harland R, Jessell TM, and Edlund T. 2000. An early requirement for FGF signaling in the acquisition of neural cell fate in the chick embryo. Curr Biol 20: 421-429.

Wohlschlegel JA, Kutok JL, Weng AP, and Dutta A. 2002. Expression of Geminin as a Marker of Cell Proliferation in Normal Tissues and Malignancies. Am J Path 161: 267-273.

Yu JY, DeRuiter SL, and Turner DL. 2002. RNA interference by expression of short-interfering RNAs and hairpin RNAs in mammalian cells. Proc Natl Acad Sci USA 99: 6047-6052.

Appendix 1

Transplacental RNAi: Deciphering Gene Function in the Postimplantation-Staged Embryo

ABSTRACT

Although the mouse is the pre-eminent model to study gene function in development, the process of targeted gene deletion using homologous recombination in ES cells can be cumbersome, costly, and slow. In addition, when there are multiple genes with overlapping, compensatory roles in development, <u>all</u> must be targeted. The application of RNA interference (RNAi) to ES cells and recently to embryos provides the opportunity to target specific or multiple regions of a particular gene, or to target multiple genes that may play redundant roles in development. When delivered via tail vein to pregnant dams, RNAi offers the opportunity to examine the role in post-implantation development of genes that cause pre-implantation lethality, and for species for which ES cells are not available, offers the opportunity to create targeted embryos.

We have delivered constituitively expressed short hairpin (sh) RNAs to pregnant mice during the early post-implantation period of development and observed gene knock-down and developmental defects that phenocopy the null embryo. In the current investigation, we have targeted seven genes singly and in combination, and describe unique phenotypes for each. Systemic delivery of shRNAs provides a potentially invaluable approach to gene silencing in the embryo.

198

INTRODUCTION

With the sequencing of the mouse genome (Waterston et al., 2002), there has been tremendous interest in teasing out the function of <u>every</u> gene. In the mouse, gene targeting using homologous recombination in embryonic stem cells (ESC) has provided a unique opportunity to probe gene function in development (Capecchi, 1989), and a number of powerful new techniques have been developed to target genes in temporal or tissue specific ways. Unfortunately, these are time consuming and often require the development of multiple strains of mice, which then must be mated to obtain the desired cell-type specific gene targeting. The recent application of post-transcriptional gene silencing using RNA interference (RNAi) to silence target genes has been an efficient way to study gene function initially in *C. elegans* and plants, later in mammalian cells in culture, and recently in embryos.

RNAi is a powerful alternative to traditional gene targeting using homologous recombination in ES cells, large scale mutagenesis, ribozymes, morpholinos, oligonucleotides, etc., for many reasons. Among these are: simplicity in design of the targeting construct, efficiency, and high throughput (reviewed in Svoboda, 2004). In addition, RNAi offers the ability to target specific exons/specific sequences within a gene (Hemann et al., 2003), to study gene dosage phenotypes, to target multiple (redundant) genes, to target multiple members of a regulatory pathway, and to produce graded levels of knock-down analogous to allelic series, which is particularly useful in analyzing the effects of genes that have "threshold" effects rather than acting as binary on-off switches. In addition, RNAi may be particularly useful to avoid the confounding genetic background effects common to gene targeting using the limited number of "germline" ESC lines, and finally, many other species (e.g., rat) can be employed.

Relatively few studies have employed RNAi to study gene function in the developing embryo. RNAi has been electroporated (Grabarak et al., 2002;

Soares et al., 2005) or microinjected into oocytes or early zygotes (Wianny and Zernicka-Goetz, 2000; Hasuwa et al., 2002; Rubinson et al., 2003; Tiscornia et al., 2003; Cao et al., 2005), siRNA transfected ES cells have been used to create germ line transgenic RNAi mice (Carmell et al., 2003), or all-ES embryos have been generated using tetraploid aggregation of RNAi targeted ESC (Kunath et al., 2003). Delivery, particularly to post-implantation staged embryos, continues to be a major limitation in the widespread application of this important technology.

Infomation regarding prenatal delivery of plasmid DNA (pDNA) comes largely from the gene therapy field where *in utero* gene targeting/therapy has been proposed as a method to treat diseases that affect the developing embryo (Coutelle et al., 1995), which may ultimately be the most effective means to treat genetic defects. Various routes of plasmid pDNA delivery have been attempted for fetal "gene therapy" including direct injection of the fetus (Baldwin et al., 1997; Larson et al., 1997; Gaensler et al., 1999), injection into the placenta or umbilical cord (Papaioannou, 1990; Turkay et al., 1999; Mitchell et al., 2000), injection into the amniotic cavity (Douar et al., 1997; Schatchner et al., 1999; Mitchell et al., 2000), or the yolk sac (Schachtner et al., 1999) typically resulting in limited transduction of the embryo.

Intravascular delivery of naked DNA is increasingly recognized as a preferred route to deliver nucleic acids to target tissues (Hodges and Scheule, 2003) because of its simplicity and effectiveness and because high levels of transgene expression can be achieved and sustained (e.g., Hagstrom et al., 2004). However, it has required either high pressure delivery to produce extravasation (Lewis et al., 2002), or a tourniquet to keep the pDNA in place (Hagstrom et al., 2004). Tail vein injection has been employed to silence genes in neonatal (Lewis et al., 2002), and adult mice (McCaffrey et al., 2003; Song et al., 2003; Sorensen et al., 2003; Soutschek et al., 2004). Based on these reports, we recently

delivered shRNAs to pregnant mice and have observed gene silencing and unique phenotypes in the embryos.

In this report, we summarize the results of silencing genes that have not yet been "knocked-out" in the mouse (geminin and Wnt8b), genes that are required during cleavage stages of development (nanog), and genes required at implantation (Bmp4, Bmp7) singly and in combination (Bmp4 + Bmp7). We have also determined a role in post-implantation development of two genes identified in a differential display RT-PCR screen of genes induced in ES cells by noggin exposure, Aggf1 and an Est (Genebank # AK008955).

RESULTS

Development of Targeting Constructs.

Based on recent evidence that DNA and short interfering (si) RNAs could be delivered to target tissues via the blood vascular system of adult and neonatal mice, we developed a targeting construct that would allow us to deliver a single plasmid containing a small hairpin RNA (driven by the constitutively active H1 or U6 promoter) and a fluorochrome reporter driven by the CMV promoter (Figure A1-1). We have delivered shRNA to more than 80 pregnant mice, and obtained both gene silencing and expression of the DsRed fluorochrome in embryonic tissues, persisting in postnatal mice. We have carried out a number of experiments to determine if implantation site correlated with knock-down. In general, embryos implanted near the vagina exhibited more complete knock-down than those near the ovaries. In most cases, there is knock-down and DsRed is expressed in embryos. Occasionally (~5% of the injections) there is no transfection, likely because injection itself fails due to an insufficient amount of DNA entering the circulation.

Because research in our laboratory has focused on the early post-implantation period of development, we have typically delivered targeting constructs at E6.5 and autopsied embryos 24h to 72h later. We have also carried out limited studies at midgestation when the placental barrier is most robust, as well as on E17.5 when the barrier thins and delivery should be more complete. We examine the extent of DsRed expression in all embryos using epifluorescence, followed by SEM, sectioning, immunohistochemistry, western blotting, and/or PCR. DsRed is typically expressed throughout the early embryo, without a preference for a particular tissue type (Figure A1-1. C). In addition to confirmation that the plasmid reached the embryonic compartment (DsRed fluorescence), we deliver empty plasmid (pRed), and hairpins containing three nucleotide substitutions (scrambled hairpins) that correspond to no known mRNA. Blast analysis confirms unique targeting of the hairpin and that no genes are targeted by the scrambled hairpin. We monitor target gene expression using PCR and at the protein level when an antibody is available. It is also important to monitor additional members of the signaling pathway, compensatory genes, irrelevant genes, and genes down-stream of the target. We also monitor the interferon response gene OAS1 (Bridge et al., 2003) to determine if our construct elicits a nonspecific response.

Geminin shRNA.

The *Geminin* gene has been both down-regulated and over-expressed in *Xenopus* embryos, reducing or expanding the neural ectoderm fields respectively (Kroll et al., 1998). Geminin is particularly interesting because, as suggested by its name, the protein has two functions; the C-terminus functions in cell cycle progression required for differentiation, the N-terminal is involved in early neural differentiation (Seo et al., 2005). Despite its provocative expression in the early neural ectoderm, and demonstrated role in amphibian, Drosophila, and zebrafish development, there is not yet a knock-out of Geminin in the mouse.

When a shRNA targeted to geminin was delivered on E6.5, and embryos examined one-three days later, we observed reductions in neural tissue, neural tube closure defects that typically affected the midbrain and posterior neuropore. In early embryos, we observed abnormally expanded nodes and failure of closure of the primitive gut endoderm (Figure A1-2). When we examined the level of Geminin expression in whole mount immunohistochemistry, wild type embryos were indistinguishable from embryos exposed to the scrambled hairpin both in morphology and in the pattern of Geminin protein expression in the newly induced neural ectoderm (Figure A1-2. A,B). Geminin was present at slightly higher levels in the anterior neural folds compared with the posterior region of early somite staged embryos (Figure A1-2 A,B). There was slight Geminin immunoreactivity in the neural ectoderm of some Geminin targeted embryos (Figure A1-2. C); while others expressed virtually no Geminin protein (Figure A1-2. D).

When semi-quantitative RT-PCR was carried out on RNA isolated from individual embryos from three litters, there was some variability in knock-down in the shRNA exposed embryos, with two embryos expressing levels similar to control, others expressing intermediate, low or no Geminin mRNA (Figure A1-3).

Nanog shRNA Exposure.

The Nanog gene encodes a varient homeodomain protein originally identified in ES cells where it is required to maintain pluripotency and inhibit lineage differentiation (Mitsui et al., 2003). Targeted deletion in embryos is lethal before implantation (Chambers et al., 2003), but additional evidence suggested that nanog was expressed in germ cells and somatic tissues later in development (Hart et al., 2004), but its role could not be assessed due to the early lethality of null embryos.   To determine Nanog's role in later stages of development, we have exposed 21 litters of pregnant mice to shRNA targeted to nanog via tail vein injection. We have observed widespread resorption of nanog targeted embryos,

and in other litters we have observed abnormalities of gastrulation and neurulation. Nanog knock-down embryos are characterized by axis abnormalities which are present in early somite embryos, considerably earlier in development than the turning process is initiated, endoderm overgrowth, and neural tube closure defects, particularly of the midbrain neural folds. Somite segmentation is also often abnormal, and we have observed abnormalities of cell migration through the primitive streak at gastrulation. Figure A1-4 and Figure A1-9. G,H illustrate some of these malformations.

In whole mount immunohistochemistry, Nanog protein expression is significantly reduced, particularly in the primitive streak of embryos exposed to the nanog shRNA (Gratsch et al., 2005). To correlate phenotype and knock-down, we carried out quantitative PCR on RNA from individual Nanog targeted embryos from an entire litter. Silencing ranged from complete in three embryos to 60% of wild type Nanog levels in the least severely affected embryo. The presence of phenotypic abnormalities correlates strongly with the degree of knock-down, as illustrated in Figure A1-4 by the largely normal appearance of the embryo from lane 6, compared with the embryo from lane 7.

Somewhat surprisingly, two Nanog shRNA embryos expressed slightly elevated levels of the OAS1 gene (Figure A1-5, lane 15). Bmp4 expression was robust, however, suggesting that there had not been widespread gene silencing. Although it is widely employed to monitor off-target effects, OAS1 is expressed in muscle, brain, and connective tissue during development (Asada-Kubota et al., 1997; Bisbal et al., 2000). In addition, OAS1 plays a role in cell cycle progression (Wells and Mallucci, 1988), suggesting the need to monitor additional interferon targets in these studies.

Targeting Multiple Genes: Bmp4, 7 RNA Interference.
When a cocktail of shRNA targeted to Bmp4 (exons 2 and 3) was delivered on E6.75 of gestation to pregnant mice, we observed defects of neural tube closure,

allantois development, and of heart and axial rotation (Figure A1-6 B) in targeted embryos. The number of primordial germ cells identified by alkaline phosphatase staining was also strikingly reduced. RT-PCR analysis of RNA obtained from individual Bmp4 shRNA exposed embryos from one entire litter identified only one embryo with low expression (Figure A1-7).

Immunohistochemical localization of BMP4 protein was carried out on sections through shRNA and pRed (plasmid lacking the hairpin) exposed embryos, and indicated significant depletion of BMP4 in targeted embryos (Gratsch et al., 2003). We also have carried out western blotting analysis of protein isolated from individual embryos exposed to Bmp4 shRNA, where there was reduced expression of phospho-Smads 1/5/8, which are phosphorylated in response to BMP4,7 signaling.

Conventional gene targeting of Bmp4 results in peri-implantation lethality (Winnier et al., 1995), while on a C57Bl/6 background embryos live until approximately 26 somite stage (Lawson et al., 1999), and are characterized by axis elongation abnormalities. The results of the Bmp4 RNAi phenocopy many defects in the Bmp4 null embryos (Winnier et al., 1995; Lawson et al., 1999; Fujiwara et al., 2002) including anomalies of: axis formation, primordial germ cell differentiation, and neural tube closure (Gratsch et al., 2003). Many of these are also observed in embryos lacking BMPR1a (Mishina et al., 1995).

Because BMP proteins have overlapping functions in development, we examined the effects of knocking-down multiple Bmps (Figure A1-6). We delivered a cocktail of shRNA targeted to Bmp4+Bmp7, as well as to Bmp7 alone. The Bmp7 shRNA embryos were the least severely affected (Figure A1-6 C) with neural tube closure defects, while the Bmp4+Bmp7 shRNA embryos had widely expanded neural folds, defects of rotation, failure of development of posterior structures, and ventral body wall closure defects (Figure A1-6 D), a more severe phenotype than either the Bmp4 shRNA, or Bmp7 shRNA embryos, but strikingly

similar to the caudal dysgenesis and the "massive brains" reported in *Xenopus* embryos following morpholino depletion of Bmp2,4, and 7 (Reversade et al., 2005).

Durability of the RNAi.

To determine how long knock-down could be maintained, we carried out tail vein injection of shRNA targeted to Bmp4 on E6.5 and examined neonatal mice. On postnatal day 1-5, neonates were characterized by cystic bladders, had rudimentary testes or ovaries, and were consistently growth retarded compared with mice exposed to the pRed control (Figure A1-8 A). Expression of DsRed was maintained in many tissues in both the mother (including milk) and in the offspring (Figure A1-8 B-F). There were also anomalies of the sub-ventricular neural stem cell zone (SVZ; Figure A1-8 B,C) which depends on Noggin-Bmp4 signaling (Lim et al., 2000).

Multiple Targets, Multiple Phenotypes.

We have delivered shRNA targeted to: Wnt8b, Bmp4, Bmp7, Bmp4+Bmp7, Geminin, Nanog, and to two Ests identified in a differential display RT-PCR screen and observed specific targeting and unique phenotypes (Figure A1-9). These studies have identified a previously unsuspected role for Nanog in gastrulation and also in somite organization (Figure A1-4, Figure A1-9 B). The two novel genes we identified in a screen, had not previously been examined during development. Aggf1 was identified as an angiogenic factor mutated in human disease (Tian et al., 2004), but no information is available about its expression or possible role in development. Given its role in vessel formation, it is not surprising that we observed hemorrhages, and failure of implantation in shRNA exposed embryos (Figure A1-9 C).

Targeting Est1 produced a severe neurulation phenotype with open neural folds, defects of embryonic rotation and differentiation of posterior structures, reminiscent of genes involved in L-R axis patterning (Figure A1-9 D). In the case of Wnt8b where there was no previously reported knock-out mouse, we observed severe axis elongation defects (Figure A1-9 F). Although Geminin targeting in amphibian and Drosophila embryos has axis patterning and neural tissue consequences, there is no information on the early expression of Geminin or targeted deletion of the Geminin gene in mouse. Since it is strongly induced by noggin, the observed neural, node and endoderm abnormalities (Figure A1-9 G,H) are not surprising.

Overall, we believe that these results are important and valid for a number of reasons. **One**. We have targeted multiple genes and observed unique phenotypes. These include: Bmp4 (phenocopies the Bmp4 null embryos, as far as is possible to determine due to early lethality of the null embryos), Bmp7 alone, Bmp4 plus Bmp7, Wnt8b, Nanog, Aggf1, and Est1. **Two.** In each case where an antibody is available to the protein (Bmp4, Nanog, Geminin) or to the downstream signal transduction cascade (PhosphoSmad1,5,8) we have demonstrated knock-down in INDIVIDUAL embryos. **Three**. In cases where an antibody is not available, we have demonstrated unique phenotypes, and knock-down by PCR. **Four.** These data also demonstrate that we can knock-down multiple targets—e.g., Bmp7 and Bmp4 and identify an additive phenotype.

DISCUSSION

With genome-wide gene sequencing data now available, there is increased interest in systematically manipulating all the genes of the mouse to understand their roles in development and disease. Many new tools to manipulate gene function have been developed including: ribozymes, microRNAs, DNAzymes, as well as a number of methods for post-transcriptional gene silencing such as morpholinos (review, Heasman, 2002), antisense oligos (review, Lavery and

King, 2003), and RNAi (review, Svoboda, 2004). RNAi is typically more robust than antisense oligos or morpholinos in embryos (Lefebvre et al., 2002; Mellitzer et al., 2002), and morpholinos have the additional problem that the translational start site must be known, so uncharacterized genes (such as Ests) cannot be targeted.

RNAi may be particularly appropriate in targeting a developmental disease such as Down's syndrome/trisomy 21 once critical duplicated genes are identified, and may also be effective in targeting upstream pathways in metabolic disease to limit disease progression, or in silencing activating gene mutations, such as in the FGF receptor-2 which produces craniosynostosis (Anderson et al., 1998). Systemic delivery will also be applicable to diseases that affect tissues with open circulations, as well as diseases in which the blood brain barrier is opened such as Duschenne muscular dystrophy, certain brain tumors, in aging and in multiple sclerosis (review, Begley, 2004).

These studies have identified unsuspected roles in development for several genes. In the case of Nanog, which in null embryos is lethal at early cleavage stages of development, a role in gastrulation, neurulation, and in endoderm differentiation. There is not a report of a knock-out of the Geminin gene in the mouse, and it will be of particular interest to study carefully the characteristics of the neural tissue in targeted embryos, as well as the characteristics of the node. Neither is there a published report of a Wnt8b knock-out, but many of the defects observed in this study are similar to those present in other Wnt null embryos. For example, Wnt3a null embryos have similar severe posterior truncations (Liu et al., 1999). The use of RNAi directed against individual Wnt mRNAs should allow rapid analysis of individual Wnt functions. In addition, some Wnts may compensate for each other, masking functions in single gene knock-outs. Combinatorial Wnt RNAi should help elucidate possible compensatory relationships between Wnts. Delivery of shRNA to pregnant dams has also provided an opportunity to rapidly determine if there was a role in early embryos

for novel genes identified in a differential display RT-PCR screen. A role for Aggf1 in later aspects of vasculogenesis was described previously (Tian et al., 2004), and given its role in vessel development, it is not surprising that targeting Aggf1 affected the implantation process.

The ability to target multiple genes with overlapping function, as in the case of Bmp4/7, is an important improvement over traditional knock-outs in which mutations in multiple genes are obtained by breeding. In the future, it will be important to target multiple genes using a single plasmid containing multiple hairpins, rather than the cocktail we have employed to target Bmp4 and Bmp7.

To date, study of the placental transport of plasmid DNA has come largely from attempts to deliver pDNA for *in utero* gene therapy, which have produced conflicting results. Thus, when pDNA complexed with liposomes was delivered by intravenous injection of pregnant mice on E2.5, 5.5, 8.5, 11.5 or 14.5, no plasmid DNA was detected in fetuses exposed on E2.5 or E5.5, while embryonic expression peaked with delivery on E8.5, compared with E11.5 or E14.5. All embryos treated on E8.5 expressed the plasmid, with sustained expression at 40 days postinjection (Tsukamoto et al., 1995). However, it has also been reported that DNA-liposome complexes were trapped in the visceral endoderm prior to placenta development on E11.5 (Kikuchi et al., 2002). Others have also reported hemodynamic transfer of genes to the fetal compartment, however. For example, intravenous delivery of plasmid DNA to pregnant mice on E9.5 successfully immunized the fetuses against HIV-1 and influenza (Okuda et al., 2001). We have avoided carriers since liposomes are often immunogenic, are generally less effective in serum and can be toxic to both the embryo and the pregnant female (Kikuchi et al., 2002).

Although we have obtained widespread expression of our construct, a number of improvements and alternative approaches can be considered. It would be possible to increase the amount of DNA injected, although 5 μg plasmid DNA

was optimal (saturating) and > 25 μg/mouse was toxic (Liu et al., 1997, 1999). Other studies have shown that transfection efficiency is not determined by volume or rate, but the amount of DNA delivered, with highest expression achieved with 1000 ng/mouse (Hagstrom et al., 2004). Given the ~1.6 ml blood volume of an 18g mouse and observations that there is less degradation of pDNA in a larger volume of carrier (Liu et al., 1999), increasing the volume delivered would be an option. Rate of injection—5 seconds is better than 30 (Liu et al., 1999; Lewis et al., 2002)—could also be considered, but very rapid injection can be lethal.

Despite careful breeding, the developmental stage of individual embryos at the time of exposure to shRNAs cannot be known precisely, and may account for some of the variability in our results. Alternatives include using exo-utero surgery of mid-gestation embryos with injection of shRNAs and electroporation (Mellitzer et al., 2002). For early post-implantation stages when exo-utero surgery is not applicable, whole embryo culture presents another option (Calegari et al., 2004). Better promoters and better control of CRE expression in the early embryonic compartment will allow the development of hybrid approaches to specifically, inducibly silence gene expression in a particular tissue/cell type (e.g., Chang et al., 2004). Interestingly, the oocyte-restricted ZP3 promoter was recently employed to drive expression of dsRNA targeted to the Mos gene, recapitulating the null phenotype, with spontaneous parthenogenetic activation (Stein et al., 2003). These and other recent investigations suggest that it will be possible to target RNAi to particular cells or tissues.

One drawback to tail vein injection is the loss of plasmid DNA to the female and unintended transfection of maternal tissues. Since the liver has an expandable circulation and is easily transfected using intravenous delivery, it is important to monitor liver function in pregnant females and neonates. Obviously, when the targeted gene is important in maternal tissues, this is a larger concern that must be constantly monitored. Additional controls might therefore include targeting of

a non-essential protein such as EGFP in the GFPU mouse (Hadjantonakis et al., 1998) which has no known down-stream targets, nor have there been deleterious effects of EGFP cleavage products. It would be possible to mate hemizygous GFPU mice to determine if there are any deleterious effects that are transmitted to the non-targeted, +/+ embryos. It would also be useful to target a gene expressed only in male embryos, so that female littermates would serve as a control for off-target and/or maternal effects.

It is impractical to carry out microarray analyses of individual, targeted embryos to determine specificity of targeting, although in previous studies when the targeting construct was specific, RNAi signatures were unique and highly specific for the target gene (Chi et al., 2003; Semizarov et al., 2003). More detailed analysis can also be carried out to verify the presence of specific mRNA cleavage products using 5' RACE, PCR to identify the cleavage fragments with sequencing (Yekta et al., 2004).   It has generally been assumed that early in development the embryo is incapable of mounting a full interferon response (Barlow et al., 1984), yet interferon responsive genes such as fragilis are expressed during very early post-implantation development (Saitou et al., 2002). Since OAS1 may have additional roles in development, monitoring other interferon-responsive genes would also be appropriate in these studies.   Recent evidence also suggests that shRNA expression can competitively inhibit endogenous miRNA function via exportin 5 (Yi et al., 2005), although inclusion of scrambled controls should control for this effect. Much remains to be understood about this technique, particularly regarding transport, uptake, and expression in the embryos and fetus

Since the first transgenic mouse was developed in 1980 by pronuclear injection of DNA (Gordon et al., 1980) there have been major improvements to the technological base for mouse functional genomics, and RNAi promises to be a powerful new addition to that tool set.

ACKNOWLEDGEMENTS

This appendix represents the contents of a published article:

O'Shea KS, De Boer LS, Slawny NA, Gratsch TE. Transplacental RNAi: Deciphering Gene Function in the Postimplantation-Staged Embryo. J Biomed Biotechnol. 2006. 2006(4):18657.

(a)

(b)

(c)

DsRed is widely expressed
in embryos as early as 24 h
after injection
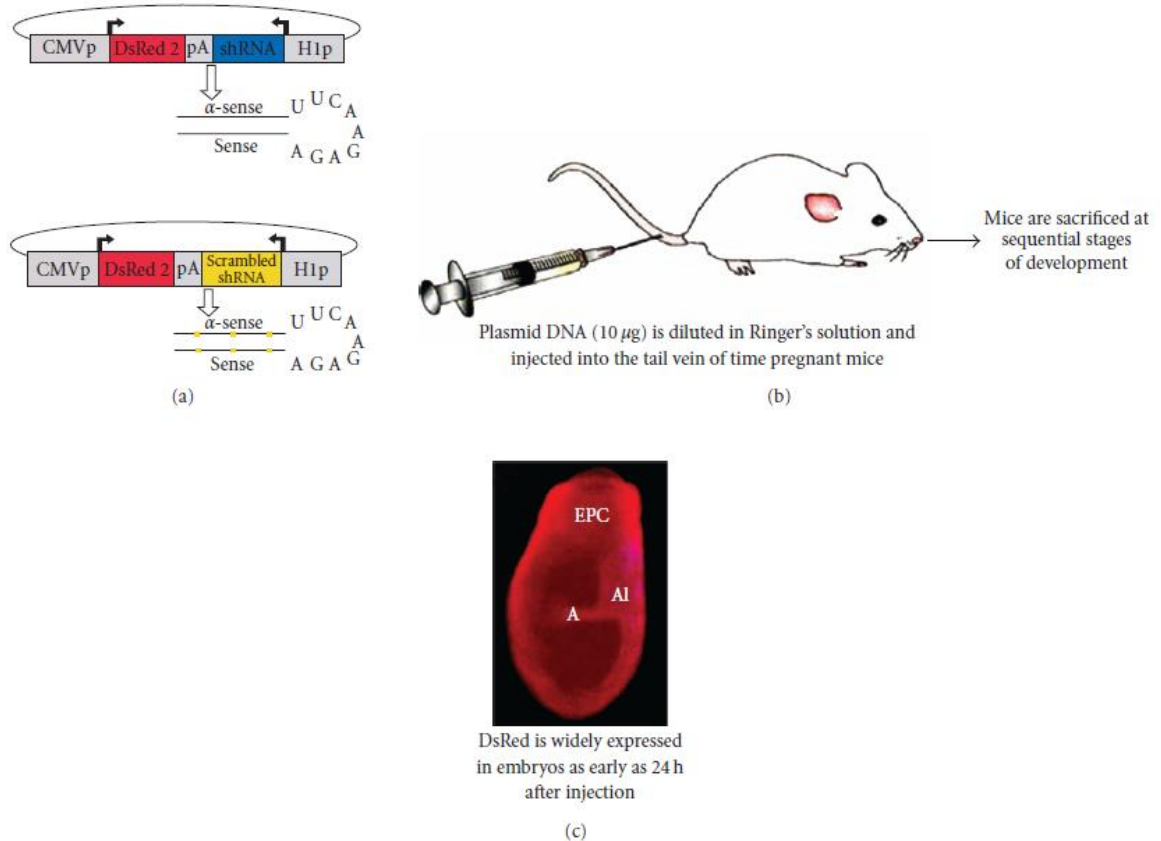
Figure A1-1. Tail vein injections.

A. shRNA expression plasmids were constructed using the pCS2 plasmid as the backbone. The DsRed 2.1 coding region was removed from the pDsRed2-1 vector (Clontech) and cloned downstream of the CMV promoter in the MCSI. The mouse H1 promoter (1040–1215 nt) of the RNAseP/PARP2 promoter, GenBank accession AF191547, was PCR-amplified from genomic DNA and cloned into MCSII. Gene-specific shRNAs (blue region) or scrambled shRNAs (yellow) are then ligated downstream of the H1 promoter.

B. Tail vein injections were carried out in pregnant mice as we have done previously (Gratsch et al., 2003).

C. Embryos are dissected from the uterus, and decidua and membranes are removed. Transmitted light and fluorescence images of embryos are captured using a Leitz-inverted fluorescence microscope to determine the extent of DsRed expression and to examine their morphology. A: amnion, AI: allantois, EPC: ectoplacental cone.
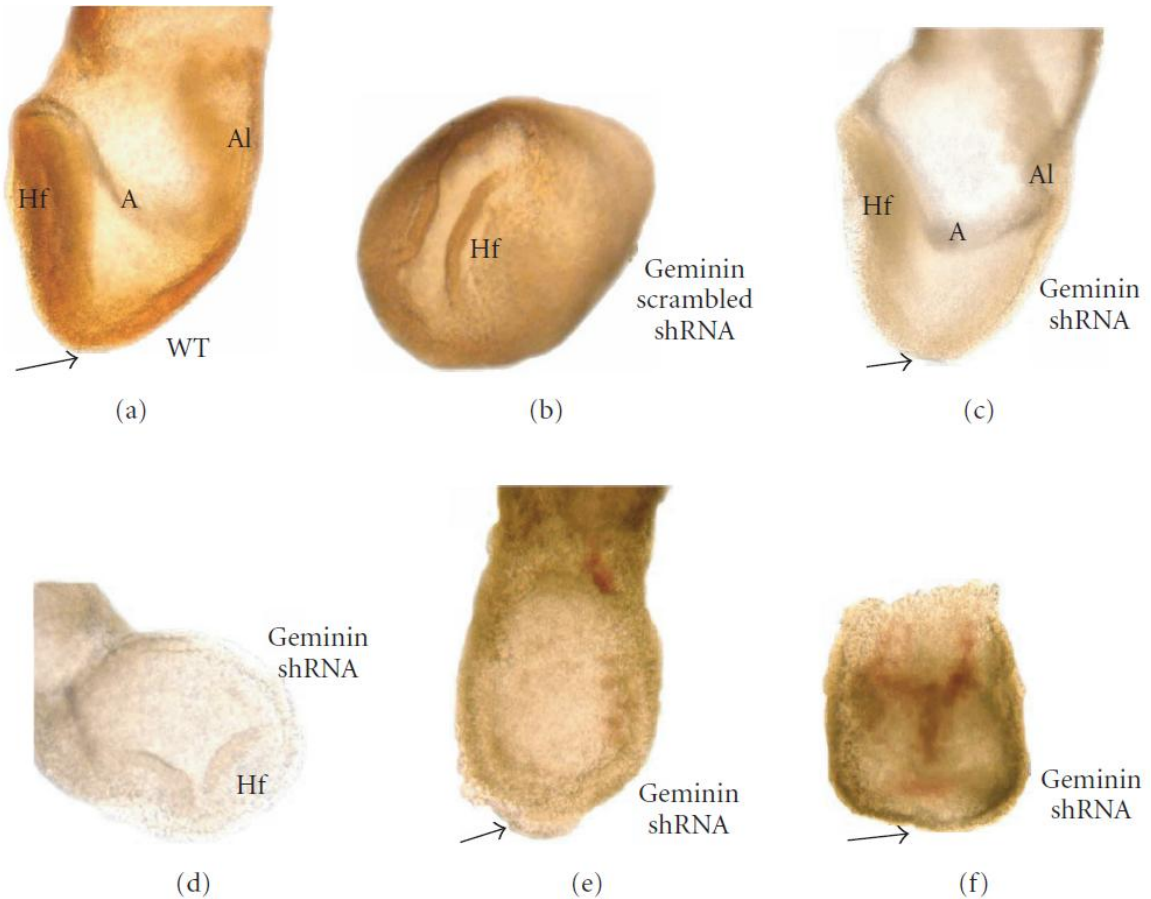
Figure A1-2. Effects of *geminin* shRNA.

Immunohistochemical localization of geminin in control (a) and (b) embryos, and in embryos exposed on E6.5 to *geminin* shRNA (c and d). In control embryos, both wild type (a) and embryos exposed on E6.5 to a scrambled *geminin* hairpin construct (b), the expression of geminin protein was high in the neural ectoderm of the head folds, although geminin was also expressed in the posterior neural ectoderm as well (brown reaction product). There is a slight background staining of the allantois and membranes in all embryos (a)–(d). (c) and (d) Embryos were exposed to the shRNA-targeting geminin, examined and fixed on E7.5 of gestation, then immunohistochemistry to identify patterns of geminin protein expression was carried out as for (a) and (b) (secondary antibody-HRP). There is low-level geminin protein remaining in the neural ectoderm in embryo (c) less than that in embryo (d). (e) and (f) Transmitted light images of embryos exposed to the *geminin* shRNA on E6.5 and examined on E7.5. (e) Many targeted embryos exhibited axis defects, abnormal expansion of the node (arrow), and in later embryos, the endoderm of the gut tube often failed to close. (f) Occasionally, the embryonic axis appeared very flattened, and there was blood within the amniotic cavity. (a), (c), (e), and (f) are sideviews with anterior located toward the left. (b) is a dorso-lateral view, and (d) is a frontal (coronal) view. A: amnion, Al: allantois, Hf: head folds, WT: wild-type control embryo. Arrows indicate the node.

214

(a)
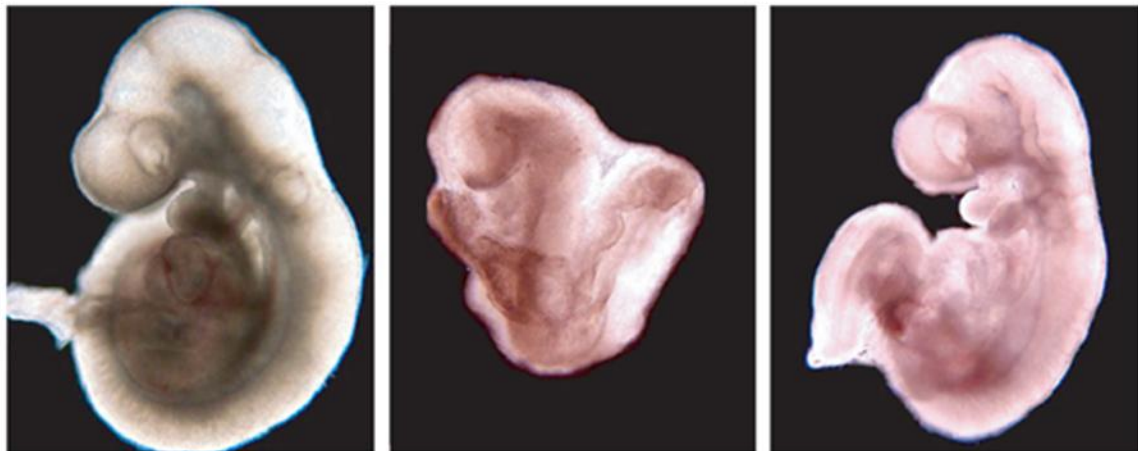
Control embryo Embryo, lane 3 Embryo, lane 4

(b)

Figure A1-3. *Geminin* knockdown.

A. Semiquantitative PCR to detect *geminin* expression in two entire litters of *geminin* shRNA-exposed embryos. Some embryos continue to express nearly normal levels of *geminin* (lanes 1, 4), while others express low (2, 3, 16), intermediate (9, 17–19), or undetectable (5–8, 10–15) levels of *geminin*. The most advanced embryos consistently expressed the highest levels of *geminin*. Two entire litters of *geminin* targeted embryos were examined; 1–8 and 9–19. (-) = no RT, (+) = E9 embryo RNA.

B. Sideview of control and embryos expressing varying levels of *geminin*.
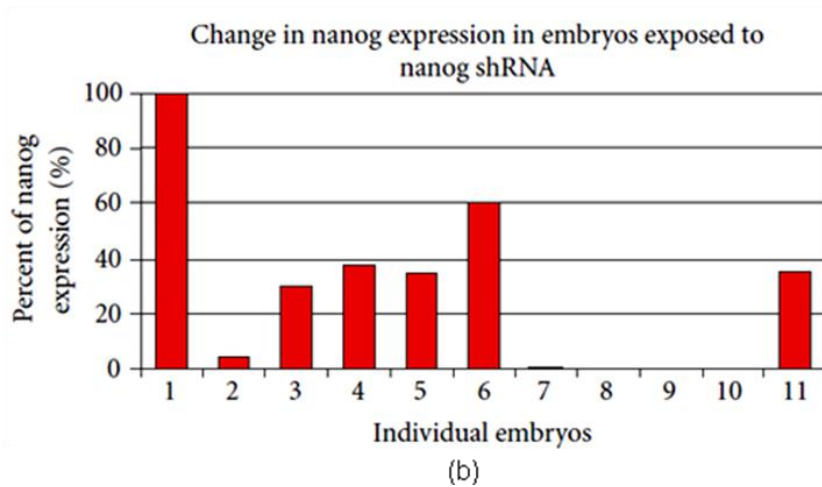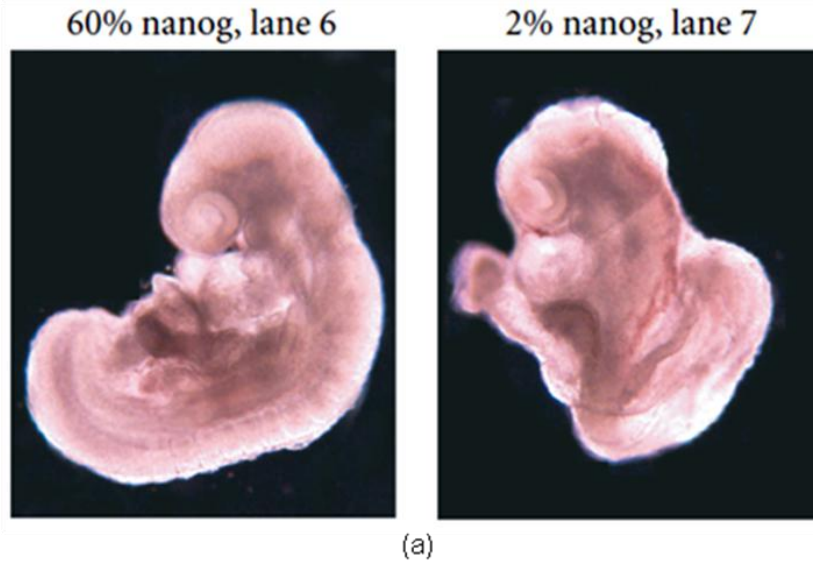
Figure A1-4. *Nanog* knockdown.

A. Sideviews of two embryos exposed to *nanog* shRNA. Although the first embryo expressed 60% of wild-type levels of *nanog* mRNA, developmental defects are minor and include an axis abnormality and a flattened posterior neuropore. When *nanog* levels are reduced to 2% of wild type, embryos were more severely affected. The embryo in the right panel is characterized by defects of somite segmentation, neural tube closure, and abnormalities of endoderm differentiation.

B. Q-PCR analysis of *nanog* mRNA expression levels in individual embryos. Embryos were exposed on E6.5 to the *nanog* shRNA and examined on E9.0. cDNA from each embryo was run in triplicate in quantitative PCR with primers to both *nanog* and *β-actin* using the Clontech Qzyme system. Levels of *β-actin* and *nanog* expression from *nanog* shRNA-treated embryos (lanes 2–11) were compared to expression in a control embryo (lane 1). *Nanog* expression ranged from 0–60% of control levels.
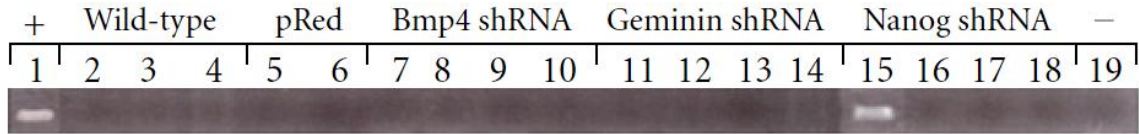
Figure A1-5. *Oas1* PCR.

Single embryo RT reactions were subjected to 40 cycles of PCR with primers for *Oas1* mRNA (71).Mouse brain RT was used as a low-level expression positive control (+). Only 2 *nanog* shRNA embryos were positive for *Oas1* expression (one shown, lane15). (-) = no cDNA control.

Figure A1-6. Effects of *Bmp* shRNA.

A. Scanning electron microscopy (SEM) view of a control embryo illustrating completed neural tube closure in the forebrain (F) region; the posterior neuropore (pnp) has not yet been closed.

B. Bmp4 shRNA-exposed embryo with widely open anterior neural folds (arrows) and posterior neuropore (lower black arrow).

C. SEM view of a Bmp7 shRNA-exposed embryo. Both the midbrain (arrows) and the posterior neuropore (pnp arrow) are widely open, but the body axis defects characteristic of Bmp4 shRNA and Bmp4 + Bmp7 shRNA embryos were not present.

D. Ventrolateral SEM view of a compound Bmp4 + Bmp7 shRNA embryo. The cephalic neural folds are unfused (arrows) and the posterior region is rudimentary (*). 1: first brachial arch, A: amnion, F: forebrain, H: heart, pnp: posterior neuropore.
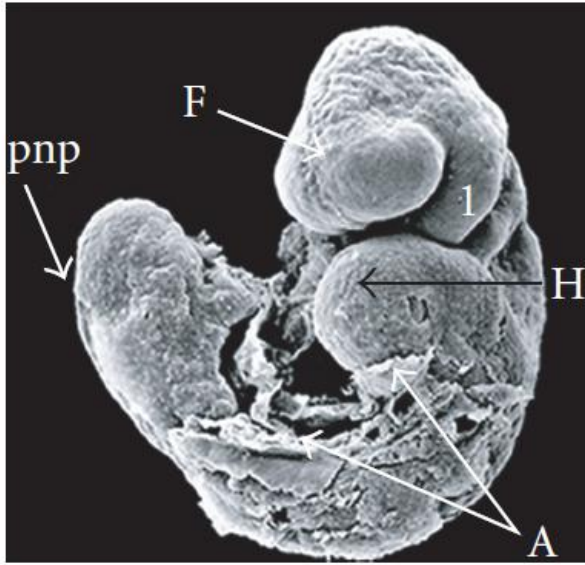
(a)
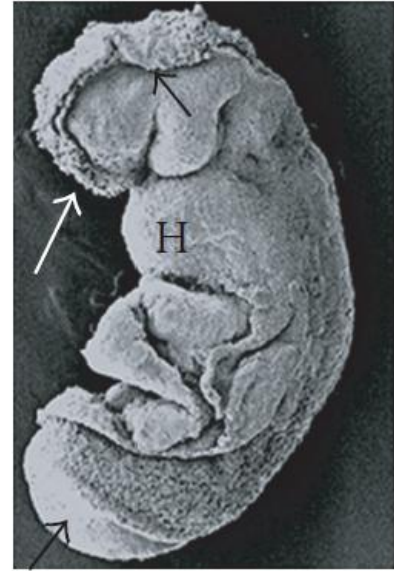
(b)
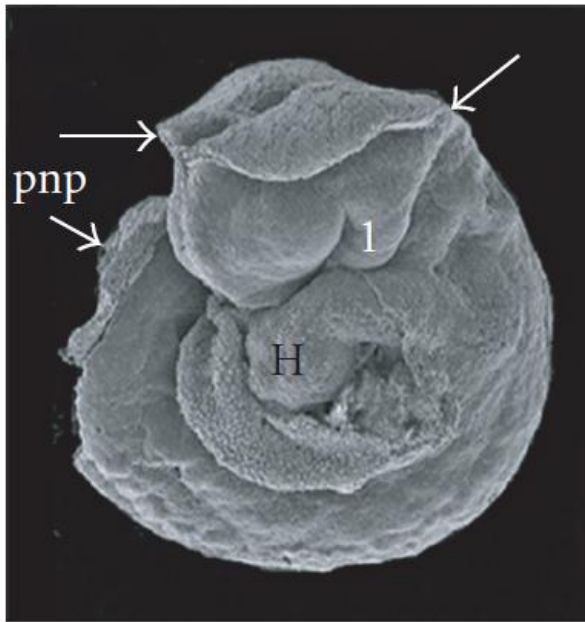
(c)
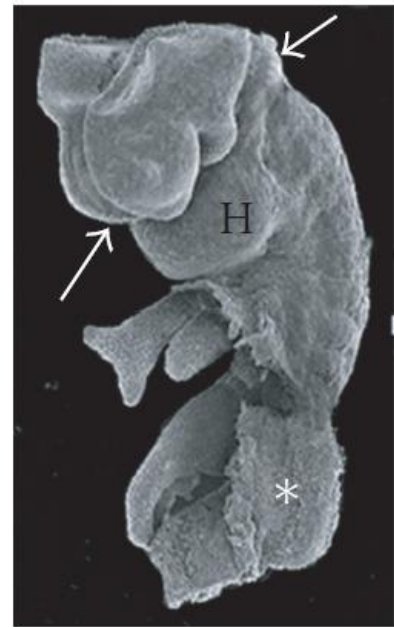
(d)
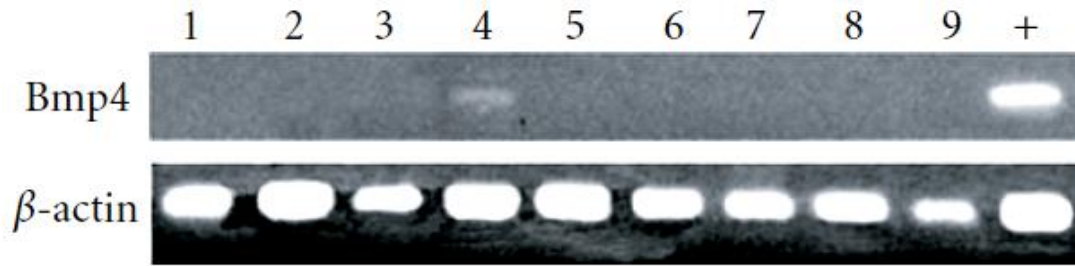
Figure A1-7. *Bmp4* knockdown.

RT-PCR analysis of individual *Bmp4* shRNA-exposed embryos from one entire litter. The positive control (+) is from an embryo exposed to pRed control vector alone. Pregnant dams were injected on E6.5 and RNA extracted from embryos on E9.0.
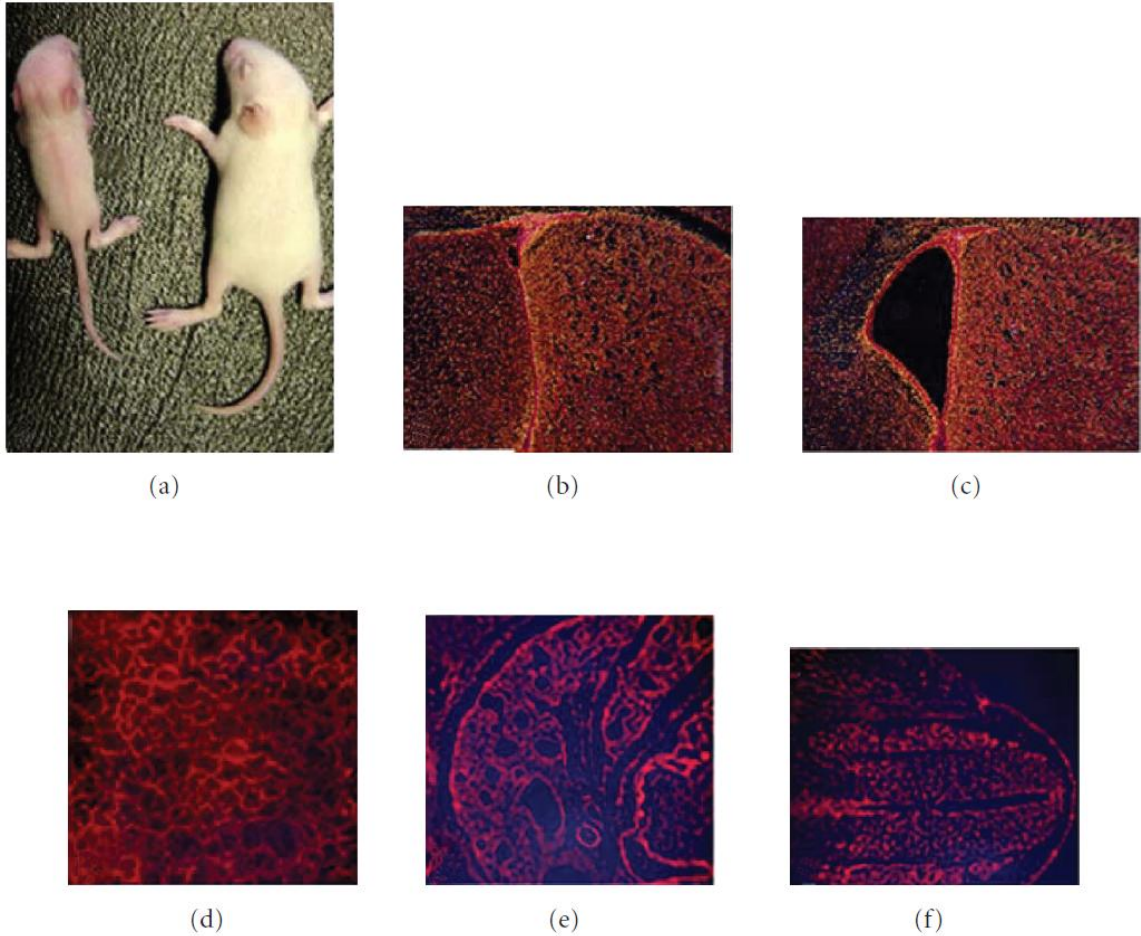
Figure A1-8. Longevity of the RNAi.

(a) Day 10 neonatal mice (PN10) obtained from litters exposed on E6.5 to the *Bmp4* shRNA (left) or to pRed (no hairpin plasmid) control (right). *Bmp4* shRNA mice were consistently developmentally delayed and lacked testis or ovaries. (b) and (c) Coronal sections through the lateral ventricles of PN3 mice exposed on E17.5 to pRed control (b) or to *Bmp4* shRNA (c). In addition to the obvious anomalies of the subventricular zone and ventricle, neural stem cells obtained from the *Bmp4* shRNA mice fail to differentiate normally. (d)–(f) illustrate the persistent expression of DsRed in liver (d), lung (e), and spinal cord (f) in neonates exposed to *Bmp4* shRNA on E6.5.

Figure A1-9. Control- and gene-targeted embryos: *nanog*, *geminin*, *Aggf1*, and *Est1*.

A. Control embryo. Sideview of an embryo exposed to pRed plasmid (no hairpin) on E6.5 and examined on E8.5, illustrating the normal appearance of the head folds (Hf), somites, and unturned body axis.

B. *Nanog* shRNA. Embryo exposed on E6.5 to shRNA targeting *nanog*, illustrating the typical lack of development of the head folds (Hf) and posterior region in the tail bud (T). Somites have also failed to segregate normally.

C-D. We carried out a differential display RT-PCR screen of genes induced in D3 ESC by noggin exposure, then targeted two using tail vein injection of shRNAs. (c) *Aggf1*-targeted embryos failed to implant normally and the primitive ectoderm often delaminated into the amniotic cavity. Hemorrhages are present within the embryo; there are striking abnormalities of turning and posterior development in the rare embryo that survived to E8.5. (d) Est1-targeted embryo. There were anomalies of primitive streak organization in these embryos. They also often failed to turn to adopt the fetal position and exhibited abnormalities of the node.

E. pRed control. Sideview of an E8.5 pRed (no hairpin) control. This embryo is beginning the turning process, the body axis is elongated, neural folds are fused in the anterior (head fold, Hf) region, although the posterior neuropore remains open in the tail bud (T).

F. *Wnt8b*-targeted embryo illustrating the shortened axis and open neural folds typical of these embryos.

G-H. *Geminin* shRNA. An embryo exposed to *geminin* shRNA on E6.5 and examined on E8.5. There are very characteristic midbrain (upper arrows) and posterior neuropore (lower arrow in (g)) defects in these embryos, which exhibit widespread DsRed fluorescence (H). All embryos are oriented with anterior toward the left. Al: allantois, H: heart, Hf: head folds, T: tail bud. Arrows indicate open neural folds.
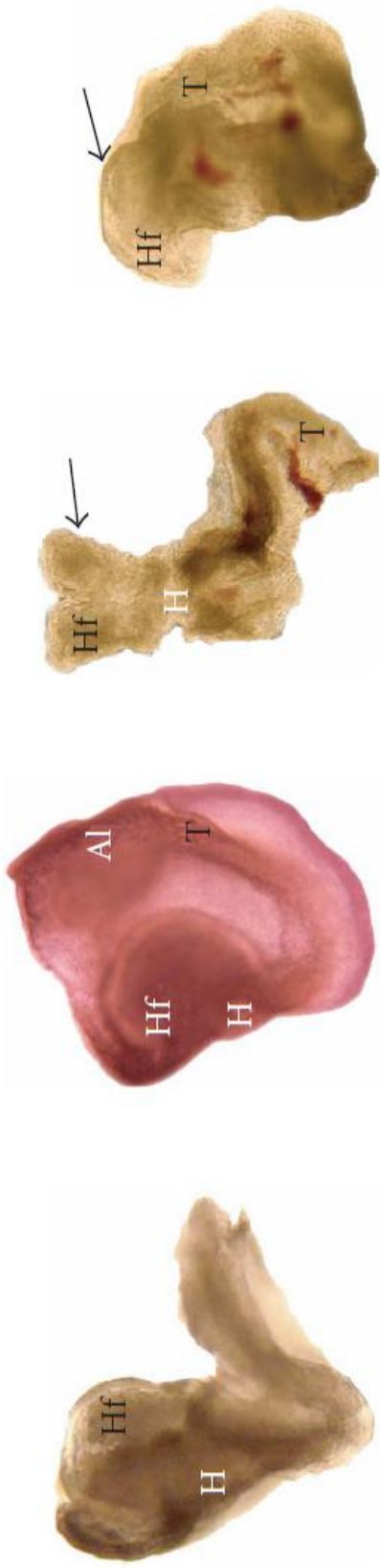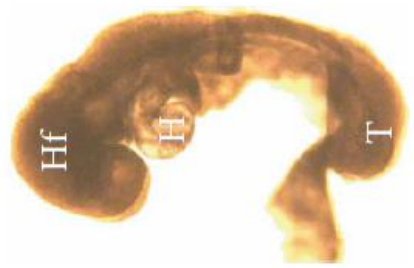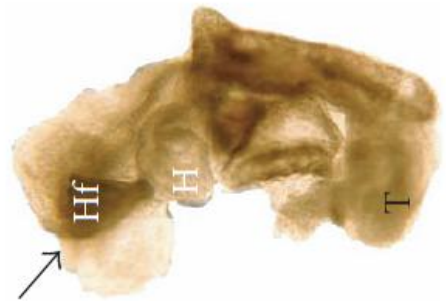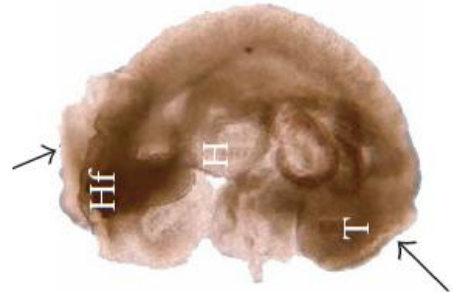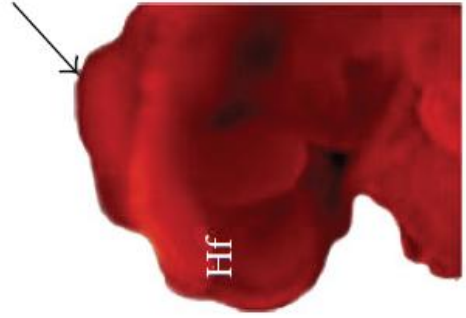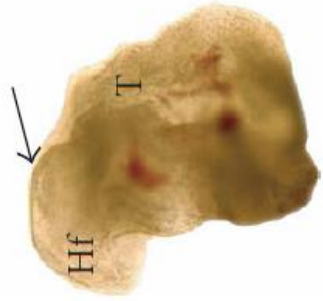
REFERENCES

Anderson J, Burns HD, Enriquez-Harris P, Wilkie AOM, Heath JK. 1998. Apert syndrome mutations in fibroblast growth factor receptor 2 exhibit increased affinity for FGF ligand. Hum Mol Genet 7: 1475-1483.

Asada-Kubota M, Ueda T, Nakashima T, Kobayashi M, Shimada M, Takeda K, Hamada K, Maekawa S, Sokawa Y. 1997. Localization of 2',5'-oligoadenylate synthetase and the enhancement of its activity with recombinant interferon α– A/D in the mouse brain. Anat Embryol 195: 251-257.

Baldwin HS, Mickanin C, Buck C. 1997. Adenovirus-mediated gene transfer during initial organogenesis in the mammalian embryo is promoter-dependent and tissue-specific. Gene Ther 4: 1142-1149.

Barlow DP, Randle BJ, Burke DC. 1984. Interferon synthesis in the early post-implantation mouse embryo. Differentiation 27: 229-235.

Begley DJ. 2004. Delivery of therapeutic agents to the central nervous system: the problems and the possibilities. Pharm Ther 104: 29-45.

Bisbal C, Silhol M, Laubenthal H, Kaluza T, Carnac G, Milligan L, Le Roy F, Salehzada T. 2000. The 2'5'oligoadenylate/Rnase L/Rnase L inhibitor pathway regulates both MyoD mRNA stability and muscle cell differentiation. Mol Cell Biol 20: 4959-4969.

Bridge AJ, Pebernard S, Ducraus Z, Nicoulaz A-L, Iggo R. 2003. Induction of an interferon response by RNAi vectors in mammalian cells. Nature Gnet 34: 263-264.

Calegari F, Marzesco A-M, Kittler R, Buchholz F, Huttner WB. 2004. Tissue-specific RNA interference in post-implantation mouse embryos using directional electroporation and whole embryo culture. Differentiation 72: 92-102.

Cao W, Hunter R, Strnatka D, McQueen CA, Erickson RP. 2005. DNA constructs designed to produce short hairpin, interfering RNAs in transgenic mice sometimes show early lethality and an interferon response. J Appl Genet 46: 217-225.

Capecchi MR. 1989. Altering the genome by homologous recombination. Science 244: 1288-1292.

Carmell MA, Zhang L, Conklin DS, Hannon GJ, Rosenquist TA. 2003. Germline transmission of RNAi in mice. Nat Struct Biol 10: 91-92.

Chambers I, Colby D, Robertson M, Nichols J, Lee S, Tweedie S, Smith A. 2003. Functional expression cloning of nanog, a pluripotency sustaining factor in embryonic stem cells. Cell 113: 643-655.

Chang H-S, Lin C-H, Chen Y-C, Yu WCY. 2004. Using siRNA technique to generate transgenic animals with spatiotemporal and conditional gene knockdown. A J Pathol 165: 1535-1541.

Chi JT, Chang HY, Wang NN, Chang DS, Cunphy N, Brrown PO. 2003. Genomewide view of gene silencing by small interfering RNAs. Proc Natl Acad Sci USA 100: 6343-6346.

Coutelle C, Douar AM, Colledge WH, Froster U. 1995. The challenge of fetal gene therapy. Nature Med 1: 864-865.

Dent JA, Polson AG, Klymkowsky MW. 1989. A whole-mount immunocytochemical analysis of the expression of the intermediate filament protein vimentin in Xenopus. Develop 105: 61-74.

Douar AM, Adebakin S, Themis M, Pavirani A, Cook T, Coutelle C. 1997. Foetal gene delivery in mice by intra-amniotic administration of retroviral producer cells and adenovirus. Gene Ther 4: 883-390.

Fujiwara T, Dehart DB, Sulik KK, Hogan BL. 2002. Distinct requirements for extra-embryonic and embryonic bone morphogenetic protein 4 in the formation of the node and primitive streak and coordination of left-right asymmetry in the mouse. Develop129: 4685-4696.

Gaensler KML, Tu G, Bruch S, Liggitt D, Lipshutz GS, Metkus A, Harrison M, Heath TD, Debs RJ. 1999. Fetal gene transfer by transuterine injection of cationic liposome-DNA complexes. Nature Biotech 17: 1188-1192.

Gordon JWS, Scangos GA, Plotkin DJ, Barbosa JA, Ruddle FH. 1980. Genetic transformation of mouse embryos by microinjection of purified DNA. Proc Natl Acad Sci USA 77: 7380-7384.

Grabarek JB, Plusa B, Glover DM, Zernicka-Goetz M. 2002. Efficient delivery of dsRNA into zona-enclosed mouse oocytes and preimplantation embryos by electroporation. genesis 32: 269-276.

Gratsch TE, De Boer LS, O'Shea KS. 2003. RNA inhibition of BMP-4 gene expression in postimplantation mouse embryos. genesis 37: 12-17.

Gratsch TE, Slawny N, Dzaman M, Morrel M, O'Shea KS. 2005. Nanog RNAi in postimplantation embryos and embryonic stem cells. Soc Neurosci Abstr, program number 597.2.

Hadjantonakis AK, Gertsenstein M, Ikawa M, Okabe M, Nagy A. 1998. Generating green fluorescent mice by germline transmission of green fluorescent ES cells. Mech Dev 76: 79-90.

Hagstrom JE, Hegge J, Zhang G, Noble M, Budker V, Lewis DL, Herweijer H, Wolff JA. 2004. A facile nonviral method for delivering genes and siRNAs to skeletal muscle of mammalian limbs. Mol Ther 10: 386-398.

Hart AH, Hartley L, Ibrahim M, Robb L. 2004. Identification, cloning and expression analysis of the pluripotency promoting nanog genes in mouse and human. Dev Dyn 230: 187-198.

Hasuwa H, Kaseda K, Einarsdottir T, Okabe M. 2002. Small interfering RNA and gene silencing in transgenic mice and rats. FEBS Lett 532: 227-230.

Heasman J. 2002. Morpholino oligos: making sense of antisense? Dev Biol 243: 209-214.

Hemann MT, Fridman JS, Zilfou JT, Hernando E, Paddison PJ, Cordon-Cardo C, Hannog GJ, Lowe SW. 2003. An epi-allelic series of p53 hypomorphs created by stable RNAi produces distinct tumor phenotypes in vivo. Nat Genet 33: 396-400.

Hodges BL, Scheule RK. 2003. Hydrodynamic delivery of DNA. Expert Opin Biol Ther 3: 911-918.

Kikuchi N, Nakamura S, Ohtsuka M, Kimura M, Sato M. 2002. Possible mechanism of gene transfer into early to mid-gestational mouse fetuses by tail vein injection. Gene Ther 9: 1529-1541.

Kroll KL, Salic AN, Evans LM, Kirschner MW. 1998. Geminin, a neuralizing molecule that demarcates the future neural plate at the onset of gastrulation. Develop 125: 3247-3258.

Kunath T, Gish G, Lickert H, Jones N, Pawson T, Rossant J. 2003. Transgenic RNA interference in ES cell-derived embryos recapitulates a genetic null phenotype. Nat Biotech 21: 559-561.

Larson JE, Morrow SL, Happel L, Sharp JF, Cohen JC. 1997. Reversal of cystic fibrosis phenotype in mice by gene therapy in utero. Lancet 349: 619-620.

Lavery KS, King TH. 2003. Antisense and RNAi powerful tools in drug target discovery and validation. Curr Opin Drug Discov Devel 6: 561-569.

Lawson KA, Dunn NR, Roelen BAJ, Zeinstra LM, Davis AM, Wright CVE, Korving JPWFM, Hogan BLM. 1999. Bmp4 is required for the generation of primordial germ cells in the mouse embryo. Genes & Dev 13: 424-436.

Lefebvre C, Terret ME, Djiane A, Rassinier P, Maro B, Verlhac MH. 2002. Meiotic spindle stability depends on MAPK-interacting and spindle-stabilizing protein (MISS), a new MAPK substrate. J Cell Biol 157: 603-613.

Lewis DL, Hagstrom JE, Loomis AG, Wolff JA, Herweijer H. 2002. Efficient delivery of siRNA for inhibition of gene expression in postnatal mice. Nature Genet 32: 107-108.

Lim DA, Tramontin AD, Trevejo JM, Herrera DG, Garcia-Verdugo JM, Alvarez-Buylla A. 2000. Noggin antagonizes BMP signaling to create a niche for adult neurogenesis. Neuron 28: 713-726.

Liu F, Qi H, Huang L, Liu D. 1997. Factors controlling the efficiency of cationic lipid-mediated transfection in vivo via intravenous administration. Gene Ther 4: 517-523.

Liu F, Song YK, Liu D. 1999. Hydrodynamics-based transfection in animals by systemic administration of plasmid DNA. Gene Ther 6: 1285-1266.

Liu PT, Wakamiya M, Shea MJ, Albrecht U, Behringer RR, Bradley A. 1999. Requirement for Wnt3 in vertebrate axis formation. Nat Genet 22: 361-365.

Mashimo T, Glaser P, Lucas M, Simon-Chazottes D, Ceccaldi PE, Montagutelli X, Despres P, Guenet J-L. 2003. Structural and functional genomics and evolutionary relationships in the cluster of genes encoding murine 2',5'-oligoadenylate synthetases. Genomics 82: 537-552.

McCaffrey AP, Nakai H, Pandey K, Huang Z, Salazar FH, Xu H, Wieland SF, Marion PL, Kay MA. 2003. Inhibition of hepatitis B virus in mice by RNA interference. Nat Biotech 21: 639-644.

Mellitzer G, Hallonet M, Chen L, Ang S-L. 2002. Spatial and temporal 'knock down' of gene expression by electroporation of double-stranded RNA and morpholinos into early postimplantation mouse embryos. Mech Dev 118: 57-63.

Mishina Y, Suzuki A, Ueno N, Behringer RR. 1995. Bmpr encodes a type I bone morphogenetic protein receptor that is essential for gastrulation during mouse embryogenesis. Genes & Dev 9: 3027-3037.

Mitsui K, Tokuzawa Y, Itoh H, Segawa K, Murakami M, Takahashi K, Maruyama M, Maeda M, Yamanaka S. 2003. The homeoprotein nanog is required for maintenance of pluripotency in mouse epiblast and ES cells. Cell 113: 631-642.

Okuda K, Xin KQ, Haruki A, Kawamoto S, Kojima Y, Hirahara F, Okada H, Klinman D, Hamajima K. 2001. Transplacental genetic immunization after intravenous delivery of plasmid DNA to pregnant mice. J Immunol 167: 5478-5484.

Papaioannou VE. 1990. In utero manipulation. In: Copp AJ, Cockroft DL (eds). Postimplantation Mammmalian Embryos. IRL Press at Oxford University Press: Oxford, pp 61-80.

Reversade B, Kuroda H, Lee H, Mays A, De Robertis EM. 2005. Depletion of Bmp2, Bmp4, Bmp7 and Spemann organizer signals induces massive brain formation in Xenopus embryos. Develop 132: 3381-3392.

Rubinson DA, Dillon CP, Kwiatkowski AV, Sievers C, Yang L, Kopinja J, Rooney DL, Ihrig MM, McManus MT, Gertler FB. 2003. A lentivirus-based system to functionally silence genes in primary mammalian cells, stem cells and transgenic mice by RNA interference. Nat Genet 33: 401-406.

Saitou M, Barton SC, Surani MA. 2002. A molecular programme for the specification of germ cell fate in mice. Nature 418: 293-300.

Schachtner SK, Buck CA, Bergelson JM, Baldwin HS. 1999. Temporally regulated expression patterns following in utero adenovirus-mediated gene transfer. Gene Ther 6: 1249-1257.

Semizarov D, Frost L, Sarthy A, Kroeger P, Halbert DN, Fesik SW. 2003. Specificity of short interfering RNA determined through gene expression signatures. Proc Natl Acad Sci USA 100: 6347-6352.

Seo S, Herr A, Lim JW, Richardson GA, Richardson H, Kroll KL. 2005. Geminin regulates neuronal differentiation by antagonizing Brg1 activity. Genes Dev 19: 1723-1734.

Soares ML, Haraguchi S, Torres-Padilla ME, Kalmar T, Carpenter L, Bell G, Morrison A, Ring CJ, Clarke NJ, Glover DM, Zernicka-Goetz M. 2005. Functional studies of signaling pathways in peri-implantation development of the mouse embryo by RNAi. BMC Dev Biol 5: 28 e-pub.

Song E, Lee SK, Wang J, Ince N, Ouyang N, Min J, Chen J, Shankar P, Lieberman J. 2003. RNA interference targeting Fas protects mice from fulminant hepatitis. Nat Med 9: 347-351.

Sorensen DR, Leirdal M, Sioud M. 2003. Gene silencing by systemic delivery of synthetic siRNAs in adult mice. J Mol Biol 327: 761-766.

Soutschek J, Akinc A, Bramlage B, Charisse K, Constien R, Donoghue M, Elbashir S, Geick A, Hadwiger P, Haarborth J, John M, Kesavan V, Lavine G, Pandey RK, Racie T, Rajeev KG, Toudjarska I, Wang G, Wuscheko S, Bumcrot D, Kotellansky V, Limmer S, Manoharan M, Vornlocher H. 2004. Therapeutic silencing of an endogenous gene by systematic administration of modified siRNAs. Nature 432: 173-178.

Stein P, Svoboda P, Schultz RM. 2003. Transgenic RNAi in mouse oocytes: a simple and fast approach to study gene function. Dev Biol 256: 187-193.

Svoboda P. 2004. Long ds RNA and silencing genes strike back: RNAi in mouse oocytes and early embryos. Cytogenet Genome Res 105: 422-434.

Tian X-L, Kadaba R, You S-A, Liu M, Timur AA, Yang L, Chen Q, Szafranski P, Rao S, Wu L, Housman DE, DiCorleto PE, Driscoll DJ, Borrow J, Wang Q. 2004. Identification of an angiogenic factor that when mutated causes susceptibility to Klippel-Trenaunay syndrome. Nature 427: 640-645.

Tiscornia G, Singer O, Ikawa M, Verma IM. 2003. A general method for gene knockdown in mice by using lentiviral vectors expressing small interfering RNA. Proc Natl Acad Sci USA 100: 1844-1848.

Tsukamoto M, Ochiya T, Yoshida S, Sugimura T, Terada M. 1995. Gene transfer and expression in progeny after intravenous DNA injection into pregnant mice. Nature Genet 9: 243-248.

Turkay A, Saunders TL, Kurachi K. 1999. Intrauterine gene transfer: gestational stage-specific gene delivery in mice. Gene Ther 6: 1685-1694.

Waterston RH, Lindblad-Toh K, Birney E, Rogers J, Abril JF, Agarwal P, Agarwala R, Ainscough R, Alexandersson M, An P, Antonarakis SE, Attwood J, Baertsch R, Bailey J, Barlow K, Beck S, Berry E, Birren B, Bloom T, Bork P, Botcherby M, Bray N, Brent MR, Brown DG, Brown SD, Bult C, Burton J, Butler J, Campbell RD, Carninci P, Cawley S, Chiaromonte F, Chinwalla AT, Church DM, Clamp M, Clee C, Collins FS, Cook LL, Copley RR, Coulson A, Couronne O, Cuff J, Curwen V, Cutts T, Daly M, David R, Davies J, Delehaunty KD, Deri J, Dermitzakis ET, Dewey C, Dickens NJ, Diekhans M, Dodge S, Dubchak I, Dunn DM, Eddy SR, Elnitski L, Emes RD, Eswara P, Eyras E, Felsenfeld A, Fewell GA, Flicek P, Foley K, Frankel WN, Fulton LA,

Fulton RS, Furey TS, Gage D, Gibbs RA, Glusman G, Gnerre S, Goldman N, Goodstadt L, Grafham D, Graves TA, Green ED, Gregory S, Guigo R, Guyer M, Hardison RC, Haussler D, Hayashizaki Y, Hillier LW, Hinrichs A, Hlavina W, Holzer T, Hsu F, Hua A, Hubbard T, Hunt A, Jackson I, Jaffe DB, Johnson LS, Jones M, Jones TA, Joy A, Kamal M, Karlsson EK, Karolchik D, Kasprzyk A, Kawai J, Keibler E, Kells C, Kent WJ, Kirby A, Kolbe DL, Korf I, Kucherlapati RS, Kulbokas EJ, Kulp D, Landers T, Leger JP, Leonard S, Letunic I, Levine R, Li J, Li M, Lloyd C, Lucas S, Ma B, Maglott DR, Mardis ER, Matthews L, Mauceli E, Mayer JH, McCarthy M, McCombie WR, McLaren S, McLay K, McPherson JD, Meldrim J, Meredith B, Mesirov JP, Miller W, Miner TL, Mongin E, Montgomery KT, Morgan M, Mott R, Mullikin JC, Muzny DM, Nash WE, Nelson JO, Nhan MN, Nicol R, Ning Z, Nusbaum C, O'Connor MJ, Okazaki Y, Oliver K, Overton-Larty E, Pachter L, Parra G, Pepin KH, Peterson J, Pevzner P, Plumb R, Pohl CS, Poliakov A, Ponce TC, Ponting CP, Potter S, Quail M, Reymond A, Roe BA, Roskin KM, Rubin EM, Rust AG, Santos R, Sapojnikov V, Schultz B, Schultz J, Schwartz MS, Schwartz S, Scott C, Seaman S, Searle S, Sharpe T, Sheridan A, Shownkeen R, Sims S, Singer JB, Slater G, Smit A, Smith DR, Spencer B, Stabenau A, Stange-Thomann N, Sugnet C, Suyama M, Tesler G, Thompson J, Torrents D, Trevaskis E, Tromp J, Ucla C, Ureta-Vidal A, Vinson JP, Von Niederhausern AC, Wade CM, Wall M, Weber RJ, Weiss RB, Wendl MC, West AP, Wetterstrand K, Wheeler R, Whelan S, Wierzbowski J, Willey D, Williams S, Wilson RK, Winter E, Worley KC, Wyman D, Yang S, Yang SP, Zdobnov EM, Zody MC, Lander ES; Mouse Genome Sequencing Consortium. 2002. Initial sequencing and comparative analysis of the mouse genome. Nature 420: 520-562.

Wells V, Mallucci L. 1988. Cell cycle regulation (G1) by autocrine interferon and dissociation between autocrine interferon and 2',5'-oligoadenylate synthetase expression. J Interferon Res 8: 793-802.

Wianny F, Zernicka-Goetz M. 2000. Specific interference with gene function by double-stranded RNA in early mouse development. Nature Cell Biol 2: 70-75.

Winnier G, Blessing M, Labosky PA, Hogan BL. 1995. Bone morphogenetic protein-4 is required for mesoderm formation and patterning in the mouse. Genes & Dev 9: 2105-2116.

Yekta S, Shih I-h, Bartel DP. 2004. MicroRNA-directed cleavage of HOXB8 mRNA. Science 304: 594-596.

Yi R, Doehle BP, Qin Y, Macara IG, Cullen BR. 2005. Overexpression of exportin 5 enhances RNA interference mediated by short hairpin RNAs and microRNAs. RNA 11: 220-226.

Appendix 2

Identification of Novel Genes in the Mouse Embryo via Laser Capture Microdissection

INTRODUCTION

At neural induction, factors are secreted from the node that first induce and then pattern the neural ectoderm. While much is known regarding the signals involved in neural induction in Xenopus and chick embryos, considerably less is known about patterning of the mammalian ectoderm. In addition, the genes that control the boundary between the neural and surface ectoderm and later convey neural identity are largely unknown. In the current investigation, laser capture microdissection (LCM) was employed to first isolate cell populations and then identify novel genes from frozen, sagittal sections of 120 stage 7.25 to 7.5 embryos. RNAs were isolated and microarray analysis conducted in order to identify genes up- or down-regulated within seven regions of the embryo including: induced versus uninduced neural ectoderm, anterior neural ectoderm versus posterior neural ectoderm, and anterior visceral endoderm, node and primitive streak. Of the approximately 7000 differentially expressed genes, we have identified clusters of genes restricted to the various regions of the embryo, including known signaling molecules. Many of these genes may be involved in fate specification or may mark early lineage differentiation of the mouse embryo at gastrulation.

MATERIALS AND METHODS

Embryos:

E7.25 to E7.5 mouse embryos were harvested from ICR dams (Harlan), fixed in 2% paraformaldehyde for 10 minutes, and embedded in OCT medium. The whole embryo illustrated is oriented with anterior to the left (Figure A2-1A).

Sections:

Sagittal sections were cut at 10 µm and adhered to plus slides. Sections were stored at –80°C with care taken to ensure slides remained dry until processed. Groups of slides were stained following the HistoGene LCM Frozen section staining protocol from Molecular Devices (Arcturus) and kept in a dessicator prior to laser microdissection (Figure A2-1B).

Laser Capture:

Slides/caps were kept a maximum of an hour from staining to laser dissection once slides were thawed from the freezer. CapSure HS caps were used on the Veritas Laser Capture Microscope. On average, the laser spot size was 11 µm and an average of 630,000 µm^2 was collected for each embryonic region.

RNA extraction:

Cell extracts were collected from the caps and stored at –80°C until all slides could be processed. RNA was isolated using the PicoPure RNA extraction kit from Molecular Devices (Arcturus) followed by a DNAse step (Qiagen). Microdissected embryo with corresponding captured regions is shown in Figure A2-1C.

Microarray and Data analysis:

RNAs were sent to the TGen consortium for double amplification and microarray analysis. Affymetrix Mouse Genome 430 2.0 arrays were used. Studies were

done in triplicate. Results obtained from the microarray were analyzed by the University of Michigan BioInfomatics Core, DAVID, and OntoExpress.

RESULTS

The data listed in Table A2-1 represent a portion of the results obtained from comparisons between two regions as indicated in the embryo cartoon.

FUTURE DIRECTIONS

Pair-wise comparison of the six regions will be analyzed against each other and genes of interest will be verified by *in situ* hybridization. Additionally, microarray data obtained from ESC lines in the lab (*i.e.* Geminin overexpressing, Ngn-1 overexpressing, and dnTCF/LEF) will be compared to regions within the embryo for an *in vitro* / *in vivo* comparison.

ACKNOWLEDGMENTS
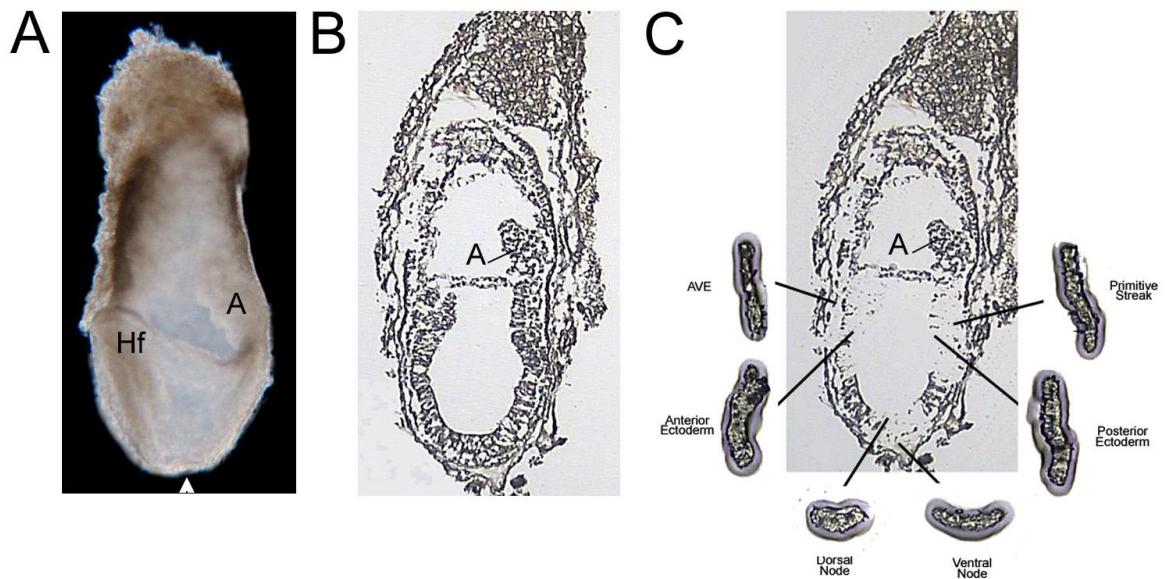
Figure A2-1. Areas collected for microarray analysis.

A. E7.25 embryo collected for LCM. A = allantois; Hf = headfolds; white arrowhead = node. Anterior is to the left.

B. E7.25 embryo section after staining prior to collection. A = allantois.

C. Image of embryo after the cells for analysis were removed. The corresponding cells removed were photographed on their respective caps.

Table A2-1. Gene comparisons.

Data shown represent comparisons between two regions. 150 similar genes were found in AVE vs. A. ectoderm; 143 genes in P. ectoderm vs. A. ectoderm; 45 genes in V. Node vs. Primitive streak; 289 genes in AVE vs. Primitive streak; 50 genes in V. Node vs. D. Node; 156 genes in AVE vs. V. Node; 108 genes in D. Node vs. P. ectoderm; and 33 genes in D. Node vs. A. ectoderm.

Unigene	Name	Pathway	Symbol	Fold Change	AVE	A. Ectoderm
Mm.100399	MAD homolog 4 (Drosophila)	Wnt & TGFb pathway	Smad4	-4.08	3.52	7.61
Mm.3400	Dishevelled, dsh homolog 1	Wnt & Notch pathway	Dvl1	-2.85	4.61	7.47
Mm.99	Ribonucleotide reductase M2	p53 signalling pathway	Rrm2	-1.90	5.66	7.56
Mm.216227	Ubiquitin B	Parkinson's Disease	Ubb	-1.46	7.70	9.15
Mm.216227	Casein kinase 1, delta	Wnt pathway	Csnk1d	-1.30	6.67	7.97

Unigene	Name	Pathway	Symbol	Fold Change	P. Ectoderm	A. Ectoderm
Mm.35389	Cytochrome c, somatic	p53 pathway	Cycs	-2.88	3.77	6.66
Mm.2206	NADH dehydrogenase (ubiquinone) flavoprotein 2	Oxidative phosporylation	Ndufv2	-2.39	5.48	7.87
Mm.379007	Ribosomal protein S6	mTor & Insulin signaling pathway	Rps6	-1.95	7.06	9.01
Mm.250332	Deoxythymidylate kinase	Pyrimidine metabolism	Dtymk	-1.67	6.19	7.86
Mm.28017	F-box and WD-40 domain protein 11	Wnt & Hedgehog pathway	Fbxw11	-1.16	5.25	6.41

Unigene	Name	Pathway	Symbol	Fold Change	V. Node	Primitive Streak
Mm.426209	Mortality factor 4 like 1	Regulation of cell growth	Morf4l1	-3.67	3.56	7.22
Mm.42249	Neogenin	Cell adhesion molecules	Neo1	-3.60	2.50	6.10
Mm.291595	Kruppel-like factor 9	Progesterone signaling pathway	Klf9	-2.88	3.49	6.37
Mm.439690	Tubulin, alpha 1A	Gap junction	Tuba1a	2.40	7.08	4.68
Mm.18714	Paxillin	VEGF signaling pathway	Pxn	-1.02	6.47	7.49

Unigene	Name	Pathway	Symbol	Fold Change	AVE	Primitive Streak
Mm.282039	ATP citrate lyase	TCA cycle	Acly	-3.93	2.87	6.80
Mm.3074	Ubiquitin-conjugating enzyme E2L 3	Parkinson's Disease	Ube2l3	-2.95	3.14	6.09
Mm.3906	Mitogen activated protein kinase kinase 7	MAPK signaling pathway	Map2k7	-1.93	6.95	8.88
Mm.19111	Protein kinase, cAMP dependent, catalytic, alpha	MAPK, Wnt, Hedgehog pathway	Prkaca	-1.89	6.41	8.30
Mm.741	Fatty acid binding protein 5, epidermal	PPAR signaling pathway	Fabp5	-1.71	8.01	9.72

Unigene	Name	Pathway	Symbol	Fold Change	V. Node	D. Node
Mm.260900	Ataxin 2	Negative regulation of body size	Atxn2	1.59	6.76	5.17
Mm.21772	SWI/SNF related, matrix associated, actin dependent regulator of chromatin, subfamily d, member 2	Chromatin modification	Smarcd2	1.59	7.67	6.08
Mm.260164	Hydroxyacyl-Coenzyme A dehydrogenase	Metabolism	Hadh	1.53	9.03	7.50
Mm.329243	Calmodulin 2	Huntington's Disease	Calm2	1.37	6.32	4.95
Mm.29368	Angiotensin receptor-like 1	Neuroactive ligand-receptor	Agtrl1	1.26	11.70	10.44

Unigene	Name	Pathway	Symbol	Fold Change	V. Node	AVE
Mm.289936	Phosphoserine aminotransferase 1	Metabolism	Psat1	2.87	6.33	3.46
Mm.141083	BCL2-like 11 (apoptosis facilitator)	Apoptosis	Bcl2l11	2.86	7.61	4.75
Mm.378921	Gap junction membrane channel protein alpha 1	Neuron migration	Gja1	2.22	6.66	4.44
Mm.43415	Cytochrome c oxidase, subunit VI a, polypeptide 1	Oxidative phosphorylation	Cox6a1	1.39	9.42	8.03
Mm.24816	Coagulation factor II (thrombin) receptor	Neuroactive ligand-receptor	F2r	1.21	7.96	6.75

Unigene	Name	Pathway	Symbol	Fold Change	D. Node	P. ectoderm
Mm.309296	Regulating synaptic membrane exocytosis 2	Neurotransmitter transport	Rims2	-4.55	2.04	6.59
Mm.66264	Syntaxin 6	Transport	Stx6	-4.11	2.34	6.45
Mm.61526	3-hydroxy-3-methylglutaryl-Coenzyme A synthase 1	Metabolism	Hmgcs1	1.13	8.21	7.08
Mm.331	Ubiquitin C	PPAR signaling pathway	Ubc	-1.07	6.97	8.04
Mm.270186	Retinoblastoma binding protein 7	DNA replication	Rbbp7	-1.07	8.24	9.32

Unigene	Name	Pathway	Symbol	Fold Change	D. Node	A. ectoderm
Mm.2108	Transthyretin	Hormone activity	Ttr	-3.18	3.09	6.27
Mm.3400	Dishevelled, dsh homolog 1	Hedgehog pathway	Dvl1	-1.40	6.07	7.47
Mm.216227	Casein kinase 1, delta	p53 signaling pathway	Csnk1d	-1.18	6.79	7.97
Mm.35389	Cytochrome c, somatic	VEGF signaling pathway	Cycs	-1.06	5.59	6.66
Mm.18714	Paxillin	Wnt & Notch pathway	Pxn	-1.05	6.16	7.20